2023

# COATES SOUTH BLOCK MINERAL RESOURCE ESTIMATE

**Technical Report and Supporting Documentation for the Coates South Block Mineral Resource Estimate**

| | |
|---|---|
| Report prepared for: | TIGA MINERALS AND METALS LIMITED<br>4 Blake Street<br>Surfdale<br>Waiheke Island 1842<br>New Zealand |
| Authors: | Mark Roux, BSc (Hons) PGCE MAusIMM<br>Jenny Love, BSc (Hons) MAusIMM<br>Sean Aldrich, MSc MAusIMM<br>Michael Gazley, PhD MAusIMM MAIG<br>Gavin Chapman, BSc PGCE<br>Olivier Bertoli, MEng FAusIMM GAA<br>Lauren Tooley, BSc (Hons) MAusIMM<br>Kat Lilly, PhD<br>Marcel Mizera, PhD<br>Annette Pocock, MSc MAusIMM |
| Competent Person: | René Sterk, MSc FAusIMM CP(Geo) MAIG (RPGeo) MSEG |
| Effective Date: | 10 February 2023 |

## Executive Summary

TiGa Minerals and Metals Limited (TiGa) commissioned RSC to prepare an independent mineral resource estimate for the Coates South Block within its Barrytown Project, West Coast, New Zealand. The work reported here, carried out by a Competent Person, and classified and reported in accordance with the JORC Code (2012), will serve to support feasibility work and ore reserve estimation for the Coates South Block. The Report's effective date is 10 February 2023.

The Barrytown Project is a coastal heavy mineral sands deposit located ~30 km north of Greymouth, New Zealand. Ilmenite, garnet, zircon, Au, and associated heavy minerals have been concentrated in a series of beach strandlines at Barrytown. Gold has been prospected for and mined from the Barrytown area since the late 1860s. Since the 1960s, Barrytown has been an ilmenite target for numerous companies.

The Barrytown Project consists of the active mining permit (MP) 60785 and two permit applications. The Coates South Block mineral resource estimate presented in this Report is fully contained within MP 60785. The commodities within the project are a mixture of Crown-owned and privately held minerals.

In 2022, TiGa drilled 257 aircore and four sonic holes on the Coates South Block for a total of 3,118 m. Data from these holes form the basis of the mineral resource estimate presented in this Report. Samples were obtained from the 45-µm to 2-mm fraction of 1-m-interval samples from the aircore and sonic drilling. A total of 2,226 pulverised samples were analysed by portable X-ray fluorescence to produce a multi-element geochemical dataset. A selection of 119 samples were analysed by laboratory X-ray fluorescence analysis to quality control the portable X-ray fluorescence data. Gold data were obtained by 50-g fire assay and bulk leach extractable gold analyses.

The abundances of ilmenite, garnet, and zircon were derived from linear regression models trained on mineral abundances measured by scanning electron microscopy-based automated mineralogy, and geochemical data from portable X-ray fluorescence analysis. In addition to determining the abundances of the heavy minerals, an assessment of impurities and other deleterious compositional qualities of these products was made using scanning electron microscopy data.

Nine geological domains were interpreted from the downhole lithological data from the 2022 drilling. Estimation domains were created using geology, Au grades, and heavy mineral abundance. The fire-assay-Au data were used to determine the mineralised Au domain. All samples from this domain were subsequently analysed by bulk leach extractable gold, on which the Au mineral resource estimate is based. The Au and heavy minerals were estimated using ordinary kriging.

The Competent Person has classified a Measured Mineral Resource of 3.15 Mt at 7.69% ilmenite, 11.49% garnet and 0.14% zircon, and an Indicated Mineral Resource of 2.5 Mt at 7.50% ilmenite, 9.70% garnet and 0.14% zircon, reported at a cut-off abundance of 1% ilmenite and within a particle size range 45 µm to 2 mm (Table 1). The specified heavy mineral products are a 45-µm to 2-mm magnetic concentrate rich in ilmenite and garnet, and a non-magnetic concentrate rich in zircon. The product specifications and marketability are considered acceptable by the Competent Person.

The Competent Person has classified an Inferred Mineral Resource for Au of 3 Mt at 400 mg/t for 3.6 koz of Au. No cut-off was applied in the classification of the Au Mineral Resource, as Au represents a by-product of the extraction and processing of the heavy minerals.

Table 1: Coates South Block Heavy Mineral Resource

| Classification | Mass (kt) | Ilmenite (%) | Garnet (%) | Zircon (%) | VHM (%) | Ilmenite (kt) | Garnet (kt) | Zircon (kt) |
|---|---|---|---|---|---|---|---|---|
| **Measured** | 3,150 | 7.69 | 11.49 | 0.14 | 19.32 | 240 | 360 | 4 |
| **Indicated** | 2,500 | 7.50 | 9.70 | 0.14 | 17.30 | 190 | 245 | 4 |
| **Total** | 5,650 | 7.60 | 10.70 | 0.14 | 18.40 | 430 | 610 | 8 |

Notes:

1. The Mineral Resource is classified in accordance with the JORC Code (2012).
2. The Mineral Resource is reported at a 1% ilmenite abundance cut-off.
3. Zircon is the tonnes of zircon within particle size range 45 µm to 2 mm.
4. Garnet is the tonnes of garnet within particle size range 45 µm to 2 mm.
5. Ilmenite is the tonnes of ilmenite within particle size range 45 µm to 2 mm.
6. VHM % is the abundance of ilmenite, garnet and zircon within a particle size range 45 µm to 2 mm.
7. The effective date of the MRE is 10 February 2023.
8. The Mineral Resources are contained within the proposed mining disturbance area.
9. Estimates are rounded to reflect the level of confidence at the time of reporting.

The linear regression model approach has produced a robust quantification of both valuable heavy mineral abundances and heavy mineral (from sink-float) data at the Barrytown Project. There is a robust relationship between the calculated mineralogy abundance data and automated mineralogy data with the sink-float data. This suggests that TiGa can reduce the quantity of sink-float analyses in future studies on the Barrytown Project.

## Contents

## List of Tables

rsc MINING & MINERAL EXPLORATION

## List of Figures

# 1 Introduction & Terms of Reference

## 1.1 Scope

TiGa Minerals and Metals Limited (TiGa) commissioned RSC to prepare an independent mineral resource estimate (MRE) for the Coates South Block within its Barrytown heavy mineral sands project, West Coast, New Zealand. The work reported here, carried out by a Competent Person, and classified and reported in accordance with the JORC Code (2012), will serve to support feasibility work and ore reserve estimation for the Coates South Block.

Any future public prospectus, presentations, website postings, or public announcements issued by TiGa that refer to the resource estimation specified in this report (Report) will be required to be reported in accordance with the JORC Code (2012) and will need to contain specific information on:

- geology and geological interpretation;
- sampling and subsampling techniques;
- estimation methodology;
- cut-off grades;
- criteria used for classification; and
- mining and metallurgical methods and parameters.

This information may be extracted from this Report to support such public reports or announcements. In addition, these public reports must contain a 'Table 1', the information for which can be extracted from this Report. RSC notes that specific written consent for the final version of the public report is required from the Competent Person before it is made public by TiGa.

## 1.2 Qualifications & Experience

### 1.2.1 Competent Person

The work completed by RSC and the subject of this Report was supervised by Rene Sterk. René is a Fellow and a Chartered Professional with the Australasian Institute of Mining and Metallurgy (AusIMM), and a Registered Professional Geologist with the AIG. He is a full-time employee and principal geologist of RSC. René holds an MSc in structural geology and tectonics from the Vrije Universiteit Amsterdam (2002), and is the managing director of RSC. He specialises in resource estimation, grade control, reconciliation, QA/QC and successful sampling and has a strong skill set in exploration management for gold and base metals. René is recognised under the JORC Code as a Competent Person for gold (alluvial, shear-zone and porphyry), base metals, seabed mineralisation, and industrial minerals (ilmenite sand, garnet sand, diatomite). René is the principal author of many Canadian NI 43-101 and JORC resource and exploration studies and has assisted clients with exploration programmes for these and other projects. He has practised continuously as a mining geologist, exploration geologist, manager and consultant for mining and exploration firms in a range of commodities since 2003.

### 1.2.2 Technical Team

The work presented in this Report was supervised by the Competent Person, and completed by the following people:

**Sean Aldrich** is RSC's General Manager of Exploration and has more than 20 years of mining and exploration experience in New Zealand, Papua New Guinea, the Middle East, Central Asia, and Africa. Sean is a Competent Person for the interpretation of exploration results of heavy mineral sand deposits. He has been involved with the evaluation, resource estimation and mining studies of both onshore and offshore heavy mineral sand deposits in New Zealand, Guinea and Greenland. Since 2012, he has held the position of Principal Geologist with RSC, where he has been involved with numerous heavy mineral sand deposits technical reviews and resource estimations in the Pacific and New Zealand. Mr Aldrich's wider experience covers project generation, resource definition and underground and open pit mine geology. Mr Aldrich has undertaken the site visit, which is discussed in section 7.2.

**Mark Roux** is a Principal Resource Consultant with RSC. He is a member of the AusIMM and holds BSc (Hons) in geology from the University of Pretoria and a Post Graduate Certificate in Geostatistics from Edith Cowan University. He has extensive experience across a range of commodities, including gold, base metals, diamonds, and manganese, and a range of linear and non-linear estimation techniques.

**Jenny Love** is a Senior Exploration Geologist with RSC and holds a BSc (Hons) in Geology from the University of Birmingham in the UK. She has over fifteen years of experience in gold and metals exploration, and mineral project assessment, including roles as exploration geologist, project manager, and consultant across both the private and public sectors. Jenny's experience also spans the public sector following a period developing and managing innovation projects for national geoscience data management, whilst working alongside tenement regulation and natural resources policy within New Zealand Petroleum and Minerals.

**Michael Gazley** is RSC's General Manager Geoscience and Principal Geochemist. He was previously a Senior Research Scientist at CSIRO Mineral Resources, based in Perth, Western Australia, for almost five years. Before joining CSIRO, Michael spent over five years working for Barrick Australia Pacific Ltd as an underground geologist based at Plutonic Gold Mine; additionally, he completed his PhD on that deposit. During his time at Plutonic, he worked across multiple Barrick sites developing pXRF best practice and utilising pXRF to gain geological insights into mineral deposits. Michael is an expert in pXRF data collection and interpretation and has written a best-practice paper on the subject. Michael is an expert in collecting, integrating, and interpreting diverse chemical and mineralogical datasets using multivariate techniques in exploration and mining settings. He has worked globally on many different mineral system types, including orogenic Au, epithermal Au, placer Au, shear-hosted Cu, IOCG, Cu-Au porphyry, Pb-Zn-Ag deposits, Li and REE pegmatites, and heavy mineral sands. Michael is also actively involved in using and developing cutting-edge data handling and machine learning techniques to maximise value from geochemical, mineralogical, and remote sensing datasets.

**Gavin Chapman** holds a BSc degree from the University of New England and a Graduate Certificate in Geostatistics from Edith Cowan University. While completing his degree, Gavin held the responsibilities of Business Development Manager and Operations/Project Manager for a fast-growing mining support company in Australia. Gavin has regulatory experience in State and Federal Governments in both Australia and New Zealand, having worked at the Geological Survey of New

South Wales before taking on a role as Data Geologist with New Zealand Petroleum and Minerals where he developed a strong background in data management principles, QA/QC, and tenement management. Prior to joining RSC, he worked for New Zealand's largest gold producer where he had a number of roles, including Underground Geologist, Mine Geologist and Project Resource Geologist. Gavin carries out resource estimation projects, covering a range of mineralisation styles including VMS Cu-Au, Sedimentary-hosted U and polymetallic nodules.

**Olivier Bertoli** has specialist training in Applied Mathematics and Geostatistics from the Paris School of Mines, complemented by 27 years of experience as a practice-leading Geostatistician. Olivier worked for five years as Technical Director of the QG Group (co-founder), five years as Technical Director of Tenzing Pty Ltd (co-founder) and for seven years with geostatistical software specialists Geovariances (including four as its CEO).

As a consultant, Olivier completed many consulting jobs for major mining companies in diverse locations and geological settings. Olivier has extensive experience in advanced geostatistical modelling: 2D methods, recoverable resource estimation (LMUC, MIK), conditional simulations and multivariate modelling. He has delivered numerous in-house and public training courses on these topics and specialises in staff mentoring on relevant applications of geostatistical techniques to mineral resource estimation. Olivier has experience with a wide range of commodities which includes precious and base metals (including nickel laterite), mineral sands, diamonds, iron ore and coal deposits.

**Lauren Tooley** is a Consultant Exploration Geologist with RSC based in Dunedin, New Zealand. She holds a Bachelor of Science (Hons) degree from the University of Otago and has worked on technical studies across numerous commodities including gold, copper, uranium, lithium, heavy mineral sands and rare earth elements. Lauren has experience in geological modelling, mineral resource estimation, code-compliant reporting, and QA/QC reviews. She has worked on resource estimates of orogenic gold, VMS and structurally-controlled copper and heavy mineral sand deposits.

**Kat Lilly** holds a PhD in Earth Science from the Australian National University and has expertise in electron microprobe analysis, scanning electron microscopy and electron backscatter diffraction. Her 10 years of experience in electron beam analytical techniques include developing new protocols for scanning electron microscope (SEM) analysis of difficult and unusual samples and have resulted in multiple publications on ore geology and mineralogy applications as well as on SEM methodology. She retrained in Computer Science in 2017–2019 and has expertise in machine learning and statistical techniques and their application to geological problems. Kat has been at the forefront of developing RSC's bespoke algorithms for validation and interpretation of geochemical data as well as building and validating workflows to derive mineralogy from geochemistry in a variety of mineral systems. She has published more than 18 peer-reviewed journal articles in diverse fields within geology and computer science including economic geology, SEM methodology, and data compression algorithms.

**Marcel Mizera** is a structural geologist with a broad knowledge on mineralisation associated with fault, vein and shear zone systems. He has worked, mapped, and published research articles on seismic active and inactive fault zones all around the world including Switzerland, Greece, Papua New Guinea, and New Zealand. During a postdoctoral research fellow employment in the Netherlands, Marcel was part of the NWO-funded research programme DeepNL where he studied shallow crustal faulting processes (<5–10 km depth) in clay- and carbonate-bearing fault zones. Prior to that, he finished

his PhD on a Marsden-funded project studying the youngest and probably best-preserved active low-angle normal fault on Earth - the Mai'iu fault in SE Papua New Guinea. His research made him an expert in using different textural and geochemical techniques to acquire and interpret diverse mineralogical datasets.

**Annette Pocock** is a geologist with over 16 years' mineral industry experience. She holds a BSc (Geology) and a BCA (Economics) from Victoria University of Wellington, and an MSc in Ore Deposit Geology from the University of Western Australia. Annette worked as an underground mine geologist for seven years for both Barrick and Goldfields in Western Australia. Then Annette spent seven years at New Zealand Petroleum & Minerals, part of the Ministry of Business, Innovation and Employment where her roles covered the Minerals Permitting Team, the Minerals Strategy Team, and the Resource Markets Policy Team. More recently, since joining RSC, Annette has been working in a range of exploration, permit management and resource estimation projects.

## 1.3 Independence Declaration

The relationship of RSC with TiGa is based on a purely professional association. This Report was prepared in return for fees based on agreed commercial rates, and the payment of these fees is in no way contingent on the results of this Report.

## 1.4 Sources of Information

The information in this Report is based on data supplied by TiGa and collected by, or collected under the supervision of, RSC. Information supplied by TiGa includes the project LiDAR DTM and a database of historical exploration. Information from the 2022 drilling programme was collected and managed by RSC and has been validated and verified by RSC.

While RSC has made every effort to verify the data provided by TiGa and used in this Report, information from third-party sources was used on the assumption that the contents were reliable and accurate.

The information relating to economic extraction, mining parameters, costs, and metallurgical processing has been provided to RSC by TiGa and its consultants involved in the Feasibility Study for Barrytown Project at Coates South. Palaris is the consulting group that has provided information relating to mine engineering and pit design, and IHC Robbins has provided information relating to metallurgical processing. Where relevant to the estimation and classification of the mineral resource, the overall Competent Person, Mr Sterk, accepts responsibility for the accuracy and precision of the third-party information.

## 1.5 Site Visit

RSC personnel, under the overall supervision of Mr Sterk, planned and managed field exploration activities at Barrytown from March 2022 to August 2022. Senior RSC geologists supervised the field activities and conducted field and laboratory visits to oversee sampling activities.

Mr Aldrich completed a site visit during the drilling programme, whereby both the drilling and sampling procedures on-site at the Coates South Block and the sample preparation procedures at the New Zealand Institute of Metals and Minerals Research (NZIMMR, Dunollie, Greymouth) facility were observed. Mr Aldrich checked whether all processes conformed to

standard operating procedures (SOPs) and checked core trays and chip trays against the database and logging sheets. Overall, Mr Aldrich and Mr Sterk confirm that the work underpinning the resource estimate at the Barrytown Project is of a good standard, and the sample and data quality are appropriate with respect to the data quality objectives. The results of the site visit are discussed in section 7.5.1 and throughout section 7.2.

## 1.6 Disclaimer

The opinions, statements and facts contained herein are effective as of 10 February 2023, unless stated otherwise in the Report.

Given the nature of the mining industry, conditions can significantly change over relatively short periods of time. Consequently, actual results and performances may be more, or less favourable, in the future and their disclosure represents no legal opinion of the authors.

For disclosure of information relating to socio-political, environmental, and other related issues, the authors have relied on information provided to RSC.

Results of evaluation and any opinions or conclusions made by RSC are not dependent upon prior agreements or undisclosed understandings concerning future business dealings with TiGa.

The authors of this Report are not qualified to provide extensive comment on legal issues associated with Barrytown Project described in this Report. Similarly, the authors are not qualified to provide extensive comment on risks of any nature (operational, sovereign, terrorist or otherwise) associated with the Barrytown Project.

This document contains certain statements that involve several risks and uncertainties. There can be no assurance that such statements will prove to be accurate; actual results and future events could differ materially from those anticipated in such statements.

The information, conclusions, opinions, and estimates contained herein are based on:

- information available to RSC at the time of preparation of this Report;
- assumptions, conditions, and qualifications set out in this Report; and
- data, reports, and other information supplied by TiGa and other third-party sources.

The opinions, conclusions and recommendations presented in this Report are conditional upon the accuracy and completeness of the existing information.

No warranty or guarantee, be it express or implied, is made by RSC with respect to the completeness or accuracy of the legal, mining, metallurgical, processing, geological, geotechnical and environmental aspects of this document. RSC does not undertake or accept any responsibility or liability in any way whatsoever to any person or entity in respect of these parts of this Report, or any errors in or omissions from it, whether arising from negligence or any other basis in law whatsoever.

The statements and opinions expressed in this document are given in good faith, and in the belief that such statements and opinions are not false and misleading at the date of this Report. RSC reserves the right, but will not be obligated, to revise this Report and conclusions, if additional information becomes known to RSC, after the date of this Report.

RSC assumes no responsibility for the actions of the company or others with respect to the distribution of this Report.

# 2 Project General Summary

## 2.1 Project Description & Location

The Barrytown Project is a coastal heavy mineral sands project located ~30 km north of Greymouth, West Coast Region, New Zealand (Figure 1). The project is located on the Barrytown Flats, a flat-lying to gently undulating coastal plain that extends over ~17 km from north to south and ~2 km from east to west. The southern end of the flats is defined by the headland Seventeen Mile Bluff, and the northern end by Razorback Point. The project area is flanked to the east by the Paparoa Ranges, and to the west by the Tasman Sea. The Coates South Block is located north of Canoe Creek, in the centre of the Barrytown Flats. The site is adjacent to the Canoe Creek Conservation Area, which is managed by the Department of Conservation.

Gold (Au) has been prospected for and mined from the Barrytown area since the late 1860s. The first gold rush occurred in the Canoe Creek area. In addition to Au, the Barrytown deposit contains ilmenite, garnet, and zircon (e.g. Wells and Haverkamp, 2020). The deposit also contains small amounts of monazite, xenotime, scheelite, cassiterite, and rutile.

## 2.2 Tenure & Ownership

New Zealand Petroleum & Minerals (NZP&M) issues permits to prospect, explore, and mine Crown-owned minerals in New Zealand. All Au, silver (Ag), uranium (U) and petroleum are statute minerals that occur naturally in New Zealand are owned by the Crown. Ownership of other minerals (e.g. ilmenite, garnet, and zircon) depends on the legislation in place at the time the land was alienated from the Crown. Exploration and mining permits are only granted over minerals that are identified as Crown-owned.

The Barrytown Project consists of one active mineral permit granted by NZP&M and two permit applications that are currently under evaluation (Table 2, Figure 1). The Coates South Block MRE presented in this Report is fully contained within the active permit: mining permit (MP) 60785.

Prior to the granting of mining permit (MP) 60785, TiGa held the Barrytown Project under exploration permit (EP) 51803, which was originally granted to Alloy Resources Ltd in November 2009. TiGa, known as Barrytown JV Limited at the time, entered the project in 2015 through an incorporated joint venture (JV). An appraisal extension was granted in October 2015 to extend the permit expiry date to November 2018. In 2017, TiGa acquired 100% of EP 51803. An extension was granted to extend the expiry of the EP a further four years to November 2022. In March 2021, TiGa applied for MP 60785 over the portion of EP 51803 north of Canoe Creek resulting in the granting of the current mining permit (MP) 60785 on 22 July 2022.

On 27 June 2022, TiGa applied for a 245-ha EP in the southeast of the Barrytown Flats (Table 2, Figure 1). On 21 November 2022, TiGa applied to extend the land within MP 60785 by 449 ha, covering the southern half of EP 51803 (Table 2, Figure 1). The exploration permit EP 51803 expired on 25 November 2022.

Non-statute minerals within MP 60785 are primarily owned by the Crown, except for several road parcels and one private land parcel in the southwest of the Coates South Block, where non-statute minerals of interest (ilmenite, garnet, zircon) are privately owned (Figure 2).

Table 2: Permit details for the Barrytown Project.

| Permit | Ownership | Status | Registered Holder | Date Granted | Expiry Date | Tier | Area (ha) |
|---|---|---|---|---|---|---|---|
| **MP 60785** | 100% | Active | TiGa Minerals and Metals Limited | 21 July 2022 | 20 July 2042 | 1 | 800 |
| **MP 60785.03 Extension of Land** | 100% | Application (Under Evaluation) | TiGa Minerals and Metals Limited | - | - | 1 | 449 |
| **EPA 60917.01** | 100% | Application (Under Evaluation) | TiGa Minerals and Metals Limited | - | - | 2 | 245 |

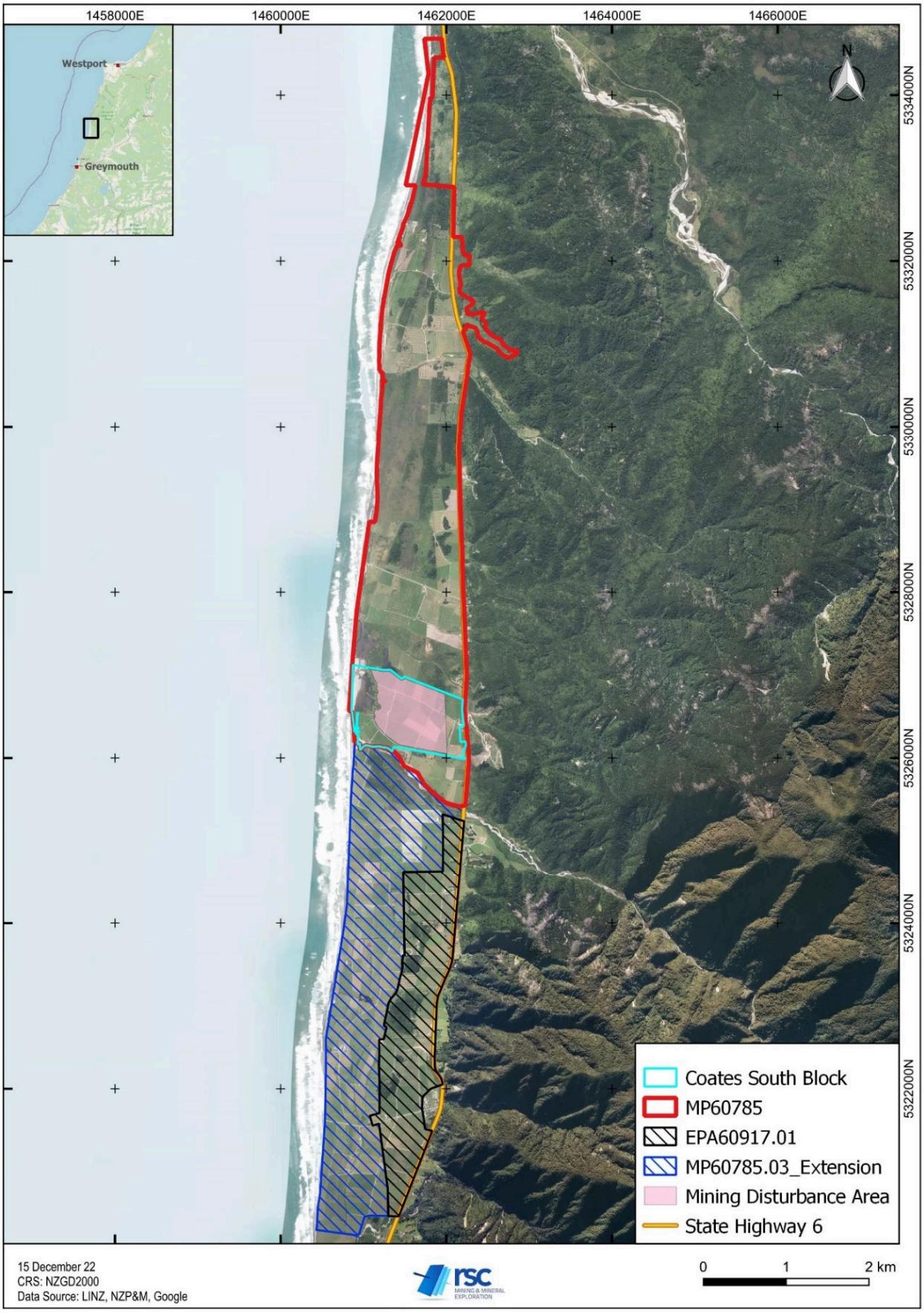


Figure 1: Map of permitted areas, Coates South property and area of study (Mining Disturbance Area).

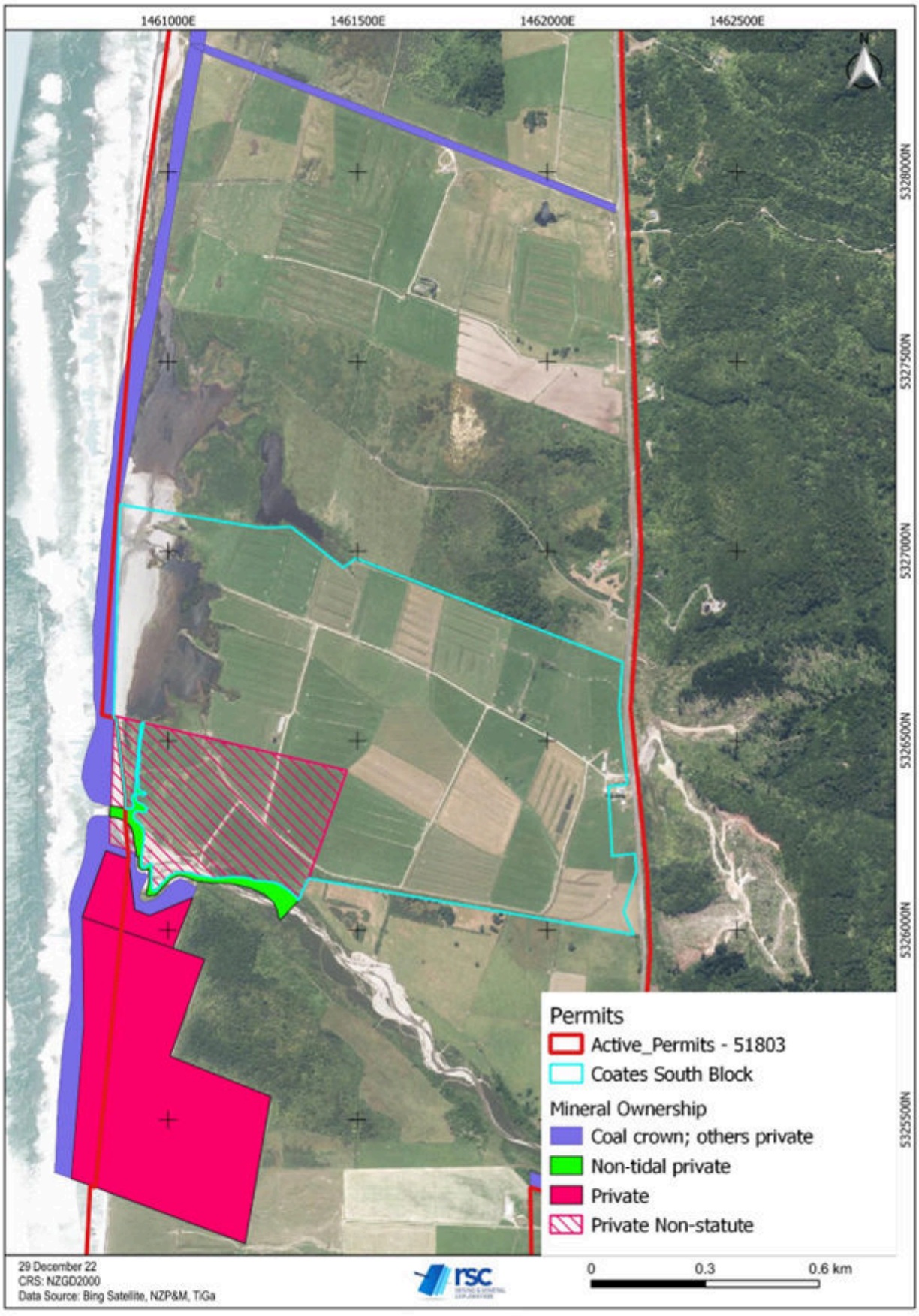


Figure 2: Non-statute mineral ownership at Coates South Block.

## 2.3 Royalties

TiGa is liable to pay royalties to the New Zealand government for Crown-owned minerals mined from its permits. For all minerals other than garnet mined from MP 60785, the royalty will be calculated in accordance with the Minerals Programme for Minerals (Excluding Petroleum) 2008. For garnet mined from MP 60785, the royalty will be calculated in accordance with the Minerals Programme for Minerals (Excluding Petroleum) 2013. The point of valuation for Au mined from MP 60785 will be at the point of sale, with the value set by the London Bullion Market Association price for Au at the time of sale. The point of valuation for heavy mineral concentrate produced from MP 60785 is the location where the product exits the permit boundary. If TiGa establishes a processing plant within MP 60785 in future, in order to process and refine the concentrate into additional product streams, the point of valuation will be the boundary of the processing plant.

Table 3: Royalty details for MP 60785.

| Mineral | Royalty Regime | Royalty Rate |
|---|---|---|
| **Gold<br>Ilmenite<br>Zircon** | Minerals Programme for Minerals (Excluding Petroleum) 2008 | 1% of annual net sales revenues (from minerals other than garnet) if net sales revenues are NZD 1.5 million or less; or<br>2% of annual net sales revenues (from minerals other than garnet) for net sales revenues that exceed NZD 1.5 million. |
| **Garnet** | Minerals Programme for Minerals (Excluding Petroleum) 2013 | 2% of the net sales revenue of the garnet obtained under the permit; and<br>10% of any accounting profits, or provisional accounting profits, as the case may be, obtained under the permit. |

## 2.4 Environmental Liabilities & Permits

Key environmental legislation concerning mining activities includes the Resource Management Act (1991) and the Wildlife Act (1953). Under the Resource Management Act, local authorities manage the environmental consenting process. Resource and land use consent must be obtained before commencing most exploration and mining activities. Other legislation regulating industrial activities, environmental effects, and the health and safety of the workplace also apply to mining activities, such as the Health and Safety at Work Act (2015) and the Heritage New Zealand Pouhere Taonga Act (2014).

The Resource Management Act (1991) (RMA) also provides for recognition of the Treaty of Waitangi and kaitiakitanga. Section 7 of the RMA requires all individuals involved with managing the use, development, and protection of natural and physical resources to have particular regard to kaitiakitanga (the process and practices of protecting and looking after the environment).

The RMA classifies activities into six primary categories: permitted, controlled, restricted discretionary, discretionary, non-complying, and prohibited. These different categories determine whether resource consent is required before carrying out an activity, and what will be considered when resource consent application is assessed. National Environmental Standards and Regional and District Plans regulate which category an activity falls in, and therefore whether resource consent is required.

The New Zealand government is currently developing a national policy statement for indigenous biodiversity, which is anticipated for gazettal in early 2023. This policy will require local governments to map significant natural areas (SNAs).

SNAs are sensitive environments that may include special landscapes with remnant native bush or native forests, wetlands, coastal vegetation, lakes and rivers or geothermal vegetation that have high ecological value due to their native plants and habitats, many of which are endangered.

North of the Coates South Block is a parcel of privately owned land that has been identified by the Grey District Council as a potential SNA (PUN-W034), which extends to the 'Canoe Creek Lagoon' which lies within the Coates South Block. The wetland area, the Canoe Creek riparian strip, and the coastline are the notable features of the site. TiGa has no intention to mine these areas, and these are therefore excluded from the mining disturbance area. Wetland vegetation is likely to be planted as a buffer for the Canoe Creek lagoon and will be specified in TiGa's consent applications. Figure 3 indicates the location of these areas with respect to the planned mining disturbance area at the Coates South Block.

TiGa must obtain resource and land-use consents from the West Coast Regional and Grey District Councils before commencing mining activities. RSC understands that TiGa is in the process of preparing updated consent applications and anticipates lodging them in 2023.

rsc
MINING & MINERAL
EXPLORATION

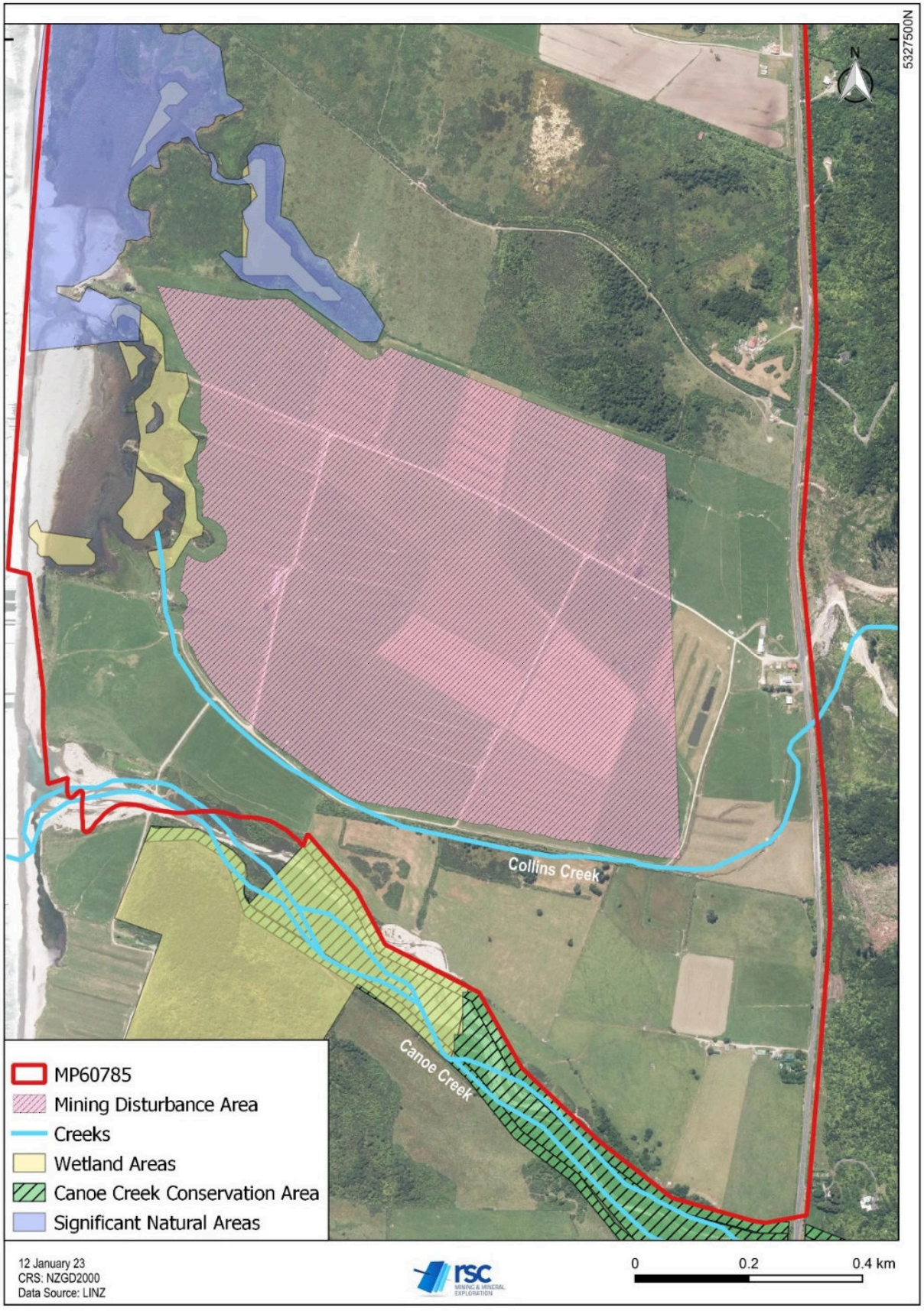


Figure 3: Coates South Block and areas of environmental sensitivity in the nearby region.

## 2.5 Access

The Project is located adjacent to State Highway 6 running north–south along the West Coast of the South Island (Figure 1). State Highway 6 is the sealed national route that provides access to the Westland region and forms the road link between Barrytown and Greymouth to the south, and Westport to the north. The Coates South Block is adjacent to State Highway 6, and local farm tracks currently provide access within the property. A direct, separate entry to the property from State Highway 6 is planned for when the project progresses to mining.

Mineral permits granted by NZP&M do not give the permit holder automatic rights of land access to the permit area. Access arrangements are required for all onshore activities other than minimum impact activities. For exploration and mining activities, the permit holder is typically required to negotiate an access arrangement with each landowner and occupier.

The Coates South Block is held under Nikau Deer Farm Limited, owned by George Coates. There is an access arrangement in place between TiGa and George Coates for the exploration and mining of the Coates South Block.

## 2.6 Climate

The climate at Barrytown Flats consists of moist cool temperatures with cloudy and windy conditions, and frequent rain showers near the coast. The climate is classified as Cfb in the Köppen climate classification (http://koeppen-geiger.vu-wien.ac.at/present.htm); a temperate oceanic climate with mild temperatures and significant rainfall. Barrytown Flats differs from much of the West Coast in that it has very few frost days. Greymouth, the closest large town, has an annual rainfall of 3,640 mm and an average temperature of 10.8°C. February is the warmest month with an average temperature of 15.3°C. The coldest month is July with an average temperature of 6.3°C. Precipitation varies by 105 mm between the driest month (February, 166 mm) and the wettest month (October, 271 mm) (Table 4).

Table 4: Greymouth monthly climate. Source: https://en.climate-data.org/oceania/new-zealand/west-coast/greymouth-19392/.

| | Jan | Feb | Mar | Ap | May | Jun | Jul | Aug | Sep | Oct | Nov | Dec |
|---|---|---|---|---|---|---|---|---|---|---|---|---|
| **Avg. Temp. (°C)** | 15.1 | 15.3 | 14 | 11.7 | 9.5 | 7.2 | 6.3 | 7.2 | 8.7 | 10 | 11.6 | 13.7 |
| **Min. Temp. (°C)** | 12.2 | 12.3 | 11.2 | 9 | 7.1 | 4.8 | 3.6 | 4.4 | 5.7 | 7.1 | 8.7 | 10.8 |
| **Max. Temp. (°C)** | 18.4 | 18.6 | 17.3 | 14.8 | 12.4 | 10.2 | 9.6 | 10.6 | 12 | 13.3 | 14.9 | 17 |
| **Precipitation (mm)** | 241 | 166 | 183 | 204 | 221 | 219 | 190 | 209 | 236 | 271 | 234 | 266 |

## 2.7 Physiography

The Project comprises the Barrytown Flats, a lowland strip within a coastal embayment. Most of the Project lies below 20 m above sea level and is backed to the east by steep slopes along an old sea cliff. The area is drained by creeks, from the Paparoa Ranges in the east, flowing west to the Tasman Sea. The Project contains several brackish, swampy areas.

The Coates South Block comprises farmland with undulating/hummocky ground caused by man-made humping and hollowing for drainage purposes. The Coates South Block is bounded to the south by Canoe Creek. The block covers a small portion of Canoe Creek and its sandy banks near the coast. As noted in section 2.4, the western extent of the block

contains the Canoe Creek Lagoon, a wetland area. Collins Creek runs along the southern edge of the Coates South property and flows into the Canoe Creek Lagoon; it is the major waterbody within the Coates South Block. Collins Creek and the wetland lagoons have been significantly modified by previous farming and mining activities. The lagoons are remnants of historically dredged areas, and the creek has been modified by farming and development for drainage purposes. Tributaries to Collins Creek are present throughout the area and are the subject of current hydrological studies on the Coates South Block.

## 2.8 Vegetation

The Coates South Block has been denuded of vegetation for pastoral farming except at the coastal interface and along Canoe Creek. The Canoe Creek Lagoon (wetland) near the coastal interface hosts wetland vegetation. There is also riparian strip planting along Canoe Creek. Very little vegetation is contained within the mining disturbance area other than pasture or occasional trees at pasture boundaries.

## 2.9 Local Resources & Infrastructure

The Barrytown Project is typically well connected by state highways and public roads to nearby towns. The settlement of Barrytown has minimal infrastructure and facilities. Greymouth is the nearest large town with a port and hospital. The nearest domestic airport is in Hokitika with flights to and from Christchurch. Christchurch airport is the closest international airport. Mobile phone coverage at the Barrytown Project area is good.

The port of Westport, to the north, can be accessed by travelling along State Highway 6 (55 km) and then along State Highway 67 (6 km). Greymouth can be reached by travelling south along State Highway 6 which crosses the rolling topography of the Barrytown Flats before skirting steep bluffs in the narrow coastal region. The road then passes through Rapahoe and Runanga, before crossing the Grey River and entering Greymouth. The ports of Greymouth (30 km to the south) and Westport (60 km to the north) are potential export routes; however, several limitations have been recognised including water depth, cargo handling, and ship capacity at both ports.

# 3 History & Previous Work

## 3.1 Tenure & Operating History

Gold (Au) has been prospected and mined from the Barrytown area since the late 1860s. The earliest mining records date from 1867 when the first gold rush occurred in the Canoe Creek area. Historical prospecting in the 1870s involved bucket line dredging and small sluice operations that worked the terraces along the Barrytown Flats for Au. Gold dredging operations were active in the southern half of the Barrytown Flats during the 1930s and 1940s. Processing efficiencies were purported to be low (50% recovery), with Au loss attributed to high slimes (Maynard and Jones, 2014). McOnie & Bull (2007) reported that historical Au mining had produced more than 62,000 oz of Au from sands at grades of 120–270 mg/m$^3$, despite poor gravity recoveries.

Records indicate that targeted exploration, including drilling, commenced in the 1930s as dredging in the area began to decline. Exploration in the 1930s and 1940s was conducted by NZ Gold Options (1931–1932), NZ Prospecting and Mining Ltd (1935–1937), Whites Electric Dredging Company (1936–1941), and Barrytown Dredging Company Ltd (1937–1945) targeting Au mineralisation.

Investigation of ilmenite potential became the main objective of most proposals over the Barrytown Project area from the 1960s onwards, including efforts by Carpentaria Exploration Company, Mineral Resources (NZ) Ltd, Amax Exploration NZ Ltd, Fletcher Challenge, and North Broken Hill Peko Limited (later known as Westland Ilmenite Ltd), Table 5. Poor market conditions in the mid-1970s put the project on hold until increased Au prices in 1979 renewed interest in the area.

Westland Titanium was established in 2013 as a wholly owned subsidiary of Pacific Mineral Resources Ltd (PMRL) following the completion of farm-in agreement put in place with Alloy Resources in July 2012. A formal joint venture was established with Alloy Resources in 2013. Subsequent work was carried out under Westland Titanium. Barrytown Joint Ventures Ltd (later TiGa) acquired full transfer of the permit in 2018 following a six-year history of assisting Alloy Resources with exploration under a work agreement.

Several phases of exploration drilling have been completed on the Barrytown Flats since the 1930s. Details of the historical drilling campaigns and an overview of the historical drillhole locations are provided Table 5 and Figure 4, respectively.

Table 5: Summary of historical drilling at the Barrytown Project.

| Company | Period | Mineral | Drillholes | Drill Type | Bulk Test Pits |
|---|---|---|---|---|---|
| **NZ Gold Options Ltd** | 1931–1934 | Au | 40 | Keystone sledge 152 mm | |
| **NZ Prospecting & Mining Ltd** | 1935–1937 | Au | 570 | Keystone 127 mm | |
| **Whites Electric Dredging Company** | 1936–1941 | Au | 11 | Handset (Banka) 89 mm | 12 shafts |
| **Barrytown Dredging Company Ltd** | 1937–1945 | Au | 229 | Keystone 152 mm | |
| **Carpentaria Exploration Company** | 1966–1976 | Au & ilmenite | 531 | 100 mm & 150 mm churn | |
| **Mineral Resources (NZ) Ltd and Amax Exploration NZ Ltd** | 1980–1984 | Au & ilmenite | Nil | Nil | Nil |
| **Fletcher Challenge** | 1984–1988 | Au & ilmenite | 136 | 150 mm churn, & 50 mm hand auger | |
| **Westland Ilmenite Ltd** | 1989–2000 | Ilmenite | 95 & 620 | Hand auger & aircore | 26 |
| **Rio Tinto Ltd** | 2000–2005 | Ilmenite | Nil | Nil | Nil |
| **NZ Gold Ltd** | 2005–2009 | Au & ilmenite | 19 | Auger (not assayed) | Nil |
| **Alloy Resources** | 2009–2014 | Au & Ilmenite | 105 | Aircore & auger | Nil |
| **Westland Titanium/Alloy Resources** | 2015–2016 | Au & Ilmenite | 120 | Aircore | 5 |

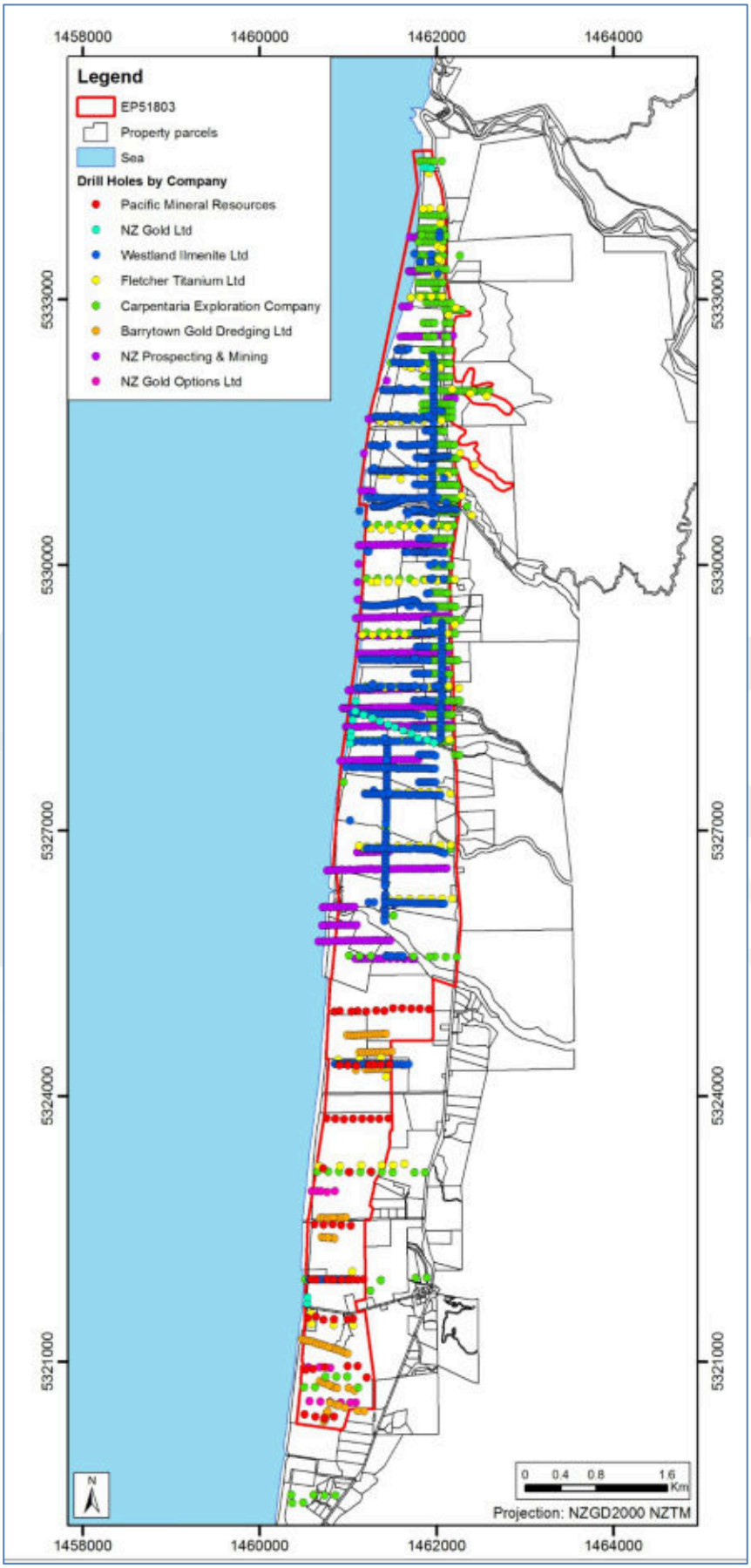


Figure 4: Distribution of historical drilling across Barrytown Flats.

Summary details of the historical drilling work outlined in Table 5 are provided in section 3.2. Since the focus of this Report is to provide supporting information for a mineral resource estimate for the Coates South Block, historical drilling completed across the Coates South Block is of particular importance. Table 6 summarises details of the historical drilling around the mining disturbance area on Coates South Block, and the data which were used to inform this MRE. Figure 5 summarises the details and extent of the historical drilling around Coates South Block, and indicates which data were used to support the MRE presented in this Report.

Table 6: Summary of historical drilling within the Coates South Block.

| Company | Date Drilled | Type | Target | # of Holes (Total m Drilled) | Holes used in this MRE | Hole IDs | NZP&M Report Reference |
|---|---|---|---|---|---|---|---|
| **Westland Ilmenite Ltd** | 1990 | RC | Ilmenite | 78 holes (712 m) | 61 holes (544 m) | NVI4100–6200 N4035–4061 NVQ3300–6200 | MR3023 |
| **Fletcher Titanium** | 1985–1986 | Churn | Ilmenite | 15 holes (129 m) | 10 holes (87 m) | BPR25, 30–36, 67–71 | MR4287, MR1424 |
| **Carpentaria Exploration Company** | 1966–1973 | Churn | Ilmenite | 11 holes (112 m) | 9 holes (88 m) | VQ3600, 4000, 4400, 4800 | MR1326 |
| **NZ Prospecting & Mining** | 1936–1937 | KSS | Gold | 67 holes (572 m) | 42 holes (384 m) | PMQ 8–17 | - |

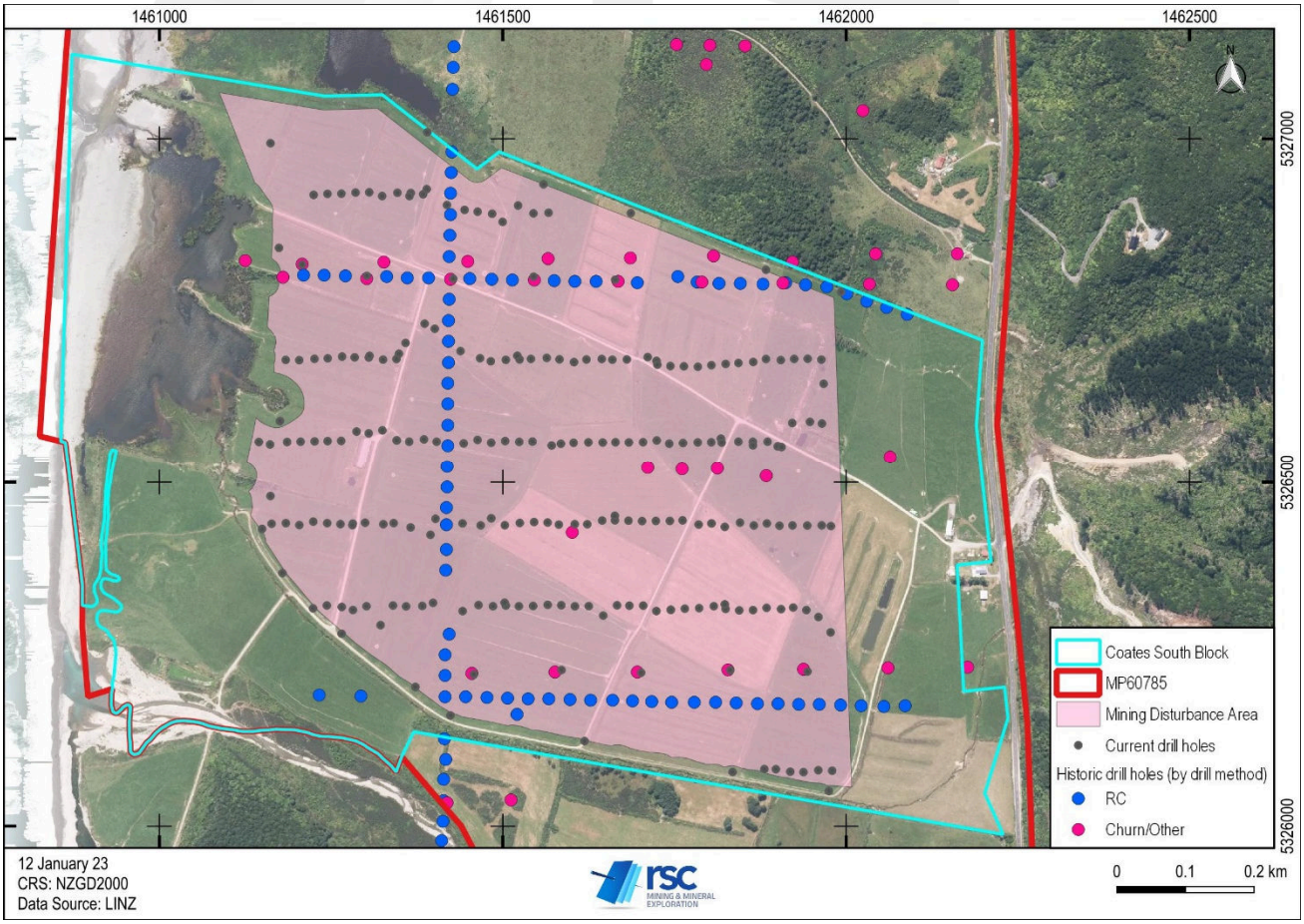


Figure 5: Distribution of historical holes and 2022 drilling at the Coates South Block.

## 3.2 Exploration History

### 3.2.1 NZ Prospecting & Mining Ltd

Drilling on the Coates South Block was first undertaken from 1936–1937 by NZ Prospecting and Mining Ltd. NZ Prospecting & Mining Ltd established systematically spaced (200-m spacing) east–west orientated drill lines that were concentrated in the north of the Barrytown Flats. This included one east-west line within the Coates South Block. Holes were drilled at 20-m centres and samples were assayed for Au. There is limited information available regarding this work, and the analytical data were not used in the MRE reported here. Geological logs from this drilling were used by RSC to guide modelling and domaining only. This is discussed further in sections 7.4.4.10 and 8.1.2.

### 3.2.2 Carpentaria Exploration Company

Several wide-spaced churn holes were drilled across the Coates South Block as part of an exploration campaign over the wider Barrytown Flats by Carpentaria Exploration Company from 1966–1973. Smaller (100-mm diameter) drilling was used in the less accessible parts of the deposit, while heavier 150-mm diameter drilling was used in areas of thick gravel overburden and old mine tailings leftover from historical Au dredging. Holes were drilled up to 20-m deep and samples were analysed for ilmenite and magnetite.

Carpentaria's ilmenite testing was initially by sink float separation, electrostatic and magnetic separation, followed by grain count (Best, 1972). Ilmenite-bearing conductors were separated from the magnetite-bearing conductors using electrostatic separation and a hand magnet. The ilmenite-bearing conductors were analysed for $TiO_2$ (by sodium bisulphate fusion at 600°C, sulphuric acid digestion, followed by atomic absorption spectrometry). The $TiO_2$ concentration was multiplied by a factor of 2.17 to calculate the ilmenite content of the sample. Geological logs and data from this drilling were used by RSC to guide modelling and domaining for the current MRE; however, the analytical data have not been used as these could not be verified. This is discussed further in sections 7.4.4.10 and 8.1.2.

Carpentaria's efforts ceased in 1976 due to poor market conditions.

### 3.2.3 Fletcher Challenge

In the mid-1980s, Fletcher Challenge (Grampian Mining Company Ltd and Fletcher Titanium Products Ltd) completed a further series of churn holes at widely spaced intervals across the property. North of Canoe Creek, the drillholes were spaced at ~120 m (east–west) with lines spaced at 600-m (north–south). Holes were drilled up to 10 m deep. All holes were surveyed by local surveyors. Fletcher also collected bulk density data. Issues with rising sands and sample recovery were recorded.

Samples were composited, with a screened magnetic fraction analysed for $TiO_2$ by XRF. Highly susceptible (magnetite) and non-magnetic fractions were not included in the sample for $TiO_2$ analysis, and only the 0.3–6.4 amp magnetic fraction was analysed. The $TiO_2$ concentrations were used to calculate the ilmenite content in each sample, using a $TiO_2$ factor of 2.17. Geological logs and data from this drilling were used by RSC to guide modelling and domaining for the current MRE;

however, the analytical data have not been used, as they could not be verified. This is discussed further in sections 7.4.4.10 and 8.1.2.

Most samples were also assayed for Au; however, the Au sampling and testing protocols were of secondary importance to the ilmenite sampling (Lee and Burlet, 2018a, b). These Au data have not been included in the current MRE.

### 3.2.4 Westland Ilmenite

Westland Ilmenite Ltd (Westland) completed several drilling campaigns mainly in the northern half of the Barrytown Flats, continuing the work undertaken by Carpentaria and Fletcher. Several RC drill lines exist within the Coates South Block from exploration in 1990 which targeted shallow ilmenite mineralisation.

The drilling was contracted to Alton Drilling Ltd who used a track-mounted Versadrill 300 rig to drill 75-mm-diameter holes. Infill holes were drilled on the same grid lines used by Carpentaria. The programme included some check drilling of Westland programmes using twin holes distanced 1 m from the original holes along the strike of the strandlines, and twin holes adjacent to the previous Carpentaria and Fletcher drillholes. The company also added the first north–south trending drill lines using 30-m spacing between holes. These north–south lines roughly follow the direction of the strandlines. All Westland holes were surveyed by professional surveyors.

Samples were collected from 1-m intervals and near-surface data were excluded from the sampling. Samples were variably composited, screened and a magnetic fraction (6.4-amp fraction) was weighed and analysed for $TiO_2$ by XRF. Composited samples were also analysed for Zr. Geological logs and data from this drilling were used by RSC to guide modelling and domaining for the current MRE; however, the analytical data have not been used as they could not be verified. This is discussed further in sections 7.4.4.10 and 8.1.2.

Westland excavated 26 test pits to assess the bulk mineral content and to determine the geotechnical characteristics of the ground to optimise potential mining practices (Lee, 1991). Backhoe pit excavations, each ~1 m x 5 m, were excavated to maximum depths of ~5 m, and from these up to about 50 kg of sand sample was retained for analysis.

Westland obtained bulk density data from these pits. A total of 26 mineralised sand samples and three overburden samples were collected (Lee, 1990). Bulk density samples were obtained by slowly pressing a thin-walled stainless-steel cylinder of 115 mm diameter into the exposed material to a depth of ~300 mm. The depth to which the cylinder was inserted was measured, then the cylinder was dug out and the material was recovered. The sample volume was determined from the cylinder circumference and measured depth. Samples were dried and weighed, and analysed for $TiO_2$. The bulk density of the dry undisturbed sand was then established, and the associated ilmenite content was recorded. All samples were collected from above the water table due to the difficulties of sampling water-saturated loose granular materials.

Westland undertook trial mining and processing on the Barrytown Project in late 1990 and early 1991; this area was located further north than the Coates South Block. The 6-tonne per hour dry mill, which was commissioned in January 1990, was designed for electrostatic treatment of concentrate where the conductive ilmenite fraction was separated from the non-conductive garnet. The plant produced a concentrate containing 80% ilmenite (overall recovery of 72%). The non-magnetic fraction containing 25% ilmenite and 5% zircon was stockpiled separately (McOnie and Bull, 2007).

In August 2000, Rio Tinto acquired North Ltd (parent company of Westland) and all its assets worldwide, including Westland's Barrytown project. Rio Tinto did not undertake any exploration or mining on the permit and surrendered the permit in 2005. The wet concentrator plant was dismantled and sold.

### 3.2.5 NZ Gold

In February 2008, NZ Gold undertook a helicopter airborne geophysical survey of the entire Barrytown Flats, comprising magnetic and radiometric data to identify Au targets (Vidanovich, 2008). The survey was flown by Thomson Aviation. The geophysical data were processed, and an interpretation was carried out using only the Carpentaria and Fletcher Au drilling and testing data for comparison. Radiometric data showed moderate responses on the thorium (Th) channel (possible mineral sources are monazite, thorite, and thorianite) and weak but detectable U responses (uraninite, and thorite), while potassium (K) counts were high. Interpretation of the radiometric data identified two main areas:

- a K anomaly indicating zones of alluvial outwash which cover the southern portion of the Coates South Block, originating from Collins Creek, and more broadly from the Canoe Creek, and associated with drainage from areas of granitic source; and
- a Th and U anomaly, where HM are exposed on the surface in strandline accumulations.

The magnetic response in the Barrytown deposits is due to the magnetite content and to a lesser extent, the ilmenite content. Vidanovich (2008) noted that magnetite is 10–100 times more magnetic than ilmenite; however, Lee & Burlet (2018a) argued that the Barrytown ilmenite should have a magnetic susceptibility closer to 1/10 of magnetite (rather than 1/100). According to Lee & Burlet (2018a), it should therefore produce a better response to the airborne magnetometer instrument. This because the Barrytown ilmenite is very fresh, with a high FeO component, making it more magnetic than the oxidised, high $Fe_2O_3$, ilmenite.

NZ Gold compared the radiometric and magnetic data with historical data to confirm that areas of magnetism and radiometric anomalies highlight and confirm the presence of buried strandlines, where elevated concentrations of Au and HM are present (Vidanovich, 2008).

NZ Gold surrendered its permit EP 40760 in June 2009 after summarising its work in two reports submitted to the New Zealand regulator, MR5265 and MR4438.

### 3.2.6 Alloy Resources Ltd

Alloy Resources Ltd was granted EP 51803 on 26 November 2009 for a period of five years. In 2013, Pacific Mineral Resources Ltd (PMRL) undertook a review of all historical digital data held by Alloy Resources as part of the process of farming in to hold a majority interest in the project. PMRL commissioned Kenex to compile all previous data into a database (Kenex, 2013a, MR4934).

Later in 2013, Alloy Resources completed drilling over the southern portion of EP 51803 for a total of 1,003 m from 105 holes. A track-mounted aircore rig was used to drill 923 m from 64 holes, and 79 m was drilled from 41 holes using a motorised auger drill. Drilling was undertaken by Horizon Drilling and holes were surveyed with differential GPS. Hole depths

ranged between 9–27 m. Samples were taken every metre, subject to a 25% split on the rig by riffle splitter, with 25% intended for gold assay, 25% for ilmenite assay, and the remainder stored in a polyweave bulk sample bag. Repeat samples were taken every 10th metre or at the end of each hole. Issues with penetrating alluvial gravels were noted, as well as difficulty in retrieving adequate samples from gravel or swampy material, and that drilling through man-made drainage humps resulted in poor sample retrieval owing to poor ground compaction in those areas. A recommendation was made that future drilling should be undertaken by sonic drill rig. Samples were analysed for ilmenite and Au by CRL Energy. Further information for this drilling can be found in Kenex (2013b, MR5069).

### 3.2.7 Westland Titanium

In 2014, Alloy combined with Westland Titanium through a joint-venture agreement and continued work on permit EP 51803. Work completed in 2014 included a scoping study and digital data compilation for the Barrytown Flats. The scoping study recommended a mining operation of 6 Mtpa with an initial 10-year mine life. A resource estimate was completed by Al Maynard & Associates, the results of which are summarised in Table 7, and the study made the following conclusions:

- the metallurgical recovery of the ilmenite may be hindered by the immaturity of the deposit;
- much of the sampling from historical drilling was not verifiable as reliable and accurate, resulting in an inferred resource estimate;
- Au mineralisation occurs coincident to ilmenite mineralisation;
- twin hole drilling is needed to verify the accuracy of historical drilling;
- closer-spaced drilling (<50-m) is required to raise the resource to an Indicated classification or above; and,
- the quality of the 2013 aircore drill programme was considered unsuitable due to poor recoveries and sample contamination below the water table.

In 2015, following a permit extension to appraise the deposit at Barrytown, Westland Titanium conducted a preliminary drilling programme over the Barrytown Flats (Kenex, 2016, MR5266). A total of 31 shallow aircore drillholes were completed for a total of 502 m. The drilling was conducted along three, east–west, traverses targeting shallow heavy mineral sands along Macmillan's Road, Burkes Road, and Cargill Road (Figure 6).

In addition to the 2015 drilling programme, Westland Titanium collected five small composite bulk samples from surface enrichments and previous drilling samples (Kenex, 2017). The exact location sources and size of each sample are not given. Samples were submitted to SGS for QEMSCAN analysis. Results from the five samples showed that:

- the ilmenite abundance is consistent with historical drilling;
- the garnet is predominantly almandine;
- the garnet-to-ilmenite ratio is ~2.64 to 1; and
- the vast majority of the garnet has a low number of inclusions.

In 2016, aircore drilling was carried out over the northern area of Barrytown Flats. A total of 985.3 m were drilled from 89 holes and holes were spaced at 10-m intervals along two east–west traverses (Figure 7). Further interpretation of the geophysical survey flown in 2008 was also undertaken by Southern Geoscience of Perth, Western Australia.

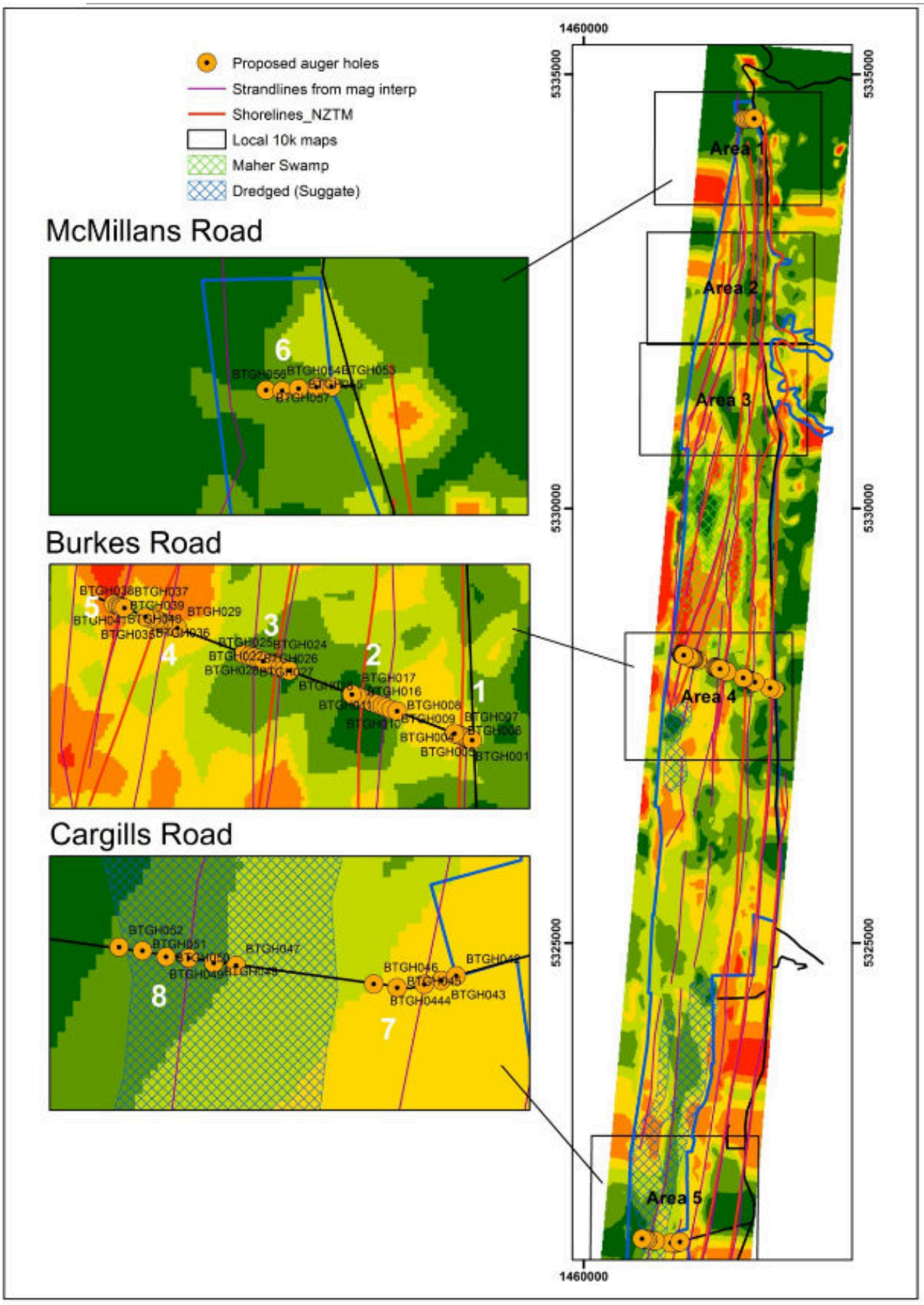


Figure 6: 2015 Drilling by Westland Titanium at Barrytown Flats.

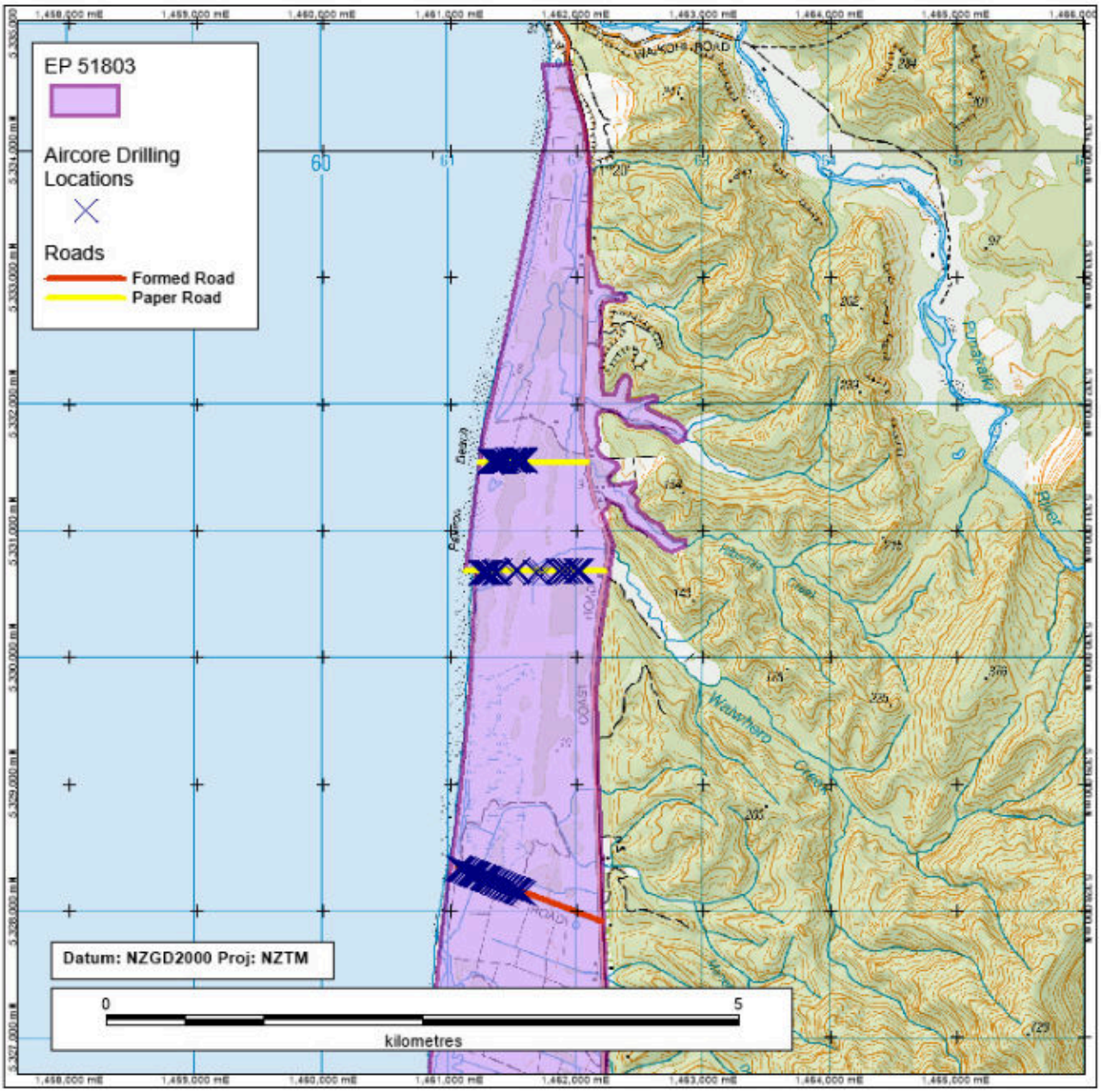


Figure 7: 2016 aircore drilling by Alloy Resources at Barrytown Flats.

## 3.3 Production History

Early production records for mining across the Barrytown Flats area are incomplete. It is known that historical prospecting in the 1870s involved small sluice operations that worked the terraces along the Barrytown Flats for Au. Despite poor recoveries McOnie & Bull (2007) estimated past production of Au from Barrytown at more than 62,000 oz Au from sands at grades of 120–270 mg/m$^3$. Most of the historical production records from Barrytown relate to areas south of Canoe Creek.

In the early 1900s, blow-up sluicing claims were worked in the vicinity of the mouths of Canoe Creek and Fagan Creek and near the fan of Bakers Creek, east of State Highway 6. No detailed information is available on these claims; however, Best (1972) indicates that the approximate extent of these worked areas are around Canoe Creek, and in the area where this

meets the beach. Most of this area is currently lagoon or tidal wetlands (Canoe Creek Lagoon, Figure 8). On the Coates South property, these areas have been excluded from the planned mining disturbance area and do not form part of the MRE detailed in this Report.

The initial operation of a pilot plant at Barrytown by Carpentaria. As of March 1972, a total of 167 tons of ilmenite had been produced, with all tailings combined and pumped to a settling pond (Best, 1972). However, there are no records of which area was mined, the quantity mined, the ilmenite abundance or where the tailings were settled. It is unlikely that it was within the Coates South Block as Carpentaria considered the Coates South Block as low-grade (Figure 8). Additionally, Figure 8 illustrates that the pilot plant was located much further north, near Lyddys Creek.

rsc
MINING & MINERAL
EXPLORATION

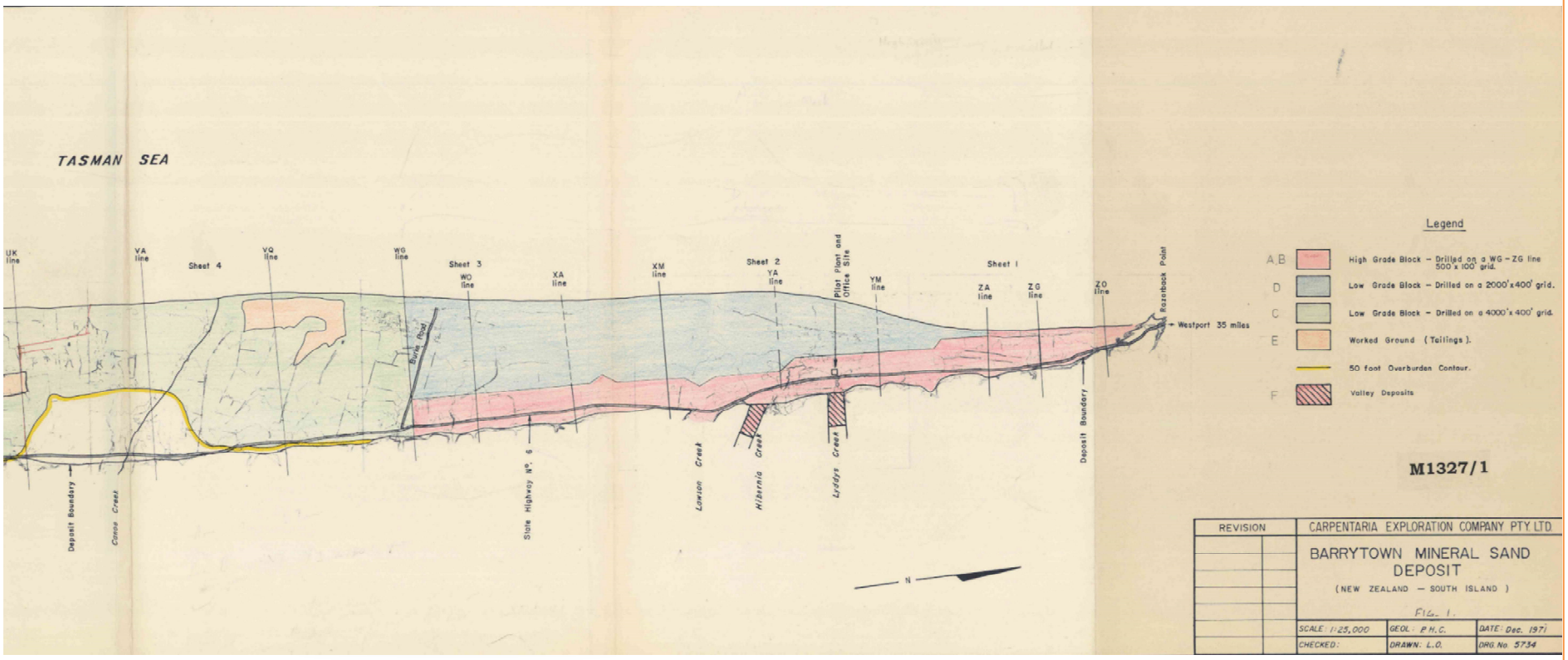


Figure 8: Carpentaria map of the Barrytown Project, that indicates worked ground (tailings) north of Canoe Creek and the pilot plant location.

## 3.4 Previous Studies

Various mineral resource estimation studies were undertaken before 2018 that were not reported or classified in accordance with the JORC Code (2012). Many of these estimates also included volumes that are now considered sterilised material, such as those covered by State Highway 6, the Punakaiki Scenic Reserve, and the buildings on the deposit. These estimates represent the wider Barrytown Flats Project area and are not directly comparable to the MRE for the Coates South property, reported in Section 8.

In 2018, TiGa commissioned Graham Lee & Associates Pty Ltd (GLA) and H&S Consultants Pty Ltd (H&SC) to undertake a resource estimate for the Barrytown Flats, resulting in an Indicated and Inferred Mineral Resource for ilmenite classified and reported in accordance with the JORC Code (2012), and an Exploration Target for garnet, zircon and Au. The results are presented in Table 7 and further details can be found in Lee et al. (2018a).

An internal study was subsequently undertaken by TiGa to establish an indicative initial mine plan to support its permitting compliance and applications (Banaszak et al., 2018). This study was based on 69 Mt @ 11.56% ilmenite, 17.3% garnet, 0.4% zircon, and 0.07 g/t Au. This study was not reported in accordance with the JORC Code (2012) and no ore reserves were reported.

### 3.4.1 Ilmenite

Several historical ilmenite resource estimates for the Barrytown deposit have been completed (Table 7). Estimates prepared in the 1970s covered the entire deposit, while estimates since 1989 have been split and cover either the portion north, or the portion south, of Canoe Creek.

Table 7: Previous Barrytown ilmenite mineral resource estimates.

| Company | Year | Cut-Off (%) | In-Situ Resource | Ilmenite (Mt) | Ilmenite Abundance (%) | Reference | Comment |
|---|---|---|---|---|---|---|---|
| **Carpentaria Exploration Company** | 1970 | 2 | 100 Mt | 12.8 | 12.3 | Caffyn (1976) | Total deposit. |
| **Carpentaria Exploration Company** | 1971 | 5 | 92.8 Mt | 11.0 | 13.0 | Caffyn (1976) | Total deposit. |
| **Mineral Resources NZ Ltd** | 1980 | Not used | 36.3 $Mm^3$ | 7.1 | 10.0 | Hancock & Associates (1980) | Total deposit. |
| **Fletcher Challenge** | 1989 | 4 | 29.6 $Mm^3$ | 6.3 | 12.3 | Robbins (1989) | Feasibility study resource estimates for the target area north of Canoe Creek. |
| **Westland Ilmenite** | 1990 | 4 | 35 Mt | 5.0 | 14.3 | Lee (1990b, a) | Manual estimates North Canoe Creek. |
| **Westland Ilmenite** | 1990 | 4 | 40 Mt | 5.6 | 13.9 | Lee (1990b, a) | Mine Map modelled Estimate North Canoe Creek. |
| **Westland Ilmenite** | 1990 | 4 | 15 Mt | 1.9 | 12.8 | Lee (1990b, a) | Manual estimates South Canoe Creek. |
| **Westland Ilmenite** | 1990 | 4 | 19 Mt | 2.3 | 11.7 | Lee (1990b, a) | Mine Map modelled estimate. |
| **Alloy Resources/Westland Titanium** | 2014 | 2.5 | 59.1–70.3 Mt | 4.7–6.4 | 6.5–10 | Maynard & Jones (2014) | Total deposit. |
| **TiGa (Barrytown JV Ltd)** | 2018 | 4 | 69 Mt | 8.0 | 11.6 | Lee & Burlet (2018a) | North of Canoe Creek. |

### 3.4.2 Zircon

In addition to the ilmenite estimates, Westland Ilmenite also estimated a zircon mineral resource of 66,000 t at 0.19% contained within the 35 Mt of in-situ resources north of Canoe Creek.

### 3.4.3 Gold

Four historical Au estimates for the Barrytown deposit have been completed covering the entire Barrytown Flats (Table 8).

Table 8: Previous Barrytown Au mineral resource and target estimates.

| Company | Year | In-Situ Resource | In-Situ Au (oz) | Gold Grade ($mg/m^3$) | Reference | Comment |
|---|---|---|---|---|---|---|
| **Mineral Resources NZ Ltd** | 1980 | 34.2 $Mm^3$ | 155,000 | 111 | Hancock & Associates (1980) | Gold resource estimate only. |
| | | 36.3 $Mm^3$ | 135,000 | 116 | | Combined Au and ilmenite resource estimate. |
| **Fletcher Challenge** | 1989 | 29.6 $Mm^3$ | 112,000 | 116 | Robbins (1989) | Feasibility study resource estimates for the target area north of Canoe Creek. |
| **N/A** | 2001 | 39 $Mm^3$ | 270,500 | 171 | James (2001) | Gold resource estimate over the area, and to the north, of the southern extent of NZ prospecting and mining drillholes. |
| **Graham Lee Associates** | 2018 | 6.4–9.61 $Mm^3$ | 51,000–316,000 | 148–150 | | Gold reported as an Exploration Target |

# 4 Geological Setting & Mineralisation

## 4.1 Regional Geology

The Barrytown Project is located in the West Coast region, South Island, which has been regionally mapped at 1:250,000 scale as part of the QMAP project (Nathan et al., 2002). The West Coast region of New Zealand has a complex geological history that is defined by multiple generations of rifting prior to and since the inception of Zealandia as a distinct landmass in the Late Cretaceous, and a shift to convergent tectonics in the Late Oligocene (Nathan et al., 1986).

Zealandia rifted away from the east coast of Gondwana throughout the Cretaceous from 125–83 Ma (Laird and Bradshaw, 2004). Extension and subsequent thinning of the continental crust were accommodated by the formation of several metamorphic core complexes (e.g. Tulloch and Kimbrough, 1989; Schulte et al., 2014). In the West Coast region, the resulting assemblage of Palaeozoic and Mesozoic basement rocks consists of an amalgamation of Ordovician metasediments (Greenland Group; Laird and Shelley, 1974), Devonian and Cretaceous intrusive plutons (Karamea Batholith; Nathan et al., 2002), and a suite of foliated granites, gneisses and mylonites (Kimbrough and Tulloch, 1989; Nathan et al., 2002) forming the exhumed footwall of the Paparoa Core Complex (Kimbrough and Tulloch, 1989).

A second stage of rifting in the Paleogene led to the formation and sedimentary infill of the Paparoa Trough (Nathan et al., 1986) that extended from Greymouth to Westport. Rifting persisted into the Late Oligocene, shifting to convergent tectonics in the Late Oligocene (Furlong and Kamp, 2013). Development of the present oblique-compressional plate boundary in the Early Miocene led to a complex Late Cenozoic history. The switch from an extensional to a compressional regime prompted basin inversion throughout the Paparoa Trough, resulting in the uplift and erosion of most of the sedimentary rocks deposited in the deepest part of the trough (Figure 9). The preserved Oligocene strata are relatively thin packages of non-marine, shelf and platform facies that would have formed along the flanks of the axis of the Paparoa Trough. Following the deposition of Tertiary sediments there was a hiatus in deposition lasting about 1.5 Myr before the deposition of the oldest Quaternary sediments in the area.

Rapid uplift of the Southern Alps since the Early Quaternary has formed the present range-and-basin topography (e.g. Nicol et al., 2017). Glaciations during cool periods in the Quaternary have resulted in downstream aggradation from moraines and down-valley glacial outwash gravels (e.g. Barrows et al., 2013). During warmer, interglacial periods, there is evidence of higher sea levels near the coast from marine terraces that have been subsequently uplifted (Pillans, 1990).

Quaternary sand formations are the result of erosion of large volumes of heavy-mineral-bearing source rocks (Figure 9). These include the quartz vein and disseminated Au deposits in the Greenland Group (Palaeozoic orogenic shear zone Au deposits) and garnet schist of the Haast Schist east of the Alpine Fault (Mesozoic orogenic Au deposits and Cenozoic orogenic alpine Au deposits) (McPherson, 1978). Gold, along with ilmenite, magnetite, garnet, zircon and other heavy minerals (Hutton, 1950; McPherson, 1978; Minehan, 1989), was concentrated into lenticular beach placers known as black sand leads along 320 km of coastline from the Karamea River in the north to Bruce Bay in the south (Christie and Brathwaite, 2006; Tay et al., 2021). Narrow, elongate Holocene beach and dune deposits typically run parallel to, and at the back of, the modern storm beach (Suggate, 1989; Tay et al., 2021).

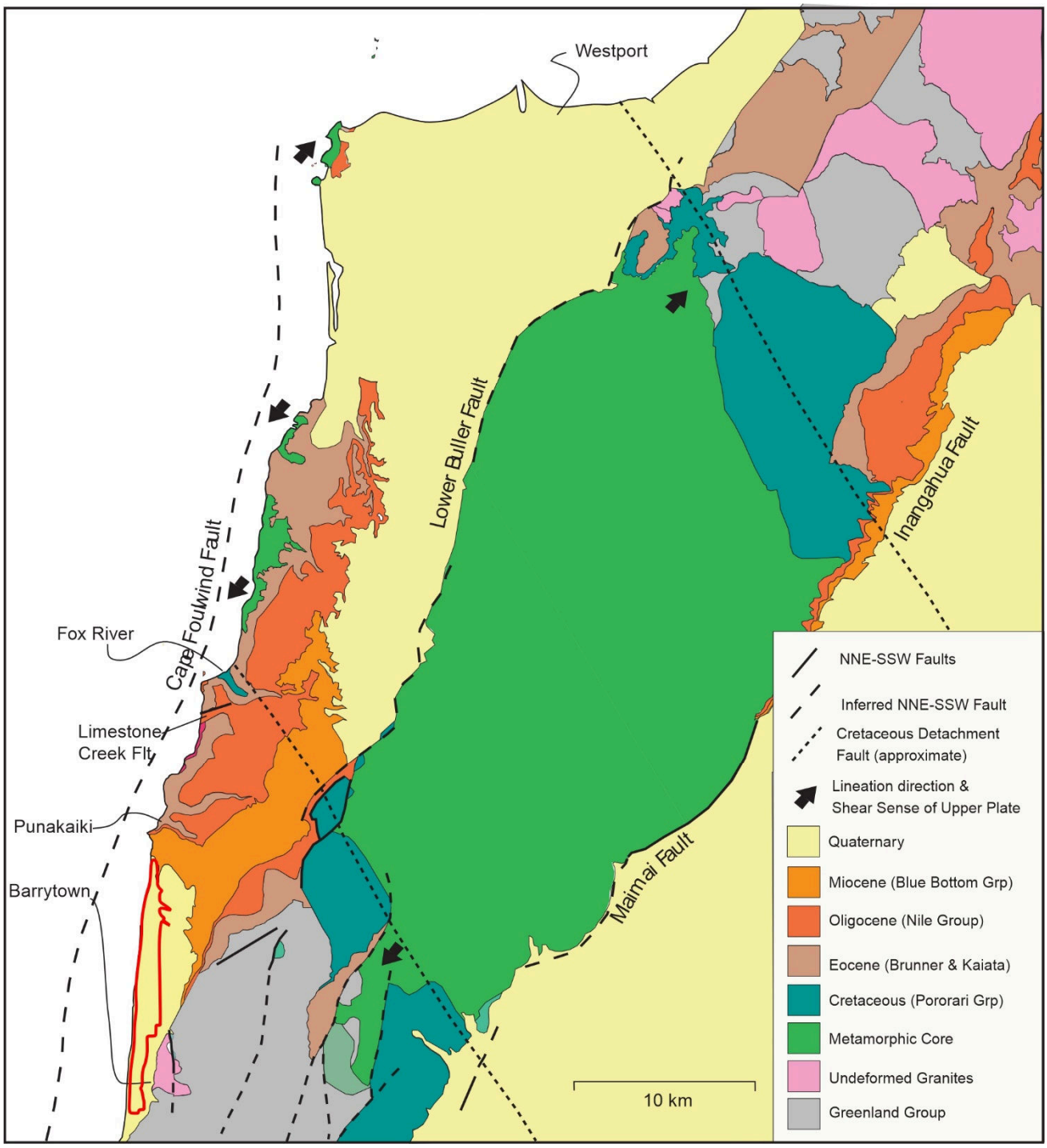


Figure 9: Simplified regional geological map of Greymouth–Westport area. Barrytown Project shown with a red outline (modified after Riordan et al., 2014).

## 4.2 Local Geology

The post-glacial coastal lowland of Barrytown (Barrytown Flats) is 17 km long and up to 1.5 km wide (Suggate, 1989). The lowland is backed by a well-marked cliff and comprises a succession of shorelines in the north, a series of fans from local creeks in the middle, and further shorelines in the south (Figure 10) (Suggate, 1989). Barrytown's lowland flats are the result of costal progradation due to northward longshore drift (Furkert, 1947). Beach and low dune ridges, with intervening

swamps, form the northern third of the Barrytown lowland. In the central part and much of the south of the lowland, fans from creeks overtop the coastal deposits, with that from Canoe Creek reaching the present coast (Suggate, 1989). The fans resulted from large amounts of resistant material transported from high, steep, hard-rock catchments; in contrast, the lower gradient northern catchments are in easily eroded soft rocks that provide only fine material, easily carried to the sea (Suggate, 1989). The lowland is interpreted to be of postglacial age based on radiocarbon dated (4720 ± 70 years BP) shoreline deposits 15 km further south (Suggate, 1968, 1989). The inland post-glacial cliff defines the eastern limit of the Barrytown Project.

Using aerial photography, topographic maps, and ilmenite drilling results, Suggate (1989) identified 10 shorelines — plus a modern shoreline with its pattern of complementary erosion and deposition cutting off preceding shorelines — in a series of three sequences at Barrytown (Figure 10 and Figure 11). The three sequences include:

- an older series of four shorelines (numbered 1–4) that developed closely parallel to the post-glacial cliff along its entire length;
- a younger series of six shorelines (numbered 5–10) that formed after a major event changed the coastal regime and represent pauses in stages of coastal advances in the north of the Barrytown Project; and
- the modern shoreline 11 that is considered to have developed after a period of major erosion along the length of the beach after the formation of Shoreline 10.

Subsequent progradation of each shoreline resulted in the preservation of the various wave-cut platforms and burial of the beach facies beneath aeolian sands. South and inland of the Barrytown Project area lies the Canoe Fault. North of the Canoe Fault, elevations of the successive older shorelines 1–4 are about 8.5 m, 7 m, 4 m, and 3.5 m above sea level (m.a.s.l.), respectively, and may reflect continuous uplift, with separate shorelines resulting from the superposition of the effects of minor eustatic sea-level fluctuations, or from successive discrete uplifts (Suggate, 1989). Uplift and displacement at Canoe Fault likely took place between 1,000 and 6,500 years ago since the sea level stabilised (Suggate, 1989). The younger shorelines are not significantly different from present sea level (Suggate, 1989).

Both the wave and aeolian-deposited sands are locally overlain by younger alluvial fan deposits of gravel and/or silt, derived from the Paparoa Range to the east. These are particularly concentrated along the toe of the coastal escarpment where streams discharge onto, and cut through, the coastal plain. Typically, the alluvial and beach sand units overlie gravel and marine sand units (Laird, 1988). The Quaternary geology at Barrytown was mapped and summarised by Laird (1988) into four units (Table 9).

The local basement in the Barrytown Project area consists of Tertiary mudstones and siltstones of the Blue Bottom Group, Carboniferous granites of the Karamea Suite, and Late Paleozoic metasediments of the Greenland Group (e.g. Nathan, 1974). These basement units are exposed to the east of the Barrytown Project (Figure 11). Blue Bottom Group sediments form the local topographic highs in the Barrytown Project area north of the Canoe Fault with elevations up to 120 m above sea level (e.g. Nathan et al., 1986). These soft sediments were partially eroded by high sea levels in the Pleistocene. South of the Canoe Fault, the inland portion of the Barrytown flats form higher, more undulating hills. This is due to the outwash

and talus materials of the more resistant granitic rocks of the Karamea intrusive suite and metasediments of the Greenland Group.

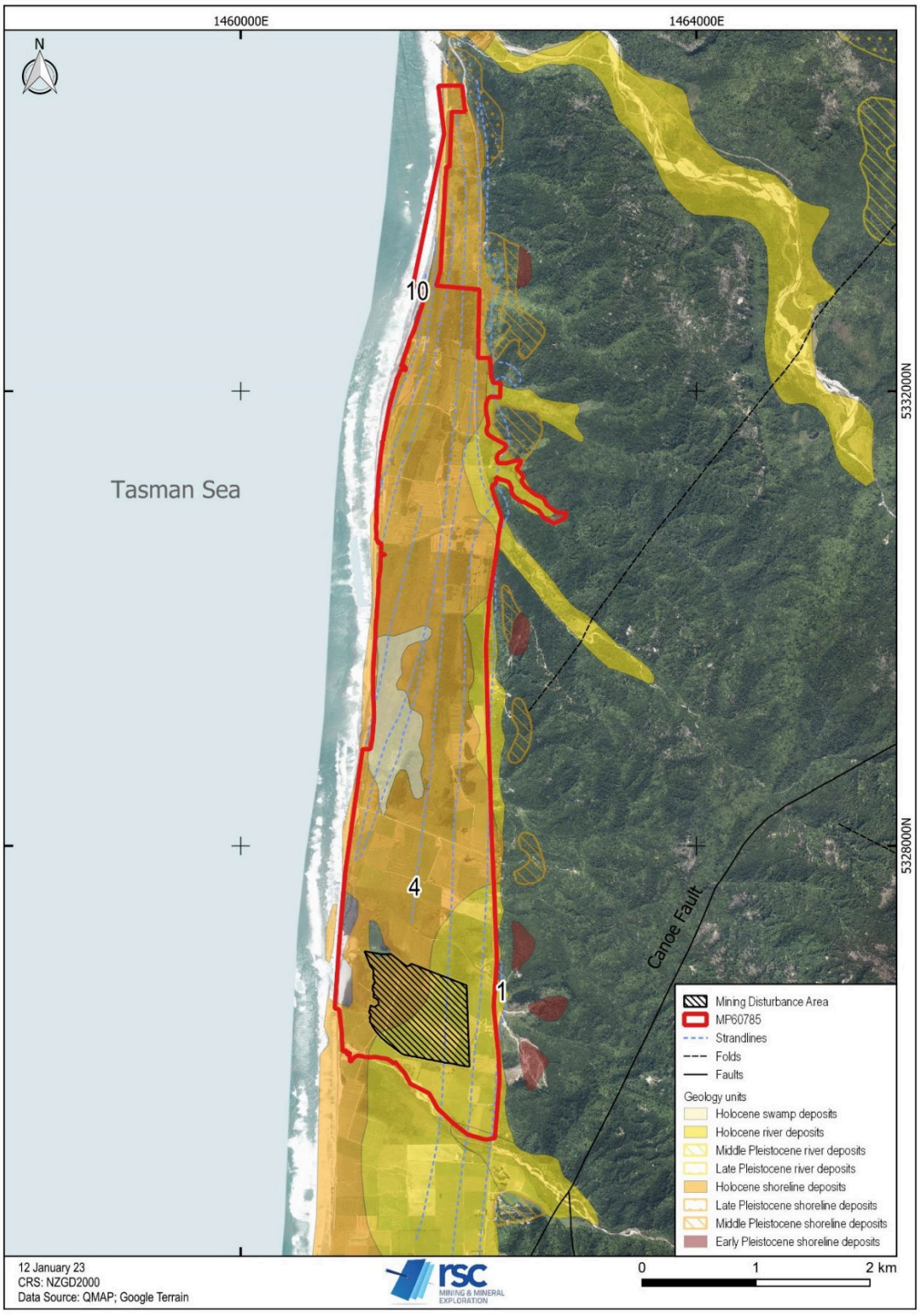


Figure 10: Sedimentary deposits and identified shorelines at the Barrytown Project area (modified after Laird, 1988; Suggate, 1989).

Table 9: Quaternary geology at Barrytown (Laird, 1988).

| Unit | Age | Description |
|---|---|---|
| **Nine Mile Formation** | Holocene | Deposits of the present-day beaches and rivers comprising unconsolidated ilmenite-rich beach sand and gravel, dredge and sluice tailings, river gravel and alluvial fans and swamp deposits. |
| **Waites Formation** | Upper Pleistocene | Gravel (mainly gneissic) forming lower-level inland river terraces and associated degradational terraces. Sand and fine gravel along the coast form a 34–36 m.a.s.l. terrace. |
| **Addison Formation** | Upper Pleistocene | Gravel (mainly gneissic) forming high-level terraces. Partly cemented, brown ilmenite-rich sand and fine gravel near the coast forming an 85–87 m.a.s.l. terrace |
| **Caledonian Formation** | Upper Pleistocene | Cemented marine sand and fine gravel near the coast form a 105–120 m.a.s.l. terrace. |

rsc MINING & MINERAL EXPLORATION

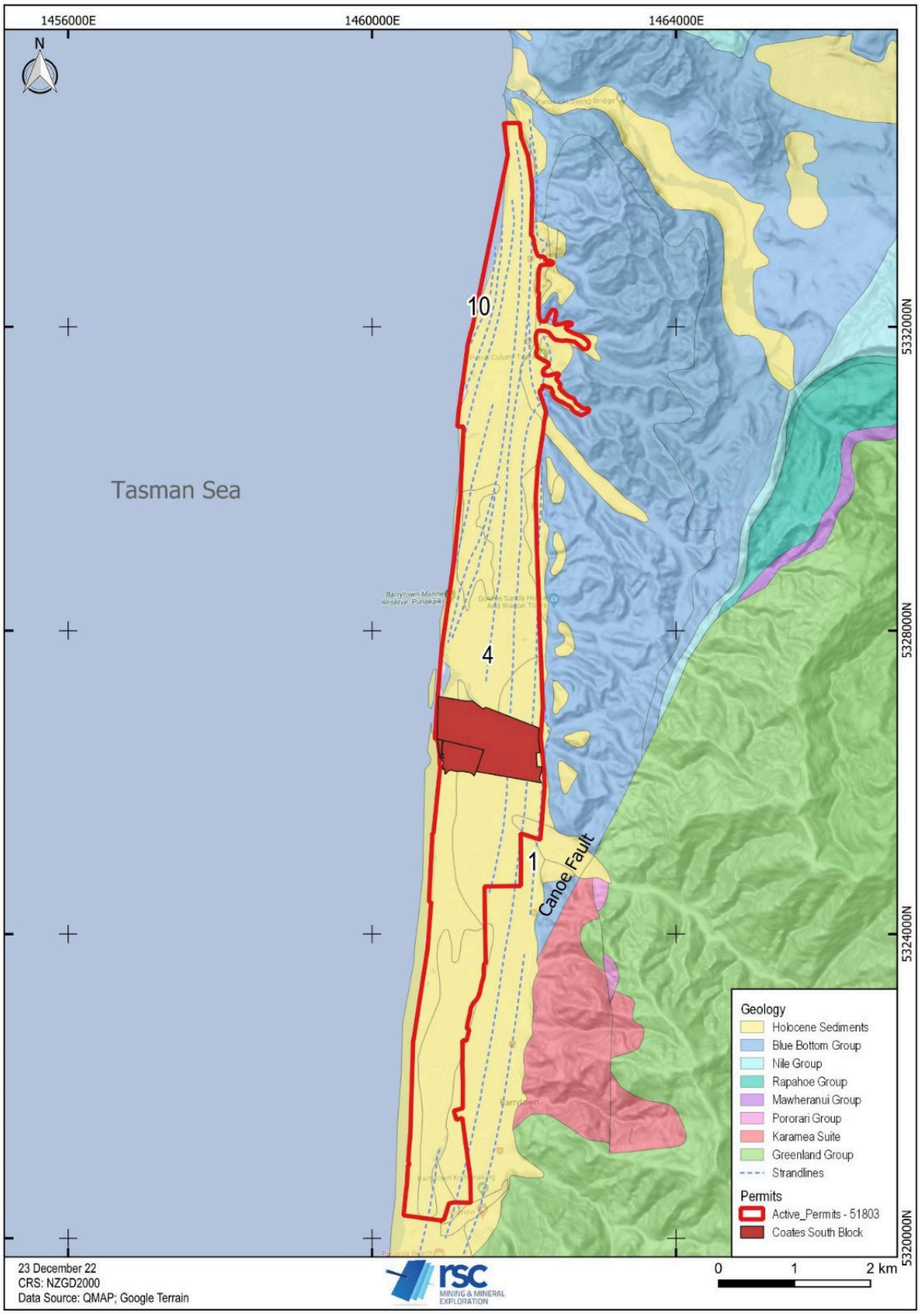


Figure 11: Geological map of the Barrytown Project area with Coates South property.

## 4.3 Deposit Geology

The Barrytown shoreline deposits are characterised by mineralogical and textural immaturity and a lack of chemical weathering. The shoreline beach deposits are quartz, feldspar, lithic (mostly grey schist fragments) sands that contain elevated heavy mineral abundances (Table 10), predominantly garnet and ilmenite with minor zircon and Au (Lee, 1991; Wells and Haverkamp, 2020). These sands are immature, as demonstrated by many composite particles present and the presence of minerals that have a low resistance to mechanical and chemical breakdown. The HM have been concentrated in the series of beach strandlines (shorelines 1 to 10) and are typically considered to have originated from the Alpine Schist of the Southern Alps, transported to the coast by rivers, mostly to the south of the Barrytown Project, and transported north by longshore drift (Bradley et al., 2002; Ritchie et al., 2019). The Au occurring in the Barrytown Project is essentially reworked detrital Au and typically occurs as very fine-grained thin flakes (Newman, 1989). Most Au grains are 50–150 µm in diameter with occasional larger fragments up to 600 µm, less than 20 µm thick and doubly or triply folded (e.g. Burlet and Lee, 2019; and references therein).

Table 10: Typical heavy mineral abundance in the Barrytown shoreline beach deposits (Newman, 1989; Haverkamp et al., 2016).

| Heavy Mineral | Abundance |
|---|---|
| **Ilmenite** | 10–15% |
| **Garnet** | 10–15% |
| **Magnetite** | 0.2–0.5% |
| **Zircon** | 0.1–0.3% |
| **Epidote** | 0.1–0.3% |
| **Heavy silicates*** | 0.1–0.3% |
| **Composite heavy particles** | 0.1–0.3% |
| **Leucoxene** | 0.02–0.05% |
| **Sphene** | 0.05–0.1% |
| **Rutile** | <0.1% |
| **Monazite** | <0.1% |

*chlorite, biotite, amphiboles, pyroxenes and actinolite.

The 2022 drilling campaign at the Coates South Block covered the interpreted shoreline deposits 2–4 from east–west, respectively (Figure 13), that overlay marine sands and gravels. The shoreline deposits are interpreted to be part of the Holocene Nine Mile Formation (cf. Laird, 1988; Suggate, 1989). Shoreline 2 beach deposits are characterised by a top beach gravel layer that extends north from the postglacial cliff close to Bakers Creek up to Scotchman Creeks in the northern part of the Barrytown Flats. Shorelines 3 and 4 are characterised by medium-grained beach sand deposits. The transition between shorelines 3 and 4 is evident further north of the Coates South Block and is defined by a 0.5 m change in altitude due to regional uplift along the Canoe Fault (Suggate, 1989). The change in altitude between shorelines 3 and 4 is not evident at the Coates South Block nor further south of it. The different shorelines might be separated by swales that contain unmineralised silt from alluvial fan deposits (e.g. schematic cross-section in Figure 12) (Lee, 1991). At the eastern part of

the Coates South Block, the shoreline deposits are covered by large quantities of alluvium derived from Canoe Creek (cf. Suggate, 1989; Lee, 1991). The thickness of the alluvial fan deposits ranges from <4-m up to 6-m at the eastern end and tapers off seaward. The shoreline and alluvial deposits are overlain by less mineralised, <1-m-thick aeolian sands and a ~0.5-m-thick top soil (Lee, 1991).

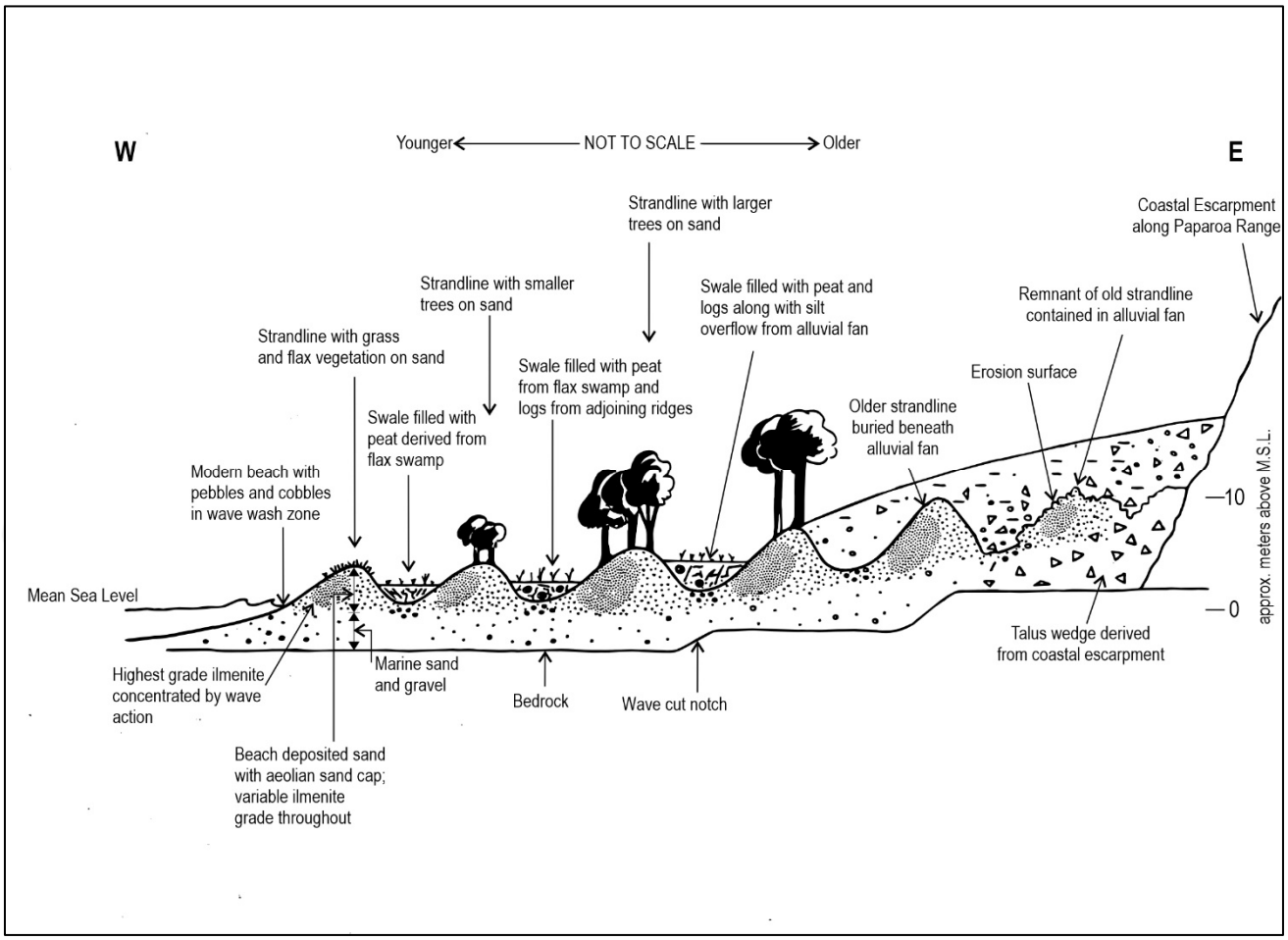


Figure 12: Generalised section of the Barrytown Project (modified after Lee, 1991; Westland Ilmenite Ltd.).

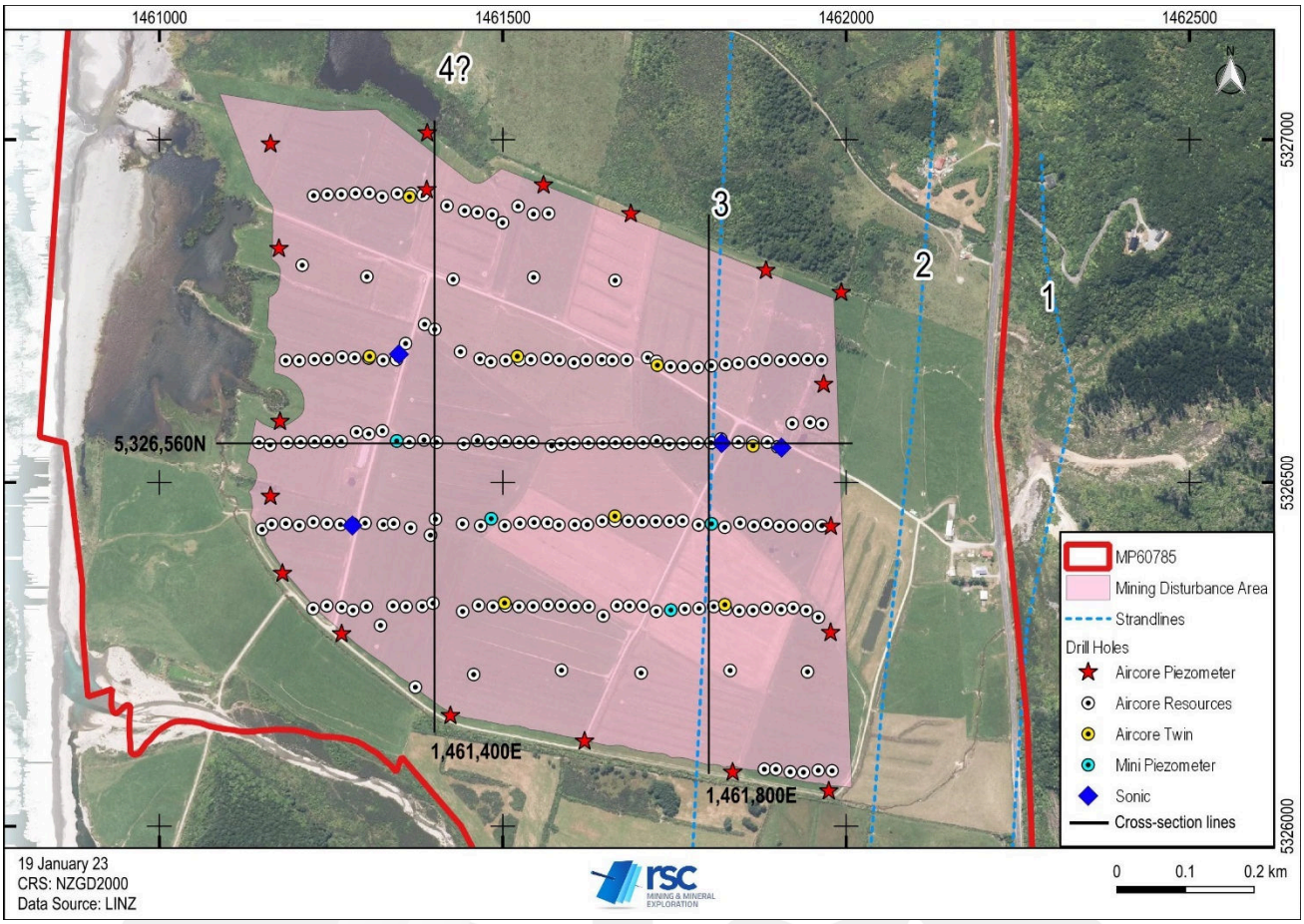


Figure 13: Coastal geology and drillhole locations at Coates South Block.

The local geology at Coates South Block was modelled in 3D using the logging from the 2022 drilling campaign. The cross sections in Figure 14–Figure 17 present the geology of the coastal deposition across the project area. The base in the project area is defined by a flat-lying, sand- and gravel-dominated layer (red in Figure 14 Figure 16) — at ~10–14 m depth from the top surface and ~2 m below mean sea level — that is interpreted as equivalent to the 'marine wave-cut platform' from previous studies in this area (cf. Suggate, 1989; Lee, 1991). Above this layer, the drilling campaign at Coates South defined an ~8–12 m-thick continuous horizon of medium-grained, ilmenite-garnet-rich sand (green in Figure 14–Figure 16). This horizon of beach sand is interpreted as the shoreline deposits 2–4. Within the eastern portion of the drilled area, the shoreline deposits are variably overlain by, or intercalated with, several draping, <2–5 m-thick fans of gravel-dominated talus (purple and light yellow in Figure 14–Figure 16). Long section views in Figure 15 and Figure 16 present the difference between the eastern and western portions of the project area, as the influence of gravel-dominated talus originating from inland in the east progrades and thins in a westerly direction towards the sea. Several buried, unmineralised, and isolated lenses of silts and debris — containing wood and vegetation — are also present within and on top of the shoreline beach sand deposits (mint green in Figure 14–Figure 16). These are interpreted as a mixture of stream channel deposits, overbank flood deposits, and brackish inter-strand lagoonal areas. The shoreline, alluvial and swale deposits are overlain by a thin layer of clay–silt (light blue) and soil (cream).

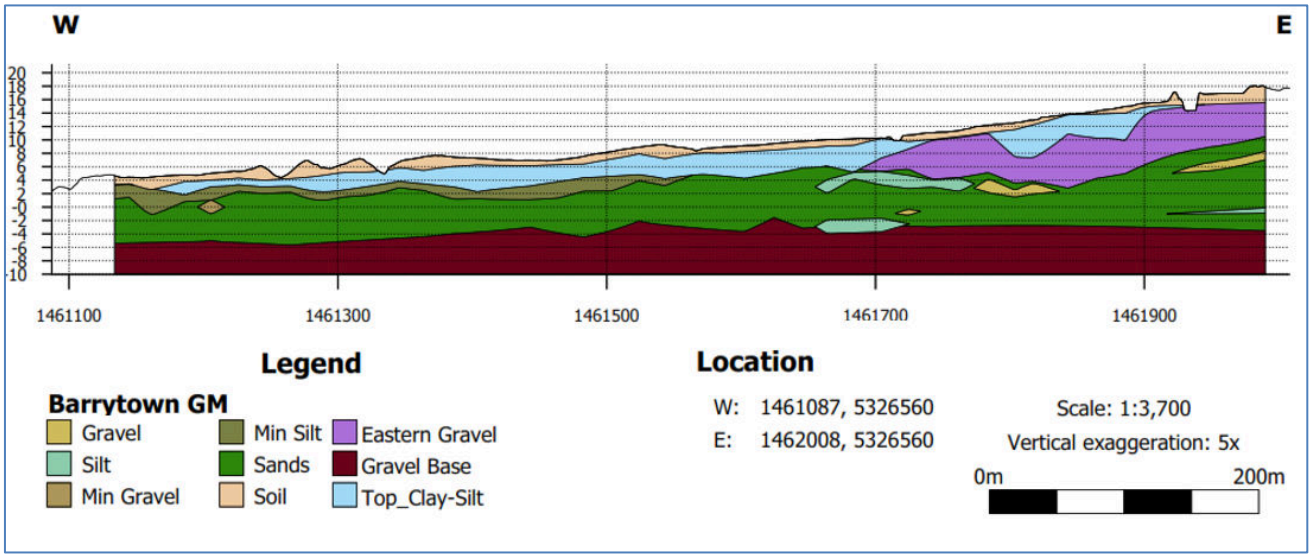


Figure 14: Representative east–west cross-section through the modelled geology along 5,326,560N (looking north).

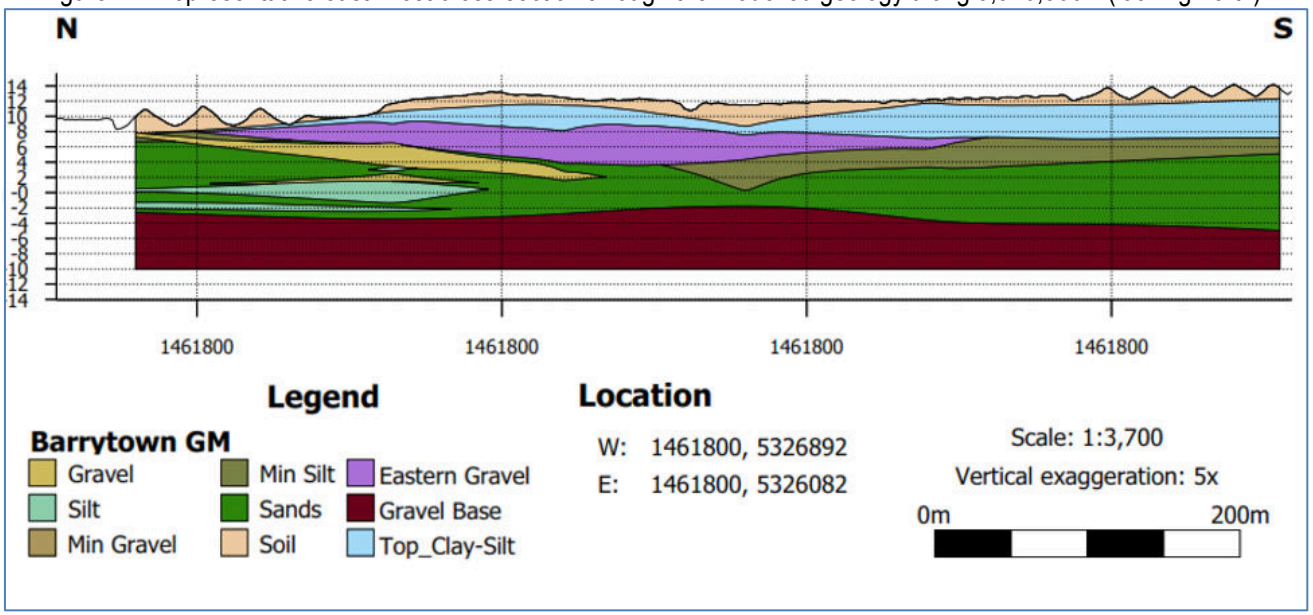


Figure 15: Long section (looking east) , representative of the eastern project area and depicting alluvial fans draping from the east and northeast (purple and yellow) (1461800E).

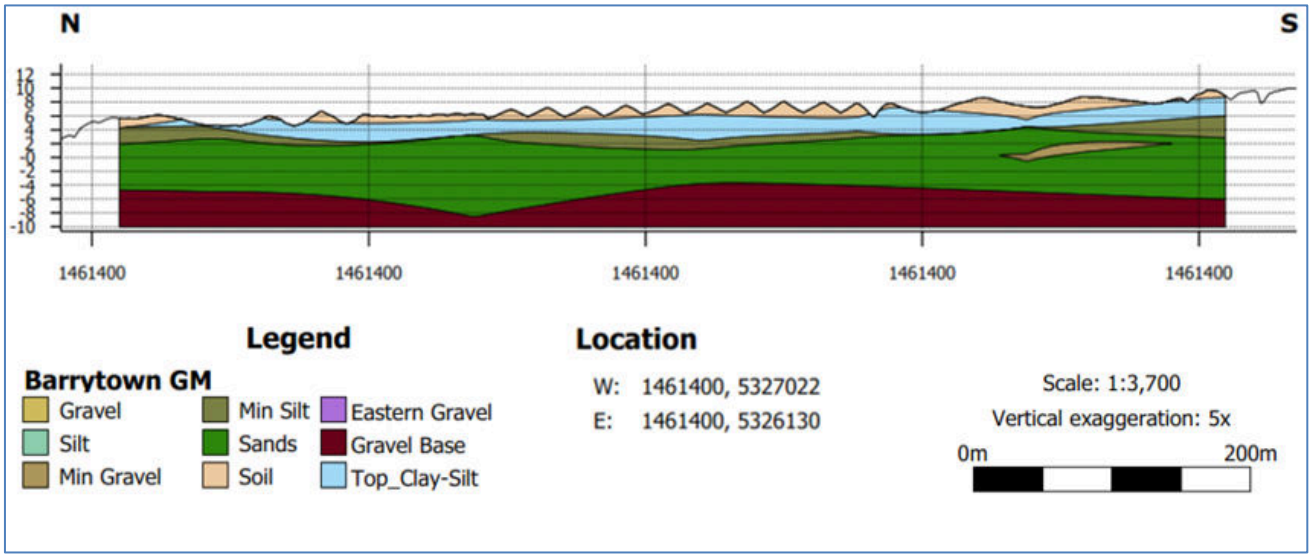


Figure 16: Long section looking east along 1,461,400E, representative of the western project area.

## 4.4 Controls on Heavy Mineral and Gold Deposition

### 4.4.1 Heavy Mineral Deposition

Drilling has confirmed the presence of three broad, north–south trending zones of concentrated HM and these appear coincident with the buried shorelines (2, 3, and 4), as interpreted as magnetic highs from geophysical studies. These strandlines contain elevated abundances of ilmenite, garnet, zircon, Au, and associated HM deposited in a marine placer environment.

Several studies on the mechanics of deposition, distribution, and enrichment of HM sands deposits have been undertaken by Suggate (1989), Force (1991), Van Gosen et al. (2014), and Gallagher et al. (2016). They discuss that the key controls on HM distribution across the Barrytown Project area are:

- the supply of HM through physical weathering;
- the downstream persistence of the HM and their availability in the fluvial or marine environment; and
- a depositional sorting process to concentrate the HM.

The mineralisation process begins inland with the erosion of metamorphic and sedimentary rocks, which supplies sand, silt, clay, and HM to stream drainages. Streams and rivers carry the sediments to a coastal area, where they are deposited and redistributed in a variety of environments, such as deltas, the beach face (foreshore), the shoreface, barrier islands, dunes, and tidal lagoons (Van Gosen et al., 2014). Aeolian dunes, the foreshore, shoreface, and lagoonal environments have been identified as the most significant sites of heavy mineral sand deposition (Force, 1991). The upper part of the beach face, the foreshore (Figure 17), also referred to as the swash zone, is the principal zone of mineral separation (Force, 1991). Breaking waves carry a charge of turbulent sediment-laden water from the lower, submerged beach face onto the foreshore.

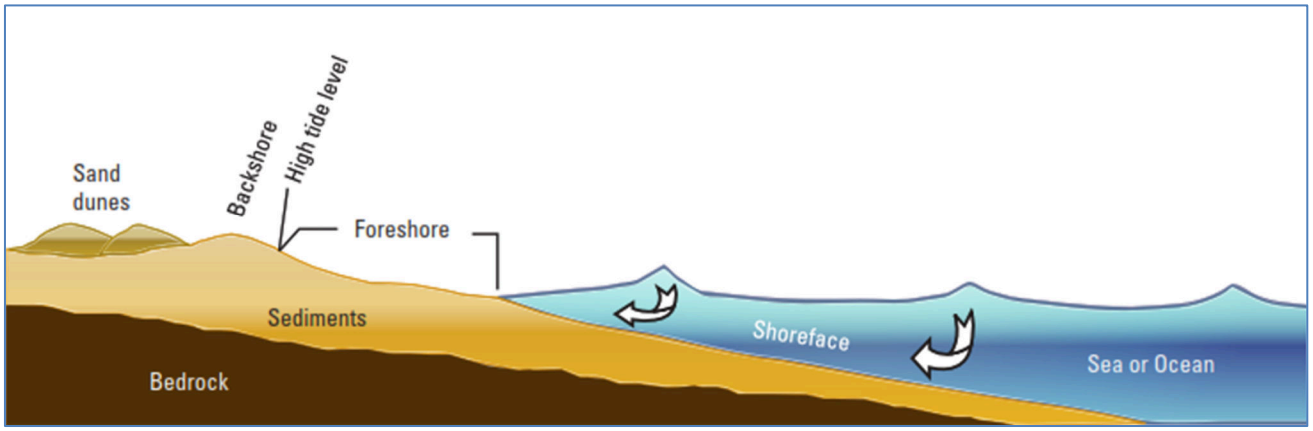


Figure 17: Idealised cross-section of a wave-dominated beach system (Van Gosen et al., 2014).

Grains with the highest settling velocities drop out first at the bottom of the foreshore, with settling velocity, a function of density and grain size. Coarser, light minerals are deposited with finer HM, resulting in a continuous spectrum of grain sizes for each mineral, with finer grains deposited toward the top of the foreshore. Subsequent backwash reworking of the grains results in 'lag enrichment' of HM in the upper portion of the foreshore (Force, 1991).

Traction flow in the lower part of the foreshore typically concentrates heavier elements into a thin, shallowly buried heavy mineral concentration occurring from backwash returning from the surf zone (Clifton, 1969). Typically, the zone of shore break reworking is about 10–40 cm deep (Gallagher et al., 2016) but thicker and more expansive layers of enrichment can form due to episodic variations in the depth and extent of the shore-break zone. These variations are known to occur as climatic and tidal sea-level variations cause the shore break to move up and down the beachfront; this further controls the lateral extent of heavy mineral deposition (Figure 12).

The most effective mineral enrichment process occurs during storms or other periods of high wave energy where HM can be transported and preserved onto the upper foreshore and areas of aeolian dunes (Force, 1991). Storm periods are optimal for the storage of heavy mineral sands, as onshore winds transport sand from the beach and deposit it in aeolian landforms above the high tide (Force, 1991).

Heavy-mineral-bearing sands developed along, and behind, the present beachfront in sandy barriers transported by longshore drift and pushed up from the sea by wave action. These sandy barrier deposits have become stranded as the coastline prograded, allowing lagoonal deposits to accumulate in the swales along the eastern side of the barriers. This has had the effect of producing elongated zones of heavy mineral enrichment on the former beaches being surrounded by lower-grade finer sands and silty sediments in the swales.

Outcrops and excavations across the wider Barrytown Flats area, as shown in Figure 18 and Figure 19, reveal a sequence of fine sand laminations of heavier and lighter minerals. Where strong storm concentrations occur, the dark heavy layers can coalesce with only minimal or no interbedded paler light mineral laminations, within the sediments deposited during that storm episode, and this can be observed in places along the high-grade eastern strandline. Finely laminated darker heavy mineral-rich layers are separated by paler quartz and feldspar light minerals laminations. The two pebbly layers represent

periods of higher wave energy where the sand was largely scoured away leaving mainly pebbles. The photograph of Figure 18 was taken from a natural exposure on Barrytown Beach looking to the east with the dipping strata appearing as horizontal.

Figure 18: Wave-cut beach face showing heavy mineral-rich layers.

Figure 19: View into Pit No 7 Excavated at drillhole YC4400) . The westerly (towards the coast) dip on the finely laminated strata is visible beneath the 0.2 m thickness of sandy soil.

### 4.4.2 Gold Deposition

The Au within the Barrytown Project area is typical of West Coast beach deposits, being essentially reworked detrital Au washed downstream by rivers and reconcentrated as very fine-grained particles in the active surf zone.

Typically, Au concentrations correlate well with HM concentrations; and the two are likely associated during deposition. Interpretations from recent drilling, and comparisons of portable X-Ray fluorescence (pXRF) with gold fire assay data, suggest that the Au is largely distributed as a component of the HM within buried strandlines. Isolated lenses of Au also occur within the overlying alluvial fan talus material, interpreted to be younger zones of alluvial outwash.

## 4.5 Known Comparable Deposits

The West Coast of New Zealand hosts numerous heavy mineral-bearing shoreline placer deposits (Figure 20) that have been the subject of exploration by both government departments and private companies for decades. These deposits are known to contain a range of HM in variable concentrations, including ilmenite, garnet, magnetite, zircon, and rutile with trace amounts of gold, monazite, cassiterite, beryl, uranothorite, scheelite and xenotime (Hutton, 1950; McPherson, 1978; Minehan, 1989; Ritchie et al., 2019).

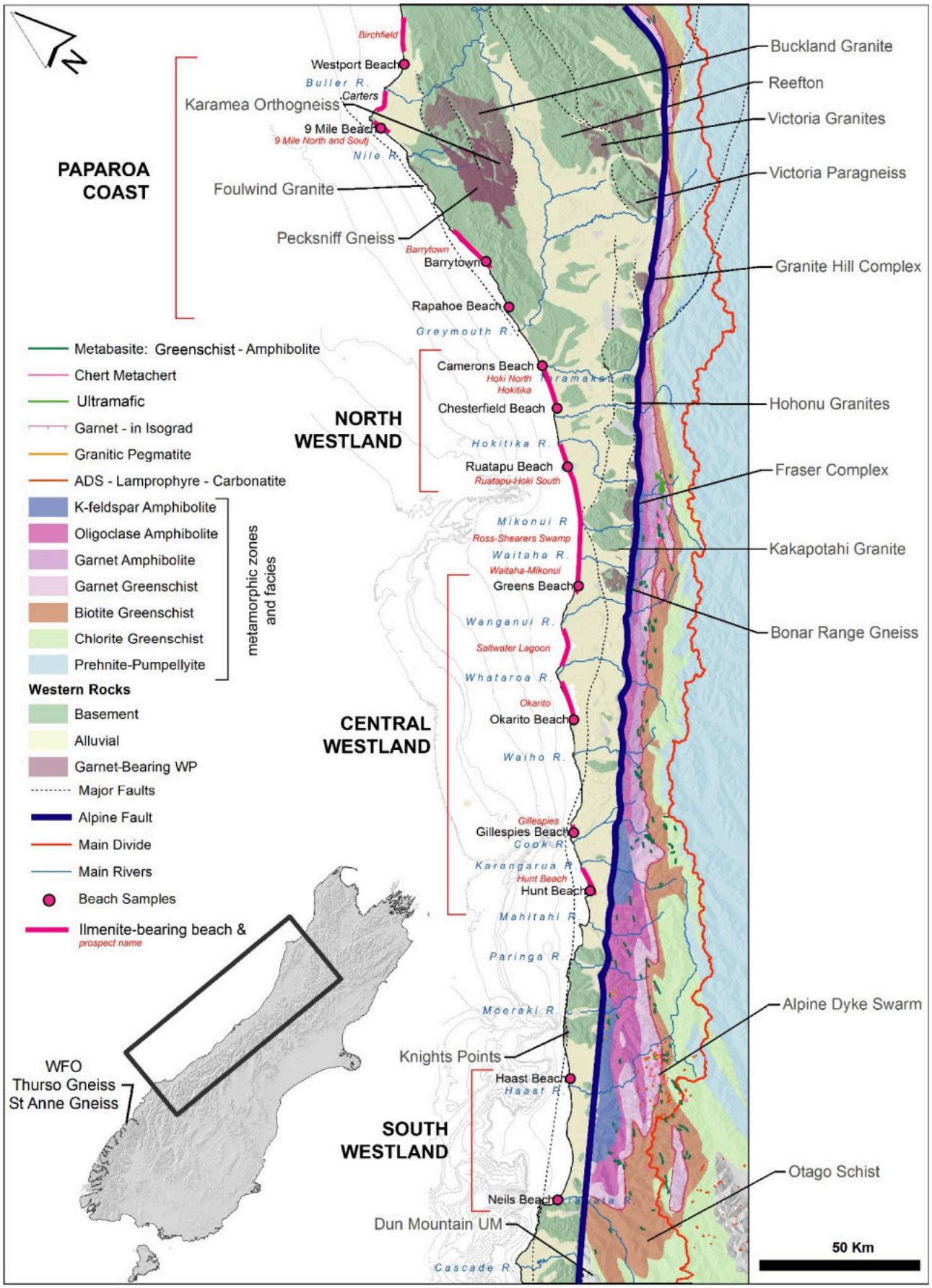


Figure 20: Geological map of Westland with heavy mineral sand prospect/deposit locations (from Ritchie et al., 2019).

Ritchie et al. (2019) assessed the heavy mineral content of samples from 13 West Coast beaches and concluded the following:

- garnet is least abundant on the South Westland beaches, intermediate in abundance along the Paparoa Coast and most abundant in Central and North Westland;
- magnetite and ilmenite abundances generally increase to the south; and
- REE HM abundance increases towards the north.

The mineralisation at Barrytown bears the most similarities to other deposits along the Paparoa and North Westland Coast, including the producing mining operation at Nine Mile and the advanced garnet deposit at Ruatapu. Sands at Barrytown and Nine Mile both contain a notable proportion of Otago Schist-derived garnet. In contrast to most other West Coast beaches, the garnet and ilmenite at Barrytown and Nine Mile have similarly fine grain sizes and high circularity. The Nine Mile Beach deposit is held by Westland Mineral Sands Co. which commenced full-scale production of a heavy mineral concentrate in January 2023. Westland Mineral Sands has reported that the North Nine Mile deposit contains over 2 Mt of heavy mineral concentrate.

Ruatapu and Barrytown sands have similar garnet/ilmenite values of 2.0 and 1.7, respectively (Figure 21; Ritchie et al., 2019). The Ruatapu deposit, targeted mainly for its garnet content, was granted a government loan for its development in 2018; However, according to a public statement published in Stuff[1], the development was cancelled by the permit holder due to changing global market conditions. The Ruatapu project (mineral mining permit MP60508) is now held by Westland Mineral Sand Co. who plans to develop the mine within the next 5–10 years[2].

[1] https://www.stuff.co.nz/national/120249249/west-coast-garnet-mine-granted-10m-government-loan-scrapped
[2] https://www.scoop.co.nz/stories/BU2301/S00023/critical-minerals-project-begins-full-scale-production-on-west-coast.htm

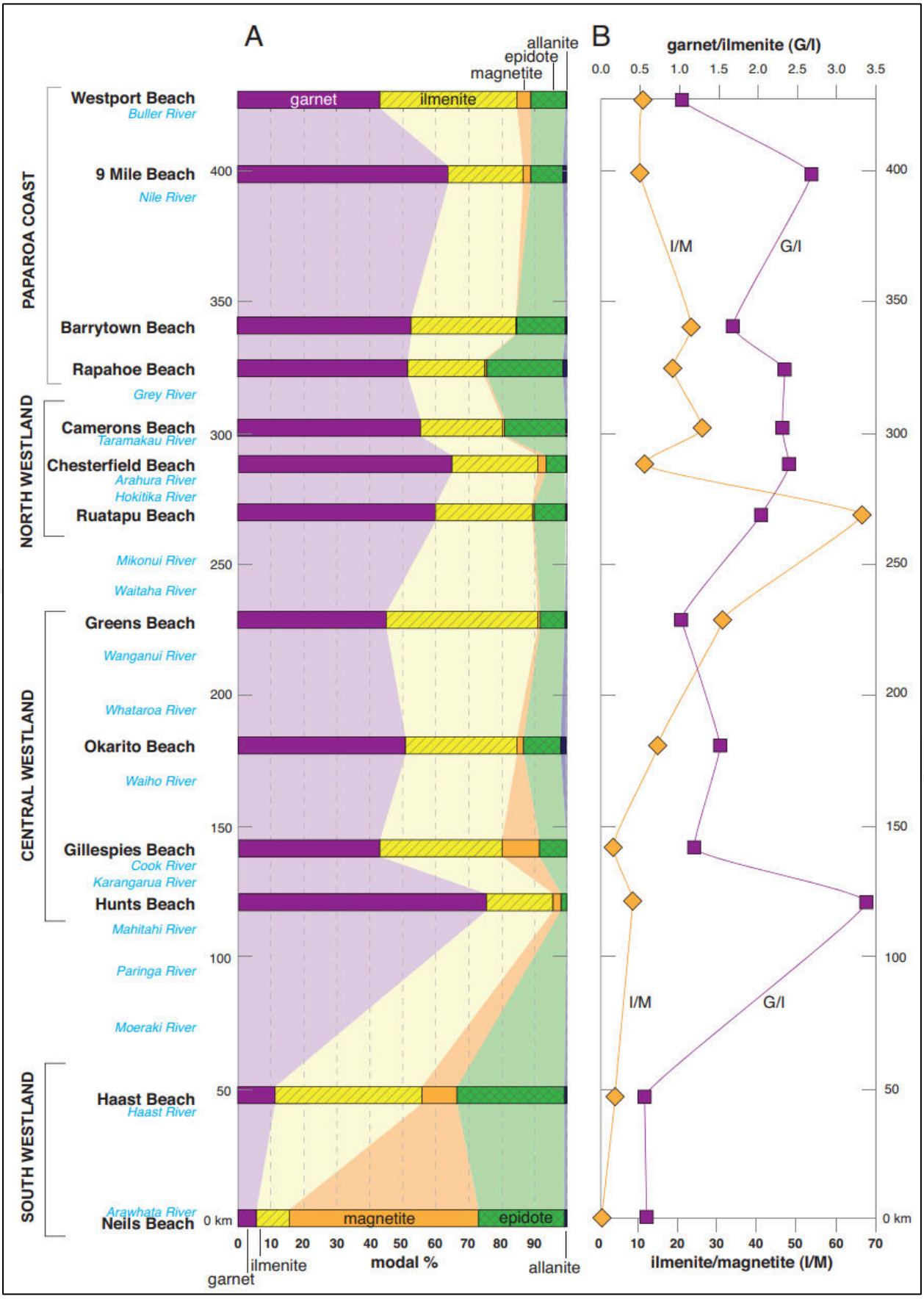


Figure 21: Summary of the lateral variation in modal abundances and ratios of garnet, ilmenite, magnetite, epidote, and allanite (recalculated to 100%) along the Westland beaches (from Ritchie et al., 2019).

# 5 Exploration by TiGa

## 5.1 Drilling

In 2022, TiGa drilled 444 holes, across two landowner blocks within MP 60785 and EP 51803, Coates South Block and Barrytown Farms, respectively (Figure 22). Details of the Barrytown Flats and Coates South Block drilling are provided in sections 5.1.1 and 5.1.2.

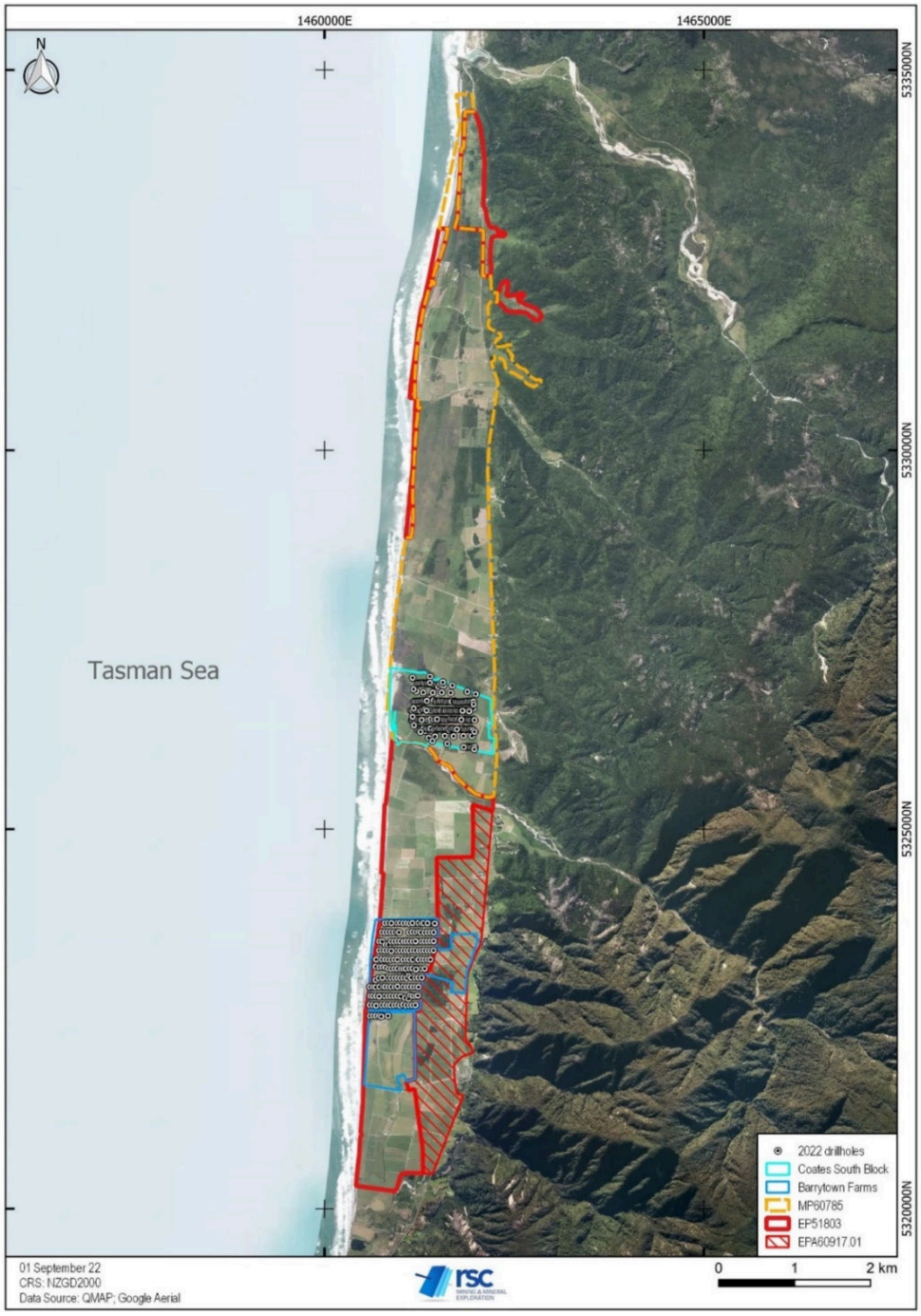


Figure 22: Overview map of the 2022 drilling programme at Coates South Block (within MP 60785) and at Barrytown Farms (EP 51803).

### 5.1.1 Barrytown Farms

TiGa completed a programme of exploration drilling at Barrytown Farms as part of exploration permit obligations for EP 51803. The drilling was supervised by RSC and targeted shallow, heavy-mineral, placer mineralisation. A total of 1,988 metres were drilled in 176 holes during April–July 2022. In addition to resource definition drilling, five holes were drilled for water monitoring and six holes were drilled for Shelby Tube density sampling (Table 11). No data from the Barrytown Farms property were used in the resource estimate reported here, and the results of this programme are therefore not discussed further in this Report.

Table 11: Summary of drilling at Barrytown Farms.

| Drill type | Barrytown Farms | |
|---|---|---|
| | No. holes | Metres (m) |
| **Aircore** | 176 | 1,910 |
| **Aircore: Water monitoring** | 5 | 55 |
| **Shelby Tube Density Drilling** | 6 | 23 |
| **Programme Total** | 187 | 1,988 |

### 5.1.2 Coates South

A total of 261 holes were drilled on the Coates South Block from April–July 2022 for a total of 3,118 m (Table 12). Data from these holes form the basis of the MRE presented in this Report. The drilling programme comprised both exploration and hydrological drilling and was designed to infill the historical drill grid and, in general, followed a grid on a line spacing of 120 m in the north–south direction and a hole spacing of 20 m in the east–west direction (Figure 23). Some holes were repositioned to allow for rig access in bogged areas. All holes were drilled vertically, approximately perpendicular to the sub-horizontal mineralisation.

Table 12: Summary of 2022 drilling on Coates South Block.

| Drill type | Coates South Block | |
|---|---|---|
| | No. holes | Metres (m) |
| **Aircore** | 192 | 2,408 |
| **Aircore: Twin** | 8 | 106 |
| **Aircore: Redrills** | 37 | 260 |
| **Sonic: Twin** | 4 | 51 |
| **Resource Definition Total** | 241 | 2,825 |
| **Aircore: Water monitoring** | 20 | 293 |
| **Programme Total** | 261 | 3,118 |

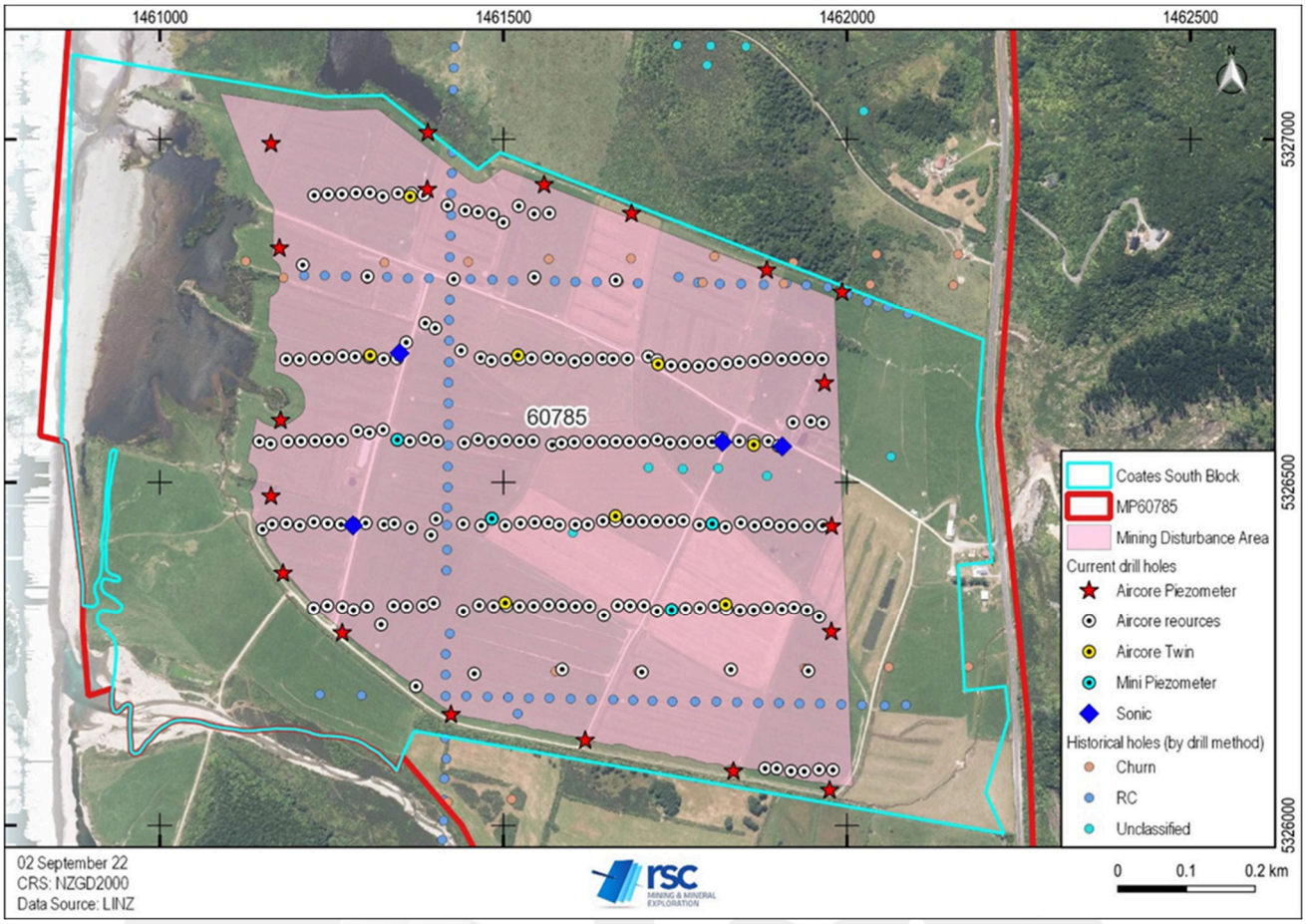


Figure 23: Distribution of 2022 drilling at Coates South Block.

Following a period of slower-than-expected drilling with the aircore rig, Alton Drilling arranged for a sonic rig to carry out trial drilling. The sonic rig was used to twin four aircore holes and demonstrated highly improved recovery (98% average for sonic core compared to 73% average for aircore) and speed of drilling (~1 minutes per sample (sonic) vs. tens of minutes for aircore). After the sonic holes were completed, TiGa decided to continue the programme with the original aircore rig.

All holes drilled range in depth from 7–19 m, with an average depth of 12.5 m. A total of 20 holes were drilled as dedicated water-monitoring holes and were installed with piezometers for monitoring by Komanawa Solutions. No samples were collected from the water-monitoring holes.

Three types of 'twin' drilling were undertaken:

- eight twin aircore holes were completed to test the short-range variability of the mineralisation;
- ten historical aircore twins were drilled to verify the quality of the historical drilling over the Coates South Block; and,
- four sonic–aircore twin holes were completed to test the quality of the aircore drilling.

Zones with high clast-size variability were difficult for the aircore bit to penetrate, typically due to the presence of large beach stones and cobbles, and a hammer bit was used to penetrate these horizons. Additionally, low recoveries were encountered

in the upper sections of the holes due to the unconsolidated nature of the sediments, and dry-plugging was used to improve sample recoveries in the top 0–6 m.

Sample recovery was poor at the start of the programme as the drillers worked to get familiar with the ground conditions. Recovery improved throughout the programme and averaged 73% across the drilled area. RSC reviewed the distribution of samples with low recovery and thirty-seven holes were fully or partially redrilled. Superseded samples that remained unprocessed by the time of drilling were eliminated from processing, dried and sent to storage.

## 5.2 Geophysics

In 2016, TiGa (then Barrytown Joint Ventures/Alloy Resources) commissioned Southern Geoscience Consultants (SGC) to reprocess and interpret the airborne geophysical (magnetic and radiometric) data obtained in 2008 by NZ Gold Ltd for heavy mineral sand (HMS) targets. The data cover the entire Barrytown deposit. The original data processing in 2008 was also completed by SGC, but it was used to establish Au targets.

The magnetic data were processed to enhance shallow magnetic features associated with HMS strandline targets. Radiometric data identified zones of elevated Th response from HM at, or very close to, surface. The processed magnetic/radiometric data, topocadastral GIS files and satellite imagery, were used to generate a 1:20,000-scale interpretation focused on HMS targets.

The interpretations were primarily based on the delineation of strandline HMS targets using magnetic images and profiles and supported by radiometric and satellite imagery. Approximately 140 magnetic strandlines and 35 associated thorium anomalies were identified over the entire deposit (Wallace and Peters, 2016). Several moderately magnetic and weakly magnetic strandline targets were identified within the Coates South area, and Coates South was also identified as an area of thicker cover.

The drilling and MRE work in this Report confirm the presence of strandlines associated with elevated concentrations of HM. Additionally, there is evidence of second-order strandlines running northeast-southwest (Figure 24) as suggested by both magnetic interpretation and variogram continuity analyses outlined in section 8.

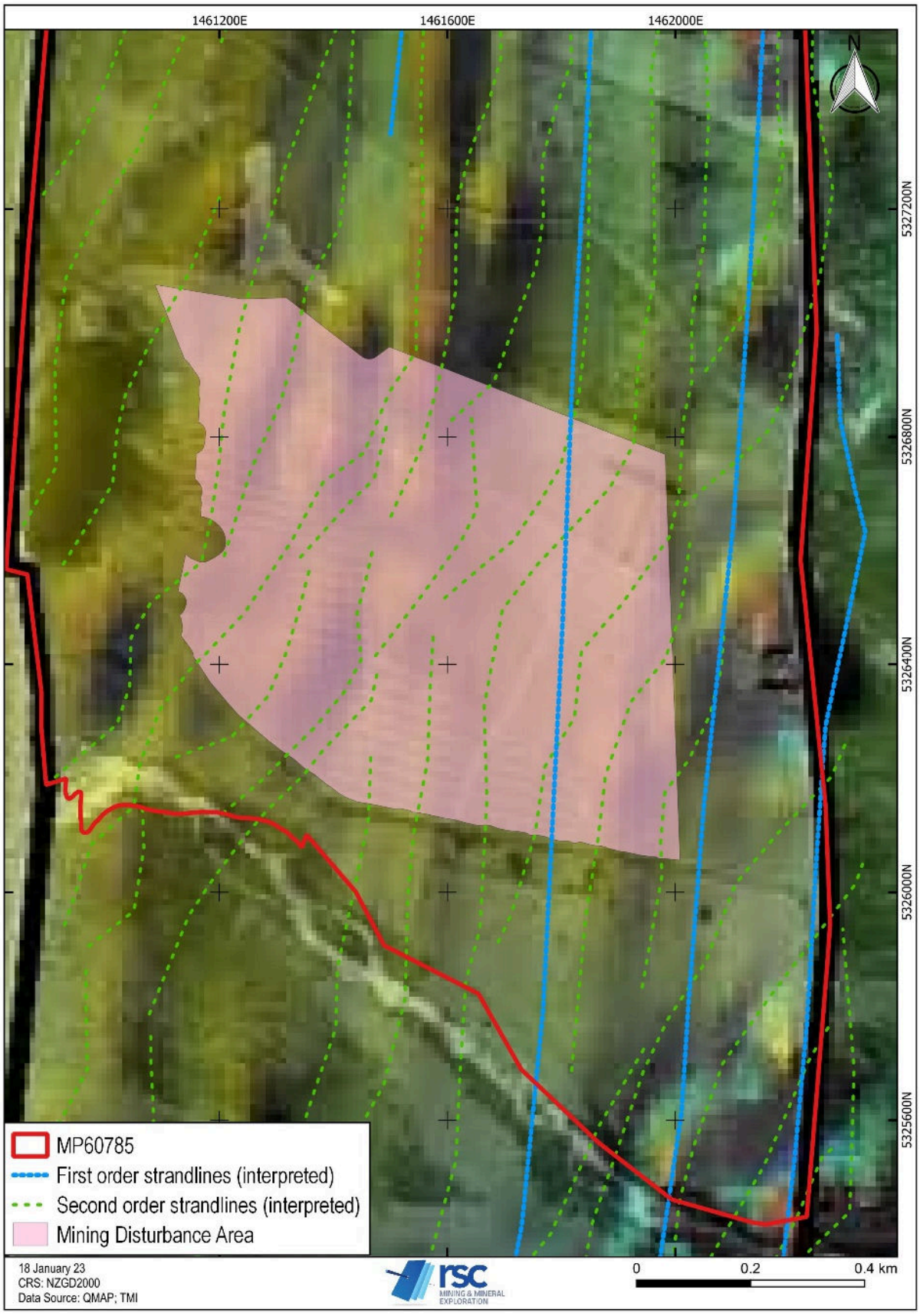


Figure 24: Interpretation of strandlines across Coates South Block from geophysical data (Vidanovich, 2008).

## 5.3 Petrography & Metallurgy

### 5.3.1 Sink-Float Testing

RSC evaluated data from sink-float test work carried out by IHC Robbins (IHC, 2022), the data were provided by email to RSC. The relationship between the Total Heavy Minerals (THM; as measured with sink-float testing) and the modelled VHM (ilmenite + garnet + zircon as modelled from pXRF geochemistry) was described by a linear regression model with a slope of 0.66 (Figure 25). In other words, 66% of the total heavy mineral fraction is comprised of the VHM minerals ilmenite, garnet, and zircon. The regression has an $R^2 = 0.87$, with the variance being the sum of both natural inherent variability in the mineral assemblage and the measurement uncertainty.

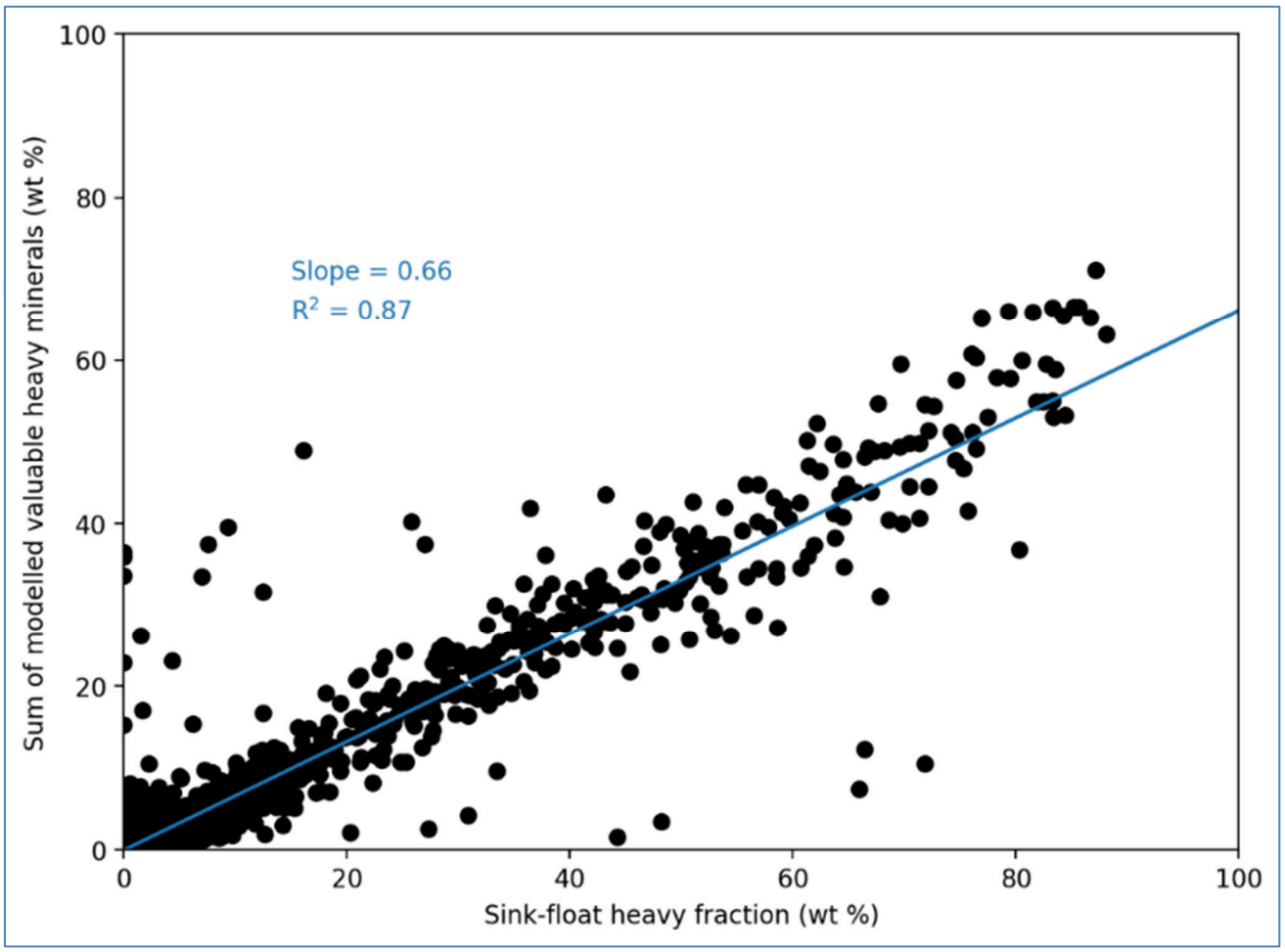


Figure 25: Comparison of modelled VHM fraction (derived from pXRF data) against the Total HM fraction (sink-float heavy fraction).

### 5.3.2 Metallurgy & Bulk Sampling

In 2017, TiGa (then Barrytown JV Ltd/Alloy Resources) completed metallurgical test work on 14 bulk samples (RSC, 2017).

Samples were analysed by Shandong Huate Magnet Technology Co Ltd (HUATE) and Allied Mineral Laboratories (AML). AML established a process flowsheet, incorporating stages of screening, gravity, electrostatic and magnetic separation. The

AML work demonstrated that ilmenite and garnet products could be produced through a simple processing circuit using electrostatic and magnet separators. Garnet products were described as visually similar but with varying yields across the composited samples.

During 2022, one bulk sample was collected by TiGa for mineral processing and characterisation work at IHC Robbins. A pit was excavated by TiGa from the Coates South Block at 1,461,374 mE / 532,6799 mN for preparation of a bulk sample. The site was selected by RSC due to the occurrence of mineralisation at surface (Figure 26), ease of access for equipment, and presence of grade representative of this area as indicated by historical data. The pit was excavated by TiGa staff to a depth of ~3.5 m, providing a ~2.5-tonne bulk sample. The material was excavated by hand, shovelled into large plastic bins, and sent to IHC Robbins in Australia.

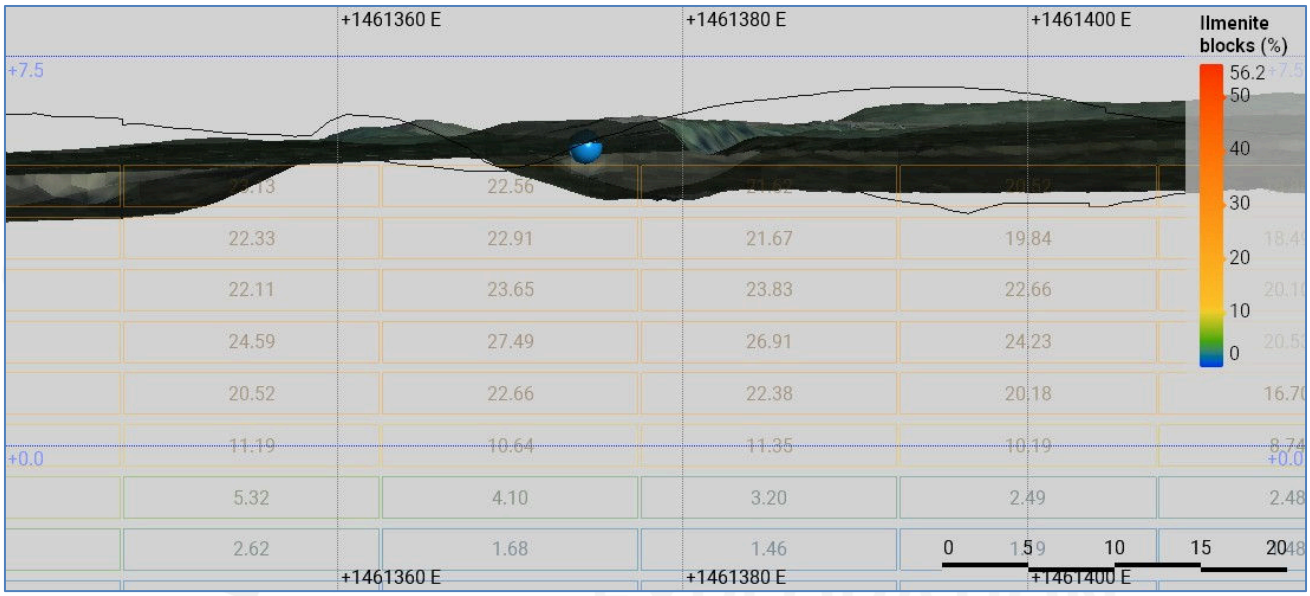


Figure 26: Cross-section showing location of bulk pit 1 (blue), looking north, with 2018 ilmenite block model.

Following RSC's recommendation to collect an additional, more broadly representative, sample, a second bulk sample was assembled from coarse crush rejects from the 2022 drilling. Approximately 1.4 tonnes of material from selected mineralised intervals across the central and eastern portions of Coates South Block was assembled (Figure 27). The results of these tests were not available on the publication date of this Report.

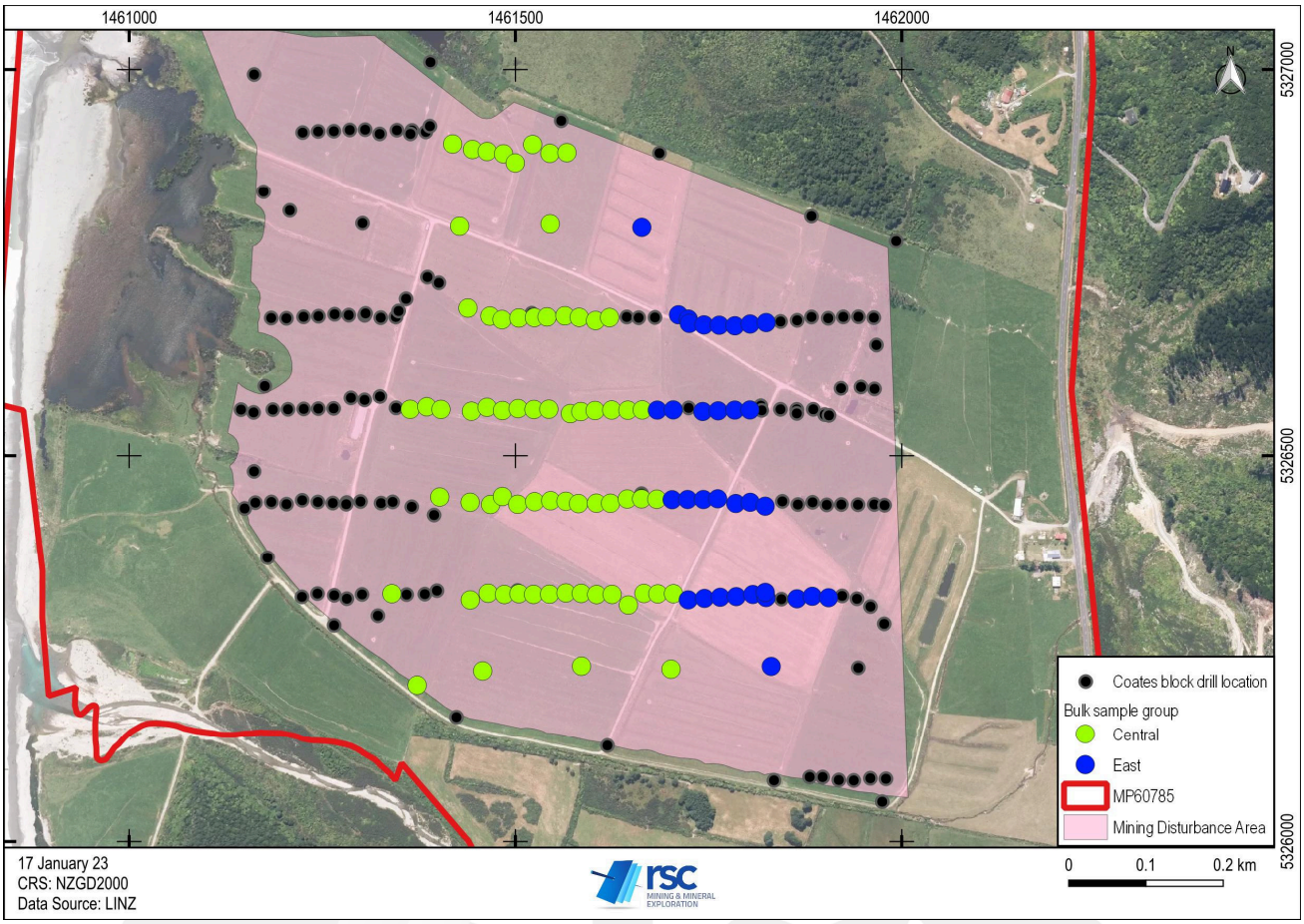


Figure 27: Distribution of samples from the central and east zones, as used in the second bulk sample.

## 5.4 Mineral Composition

Mineral inclusion data provide important information for product specification. Product specification is an important principle in the estimation of industrial minerals and must be addressed by the Competent Person under clause 49 of the JORC Code (2012). This means that, in addition to determining the abundances of heavy minerals, garnets or ilmenite (i.e. the 'products), an assessment of any impurities and any other deleterious compositional qualities of these products must be made.

### 5.4.1 Garnet

Quantitative Energy Dispersive Spectroscopy (EDS) analyses were undertaken on a representative selection of 120 garnet grains. This shows that the chemistry of the garnets at Barrytown falls within the expected range published in the literature (e.g. Ritchie et al., 2019; Figure 28). The garnet population is dominated by almandine, along with a more spessartine-like composition and a population intermediate between the two (Table 13). The garnet grains are largely free of mineral inclusions.

The median grain size for garnet, as observed by SEM automated mineralogy is ~100 µm. Figure 29 presents particle size distributions for each of the samples analysed by SEM, with the mean of 59 samples shown in black.

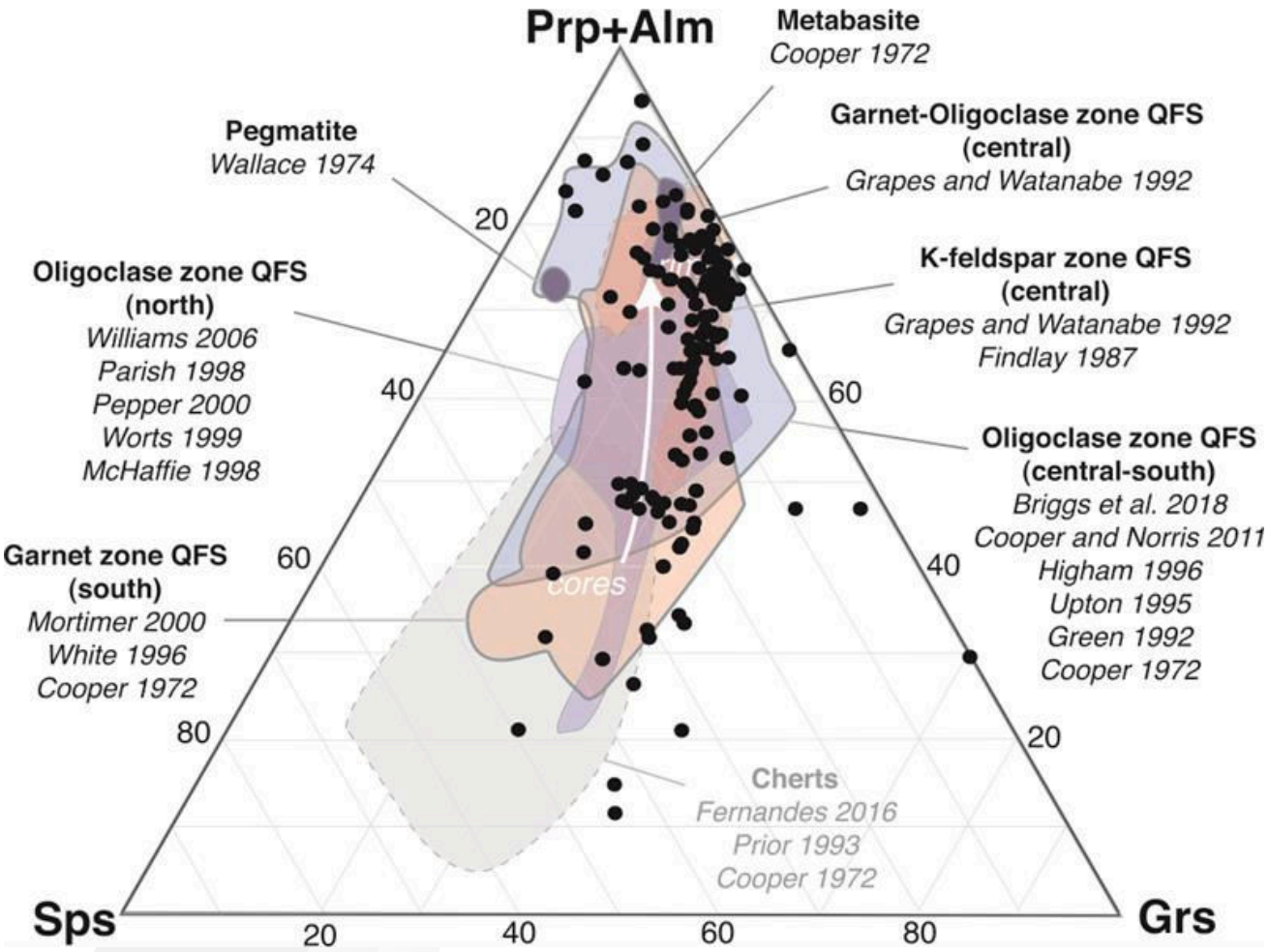


Figure 28: Garnet compositions from Barrytown samples (black circles) plotted over garnet compositions in the literature (e.g. Ritchie et al., 2019).

Table 13: Average compositions by an average of measurements on twelve grains of almandine, spessartine and intermediate compositions.

| | MgO (wt%) | $Al_2O_3$ (wt%) | $SiO_2$ (wt%) | CaO (wt%) | $TiO_2$ (wt%) | MnO (wt%) | FeO (wt%) | Total (wt%) |
|---|---|---|---|---|---|---|---|---|
| **Almandine** | 1.81 | 22.41 | 29.17 | 8.48 | 0.12 | 1.56 | 36.02 | 99.57 |
| **Spessartine** | 0.74 | 22.00 | 28.74 | 11.36 | 0.32 | 12.28 | 23.84 | 99.28 |
| **Intermediate** | 1.11 | 22.11 | 28.81 | 10.73 | 0.17 | 6.37 | 29.74 | 99.03 |

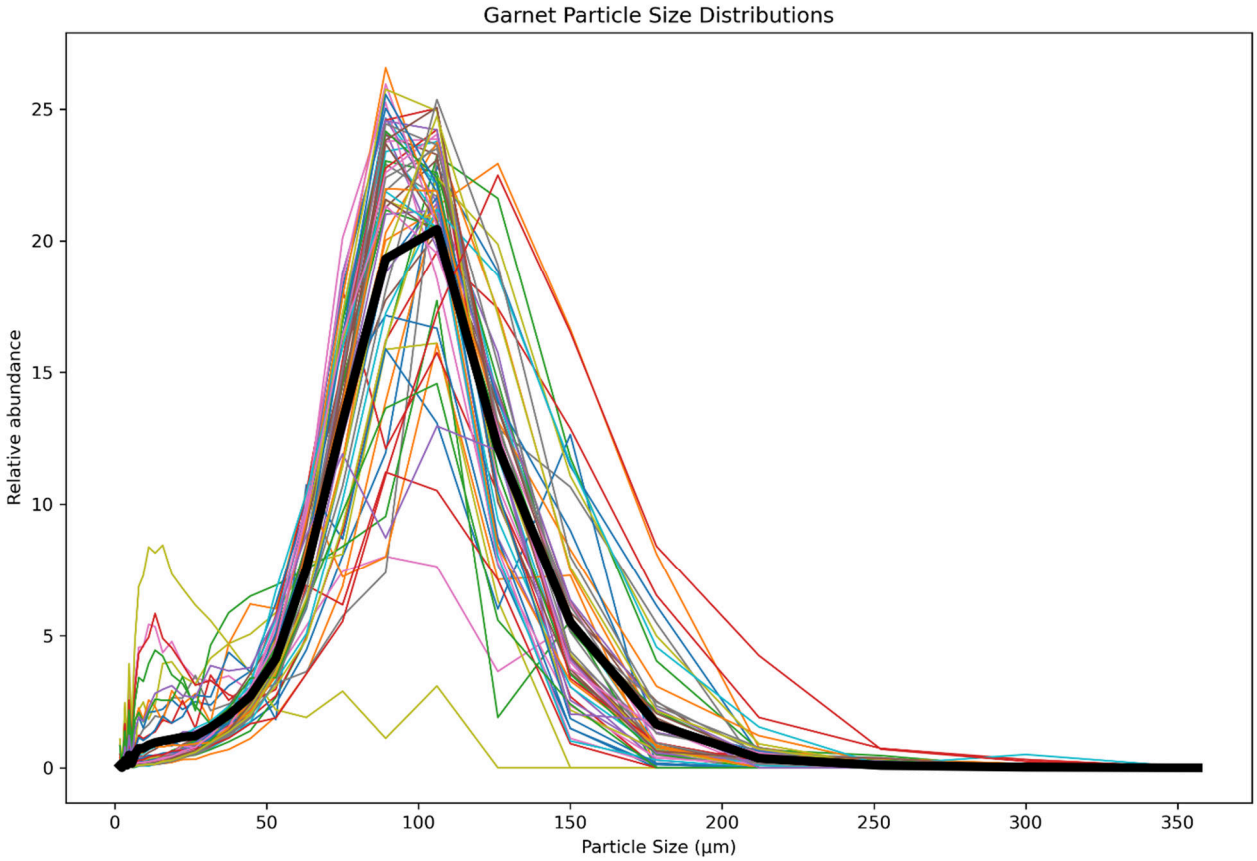


Figure 29: Particle size distributions of garnet grains from SEM analysis. The mean of all measured samples is shown by the bold black line.

### 5.4.2 Ilmenite

Ilmenite grains in the Barrytown deposit contain multiple large inclusions of other minerals; an example of the inclusions within ilmenite as mapped by SEM is presented in Figure 30. The median grain size for ilmenite, as measured by SEM automated mineralogy is ~75 microns. Figure 31 presents particle size distributions for each of the SEM samples, with the mean of 59 samples shown in black.

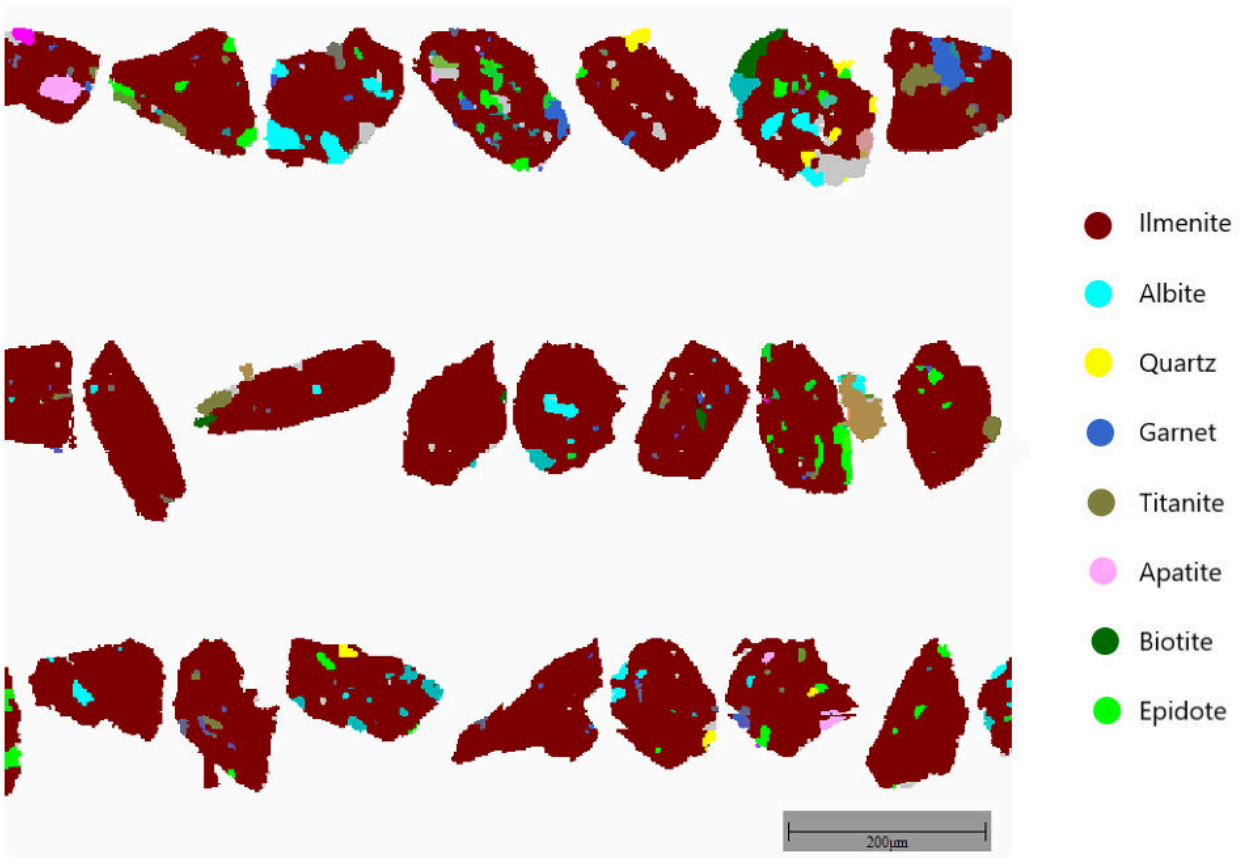


Figure 30: Example image of inclusions within ilmenite as observed by SEM automated mineralogy. These grains are from sample 202910, and are typical of the size, abundance and diversity of mineral inclusions seen across the entire deposit.

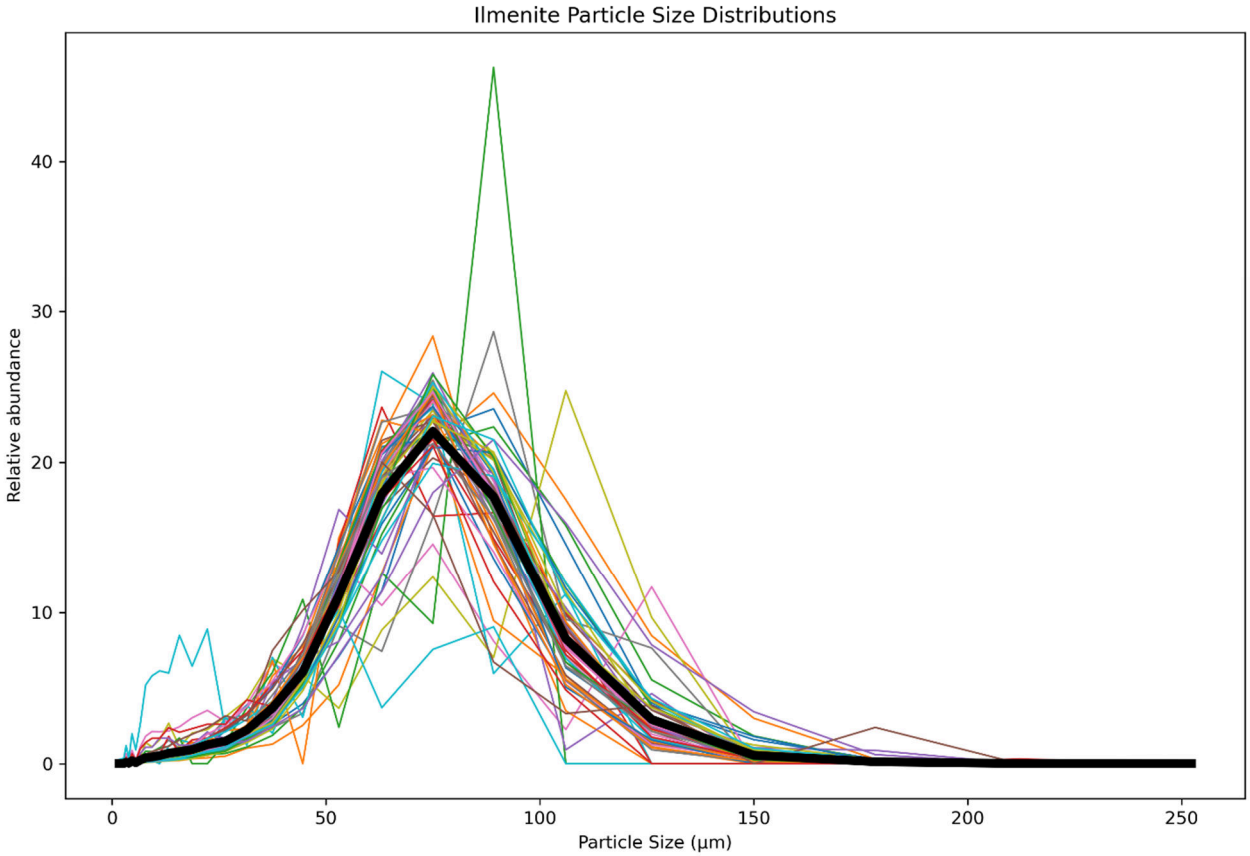


Figure 31: Particle size distributions of ilmenite grains from SEM analysis. The mean of all measured samples is shown by the bold black line.

## 5.5 Surveying, Topography, DTM

LiDAR data for the Project were collected in 2020 and 2021. The LiDAR survey was flown by Aerial Surveys Ltd. The associated 1-m resolution digital elevation model (DEM) was provided to TiGa by Aerial Surveys in NZTM2000 horizontal and NZVD2016 vertical datums, with accuracy specifications of ± 1.0 m (95%) horizontal and ± 0.2 m (95%) vertical. This DEM was used in the geological and estimation domain modelling described in section 8.

# 6 Sampling, Preparation, Analysis

## 6.1 Drilling

The 2022 drilling programmes comprised of aircore and sonic drilling for resource definition and hydrological purposes. All drillhole collar locations were surveyed in place in advance of drilling by Mike Robbins of Davis Ogilvy & Partners Ltd using a Trimble RTK GNSS with R10 rover and base units. To establish local control, two survey reference marks were used: LINZ geodetic code EV77 (OITI DP3017) for the Coates South Block and ADQ1 (Barrytown) for the Barrytown Farms' block. All collars were surveyed during the programmes and resurveyed at the end of the programme by RSC using handheld Garmin GPS Map60.

All aircore drilling was undertaken by Alton Drilling using an ADL Manufactured Multipurpose Rig mounted on an MST-600VD crawler using a 3-inch hammer (~76 mm) and a 200 psi (400 cfpm) compressor (Figure 32). The aircore samples were collected at 1-m intervals from the cyclone into labelled plastic bags by drill assistants.


Figure 32: Aircore drilling on Coates South Block.

The sonic drillholes were drilled by Pro-Drill using a FrasteXL1 remote tracked rig, using 150 Hz frequency and 127 mm casing, and producing 83-mm diameter core. Samples were drilled in 1-m intervals and core was collected from the drill string into a plastic receiver and slotted directly into a labelled core box. The core trays were wrapped in preparation for density measurements and sampling at NZIMMR.

No downhole surveys were conducted on any holes due to the vertical orientation of the drillholes, and shallow nature of the drilling (< 19-m).

All samples were weighed in the field-by-field assistants using spring scales. RSC geologists then logged each sample using a logging board for visual representation, and a small portion was placed into chip trays. Groups of ~40–60 samples were packed into large polyweave bulk bags prior to transportation to the sample preparation facility at NZIMMR.

## 6.2 Sample Preparation

A laboratory sample preparation process was developed by RSC (Figure 34), and adapted during the programme following consultation with TiGa, Palaris, IHC Robbins, and NZIMMR. The sample preparation plan was adjusted several times at TiGa's request, to improve sample processing times, and minimise transportation costs due to sample weights. These adaptations and adjustments resulted in differences in sample preparation over time, which in turn resulted in differences in sample data quality. This has been taken into consideration in the classification by the Competent Person. Sample preparation and analyses were carried out at several facilities due to the wide range of data required, and limitations with laboratory capacity on the West Coast. The flow chart presented in Figure 33 and Figure 34 presents the entire sample preparation procedure and highlights which parts of the procedure changed over time.

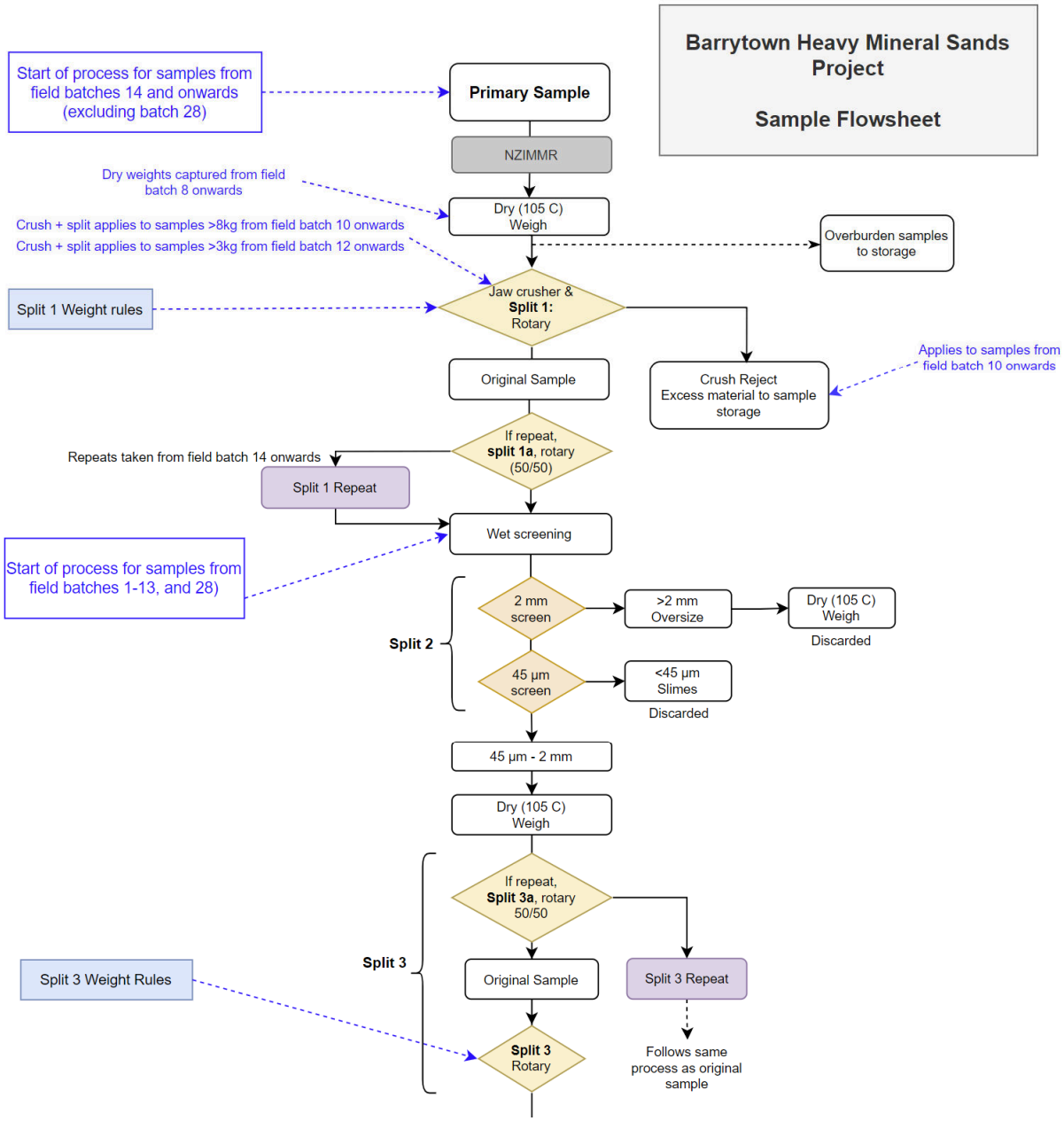


Figure 33: 2022 TiGa drill sample processing flow chart (continues in Figure 34).

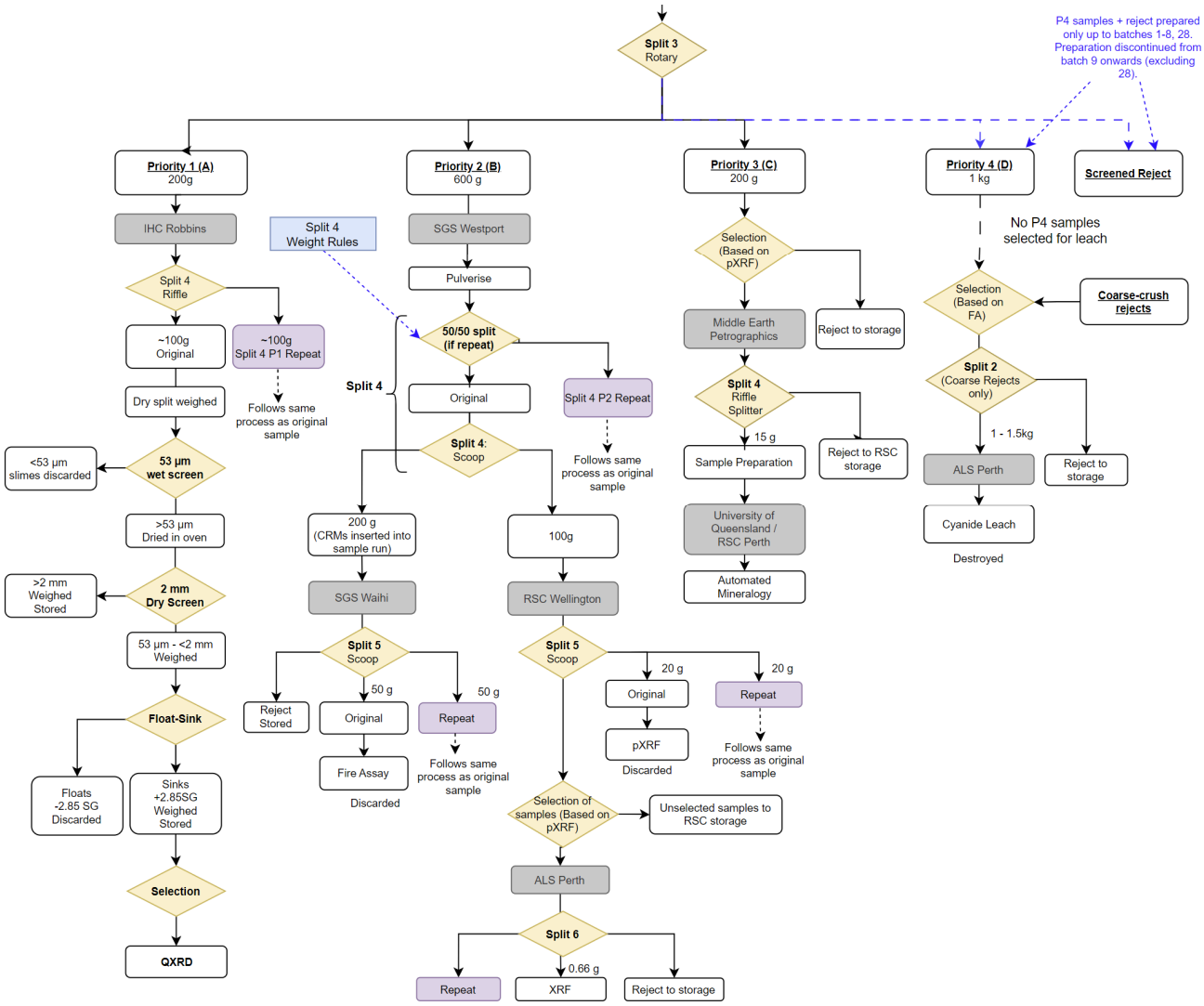


Figure 34: 2022 TiGa drill sample processing flow chart (continues from Figure 33).

NZIMMR processed samples in order of field batch number, according to the sample preparation flowsheet and associated splitting and weight guidance. Overburden samples were stored without any preparation other than being dried. A total of 67 field batches were created, with an average of 47 samples in each (ranging from 29–62).

At the start of the project, the samples went straight to the wet screening stage (field batches 1–9 and 28). During this time, it was noted that the drying time of the 0 µm to 45 µm slimes fraction was much longer than anticipated, causing significant delays to the project timeline. To mitigate this, the process was adapted to include a primary drying stage to obtain a dry sample weight of the entire sample prior to wet screening. This eliminated the need to dry the slimes fraction.

Samples of field batches 10–27 and 29–67 were dried in an Alsto M2, 2-m$^3$ drying oven for ~12 hours at 105°C and weighed.

As a result of the drying, many samples solidified and required deagglomerating using a jaw crusher. Samples of field batches 10–14 were crushed, and the entire crushed sample was wet-screened.

Following the completion of field batch #14, TiGa decided to reduce the sample size to improve the efficiency of the screening and drying procedures. Samples from field batch #14 onwards were crushed and split (Split 1) in a Rocklabs Boyd Elite jaw crusher and rotary sample divider combo (Figure 35). Fluctuating sample recoveries in combination with variable water content caused high variability in sample weights (0–30 kg). NZIMMR developed weight guidance rules to achieve targeted split weights (Table 14).

Repeat samples were collected approximately once every 20 regular samples. In the case of repeat samples, the first split stage consisted of two separate steps. First, the primary sample was passed through the crusher-RSD combo to create a subsample with a weight approximately twice that of a regular sample (~8 kg, split step 1). Next, this subsample was passed through the crusher-RSD combo again to create two subsamples with equal weights (~4 kg each, split step 1a).

For selected samples from field batches 10–27 and 29–67, about 1–1.5 kg was split from the split 1 rejects using the crusher-RSD combo and sent to ALS Perth for bulk leach extractable gold (BLEG) analysis using ALS sample code Au CN11. The samples were selected for BLEG analysis based on fire assay (FA) Au results.


Figure 35: The RockLabs crusher-splitter at NZIMMR.

Table 14: NZIMMR Split 1 weight rules for regular and repeat samples.

| Regular sample | | |
|---|---|---|
| **Dry Weight** | **% Split to Sample** | **% Split to Reject** |
| **<3.75 kg** | 100 | 0 |
| **>3.751–<5.0 kg** | 80 | 20 |
| **>5.01–7.5 kg** | 60 | 40 |
| **>7.51–15.0 kg** | 40 | 60 |
| **>15.01 kg** | 20 | 80 |
| **If repeat required** | | |
| **Dry Weight** | **% Split to Sample** | **% Split to Reject** |
| **<7.5 kg** | 100 | 0 |
| **>7.51–10 kg** | 80 | 20 |
| **>10.01–15 kg** | 60 | 40 |
| **15.01–30 kg** | 40 | 60 |

After Split 1, the samples were wet-screened (Split 2) using a 2-mm screen, followed by a 45-µm screen. The >2-mm (oversize/coarse) fraction was dried, weighed, and discarded. The 45 µm to 2 mm (silt/sand) fraction was dried at 105°C and weighed and retained; and the <45-µm (slimes) fraction was discarded with the wastewater. The slimes weights were determined by subtracting the weights of the dried reject and the weights of the dried 45 µm to 2 mm and >2-mm fractions from the dry weight of the full sample.

The dried 45 µm to 2 mm (silt/sand) fraction was split (Split 3) with a Rocklabs Rotating Sample Divider (Figure 35), producing four sub-samples.

- Priority 1 (P1', also labelled 'A): ~200 g for sink-float testing at IHC Robbins and Quantitative X-Ray Diffraction (QXRD) at Bureau Veritas.
- Priority 2 (P2', also labelled 'B): ~600 g which was sent to SGS Westport for further preparation to create two sub-samples:
  - 200-g pulp for 50 g Au fire assay (FA) at SGS, Waihi (SGS method code: FAA505); and
  - 100-g pulp for pXRF analysis at RSC, Wellington, and XRF analysis at ALS Geochemistry, Brisbane.
- Priority 3 (P3', also labelled 'C): ~100 g for automated mineralogy using AMICS scanning electron microscopy at the University of Queensland, Brisbane, and RSC, Perth, on a Hitachi SU-3900 scanning electron microscope (SEM). The sample preparation and analytical conditions are discussed in section 6.3.
- Priority 4 (P4', also labelled 'D): 1–1.5 kg intended for BLEG analysis (method code Au-CN11) at ALS, Perth. Ultimately, none of the P4 samples were submitted for analysis.

NZIMMR developed a set of splitting rules for Split 3 to prioritise sample preparation where samples were underweight (Table 15). Split 3 repeat samples were collected approximately once every 20 regular samples, but only from samples with a silt/sand fraction weighing >2 kg. In the case of repeat samples, the third split stage consisted of two separate steps. First, the sand/silt fraction sample was passed through the crusher-RSD combo to create two subsamples with equal weights

(Split step 3a). Next, each subsample was passed through the crusher-RSD combo again to create the P1 to P4 subsamples (Split step 3).

Table 15: NZIMMR Split 3 weight and prioritisation rules.

| Sample Weight | Tray 1 (20%) | Tray 2 (20%) | Tray 3 (60%) |
|---|---|---|---|
| **<0.799** | Combine to P1 | | |
| **>0.8–1 kg** | Combine to P1 | | P2 |
| **>1.01–<1.5 kg** | P1 | P3 | P2 |
| **1.501–2.0 kg** | P1 | P3 | P2 |
| **2.001–4.0 kg** | P1 | P3 | P2 |

The P1 samples were sent to IHC Robbins, Brisbane, for float-sink test work and prepared according to the flow chart in Figure 36. Samples were reduced to 100 g using a riffle splitter, soaked in buckets overnight and screened using a 53-µm sieve. The soaking and use of the finer screen were employed to break any agglomerated particles and prevent them from misreporting to the oversize fraction. The oversize was dried and screened using a 2-mm sieve and the undersize was discarded. The +2-mm fraction was weighed, bagged, and stored. Approximately 100 g of sample was separated using heavy liquid (lithium heteropolytungstate) separation to separate the ±2.85 g/cm$^3$ fraction. Repeat samples were collected approximately once every 20 regular samples.

The P2 samples were pulverised at SGS Westport to 85% passing <75 µm, and split using a scoop to create two, 200-g subsamples. One subsample was analysed by pXRF by RSC (see section 6.3 for details), the other by 50-g FA at SGS Waihi (SGS method code FAA505). Repeat samples were collected at SGS Westport for both sample streams at a rate of ~5% (or 1 in 20). Splitting rules were developed to manage the division of material for low-weight samples (Table 16).

Table 16: Splitting rules for P2 samples at SGS Westport.

| P2 Sample Weight | Sample Weight FA Split | Sample Weight pXRF Split |
|---|---|---|
| **>250 g** | 200 g | >50 g |
| **150–250 g** | 100 g | 50–100 g |
| **70–150 g** | 50 g | 20–100 g |
| **30–70 g** | 30 g | <40 g |
| **<30 g** | Record as No Sample for FA | <30 g |

The P3 samples were prepared for SEM analysis by the methods outlined in section 6.3.4.1.

The P4 samples were prepared from the Split 2 silt/sand fraction for all samples from field batches 1–9, and 28. Preparation of the P4 samples was discontinued part-way into the programme, at the instruction of TiGa, to improve sample preparation times. Fire assay results from the P3 samples were used to determine which samples to submit for cyanide leach assay. None of the P4 samples were assayed.

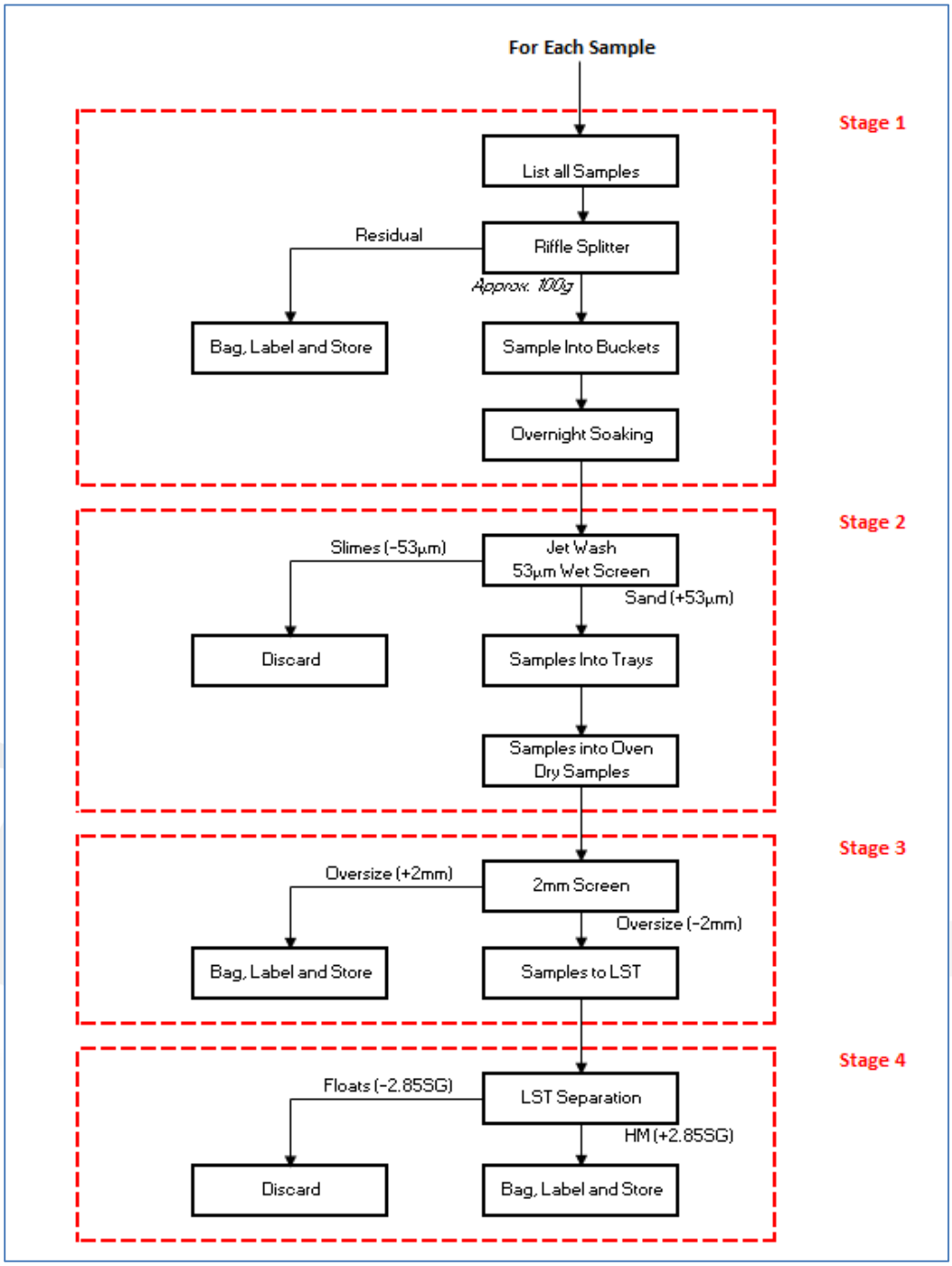


Figure 36: IHC Robbins' sample preparation process for sink-float analyses.

## 6.3 Analysis

### 6.3.1 Portable X-Ray Fluorescence

A total of 2,226 samples were analysed by pXRF by RSC to produce a multi-element geochemical dataset. All pXRF samples are derived from a pulverised split of the Priority 2 split of the 45 µm to 2 mm screened fraction (see section 6.2). Samples were analysed with an Olympus Vanta VMR instrument with a 4 W, 50 kV rhodium anode and a large-area silicon-drift detector. The instrument was operated using a field test stand and a laptop with the Vanta PC Software (software

version 3.30.106). The approach adopted by RSC follows industry best practice as outlined in Fisher et al. (2014) and Gazley and Fisher (2014).

To prepare the sample for analysis, about 20-g of sample material was collected from the plastic sample bag using a spoon and poured into a 40-mm sample cup with one end covered by 4-µm polypropylene film. The sample cup was put in the test stand and analysed using 3-beam Geochem mode. A beam — also referred to as a filter — is a combination of voltage and amperage that allows different elements to be detected. Analysis times were set to 15 s for each beam. To ensure the quality of the pXRF data, standard operating procedures were strictly adhered to, which included a solid quality control framework.

The pXRF data were corrected using calibration plots derived from certified reference materials (CRMs) inserted and analysed for each analytical session. The calibration plots are based on the expected values of the CRM plotted against the measured values of the CRM samples (Fisher et al., 2014). The gradient of the linear fit between the expected and the measured values defines the correction factor used to correct the elemental data (Figure 37).

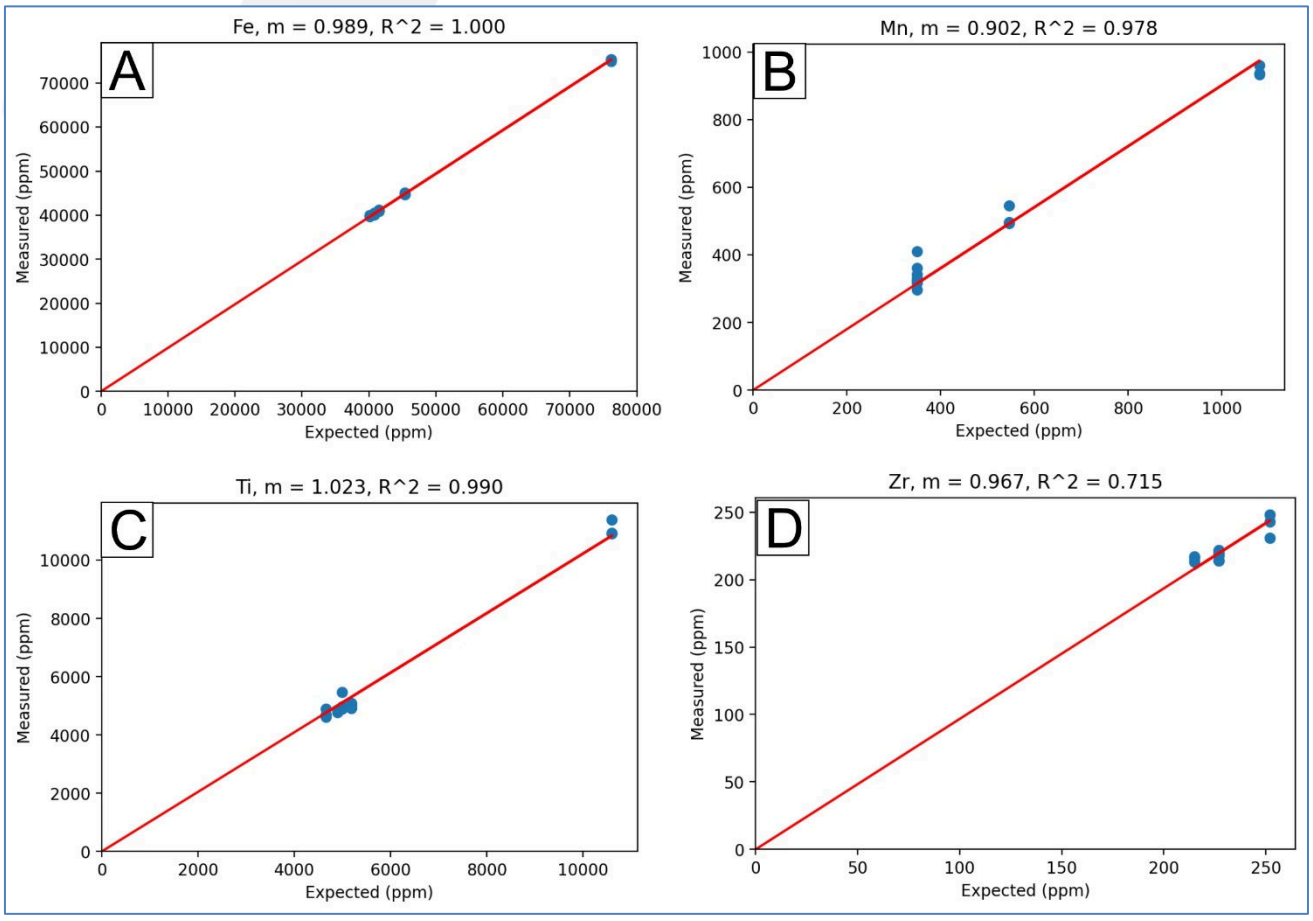


Figure 37: Example of calibration plots to correct geochemical data collected on the 20/09/2022 for: A) Fe; B) Mn; C) Ti; and D) Zr.

### 6.3.2 Laboratory XRF

A total of 119 samples were selected from pXRF data and sent for laboratory XRF analysis at ALS Geochemistry, Brisbane. The samples were selected to cover the full range of variability of the geochemistry dataset. This means that the validation sample set includes samples with close to the highest and lowest measurements as well as a range of intermediate measurements in every element used in the mineral abundance models. Three tablespoons of material were scooped from each sample and poured into paper bags labelled with the sample ID. The subsamples were analysed for whole-rock geochemistry using ME-XRF21u + ME-GRA05, with 24 analytes (plus total and LOI) as presented in Table 17. For laboratory XRF, a 0.66 g sample was scooped from the bag, fused with a Li-borate flux (including Li-nitrate) and poured into a platinum mould creating a disk. The disk was then analysed by X-ray spectrometry directly by the instrument; a summary of analytes and reporting ranges is provided in Table 17. Lithium-borate fusion and XRF finish is the standard industry method for the analysis of oxide iron (Fe) ores. Loss-on-ignition was calculated from thermogravimetric analysis using a TGA furnace. These laboratory XRF analyses also provided a quality check on the pXRF data (Section 6.3.1); the latter forms a key input to the MRE via a linear regression model to convert pXRF chemistry to mineralogy.

Table 17: ALS Brisbane detection limits for XRF analysis.

| Method Code | | Analyte | | | Unit | | | Lower Limit | | Upper Limit | |
|---|---|---|---|---|---|---|---|---|---|---|---|
| ME-GRA05 | | LOI | | | % | | | 0.01 | | 100 | |
| ME-XRF21u Analytes and Reporting Ranges | | | | | | | | | | | |
| | | Lower | Upper | | | Lower | Upper | | | Lower | Upper |
| Analyte | Units | Limit | Limit | Analyte | Units | Limit | Limit | Analyte | Units | Limit | Limit |
| $Al_2O_3$ | % | 0.01 | 100 | As | % | 0.001 | 1.5 | Ba | % | 0.001 | 10 |
| CaO | % | 0.01 | 40 | Cl | % | 0.001 | 6 | Co | % | 0.001 | 5 |
| $Cr_2O_3$ | % | 0.001 | 10 | Cu | % | 0.001 | 1.5 | Fe | % | 0.01 | 74.8 |
| $K_2O$ | % | 0.001 | 6.3 | MgO | % | 0.01 | 40 | Mn | % | 0.001 | 25 |
| $Na_2O$ | % | 0.005 | 8 | Ni | % | 0.001 | 8 | P | % | 0.001 | 10 |
| Pb | % | 0.001 | 2 | S | % | 0.001 | 5 | $SiO_2$ | % | 0.01 | 100 |
| Sn | % | 0.001 | 1.5 | Sr | % | 0.001 | 1.5 | $TiO_2$ | % | 0.01 | 30 |
| Total | % | 0.01 | 110 | V | % | 0.001 | 5 | Zn | % | 0.001 | 1.5 |
| Zr | % | 0.001 | 1 | | | | | | | | |

### 6.3.3 Gold Analysis by Fire Assay and Cyanide Leach

The P2 subsamples were analysed by 50-g FA at SGS, Waihi (SGS Code FAA505). The FA data were modelled in Leapfrog to create mineralisation domains. These domains were then used to select a number of samples for which a larger sample derived from the split 1 reject was submitted to ALS, Perth for BLEG analysis (ALS method code Au-CN11). BLEG provides more precise results than FA because the sample is larger and grouping-and-segregation errors are eliminated.

### 6.3.4 SEM-based Automated Mineralogy

The MRE presented in this Report is based on the *abundance* of several *minerals* (ilmenite, garnet and zircon), collectively labelled 'VHM', and collectively called 'the product' from a JORC Code (2012) reporting perspective (see comments in section 5.4). The abundances of these minerals were calculated from geochemical data using linear regression models trained on mineral abundances measured in the same sample using automated mineralogy.

The geochemical data derived from pXRF, in combination with quantitative SEM-based automated mineralogy, were used to build a model to derive quantitative mineralogy for each sample, as inputs to the estimation process. Quantitative mineralogical data were obtained for each sample by automated mineralogy, and then using regression algorithms applied to multi-element geochemistry as discussed in section 6.3.4.4. The quantitative mineralogy data either directly measured by SEM or derived from the geochemistry provide the main input into the MRE.

The collection of quantitative mineralogical data by SEM-based energy-dispersive X-ray spectroscopy (EDS) is known as automated mineralogy. The sample surface is scanned by the SEM with a focused beam of electrons. The electron beam interacts with the atoms in the sample, and the reflected signal is detected to produce a backscattered electron (BSE) image of the scanned surface. The brightness of a BSE image is proportional to the mean atomic number of the material, which means that different minerals can be distinguished from each other using this image. The BSE images are used to segment the sample based on back-scatter intensity. Each segment is allocated an EDS analysis point, which the SEM collects automatically. The EDS spectra for each point are compared to a library or database of minerals which allocates a mineral to each point analysis and thus each area of the sample. This allows an abundance of each mineral to be calculated for each sample.

A total of 63 samples were analysed by SEM by RSC in October 2022. Samples were selected to represent the full chemical variability of the dataset as indicated in the principal-components analysis of eight elements (Figure 38).

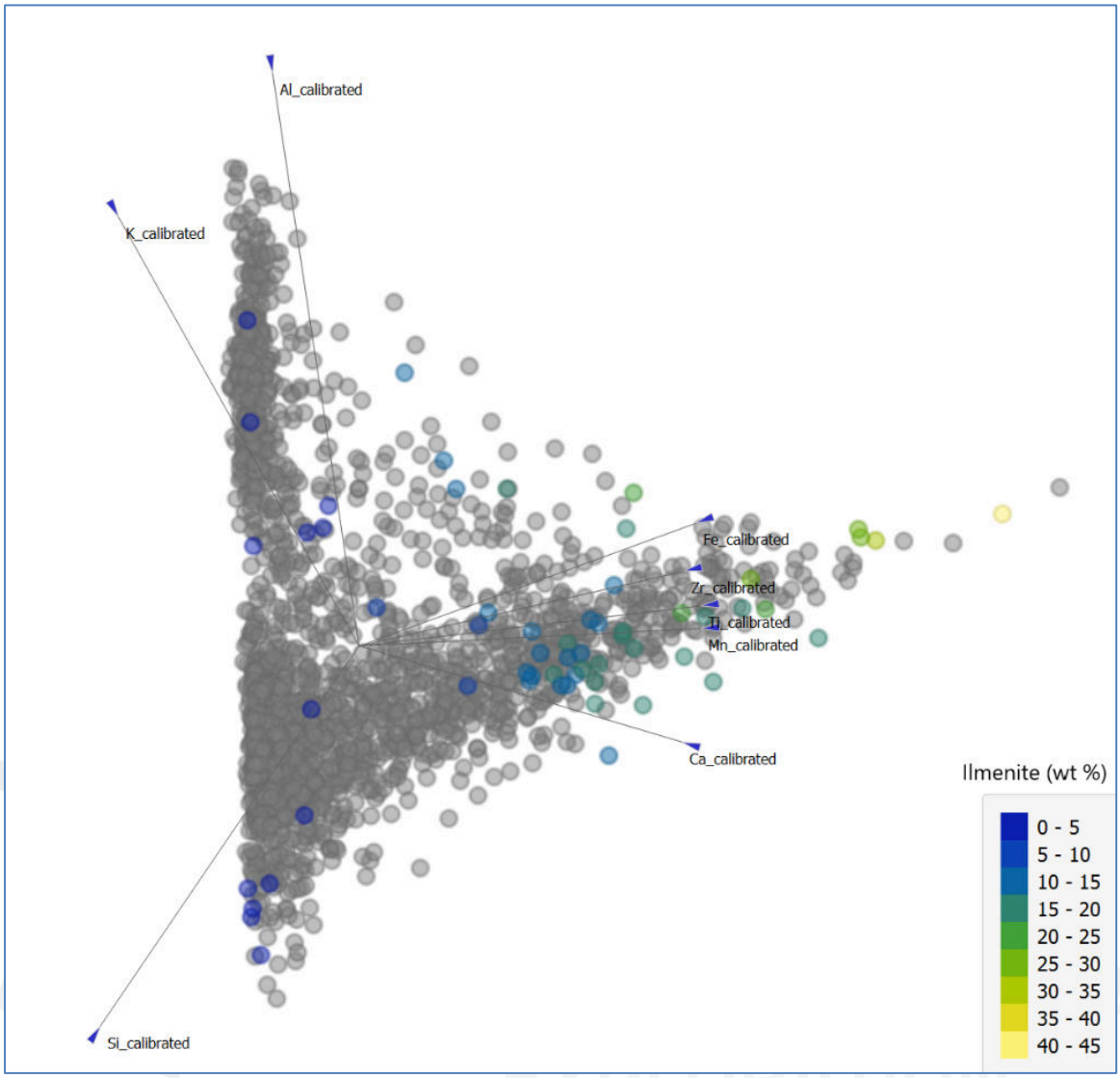


Figure 38: Principal Components Analysis of all samples for an eight-element sub-composition with samples selected for SEM analysis coloured by their ilmenite abundance.

### *6.3.4.1 SEM Sample Preparation*

Sample material used for the SEM analyses was derived from 70 P3 samples (200-g splits of the screened ~45 µm to 2 mm size fraction material) and was prepared by Middle Earth Petrographics. Samples were split to ~15 g using a Humboldt Micro and Precision Riffle Splitter and then set in a 25-mm epoxy round. Repeat samples were created at this stage. The hardened epoxy round was then cut in half vertically and remounted in a 30-mm epoxy round to expose the two cut faces for SEM analysis (Figure 39). Cutting the 25-mm round reduces the impact of any differential settling of the sample in the epoxy round by grain size and density. The sample face of the epoxy mount was then polished with water-soluble, polycrystalline diamond suspension (from 3 µm down to 1 µm) to produce a highly smoothed surface. The polished surface was coated with a 15–20 nm conductive carbon film before SEM analysis.

Figure 39: Prepared Barrytown samples loaded for SEM analysis.

### 6.3.4.2 *SEM Data Acquisition and Processing*

Samples were analysed in a Hitachi SU-3900 SEM with Quantax Q655-60-129 XFlash® EDS silicon-drift detectors using Bruker's AMICS software to control the SEM and process the data. Analysis was undertaken in particle mode, whereby backscatter intensity was used to segment the sample into individual grains for EDS spot analyses, for each grain to quantify the mineralogy of the sample in a fast and efficient manner. The EDS spectra for each point are compared to a library or database of minerals that was updated from the generic database to be specific to the Barrytown project. This library allocates a mineral to each point analysis and thus each area of the sample. Therefore, mineral abundances can be calculated for each sample.

### 6.3.4.3 *SEM Geochemical Reconciliation*

As part of processing the AMICS data, a geochemical composition for each sample was calculated from the measured mineral abundances in the samples, and this was used as an internal check on the chemistry of the minerals (Figure 40 and Figure 41). This step provides information to optimise the choice of chemistry for each mineral in the library and allows for a project-specific library to be generated where the composition of each mineral matches those present in the samples.

Data from only 59 samples were used, as quality issues and/or anomalies warranted the exclusion of data from some of the samples. Many of the excluded samples contained remnant agglomerations of fine material (Figure 42), which likely indicates incomplete washing and screening by NZIMMR. The presence of fine particles led to substantially longer SEM analysis times than clean (well-washed) samples and resulted in erroneous data. A couple of the samples contained organic material (Figure 43); data from these parts of these samples were excluded.

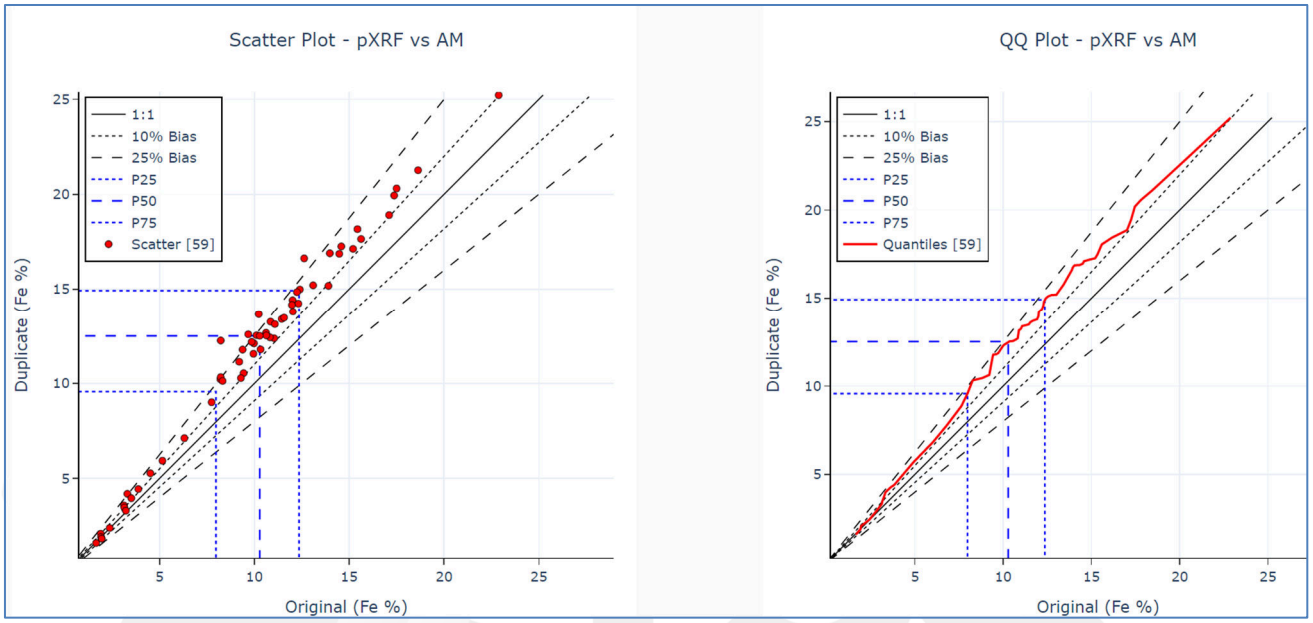


Figure 40: pXRF geochemistry compared with SEM-derived geochemistry for Fe. Left panel: point scatter; right panel: QQ plot.

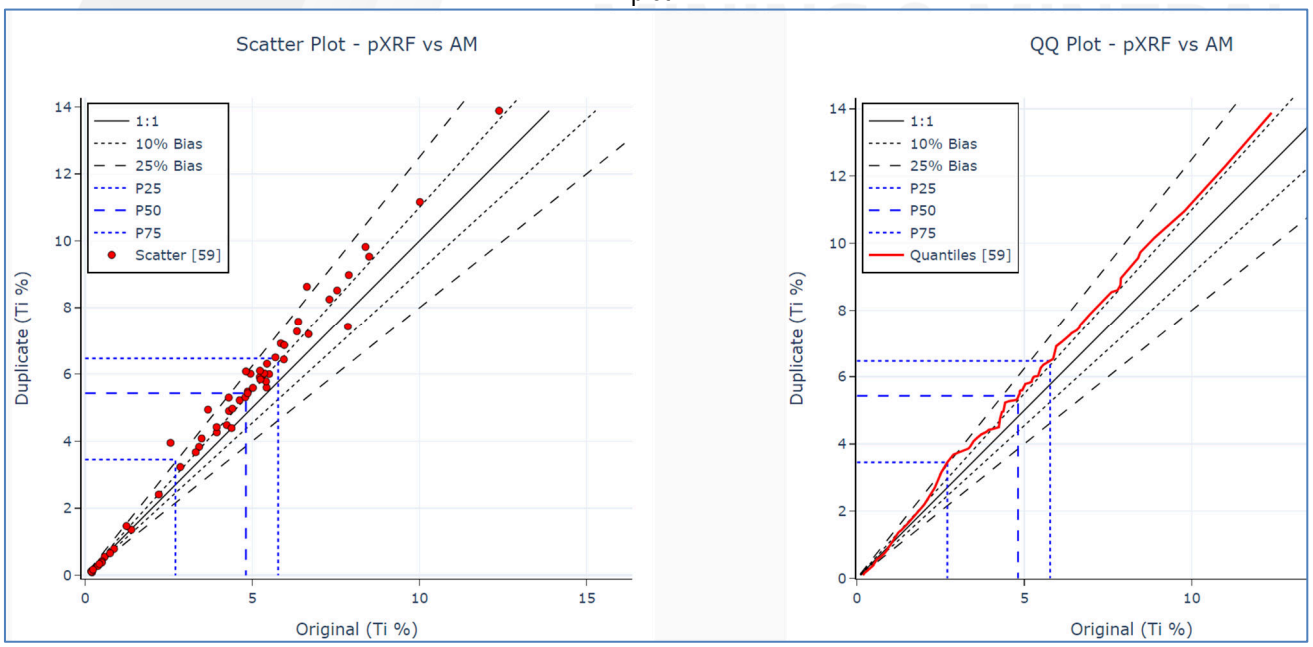


Figure 41: pXRF geochemistry compared with SEM-derived geochemistry for Ti. Left panel: point scatter; right panel: QQ plot.

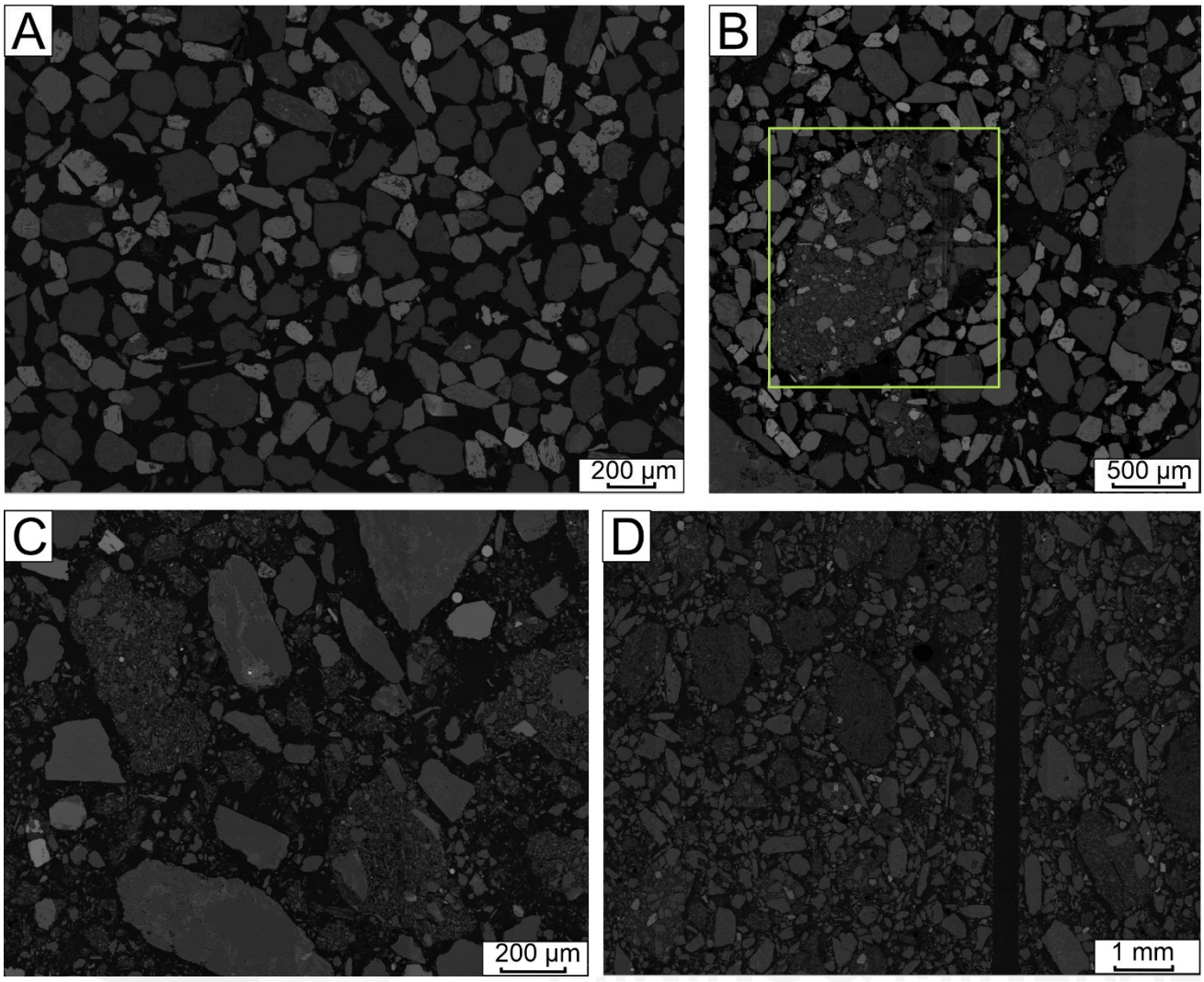


Figure 42: SEM BSE images of (A) a clean sample; (B-D) agglomerations of particulate material.

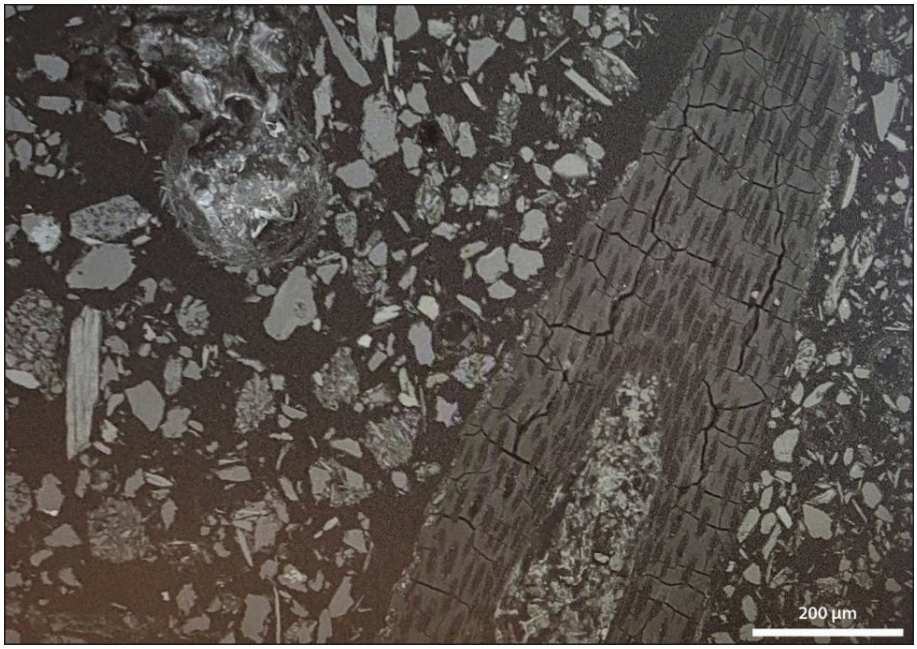


Figure 43: SEM BSE image of organic material.

#### 6.3.4.4 *Heavy Mineral Abundance from SEM-Chemistry Regression*

Linear regression models were built using the linear regression algorithm in the scikit learn package in Python (sklearn.linear_model.LinearRegression), to model abundances of ilmenite, garnet, and zircon from pXRF data based on nine elements: Al, Ca, Fe, K, Mn, Si, Ti, Y, Zr. The mineral abundances, measured by SEM automated mineralogy from 59 samples were used as the training data.

The performance of the models in estimating mineral abundances for samples unseen[3] in the training dataset was estimated using test-and-train datasets with bootstrap sampling. RSC used Python's scikit-learn machine-learning library for the bootstrap sampling. The models used to calculate the mineral abundances were trained on the full set of available automated mineralogy data; however, the performance metrics reported in Table 18 were calculated using data previously unseen by models that were trained on a same-sized sample of the data created with bootstrap resampling (Figure 44). Lastly, calculated mineral abundances based on the laboratory-derived XRF geochemistry data were compared with SEM-derived mineral abundances as a check of model performance (Figure 45).

Table 18: Model performance metric mean-absolute error (MAE) expressed as percentages of measured mineral abundance. The relative errors are largest for the lowest grade samples. The performance metrics are calculated below for test samples above 1%, 2%, and 4% ilmenite cut-off abundances.

| Model | MAE 1% cut-off | MAE 2% cut-off | MAE 4% cut-off | $R^2$ |
|---|---|---|---|---|
| **Ilmenite** | 16% | 9% | 10% | 0.98 |
| **Garnet** | 10% | 9% | 8% | 0.98 |
| **Zircon** | 24% | 18% | 19% | 0.95 |

Some holes in the ilmenite abundance training data were identified at both high abundances and around the likely resource cut-off. Hence, a further 16 samples were selected for analysis by SEM after the initial linear regression model was built to validate the calculated mineral abundance. These samples are not included in the statistics presented in (Table 18). The results are presented in Figure 45 and demonstrate that the model provides accurate and precise results.

[3] 'Unseen' refers to a blind dataset, that has not been involved in training the algorithms, its sole purpose is to define the performance of the classification/regression.

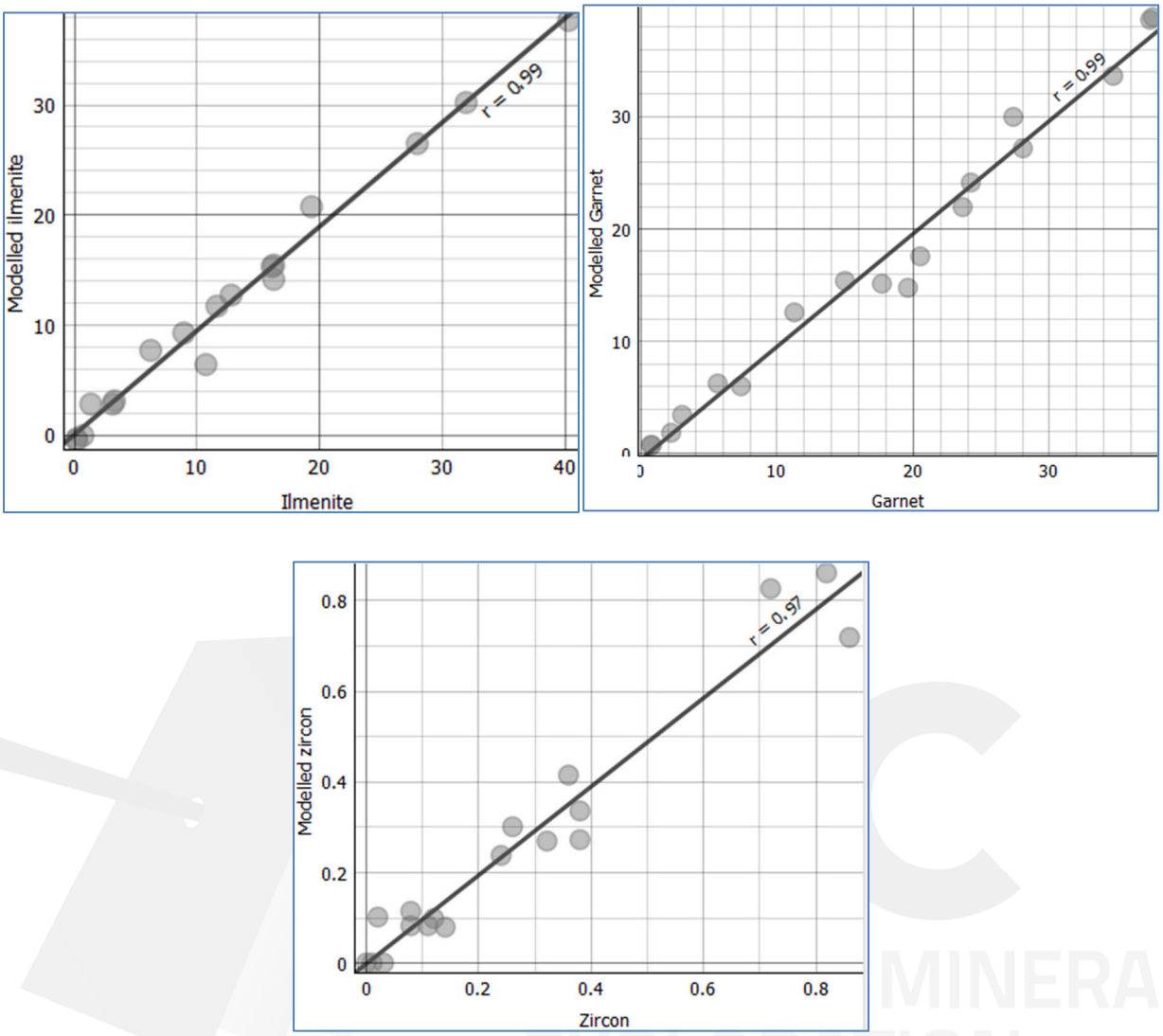


Figure 44: Modelled vs measured mineral abundances for the test dataset that were excluded from the training data for the purpose of model evaluation. All units are wt.%, with measured (SEM) values (x-axes) and modelled values (y-axes).

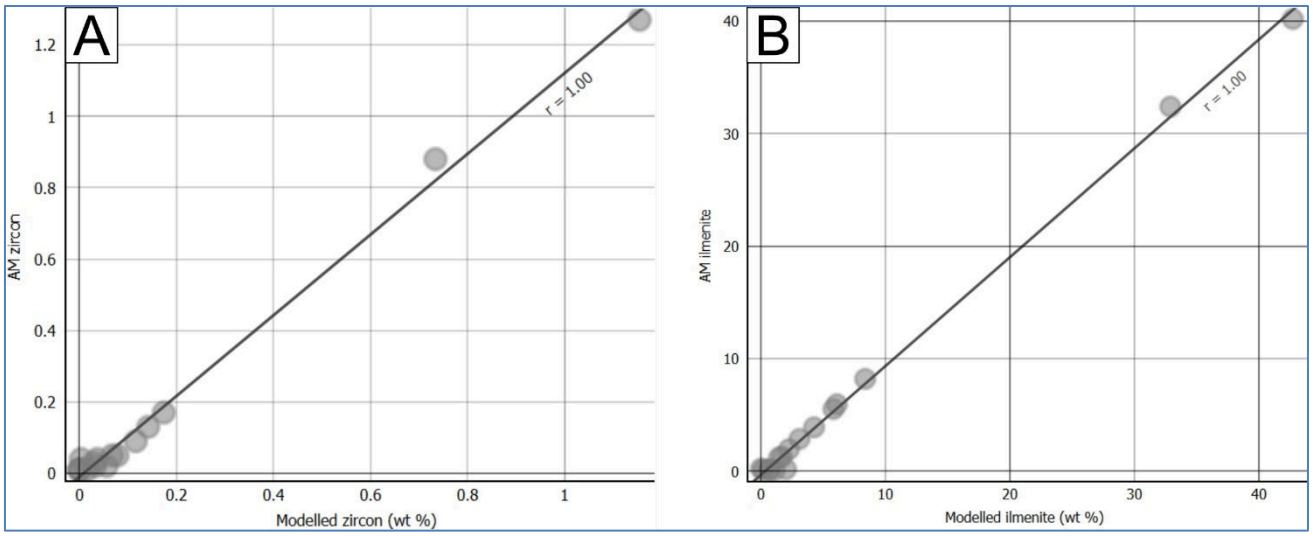


Figure 45: SEM-measured mineral concentrations (y-axes) versus modelled mineral concentrations (x-axes) for (A) zircon and (B) ilmenite.

## 6.4 Bulk Density

The Mineral Resource is estimated and classified as bulk dry tonnes (section 8.11)[4]. RSC has calculated dry bulk density data from sonic drill core using the 'core tray method'.

The length of the core in the core tray was measured in the field using a tape measure prior to sample transportation to the NZIMMR lab. At the NZIMMR lab, RSC staff weighed the core boxes with the wet core using digital industrial scales with an accuracy of 100 g. Next, the wet core was split into 1 m intervals which were put onto trays and weighed. If a metre interval extended across two different boxes, the partial intervals were placed on separate trays and weighed. The empty core boxes were weighed separately to determine the total weight of the wet core. The trays were put in an Alsto drying oven and the samples were dried overnight (~12 hours) at 105°C. After drying, the combined weight of the tray and the dry sample was determined using Ohaus Valor digital scales with an accuracy of 1 g.

To determine the dry bulk density of a sample, the dry sample weight and the sample volume are required. The sample weight was determined by subtracting the mass of the tray from the combined dry sample and tray mass. The sample volume was calculated using the length of the sample and the core diameter. The diameter of the core could not be measured using a calliper due to the unconsolidated nature of the sediments, the internal diameter of the bit (77 mm) was therefore used. The dry bulk density of the samples was calculated by dividing the dry weight of the sample by its volume. The moisture content of the samples was determined by comparing the wet and dry weights of the samples.

[4] Commonly, alluvial Au resources are reported and classified as volumes (as opposed to either dry or wet tonnes). Given that the primary commodity is heavy minerals, which are reported and classified as bulk dry tonnes, the Mineral Resource is expressed as bulk dry tonnes.

# 7 Data Quality

## 7.1 Data Quality & Quality Objectives

Every data collection process implicitly comes with expectations for the accuracy and precision of the data being collected. Data quality can only be discussed in the context of the objective for which the data are being collected. In the minerals industry the term 'fit for purpose' is commonly used to convey the principle that data should suit the objective. In the context of data quality objectives (DQO), fit for purpose could be translated as 'meeting the DQO'.

For the Barrytown Project, data from the 2022 drilling programme should be of a quality that is fit for the purpose of classifying at least Indicated Mineral Resources for ilmenite, garnet, and zircon, and at least Inferred Mineral Resources for Au, in accordance with the JORC Code (2012). These Mineral Resource classification objectives set a requirement for the level of quality of the data and determine the DQO.

## 7.2 Quality Assurance

Quality assurance (QA) is about error prevention and establishing processes that are repeatable and self-checking. The simpler the process and the fewer steps required the better, as this reduces the potential for errors to be introduced into the sampling process. This goal can be achieved using technically sound, simple prescriptive SOPs, and management systems.

In discussing the suitability of QA systems for the data collection that underpin the MRE reported here, and the potential impact of these processes on the resource classification, RSC has applied the process summarised in Figure 46. This summary discusses whether:

- processes are clearly documented in an SOP, and they represent good practice;
- the SOP includes statements on clear data quality objectives;
- the SOP includes clear details on quality control (QC) measures; and
- the site visit confirmed adherence to the SOPs.

For each part of the sampling, preparation and analytical process, a comment on the expected associated risk with respect to resource classification is provided.

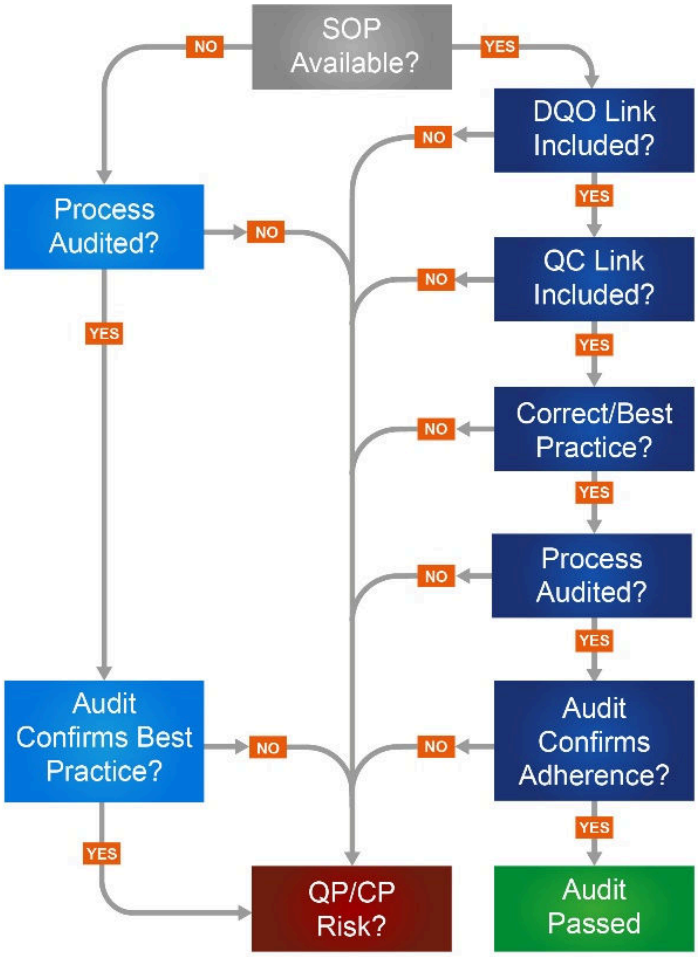


Figure 46: Flow chart of RSC's QA review process.

### 7.2.1 Location

#### *7.2.1.1 Collar Location*

The drillhole collars were pegged by a professional surveyor using a Trimble RTK GNSS with R10 rover and base units. The measurement accuracy of this survey is reported at better than ±2–3 cm both horizontally and vertically. Local control was established with temporary survey marks. Survey field checks were made on the establishment of each day's fieldwork to ensure the survey equipment was reliably operating in terms of the established network. The third-party surveyor SOPs were not available for review and this process was not audited.

Due to logistical issues with working on an active dairy farm, and the surveyor's limited availability, the final drillhole collar locations were captured each day using a hand-held GPS with ~3 m accuracy. Drillhole collar elevations were draped to the DTM with accuracy specifications of ± 0.2 m (95%) vertical. While the use of hand-held GPS may have resulted in lower horizontal accuracy, given the flat, open areas of the Coates South Block, and relatively strong grade and geological continuity in the deposit, the Competent Person considers that there is low risk of using hand-held GPS with respect to the classification of the mineral resource.

#### *7.2.1.2 Downhole Survey*

No downhole surveys were conducted for any of the 2022 drillholes. The Competent Person considers that this is appropriate given the vertical orientation and shallow nature of the drilling and considers that there is low risk with respect to the location of the samples on the quality of the estimate.

### 7.2.2 Dry Bulk Density

RSC staff collected dry bulk density data from the dried sonic drill core at the NZIMMR laboratory in Greymouth, both at metre intervals, and by core box, using the core tray method as described by Lipton and Horton (2014) and explained in the SOP. The procedure is not best practice, but the Competent Person considers it to be appropriate for obtaining bulk density data from unconsolidated material. Weight standards were weighed during the process to ensure that the scales were providing consistent data.

The Competent Person considers the bulk density data collection process poses a minor risk with respect to the accuracy of the tonnage estimation.

### 7.2.3 Geological Logging

An SOP was in place for the process of collecting geological data and information from the aircore samples, which included appropriate sections on QC and objectives. For each metre, a handful of sample material was placed on a logging board and logged. The geological data captured include lithology, grain size, colour, rounding, clay content, garnet content, dark heavy-mineral (HM) content and the number of Au grains. Other details logged include sample weight, sample moisture and depth to the water table. Logging details were entered in dropdown-validated MS Excel spreadsheets.

This process was audited internally during a site visit by Mr Aldrich. The Competent Person considers the aircore logging procedures to be carried out well. The Competent Person considers that there is low risk with respect to the objectives, and any minor logging inconsistencies have been taken into consideration when classifying the resource.

### 7.2.4 Grade

#### *7.2.4.1 Primary Sample*

The primary sample was collected at the drill bit. Quality assurance of the primary sample for aircore drilling generally consisted of selecting the correct drill bit, applying the correct air pressure, ensuring correct placement of metre marks on the drill mast, maintaining adequate moisture content to minimise loss of fines, minimising sample loss by choosing the right tolerance between bit and shroud, and ensuring the sample system was clear to minimise cross-contamination between samples. These decisions were continually adjusted based on encountered lithologies to make sure delimitation errors and extraction errors are prevented. A good SOP for the drilling process details how these decisions are made, by whom, and with a particular focus on recovery management. However, in practice, such decisions and processes are typically not documented, and quality is dependent on the experience of the driller.

During the site visit, Mr Aldrich noted that drilling encountered some challenges:

- high water tables creating wet samples;
- high rainfall and surface water creating wet samples;
- rising sand causing overweight samples;
- loss of pressure in the top 1–3 m resulting in low-weight samples, and
- areas with beach cobbles or wood debris that caused blockages in the drill string, and resulted in low-weight samples and potential loss of fine material.

Mr Aldrich observed that the drilling was actively monitored by staff on site and that instructions and training were provided to both drilling and field staff regarding the drilling procedures. Any issues affecting the quality of the primary sample were noted in drilling daily logs and on log sheets.

Recovery was monitored by weighing the primary sample on site and recording these weights on paper. Alton Drilling actively worked to resolve sample recovery issues. The driller paused at the end of each metre to allow the sample to fully pass through the system, and the sample return hose and cyclone were cleaned continuously.

TiGa decided to use the aircore rig instead of a sonic rig for logistical, timing and cost reasons. Notwithstanding the assurance measures in place, the Competent Person considers that there is some risk associated with the aircore sampling that affects the quality of the resource estimation. This led to the redrilling of several holes, which demonstrates commitment to the established QA principles. Where recovery is not optimal and redrilling has not occurred, this has been considered in classifying the resource.

#### *7.2.4.2 First Split*

The first split (Split 1) of the primary sample occurred at the NZIMMR laboratory, where the primary sample was passed through a Rocklabs Boyd Elite jaw crusher and RSD combo. In the case of samples for which a repeat sample was to be collected, this first-split stage consisted of two separate steps. First, the primary sample was passed through the crusher-RSD combo to create a subsample with a weight approximately twice that of a regular sample (Split step 1). Next, this subsample was passed through the crusher-RSD combo again to create two subsamples with equal weights (Split step 1a).

The first split process was not audited, as the NZIMMR laboratory was not processing samples during the site visit. However, the first split process was regularly observed by RSC field personnel, and it was undertaken in accordance with the established and well-communicated procedures. The Competent Person considers using an RSD to split the primary sample industry good practice. The Competent Person considers the risk associated with the first split procedure to be low with respect to the quality objectives.

#### *7.2.4.3 Second Split*

The second split (Split 2) occurred at the NZIMMR laboratory when the first split was wet-screened using a 2-mm and a 45-µm sieve. The second split process was not audited, as the NZIMMR laboratory was not processing samples during the site visit. However, the second-split process was regularly observed by RSC field personnel, and it was generally undertaken in accordance with the established procedures. RSC notes that the trays used were not always cleaned between every

sample. In future, RSC recommends that NZIMMR completes sizing tests to ensure the quality of the wet-screening process, and ensures the sample trays are cleaned between each sample to reduce contamination.

The Competent Person considers that even though improvements to this process should have been made, the risk associated with the second split procedure is low with respect to the objectives.

#### *7.2.4.4 Third Split*

The third split (Split 3) occurred at the NZIMMR laboratory when the 2-mm to 45-µm subsample was passed through a Rocklabs Boyd Elite jaw crusher and RSD combo to create P1, P2, P3 and P4 subsamples (priority subsamples). The process was governed by a sample process flowsheet and splitting rules developed between RSC, TiGa, NZIMMR, and IHC Robbins. Every 30th sample, a duplicate sample pair was created by passing the 2-mm to 45-µm subsample through a Rocklabs Boyd Elite jaw crusher and RSD combo to create two equal splits (Split step 3a) before creating the P1, P2, P3 and P4 subsamples. The duplicates were collected to monitor the consistency of this step. P1, P2, P3 and P4 subsamples were subsequently created from the 3a splits.

The third split process was not audited, as the NZIMMR laboratory was not processing samples during the site visit. However, the third split process was regularly observed by RSC field personnel, and it was generally undertaken in accordance with the established procedures.

The Competent Person considers using an RSD to create the third split subsamples industry good practice. The procedures outlined in the flowsheet and the splitting rules are considered industry standard practice. The Competent Person considers the risk associated with the third split process to be low with respect to the resource classification target.

#### *7.2.4.5 Priority 1 Subsample (P1)*

The P1 subsample was sent to IHC Robbins' facility in Brisbane for further processing and sink-float analysis. At IHC Robbins' facility, the P1 subsample was split using a riffle splitter to create a ~100-g subsample (P1 fourth split). Fourth-split repeat samples were collected approximately once every 20 regular samples. The fourth-split subsamples were jet-washed through a 53-µm screen, eliminating the slimes from the sample (P1 fifth split). The fifth-split oversize material was dried and passed through a 2-mm sieve (P1 sixth split). The sixth-split 53-µm to 2-mm fraction was submitted to IHC Robbins' heavy liquid laboratory for sink-float analysis.

The P1 fourth, fifth and sixth split processes were not audited as the Competent Person did not visit IHC Robbins' facility; however, the Competent Person considers the processes outlined in the flowchart (Figure 36) industry standard practices. IHC Robbins is an internationally recognised independent laboratory that specialises in testing HM samples, and, even though there is some residual risk in this part of the process not having been audited, the Competent Person considers the risk associated with the P1 subsampling processes to be low with respect to the quality of the resource estimation.

#### 7.2.4.6 Priority 2 Subsample (P2)

##### 7.2.4.6.1 P2 Fourth Split

The P2 subsamples were sent to SGS Westport for pulverisation and splitting. Following pulverisation, a 200-g and a 100-g subsample were created using a scoop (P2 fourth split). No SOP outlining the P2 fourth split procedure was available for review and the process was not audited.

SGS Westport is an ISO/IEC 17025 accredited laboratory, and, even though there is some residual risk with this part of the process not having been audited, the Competent Person has deep knowledge of SGS laboratories and its SOPs around the world, and considers the risk associated with the P2 fourth split to be low with respect to the quality of the resource estimation.

##### 7.2.4.6.2 P2 Fifth Split

*SGS Waihi*

At SGS Waihi, a 50-g aliquot was extracted from the P2 fourth-split subsamples using a scoop (P2 fifth split). Fifth-split repeat samples were created approximately once every 20 regular samples. No SOP outlining the P2 fifth-split procedure at SGS Waihi was available for review and the process was not audited.

SGS Waihi is an ISO/IEC 17025 accredited laboratory, and, even though there is some residual risk with this part of the process not having been audited, the Competent Person has deep knowledge of SGS laboratories and its SOPs around the world, and considers the risk associated with the P2 fifth split at SGS Waihi low with respect to the quality objectives.

*RSC Wellington*

At the RSC Wellington Office Laboratory, about 20 g of sample material was extracted from the P2 fourth-split subsamples using a spoon, using the “many increments” approach to obtain a fit-for-purpose split of the sample. Fifth-split repeat samples were created approximately once every 30 regular samples to check and monitor this. The Competent Person considers the risk associated with the P2 fifth split at RSC Wellington low with respect to the quality of the regression model on which the abundance calculations are based, and, in turn, the quality of the resource estimation as determined by its accuracy and precision.

##### 7.2.4.6.3 P2 Analytical (Fire Assay and Portable XRF) Process

*SGS Waihi*

The gold content of the P2 samples was determined at SGS Waihi by 50-g fire assay. The SOP describing this process was not available for review and the process was not audited. SGS Waihi is an ISO/IEC 17025 accredited laboratory, and the Competent Person has deep knowledge of SGS laboratories, and in particular its SOPs, and its controls around the FA process. These data were only used for domaining and further selecting samples for higher-quality BLEG analysis. BLEG provides more precise results than FA because the sample is larger and grouping-and-segregation errors are eliminated.

The Au FA data were not used for estimation and therefore, the risk associated with the FA analytical stage at SGS Waihi is low.

*RSC Wellington Office Laboratory*

Multi-element analysis of the P2 samples was completed at RSC's office in Wellington using an Olympus Vanta VMR pXRF instrument and followed industry best practice and RSC's pXRF analysis SOP. A robust QC framework was in place to ensure that the instrument was working according to its specifications and that no special-cause variation was introduced. The process was not audited, but it was supervised by RSC's Principal Geochemist, and the Competent Person considers that the risk associated with the pXRF analysis at RSC Wellington is low with respect to the quality objectives.

#### *7.2.4.6.4 P2 Sixth Split*

Based on the pXRF results, a subset of samples reflecting the geochemical variety of the total sample population was selected for laboratory whole-rock XRF analysis. At RSC Wellington, three tablespoons were scooped from the sample bags of the selected samples and poured into labelled paper bags that were sent to the ALS laboratory in Brisbane. No SOP describing this process was available for review and the process was not audited. Because the samples are finely pulverised and because the XRF analysis determines the concentrations of common rock-forming elements that have a very low natural inherent variability, the Competent Person considers the risk associated with the P2 sixth split process at RSC Wellington to be low with respect to the resource estimation quality.

#### *7.2.4.6.5 P2 Seventh Split*

At ALS Brisbane a 0.66-g aliquot was extracted from the P2 sixth-split subsamples using a scoop (P2 seventh split). Seventh-split repeat samples were created once every ~20 samples to control the consistency of this process. No SOP outlining the P2 seventh-split procedure at ALS Brisbane was available for review and the process was not audited. As ALS Brisbane is an ISO/IEC 17025 accredited laboratory, the Competent Person considers the risk associated with the P2 seventh split at ALS Brisbane to be low with respect to the quality objectives.

#### *7.2.4.6.6 P2 Analytical (XRF) Process*

At ALS Brisbane, the whole-rock geochemistry of the P2 subsamples was determined using methods ME-XRF21u and ME-GRA05. The SOP describing this process was not available for review and the process was not audited. ALS Brisbane is an ISO/IEC 17025 accredited laboratory, and the Competent Person is very familiar with its processes and standards and the Competent Person considers the risk associated with the analysis of samples by ME-XRF21u and ME-GRA05 at ALS Brisbane to be low with respect to the resource classification objectives.

### *7.2.4.7 Priority 3 Subsample (P3)*

#### *7.2.4.7.1 P3 Fourth Split*

The P3 samples were shipped to Middle Earth Petrographics where they were split to ~15 g, using a Humboldt Micro and Precision Riffle Splitter and then set in a 25-mm epoxy round. Repeat samples were collected from five of the 60 samples

to monitor process consistency. The hardened epoxy round was cut in half vertically and remounted in a 30-mm epoxy round to expose the two cut faces for SEM analysis. Cutting the 25-mm round vertically reduces the impact of any differential settling of the sample in the epoxy round by grain size and density. No SOP is available for review, but the process was reviewed by senior RSC staff. The Competent Person considers this sample preparation method to be best practice and considers there is low risk of this process generating excessive inaccuracies or imprecision.

#### *7.2.4.7.2 P3 Analytical (SEM) Process*

SEM data collected at the University of Queensland and RSC Perth were collected in accordance with standard AMICS workflow as outlined in the manual (Bruker, 2020). The work was supervised by RSC's Principal Geochemist. The Competent Person considers the AMICS workflow industry good practice, and this process therefore presents minimal risk with respect to the quality of the resource estimate.

### *7.2.4.8 Priority 4 Subsample (P4)*

The P4 subsamples were not submitted to ALS for further processing and analysis.

### *7.2.4.9 Cyanide Leach Samples*

#### *7.2.4.9.1 Second Split*

Samples selected for BLEG analysis were sub-sampled from the Split 1 rejects. At NZIMMR, 1–1.5 kg was split from the Split 1 rejects using a Rocklabs Boyd Elite jaw crusher and RSD combo. The process was governed by a sample process flowsheet developed between RSC, TiGa, NZIMMR, and IHC Robbins. The second split process for the BLEG samples was supervised by senior RSC staff. The second split process was completed in accordance with the steps outlined in the flowsheet; however, it is noted that some of the coarse-crush rejects used had already been sampled by TiGa to create the second bulk metallurgy sample.

The Competent Person considers using large samples for BLEG and using an RSD to create these second split subsamples industry good practice. The procedures outlined in the flowsheet are considered industry standard practice. The risk associated with the second split process for the BLEG samples is considered to be low with respect to the quality of the Au estimate.

#### *7.2.4.9.2 Analytical (BLEG) Process*

The Au content of the P4 samples was determined at ALS Perth by means of BLEG analysis (method code Au-CN11). The SOP describing this process was not available for review and the process was not audited; however, RSC is familiar with ALS Perth's SOPs and has audited this laboratory and process before and considers the risks associated with the BLEG analysis process are low.

## 7.3 Quality Control

The purpose of quality control (QC) is to detect and correct errors while a measuring or sample-collection system is in operation. The outcome of a good QC programme is that it can be demonstrated that any errors were fixed during operation and that the system delivering the data was always in control. Together with good QA (section 7.2), QC ensures that the data quality objectives are met. Good QC is achieved by inserting and constantly evaluating checks and balances. These checks and balances can be incorporated at every stage of the sample process (location, primary sample collection, preparation, and analytical phases) and, if in place, should be monitored during data collection, allowing the operator to identify and fix errors as they occur.

### 7.3.1 Sample Location

Quality control of the sample location data, usually derived from a combination of drillhole collar positions and downhole surveys, should occur on site as surveys are being conducted by conducting check measurements. Quality control of the collar location data should take place on site as measurements are being collected.

#### *7.3.1.1 Collar Location*

GPS survey field checks were made at the start of each day's fieldwork; with any accuracy checks or repeat readings for each collar used to check, correct and repeat the collar-recording process if necessary. Even though the accuracy and repeat metadata were not recorded in the database, these QC measures are good practice. Final drillhole collar locations, captured each day by hand-held GPS, were compared against the pegged values from the professional surveyor as an additional check. The Competent Person considers the accuracy and precision of collar data to be well-controlled, resulting in fit-for-purpose collar data.

#### *7.3.1.2 Downhole Survey Data.*

No downhole surveys were conducted for any of the 2022 drillholes.

### 7.3.2 Dry Bulk Density

Reference weights were recorded during the weighing process. Repeat measurements were not carried out. The reference data indicate that the scales were operating consistently, and providing data that can be confidently used in density calculations.

### 7.3.3 Geological Logging

Geological logging was completed by field geology staff with some check logging completed by the cross-shift geologist, senior RSC staff during the drill campaign and by Mr Aldrich during the site visit. No significant discrepancies were identified during this process, demonstrating consistent data capture. Hence, the logging data can be confidently used in the building of geological domains.

### 7.3.4 Grade

#### *7.3.4.1 Primary Sample*

The quality of the primary sample was monitored by reviewing sample weights as the drilling was ongoing (Figure 47). Sample recovery was calculated at the drill rig from the sample weights.

Improvement of recovery with time is demonstrated in the data, which indicates that both the QA and QC processes are working as intended. RSC staff reviewed the distribution of samples with low recovery during the drill campaign and thirty-seven holes were fully or partially redrilled. Superseded samples that remained unprocessed by the time of drilling were eliminated from processing, dried, and sent to storage. The average recovery was 73%. Where recovery is not optimal and redrilling has not occurred, this has been considered in classifying the resource. There is a noticeable drop in the sample weight (recovery) at approximately sample sequence ID #1452 (TAC187, 25 May 2022). This drop in performance roughly aligns with when drilling moved to a different paddock and when the driller's first assistant changed.

The quality control data, by proxy of recovery data, show that the aircore drilling process was not always in control, with trends, step-drops and out-of-threshold recoveries demonstrated throughout the drilling campaign. Notwithstanding the improvements in the recovery data, the Competent Person considers that there is some risk associated with the aircore sampling that carries some risk forward in the accuracy and precision of the resource estimation, and requires further investigation of the implication of the recovery issues (see section 7.4.4.1).

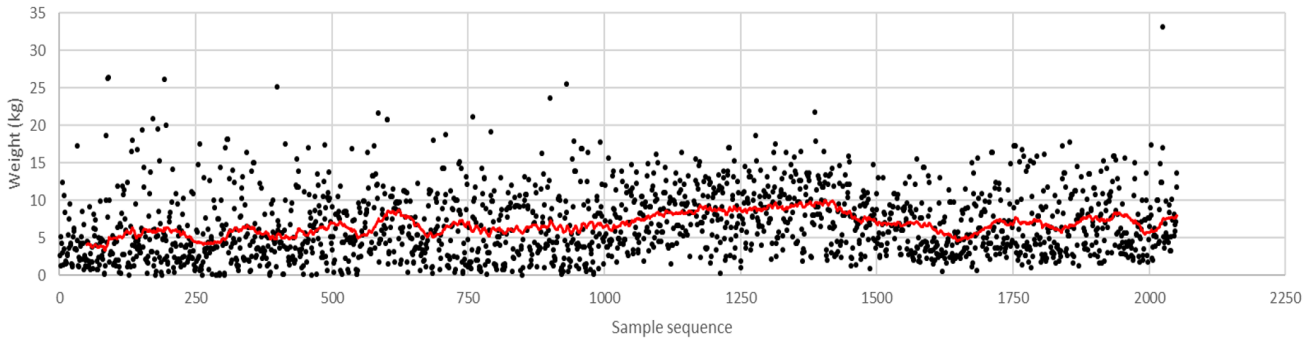


Figure 47: Sample weights against sample sequence (time); 50 period moving average trendline in red.

#### *7.3.4.2 First Split*

The consistency of the splitting process was assessed by tracking the relative difference of the repeat pairs over time. The quality control data for the first split, by proxy of repeat elemental data for Ti, Fe and Zr (Figure 48, Figure 49 and Figure 50, respectively), show that the splitting process was in control, showing no trends, step-drops or threshold breaches. The Competent Person considers the splits generated here to be consistently executed and usable in down-stream processes

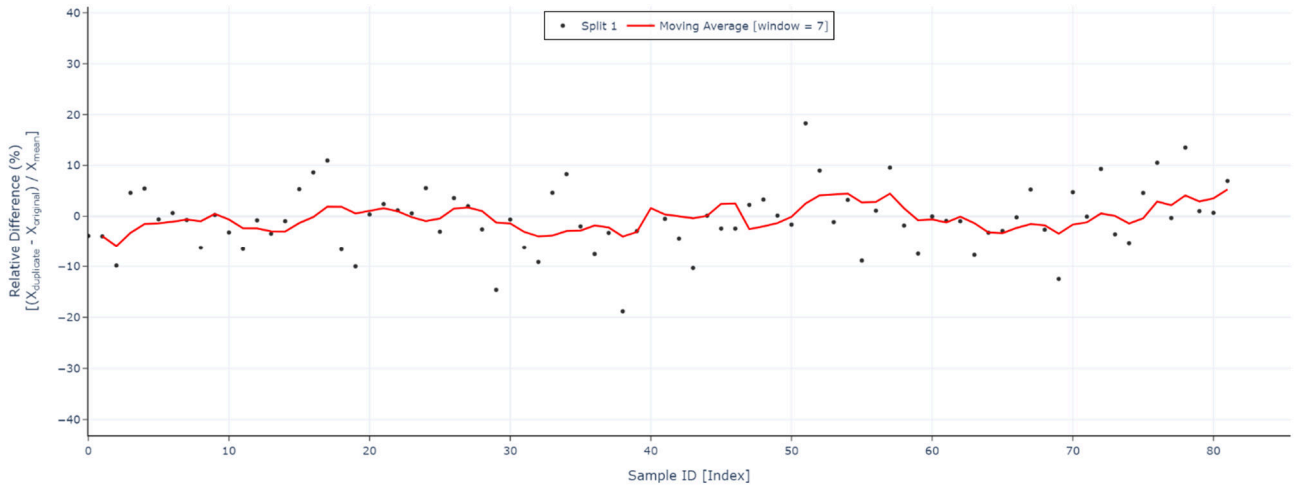


Figure 48: RD plot Ti pXRF first split, showing the relative differences in grades between original and repeat samples against time, collected at the first-split stage.

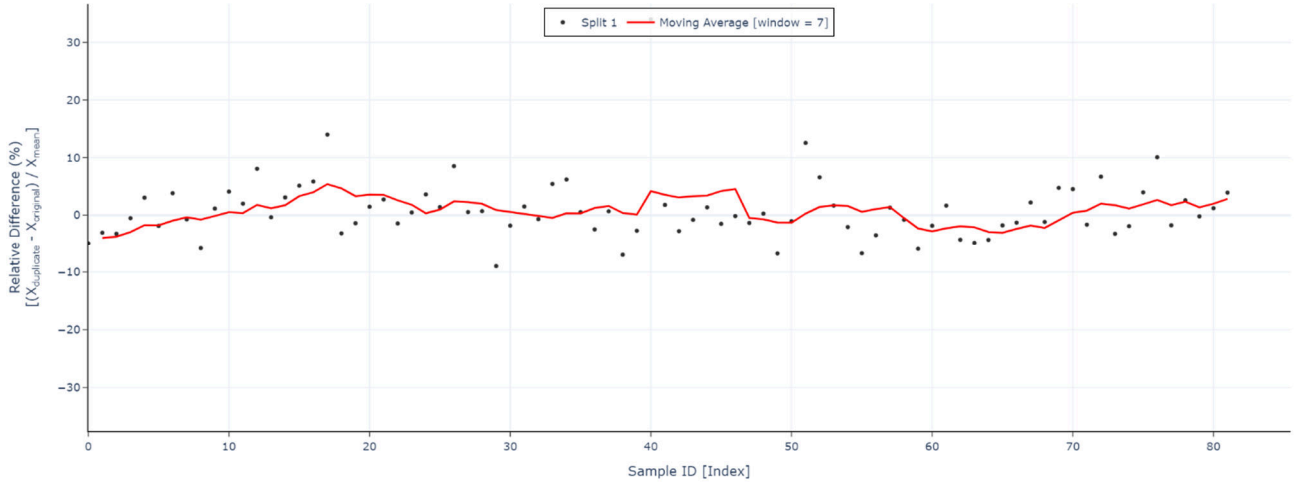


Figure 49: RD plot Fe pXRF first split, showing the relative differences in grades between original and repeat samples against time, collected at the first-split stage.

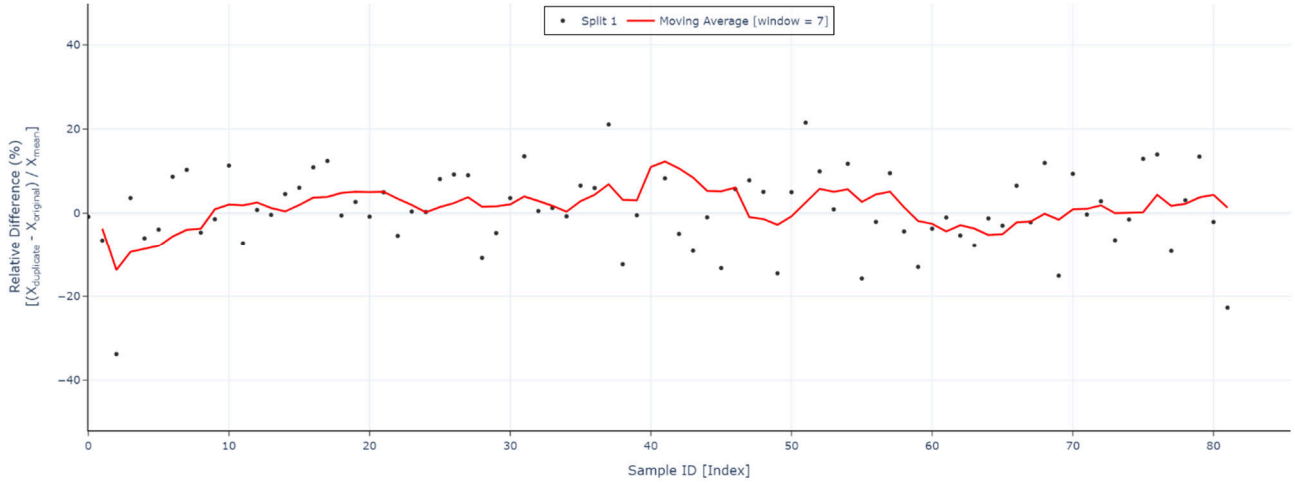


Figure 50: RD plot Zr pXRF first split, showing the relative differences in grades between original and repeat samples against time, collected at the first-split stage.

### 7.3.4.3 *Second Split*

The second split occurred at the NZIMMR laboratory when the first split samples (including first-split repeats) were wet-screened using a 2-mm and a 45-µm sieve. The consistency of the wet-screening process was assessed by reviewing repeat data only as no screen-size testing data were not available.

The quality control data for the second split, by proxy of repeat elemental data for Ti, Fe and Zr (Figure 51, Figure 52 and Figure 53, respectively), show that the splitting process was mostly in control, with no threshold breaches, and perhaps a few minor trends throughout the measuring cycle.

The Competent Person considers the splits generated here to be consistently executed and usable in downstream processes.

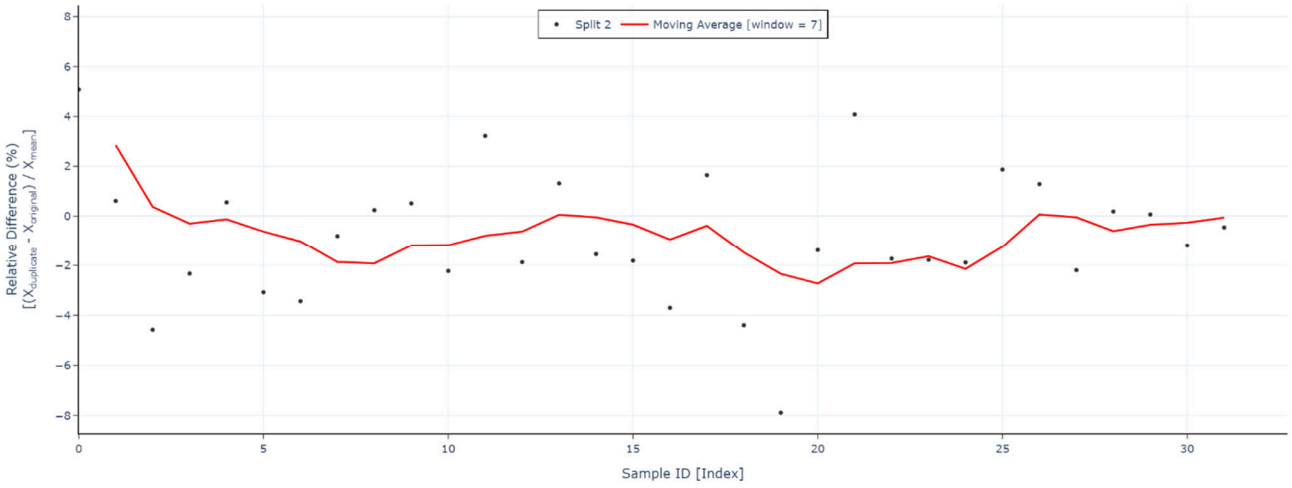


Figure 51: RD plot Ti pXRF second split, showing the relative differences in grades between original and repeat (collected at the first-split stage) samples against time.

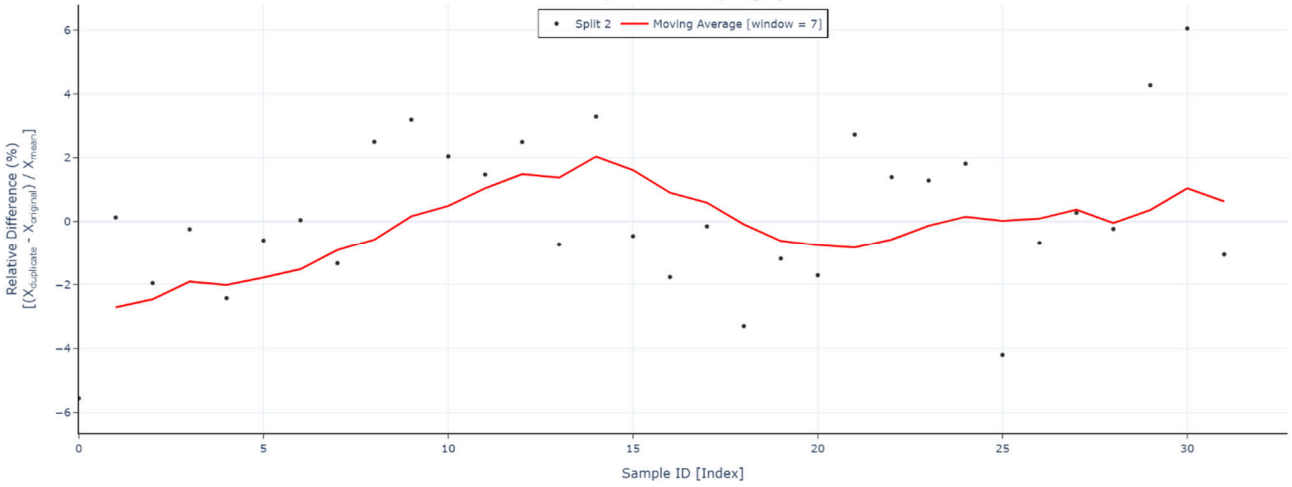


Figure 52: RD plot Fe pXRF second split, showing the relative differences in grades between original and repeat (collected at the first-split stage) samples against time.

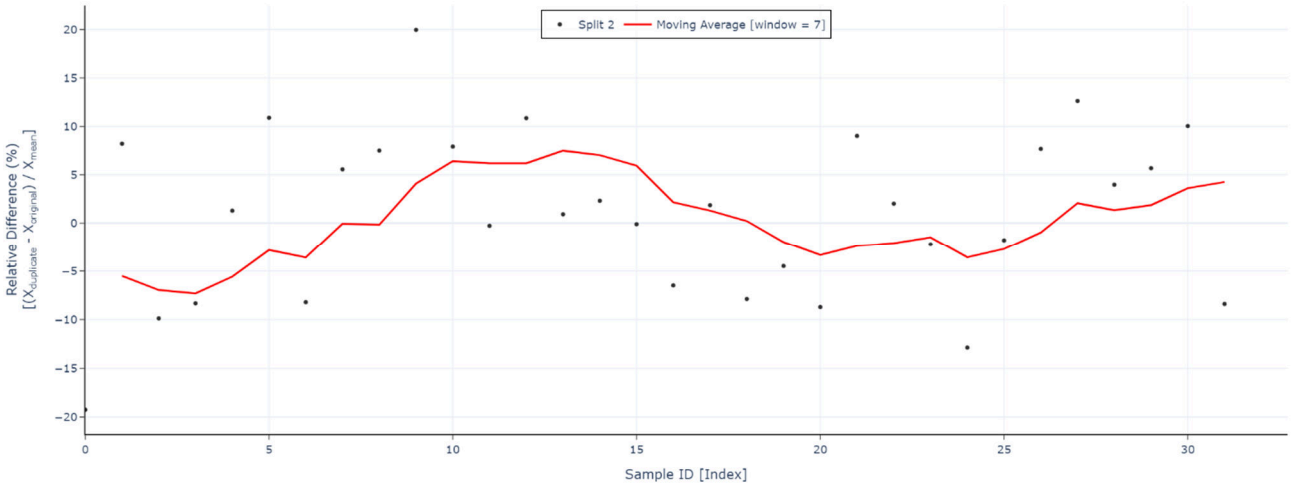


Figure 53: RD plot Zr pXRF second split, showing the relative differences in grades between original and repeat (collected at the first-split stage) samples against time.

### 7.3.4.4 *Third Split*

The quality control data for the third split, by proxy of repeat elemental data for Ti, Fe and Zr (Figure 54, Figure 55 and Figure 56, respectively), show that the splitting process was in control, showing no trends, step-drops or threshold breaches. The Competent Person considers the splits generated here to be consistently executed and usable in downstream processes.

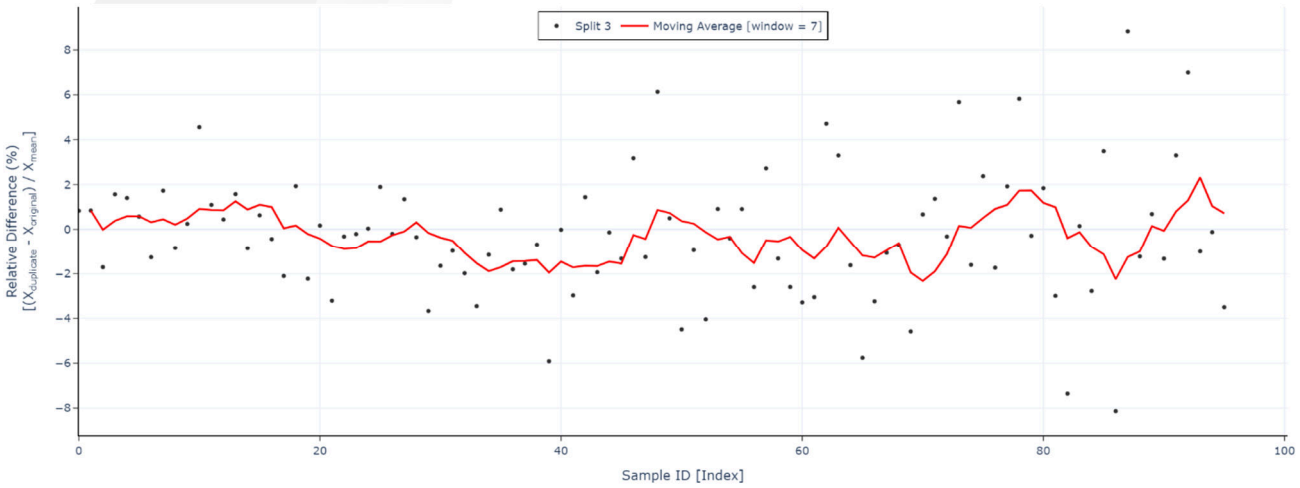


Figure 54: RD plot Ti pXRF third split, showing the relative differences in grades between original and repeat samples against time, collected at the third-split stage.

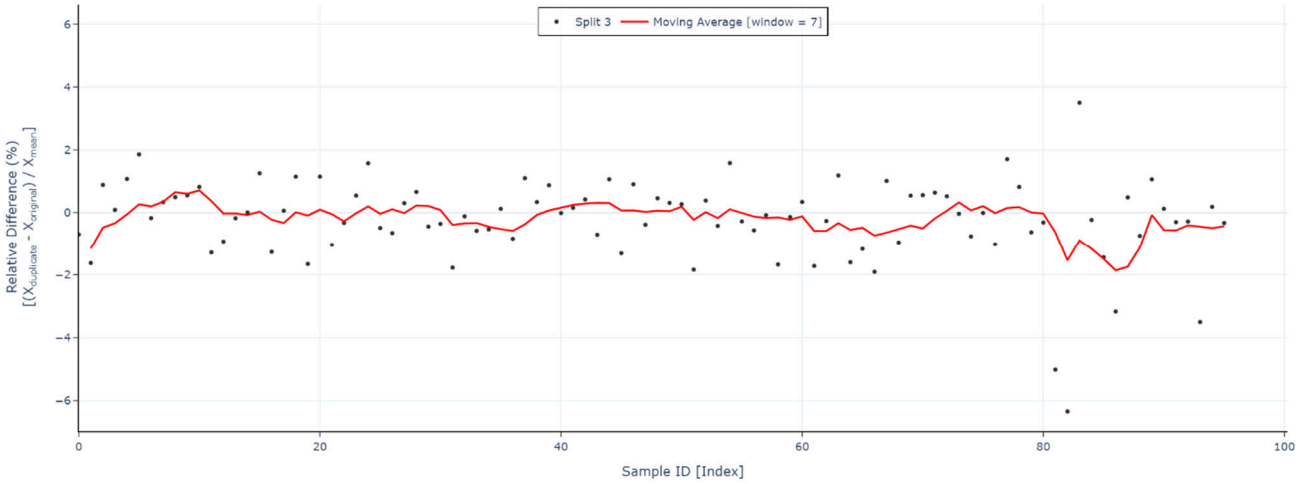


Figure 55: RD plot Fe pXRF third split, showing the relative differences in grades between original and repeat samples against time, collected at the third-split stage.

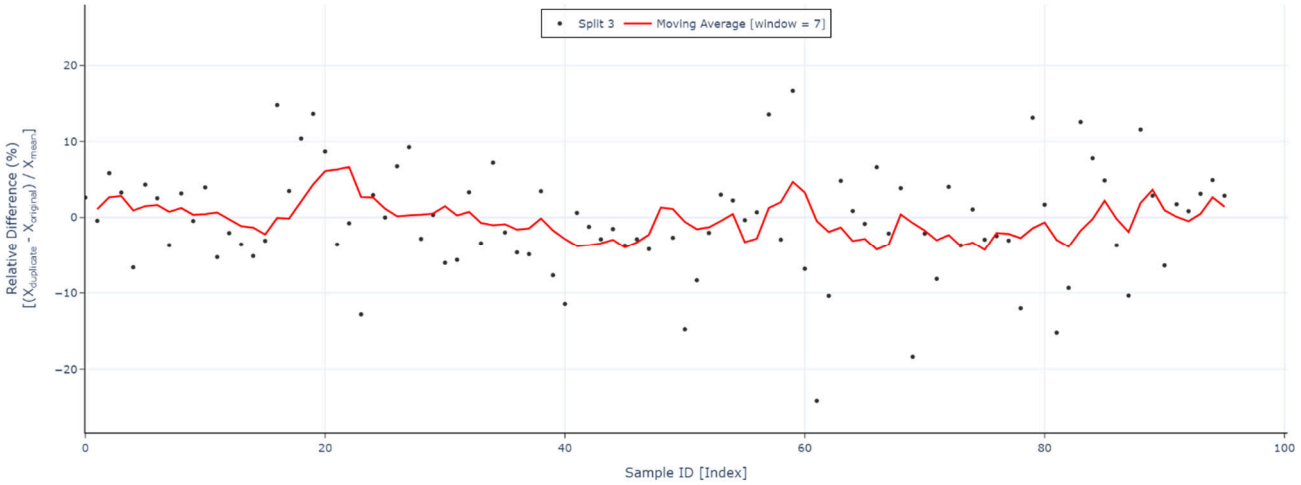


Figure 56: RD plot Zr pXRF third split, showing the relative differences in grades between original and repeat samples against time, collected at the third-split stage.

### *7.3.4.5 Priority 1 Subsample (P1)*

#### *7.3.4.5.1 P1 Fourth Split*

The quality control data for the P1 fourth split, by proxy of repeat heavy mineral abundances and repeat weight data (Figure 57, Figure 58), show that the splitting process was mostly in control, with no threshold breaches, no step-changes and perhaps a few minor trends throughout the measuring cycle. One split weight pair (samples 461 and 462) has an unusually large weight difference (41.1 g vs 94.9 g), which is considered an error and these samples were removed from the assessment.

The Competent Person considers the splits generated here to be mostly consistently executed and usable in downstream processes.

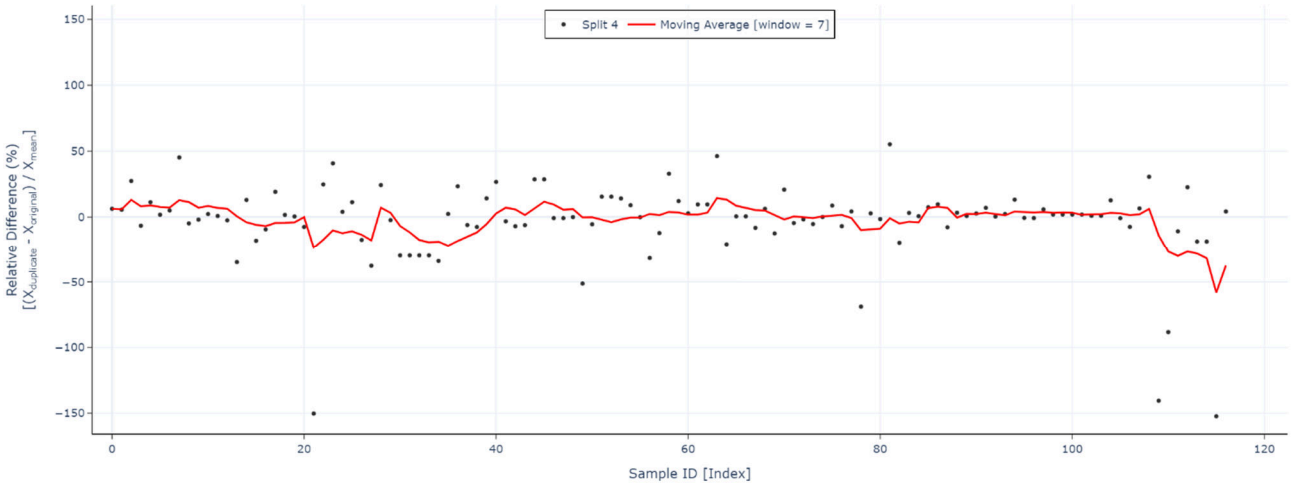


Figure 57: RD plot HM abundance P1 fourth split, showing the relative differences in abundance between original and repeat samples against time, collected at the P1 fourth-split stage.

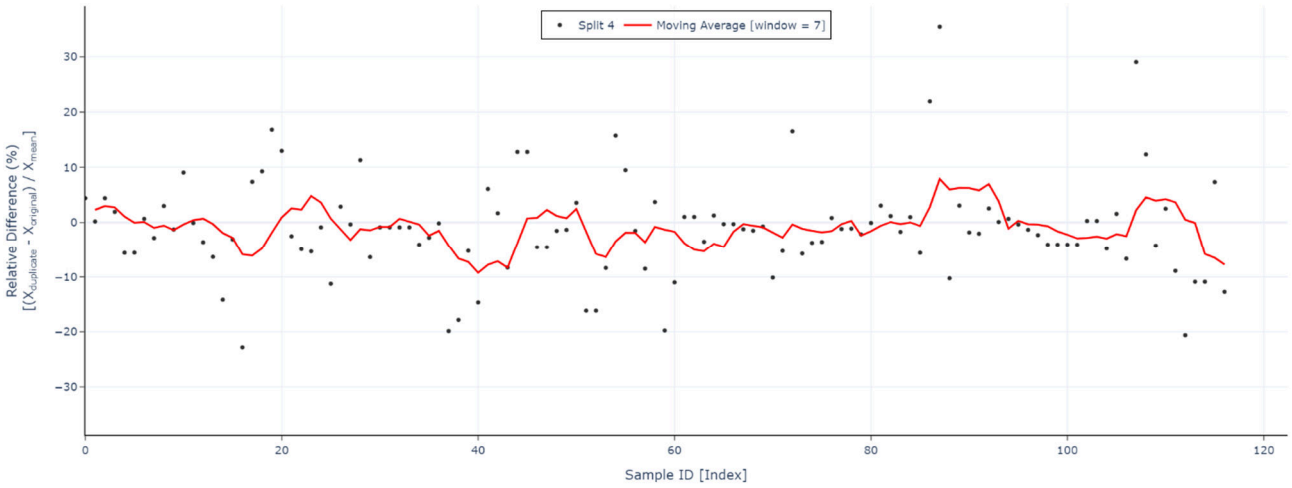


Figure 58: RD plot sample weight P1 fourth split, showing the relative differences in weights between original and repeat samples against time, collected at the P1 fourth-split stage.

#### *7.3.4.5.2 P1 Fifth Split*

The consistency of the P1 fifth split (slime screening) process was monitored by proxy of weight data of the dried slimes from the P1 fourth split repeat pairs (Figure 59). The data show that the IHC Robbins splitting process was mostly in control, with no trends or step-drops or threshold breaches. However, four instances were identified where the repeat sample is a lot heavier. This could indicate that the slime removal process is not always consistent.

The Competent Person considers the splits generated here to be mostly consistently executed, and has considered any inconsistencies in the data in downstream processes with respect to the resource classification.

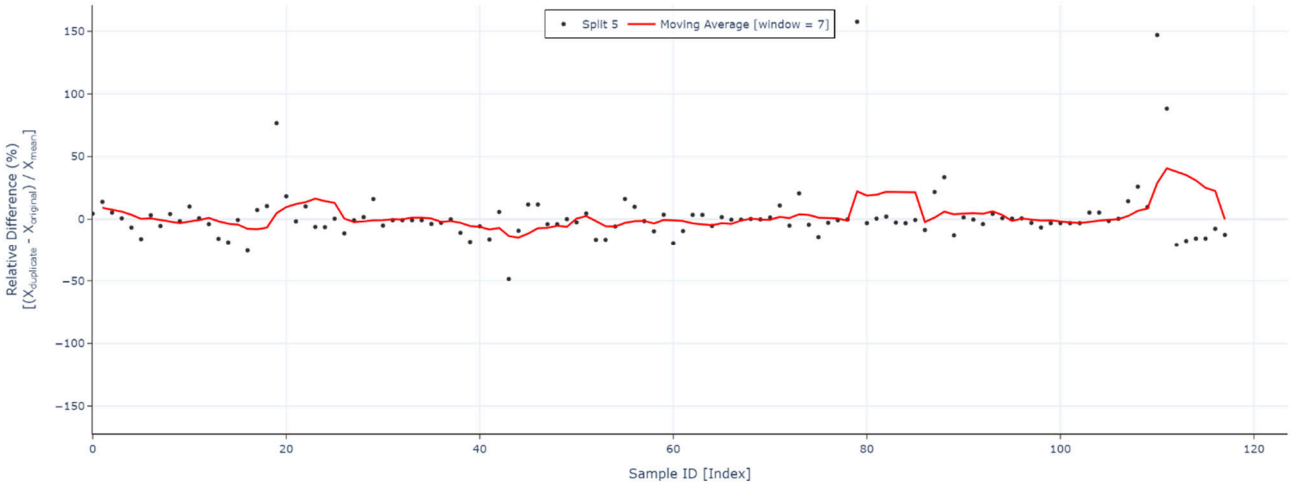


Figure 59: RD plot slime (-53 µm) weights P1 fifth split, showing the relative differences in weights between original and repeat (collected at the P1 fourth-split stage) samples against time.

### 7.3.4.5.3 *P1 Sixth Split*

The consistency of the P1 sixth split (screening) process was monitored by proxy of weight data of the dried oversize (+2-mm) material from the P1 fourth split repeat pairs (Figure 60). There are not enough points available for a proper statistical process control analysis, because these samples were already screened using a 2-mm sieve at NZIMMR (Split 2). The analysis shows that the IHC Robbins splitting process was not quite in control, showing excessive variance or threshold breaches. This means that some minor unwanted inaccuracies and imprecision will be carried forward into the estimation process, which has been considered by the Competent Person in classifying the mineral resource.

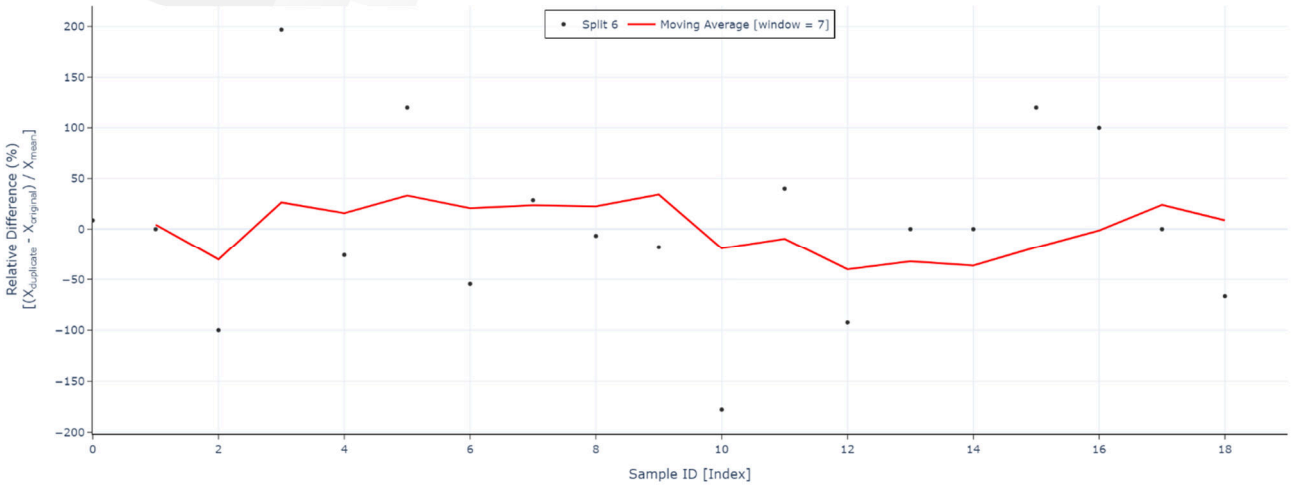


Figure 60: RD plot oversize (+2 mm) weights P1 sixth split, showing the relative differences in weights between original and repeat (collected at the P1 fourth-split stage) samples against time.

#### 7.3.4.5.4 P1 Analytical Process

No CRM or blank sample data are available for the sink-float analyses, hence the consistency of the analytical process cannot be quantitatively determined.

### 7.3.4.6 Priority 2 Subsample (P2)

#### 7.3.4.6.1 P2 Fourth Split

No quality control data are available for review hence the consistency of the P2 fourth split process cannot be quantitatively determined.

#### 7.3.4.6.2 P2 Fifth Split

*SGS Waihi*

No quality control data are available for review hence the consistency of the P2 fifth split process at SGS Waihi cannot be quantitatively determined.

*RSC Wellington*

The quality control data for the P2 fifth split, by proxy of repeat elemental data for Ti and Fe (Figure 61 and Figure 62, respectively), show that the splitting process was in control, with no trends, step-drops or threshold breaches.

The Competent Person considers the splits generated here to be consistently executed and usable in downstream processes.

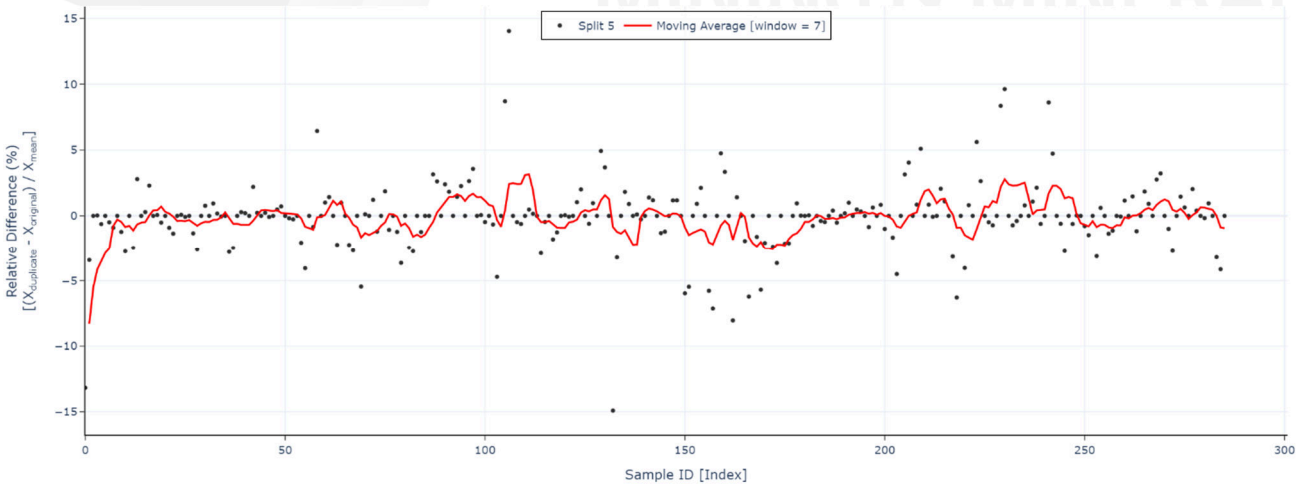


Figure 61: RD plot Ti pXRF P2 fifth split, showing the relative differences in grades between original and repeat samples against time, collected at the P2 fifth-split stage.

.

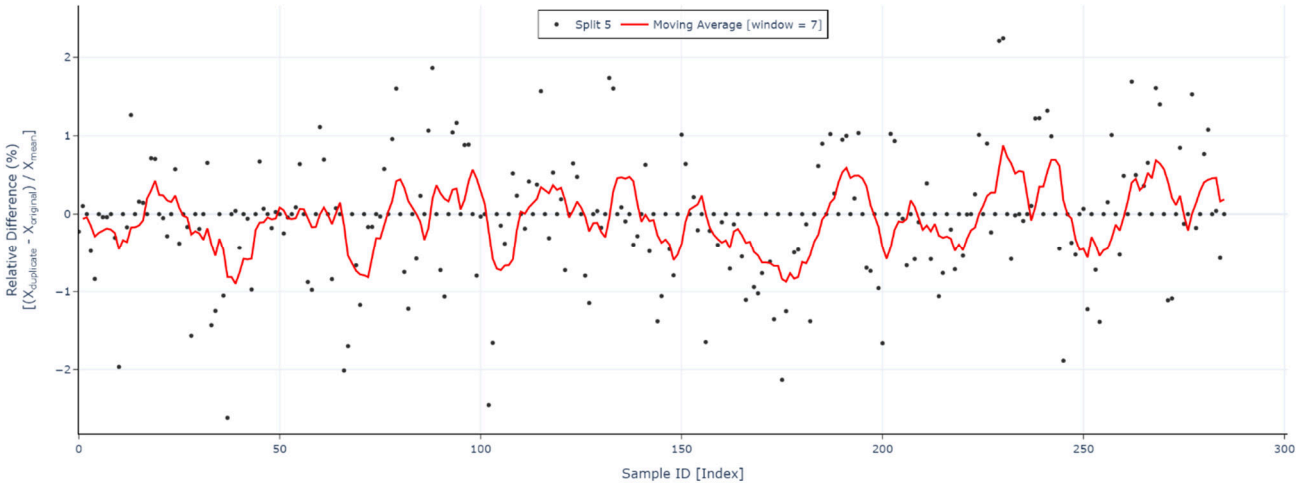


Figure 62: RD plot Fe pXRF P2 fifth split (pXRF), showing the relative differences in grades between original and repeat samples against time, collected at the P2 fifth-split stage.

#### *7.3.4.6.3 P2 Analytical (Fire Assay and pXRF) Process*

The QC of the fire assaying and analytical process involves the repeated and continuous evaluation of CRMs. The laboratory inserts such reference materials into the sample stream, evaluates these, and makes corrections to the system when errors occur, as part of its requirements under ISO accreditation. RSC notes that when clients receive the analytical results of *internal* reference material used by the laboratory, these are typically already corrected (e.g. QC has already taken place, the system stopped when transgressions were identified, and the values replaced by new and correct values).

It is common in the minerals industry for companies to submit their own (disguised) CRMs. However, in RSC's experience, this only achieves its intended purpose when data are immediately and properly analysed, and correct decisions are drawn from the data. The timeframe between analysis and evaluation of results means that correcting a system in real-time is not possible, and therefore QC cannot be effectively exercised. This frequently leads to frustration between the laboratory and operator as both are effectively looking at results for two different datasets that are acted on at different times in the process.

RSC regularly inserted six different CRMs in the sample stream throughout the duration of the programme.

*Fire Assay*

The analytical consistency was assessed using RSC's in-house QC tool. Unwanted, *special*-cause variation (as opposed to "*common*-cause variation") was assessed for each CRM, using statistical process control plots. The statistical process control charts (SPCs) were created using the process mean and the CRM-certified standard deviation. Westgard rules 1(3s), 2(2s), 4(1s), R(4s), 7X, 6T, J-Chart and 14O (Westgard et al., 1981) were used to identify special cause variation.

The SPC chart for CRM OREAS 235, inserted by RSC, is presented in Figure 63. The results show a relatively consistent process with no trends, major step-changes or statistically significant occurrences of special-cause variation, suggesting that the analytical process was in control. The results of the laboratory's internal CRM result support this (Figure 64).

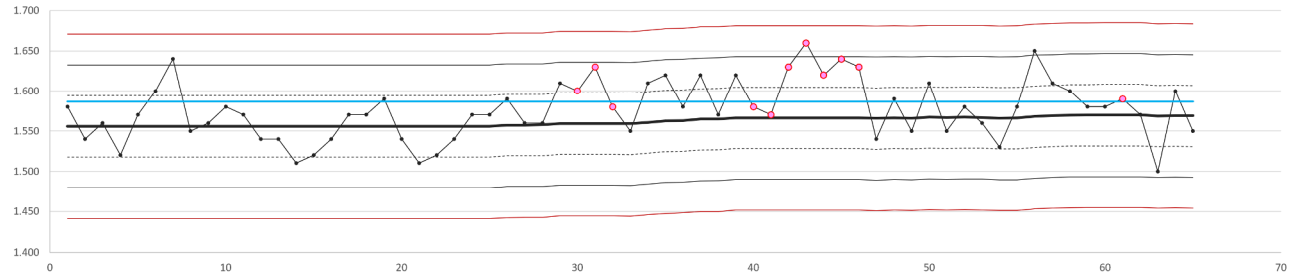


Figure 63: Shewhart control plot for FA Au for CRM OREAS 235.

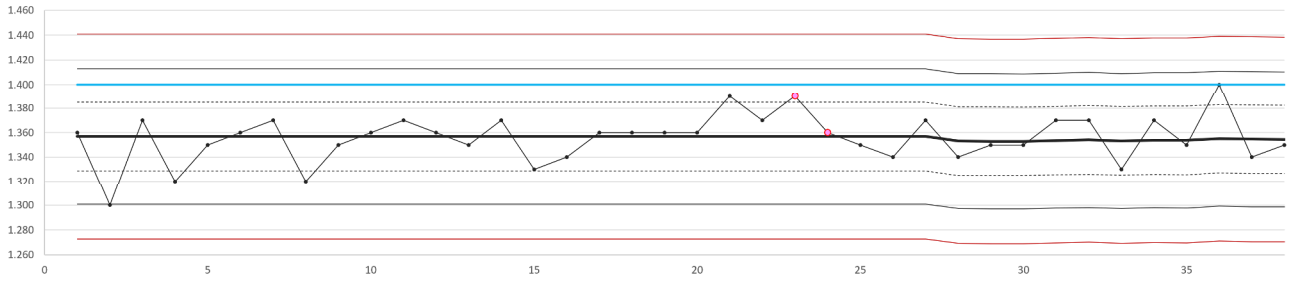


Figure 64: Shewhart control plot for FA Au for laboratory CRM SH98.

*pXRF*

Certified reference materials (OREAS24C, OREAS232, OREAS235, OREAS239, and OREAS501B) were inserted in the sample stream for quality control during pXRF operation. Every pXRF operator started their measurements with the blank and five CRMs. After that, only one of the five CRMs was measured, at a frequency of 1 in 20 (the maximum frequency is 1 to 30) starting with OREAS24C. A repeat measurement and a repeat sample (second scoop from the sample bag) were measured at a frequency of 1 in 20 (if enough sample material was available). All five CRMs followed by the blank were measured again at the end of each shift. Standard samples were inserted in the sample stream to allow post-processing correction of the data, as well as to monitor the consistency of the pXRF analytical process during the measuring process. Blanks were inserted to ensure that any contamination of the instrument was identified before samples were analysed. Repeat measurements were used to test the precision of the instrument.

All pXRF measurements were calibrated against the OREAS standards. The geochemical data collected with the pXRF were corrected using calibration plots after every shift (section 6.3.1; Figure 37). The calibration plots are based on the expected values of the CRM standards plotted against the measured values of the standards. The gradient of the linear fit between the expected and the measured values defined the correction factor used to calibrate the collected geochemistry data. Repeat measurements were performed for 95 samples (Figure 48–Figure 50).

No step changes, trends or major deviations were observed during the pXRF analytical process, suggesting that the process was in control and delivered consistent data.

#### *7.3.4.6.4 P2 Sixth Split*

No repeat data are available for the P2 sixth split hence the consistency of the P2 sixth split process cannot be quantitatively determined.

#### 7.3.4.6.5 P2 Seventh Split

The ALS repeat data were briefly reviewed in sighted laboratory reports and indicate that the splitting process provided consistent data.

#### 7.3.4.6.6 P2 Analytical (XRF) Process

RSC did not insert CRMs into the sample stream. The laboratory blank and CRM data were briefly reviewed in sighted laboratory reports and suggesting that the analytical process was in control.

### 7.3.4.7 Priority 3 Subsample (P3)

#### 7.3.4.7.1 P3 Fourth Split

Only five repeat samples were collected, hence there are not enough data points available for a proper statistical process control analysis of the consistency of the splitting process.

#### 7.3.4.7.2 P3 Analytical (SEM) Process

It is not possible to insert QC samples into the P3 analytical process. However, as part of processing the AMICS data, a geochemical composition for each sample was calculated from the measured mineral abundances in the samples, and this was used as an internal check on the chemistry of the minerals (section 6.3.4.3; Figure 40 and Figure 41).

### 7.3.4.8 Priority 4 Subsample (P4)

No priority 4 samples were submitted for analysis.

### 7.3.4.9 Cyanide Leach Samples

#### 7.3.4.9.1 Second Split

No repeat data were collected (due to insufficient sample material) hence the consistency of the process cannot be verified.

#### 7.3.4.9.2 Analytical (BLEG) Process

CRMs are not commonly inserted in BLEG analysis, and no information is available to quantitatively assess any special-cause variation in the BLEG analytical process.

## 7.4 Quality Acceptance Testing

### 7.4.1 Location

#### 7.4.1.1 Collar Location

There are no quantitative quality data for the collar location collection process; hence, accepting the quality (accuracy and precision) of the collar location data based on statistically defined thresholds is not possible. Based on the review of processes, systems and tools available to determine collar locations (section 7.2.1.1), including the quality control process

to monitor any inconsistencies in GPS readings (section 7.3.1.1), the collar location data are considered fit for the purpose of estimation and high-confidence resource classification.

#### *7.4.1.2 Downhole Survey Data.*

No downhole surveys were conducted for any of the 2022 drillholes. The Competent Person deems this appropriate given the vertical orientation of the drillholes and shallow nature of the drilling, and considers there is low risk with respect to the data quality objectives.

### 7.4.2 Dry Bulk Density

Based on the review of processes, systems and tools available to determine bulk densities (section 7.2.2), including the quality control process to monitor any inconsistencies in scales readings (7.3.2), the density data are considered fit for the purpose of estimation and high-confidence resource classification.

### 7.4.3 Geological Logging

Based on the review of processes, systems and tools available to collect geological data from the drill core (section 7.2.3), including the quality control process to monitor any inconsistencies in logging (section 7.3.3), the logging data are considered fit for the purpose of supporting high-confidence estimation domains for use in resource estimation.

### 7.4.4 Grade

#### *7.4.4.1 Primary Sample*

A practical way to check and verify the quality of a primary sample is to validate it against, or compare it with, a sample of a known grade. In simple terms, the difference between the measured value and the 'known' value is then defined as the bias, a measure of sample quality. Precision can be benchmarked by comparing the variance in the measurements of samples with the variance in the check samples. This is the principle, for instance, behind the utility of laboratory CRMs.

For the *primary* sample, i.e. the sample collected at the drill bit, such options do not readily exist. The next practical way to determine the quality of the primary sample is to compare it with a sample of better quality, taken at the same location. Practically, in unconsolidated ground conditions, sonic drill core is regarded as providing the highest-quality sample and is often used to check the quality of lower-quality drilling or sampling methods, usually aircore or reverse circulation (RC) drilling. This process is often called 'twinned drilling', but it can be used anywhere where a sample from drill type A is close enough to a sample from drill/sample type B

The evaluation of bias between two different populations (in this case aircore and sonic), and the rejection of the hypothesis that the statistically significant bias is solely caused by the difference in sampling technique, is complicated by several factors:

1. The fact that these two populations themselves may be drawn from different or overlapping statistical populations, such as those caused by the presence of different geological domains — this would invalidate any hypothesis testing.

2. The presence of variance due to different analytical or sample preparation techniques.
3. The presence of variance due to distance between Aircore and Sonic samples, as indicated by the variogram.
4. The presence of variance due to differing sample intervals and differing sample support.
5. The presence of outliers.

A review of the results of a distance-buffered QQ plot of ilmenite abundances for 2022 aircore vs sonic samples, created in Phinar X-10 software, is presented in Figure 65. RSC notes that only four sonic drillholes were drilled during the drilling campaign (section 5.1.2), hence the number of samples in the assessment is low (n=23) and the assessment is sensitive to outliers. The QQ plot in Figure 65 suggests that the aircore data are biased slightly low (~10%) compared to the sonic data; however, the scatterplot shows the data are also highly variable. The outlying pair with the largest difference (~16% ilmenite sonic vs ~4% ilmenite aircore) had extremely poor recovery in the aircore sample (~7%), which is not representative of the overall aircore dataset (~73% recovery). While the data suggest some inaccuracy between sonic and aircore ilmenite abundances, there are not enough data to reach confident conclusions relating to accuracy of the aircore drilling. If a low bias exists in the aircore data, the overall abundance estimation is possibly slightly conservative and reflect a potential minor upside in the estimation of ilmenite abundance.

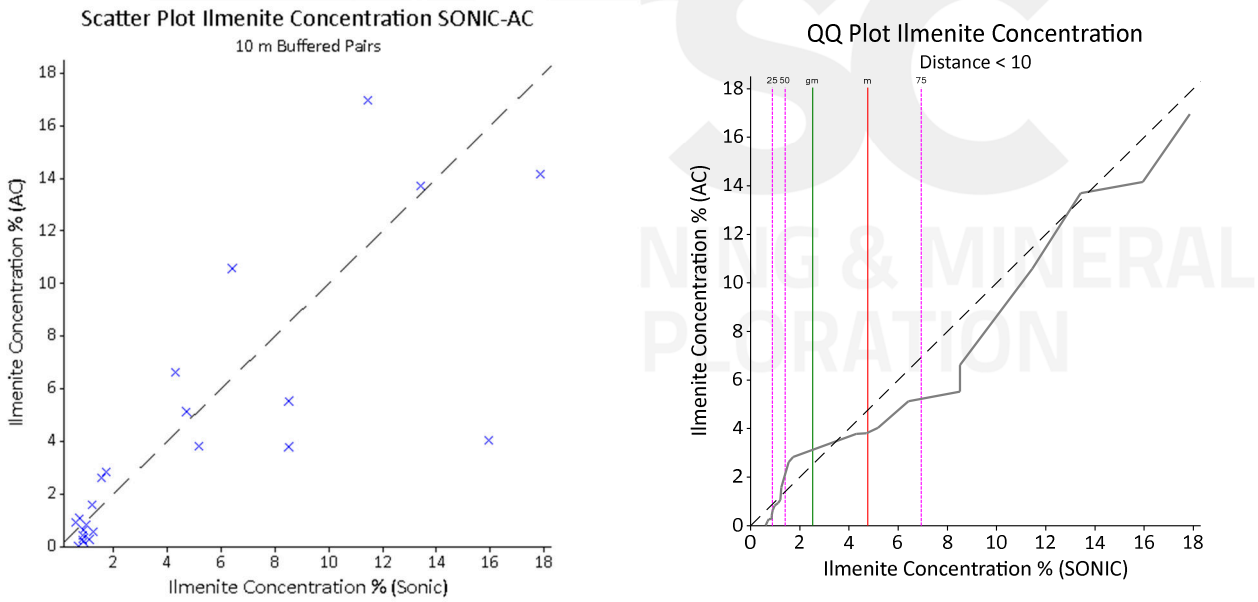


Figure 65: Scatterplot (left) and distance-buffered QQ plot (right) of sonic vs aircore at 10 m buffer distance.

As another back-door check for primary sample quality, sample recovery can be used as a proxy to investigate impact on the grade distribution. Noting that some trends were visible in the quality control data (section 7.3.4.1), and that the site visit had indicated some challenges with wet ground (section 7.2.4.1), it is important to review the impact of recovery on grade. Figure 66 shows that low-recovery samples have relatively high Au grades. This apparent bias is one of the key reasons limiting a high-confidence Au resource classification.

This trend is not visible in Ti, Zr, Fe, garnet, ilmenite and zircon data, providing another key support for aircore drilling to support the high-confidence classification categories, in addition to the twin drilling results (Figure 67–Figure 69).

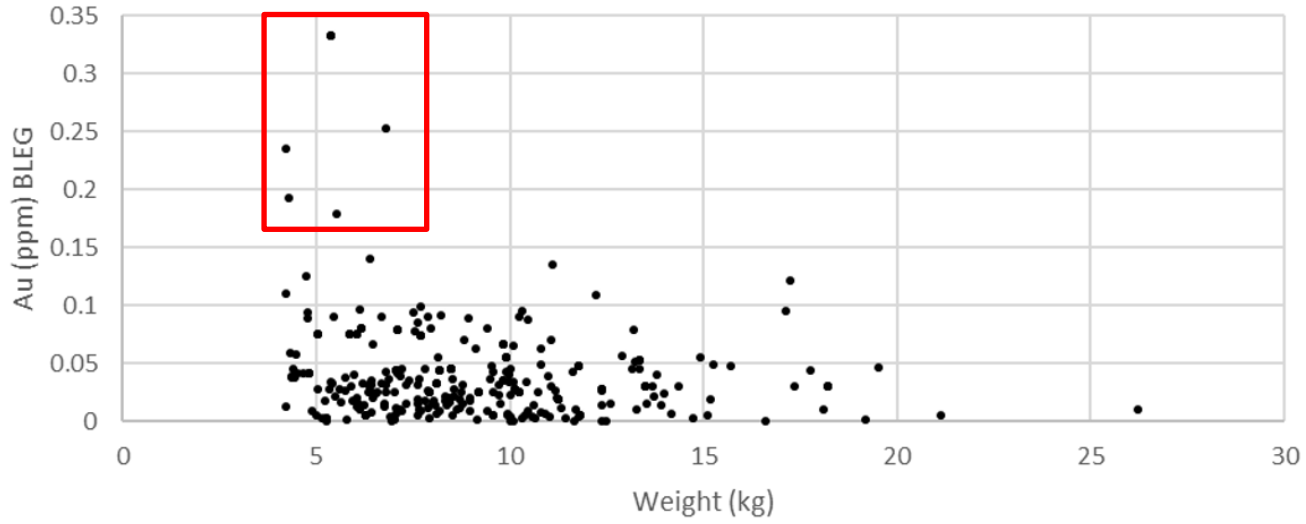


Figure 66: BLEG Au (ppm) grade vs sample weight plot.

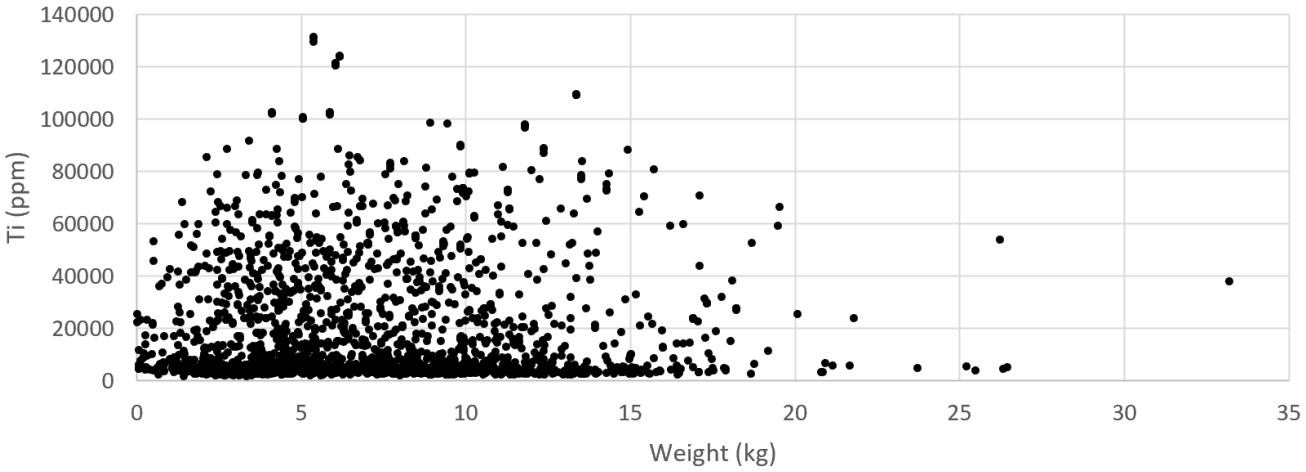


Figure 67: Ti grade (pXRF) vs sample weight plot.

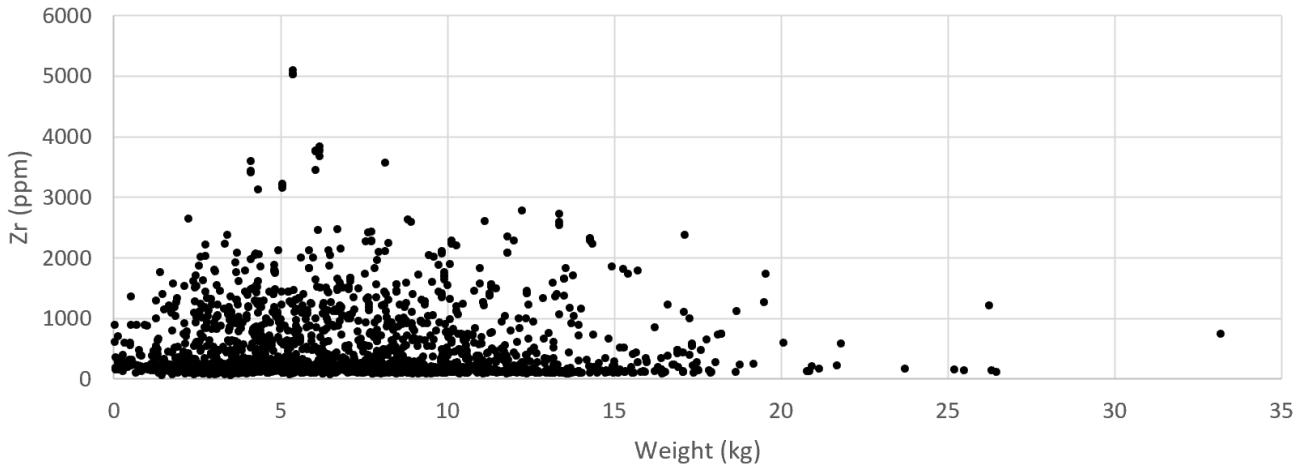


Figure 68: Zr grade (pXRF) vs sample weight plot.

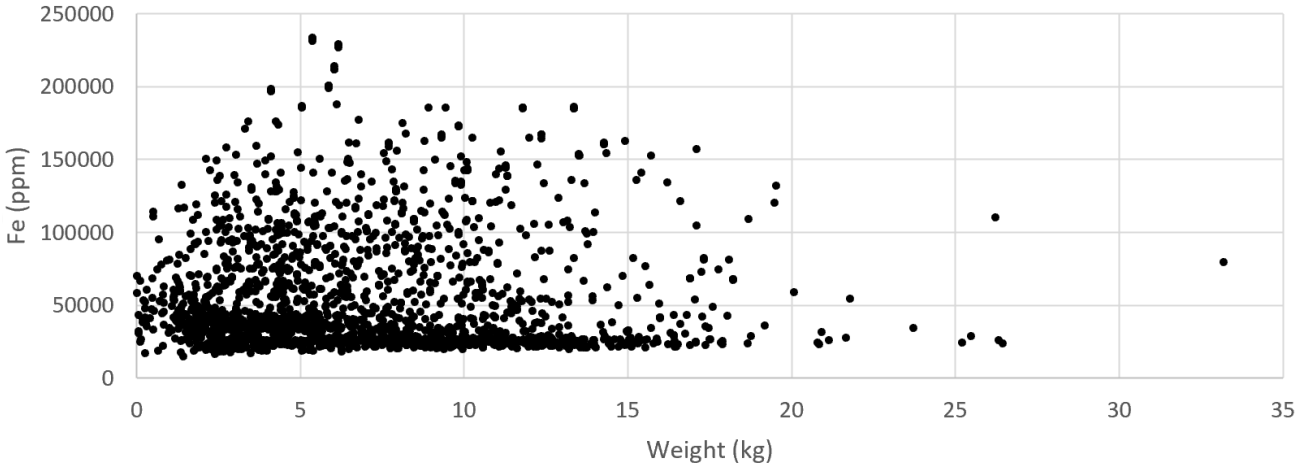


Figure 69: Fe grade (pXRF) vs sample weight plot.

### 7.4.4.2 *First Split*

The data quality of the first (rotary) splitting stage was determined following the determination that these processes were appropriately controlled and provided consistent data (section 7.3.4.2).

No Au data are available for first split repeat pairs. Scatter and QQ plots of the first split repeats (n=82) are presented in Figure 70, Figure 71, and Figure 72 for pXRF Ti, Fe and Zr data, respectively. The scatterplots show very low scatter. This is also reflected in the precisions (measured by the coefficient of variation[5]) of ~7%, ~5% and ~10% for Ti, Fe and Zr, respectively. A CV of 5–10% is similar to the expected range for field duplicates from detrital ilmenite sand deposits, as calculated by Abzalov (2008). The QQ plots do not indicate significant bias and ranked Wilcoxon tests confirm that there are no statistically significant biases at 95% confidence.

The data resulting from the first split are accurate and highly precise, and therefore fit for the purpose of resource estimation in high-confidence classification categories.

[5] Root mean square CV (Stanley and Lawie, 2007; Abzalov, 2008).

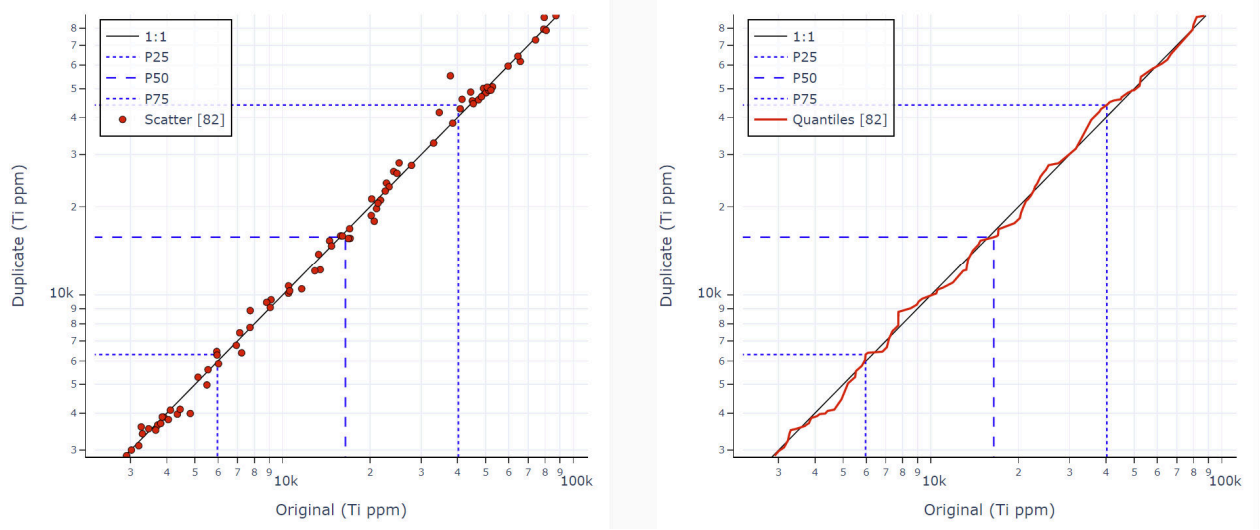


Figure 70: Scatter and QQ plot Ti pXRF first split repeats.

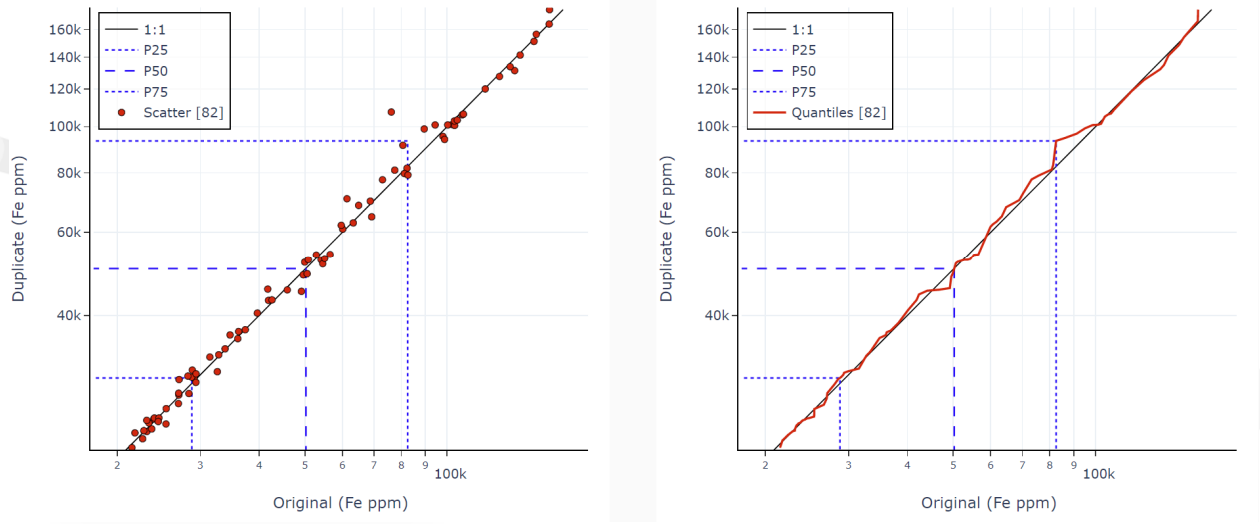


Figure 71: Scatter and QQ plot Fe pXRF first split repeats.

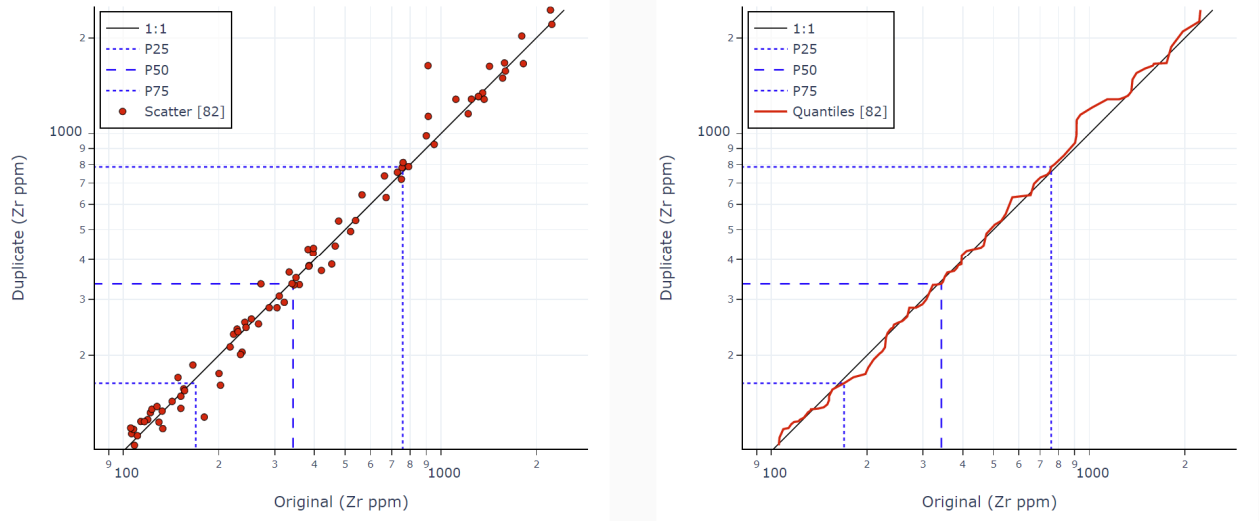


Figure 72: Scatter and QQ plot Zr pXRF first split repeats.

### *7.4.4.3 Second Split*

The data quality of the wet-screening and second splitting was assessed following the determination that these processes provided consistent data (7.3.4.3).

Screen-size data from the NZIMMR wet-screening process was not available. However, the P1 fifth and sixth split data from IHC Robbins and SEM data were used to review the quality of the NZIMMR wet-screening process.

The P1 fifth split data presented in Figure 59 suggest that the NZIMMR slime removal process may not always be completely effective, as finer than 45 µm material (slime) should have been removed before the P1 fifth split process; however, a direct comparison is not possible because of the size difference in the slime fraction removed at NZIMMR (-45 µm) and IHC Robbins (-53 µm). Observations in the SEM data (section 7.4.4.7.2) further suggest that the NZIMMR wet-screening process to remove slimes (-45 µm) did not always provide consistent data. Of the original 70 SEM samples, 17 samples had more than 10 wt% of -45 µm material (slime) as measured by the SEM; five of those had more than 20 wt% of finer than 45 µm material. The highest slime content measured in a sample was 46 wt%.

The P1 sixth split data (18 data points) presented in Figure 60 demonstrate that the NZIMMR oversize removal process is not always completely effective, as oversize (+2 mm) material should have been removed during the NZIMMR wet screening, well before the P1 sixth split stage.

No Au data are available for second split repeat pairs. Scatter and QQ plots of the second split repeat data (n=32) are presented in Figure 73, Figure 74 and Figure 75 for pXRF Ti, Fe and Zr data, respectively. The scatterplots show very low scatter. This is also reflected in the precisions (CV[5]) of ~2%, ~2% and ~8% for Ti, Fe and Zr, respectively. These are in range with expectations for the mineralisation style and comminution stage. The QQ plots do not indicate significant bias and ranked Wilcoxon tests confirm that there are no statistically significant biases at 95% confidence.

The data resulting from the second split are accurate and highly precise, and therefore fit for the purpose of resource estimation in high-confidence classification categories.

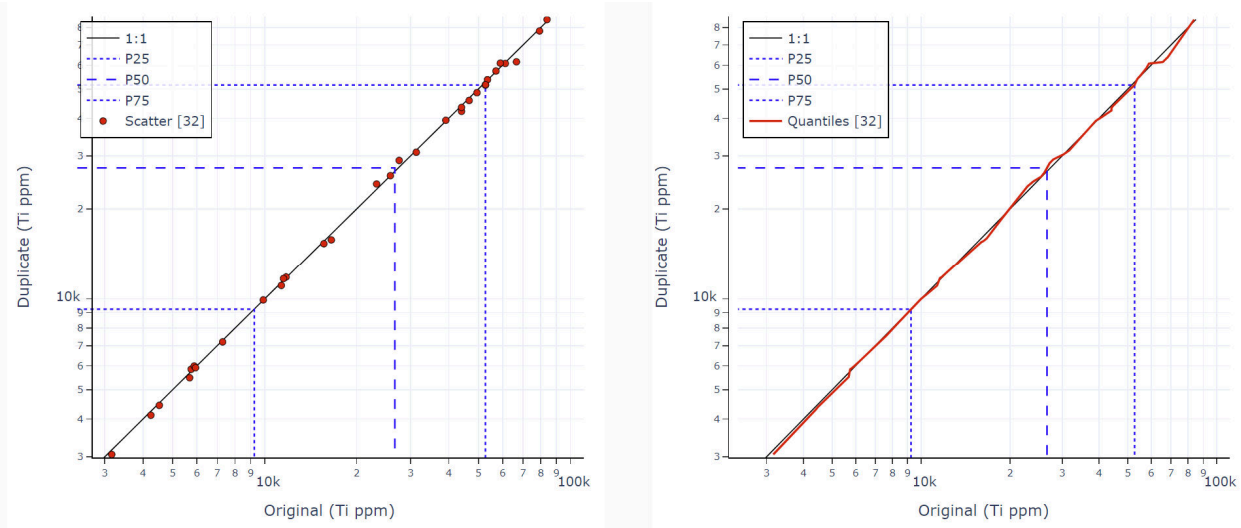


Figure 73: Scatter and QQ plot Ti pXRF second split repeats.

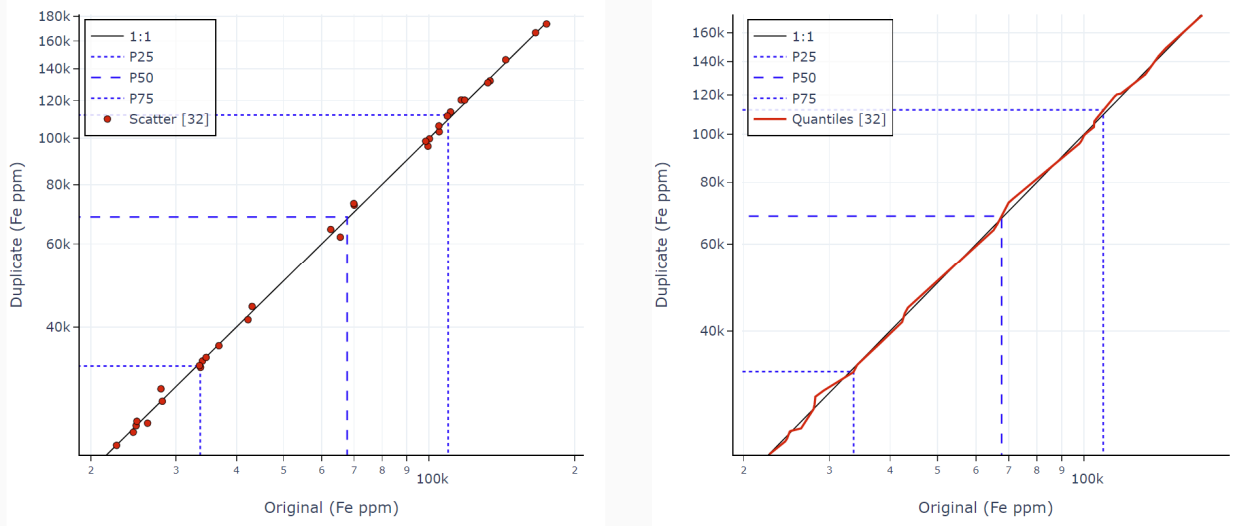


Figure 74: Scatter and QQ plot Ti pXRF second split repeats.

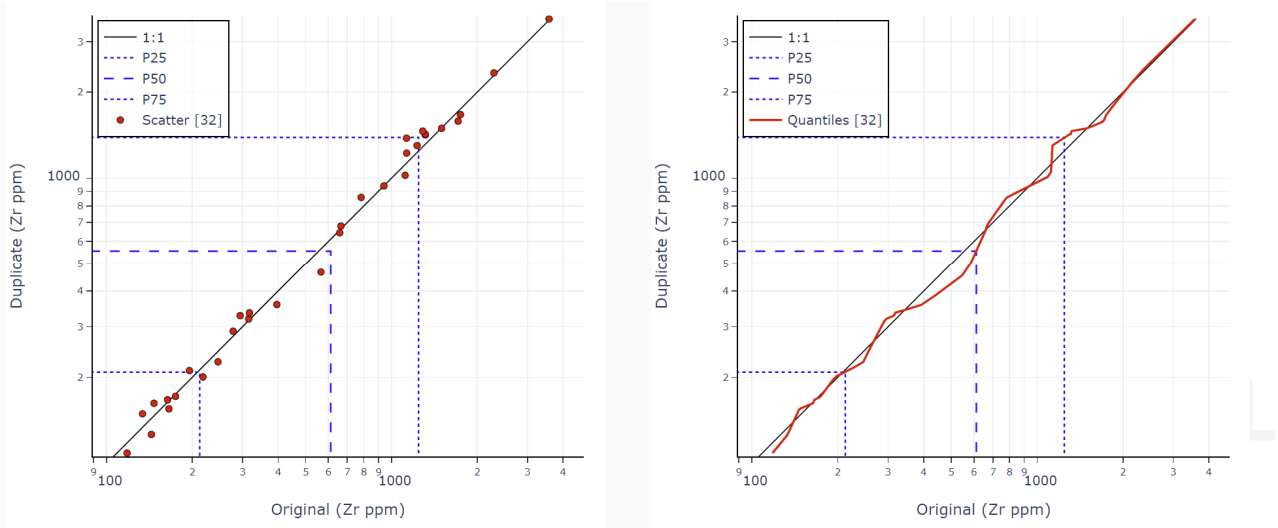


Figure 75: Scatter and QQ plot Zr pXRF second split repeats.

### 7.4.4.4 *Third Split*

The data quality of the third splitting was assessed following the determination that these processes provided consistent data (7.3.4.4).

No Au data are available for third split repeat pairs. Scatter and QQ plots of the third split repeat data (n=96) are presented in Figure 76, Figure 77 and Figure 78 for pXRF Ti, Fe and Zr data, respectively. The scatterplots show very low scatter. This is also reflected in the precisions (CV[5]) of ~2.5%, ~1% and ~7% for Ti, Fe and Zr, respectively. These are in range with expectations for the mineralisation style and comminution stage. The QQ plots do not indicate significant bias and ranked Wilcoxon tests confirm that there are no statistically significant biases at 95% confidence.

The data resulting from the third split are accurate and highly precise, and therefore fit for the purpose of resource estimation in high-confidence classification categories.

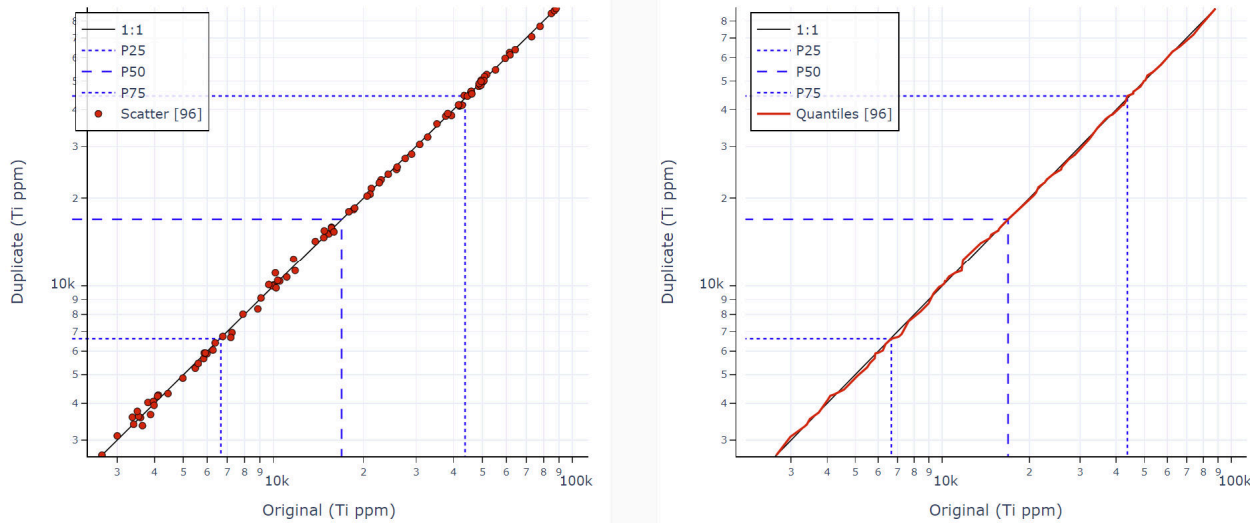


Figure 76: Scatter and QQ plot Ti pXRF third split.

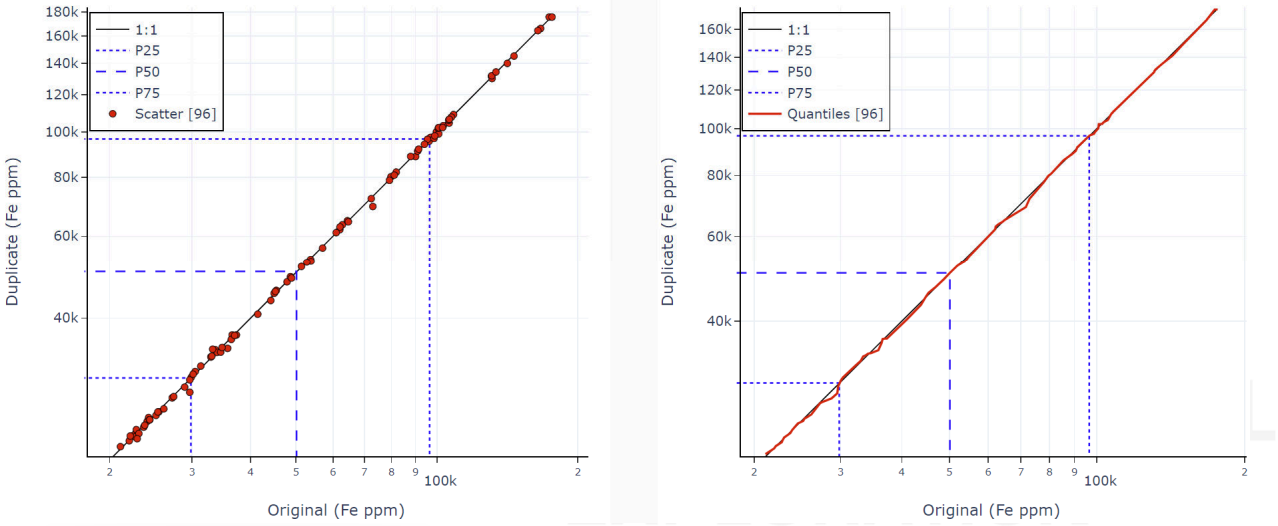


Figure 77: Scatter and QQ plot Fe pXRF third split.

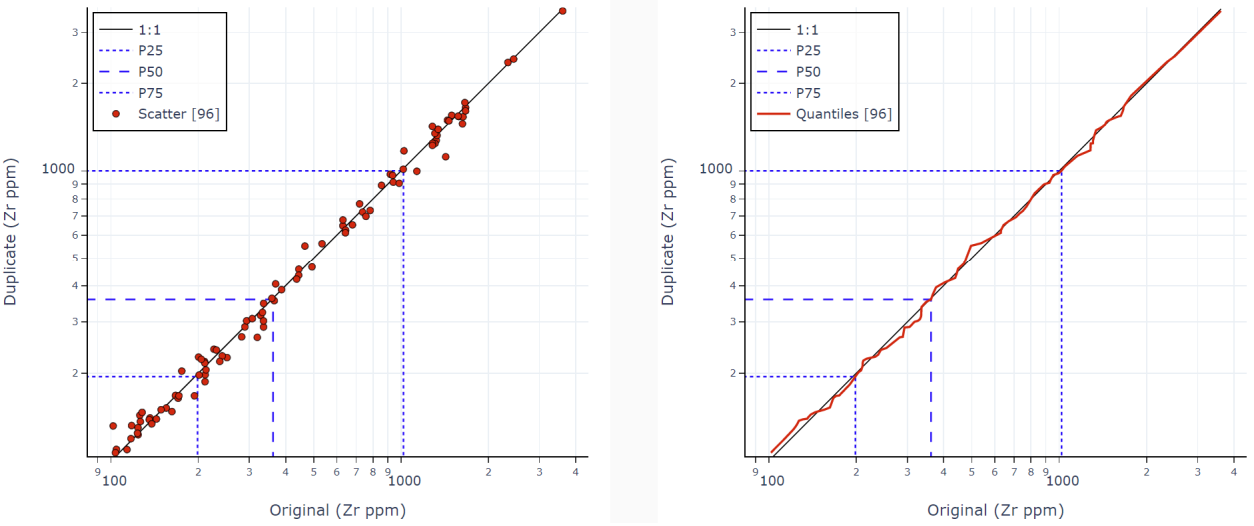


Figure 78: Scatter and QQ plot Zr pXRF third split.

### 7.4.4.5 *Priority 1 Subsample (P1)*

#### 7.4.4.5.1 *P1 Fourth Split*

The data quality of the P1 fourth split (riffle splitter) was assessed following the determination that the process provided consistent data (7.3.4.5.1).

Scatter and QQ plots of the P1 fourth split HM repeat data (n=117) are presented in Figure 79. The scatterplot shows some variability. This is also reflected in the precision ($CV^5$) of ~28%, which is on the high side for this stage of comminution. The QQ plot suggests a minor bias towards the original sample in samples below 20% HM; However, a ranked Wilcoxon test confirms the bias is not statistically significant at 95% confidence, and even though there are a few outliers causing high variance, the data are considered fit for purpose.

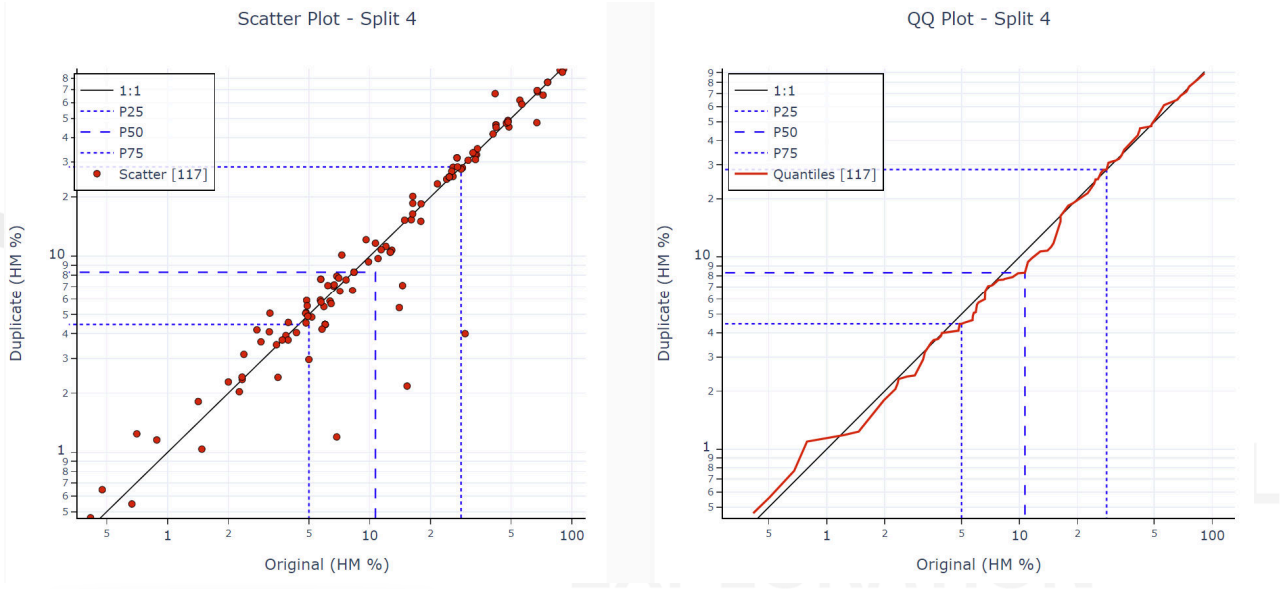


Figure 79: Scatter and QQ plot HM (%) P1 fourth split (riffle).

#### 7.4.4.5.2 *P1 Fifth and Sixth Split*

IHC Robbins is an internationally recognised independent laboratory that specialises in testing HM samples. Based on the industry standard practices implemented by IHC Robbins (section 7.2.4.5), including the quality control process to monitor any inconsistencies in screening (sections 7.3.4.5.2 and 7.3.4.5.3), the data resulting from the P1 fifth and sixth splits are considered fit for the purpose of estimation and high-confidence resource classification

#### 7.4.4.5.3 P1 Analytical

No CRM or blank sample data are available for the sink-float analytical process, and therefore accuracy and precision cannot be determined. There is some residual risk since there are no quality data available for this part of the process; however, the risk is considered low based on the accreditation of the laboratory and the use of industry-standard processes (section 7.2.4.5). Hence, the data are considered fit for purpose.

### 7.4.4.6 Priority 2 Subsample (P2)

#### 7.4.4.6.1 P2 Fourth Split

No quality data are available for the P2 fourth split, hence the quality of the P2 fourth split scooping process cannot be quantitatively determined. However, the Competent Person has deep knowledge of SGS laboratories and considers the risk associated with the P2 fourth split low. The data resulting from the P2 fourth splits are considered fit for the purpose of estimation and high-confidence resource classification.

#### 7.4.4.6.2 P2 Fifth Split

*SGS Waihi*

No quality data are available for the P2 fifth split, hence the quality of the P2 fifth split scooping process cannot be quantitatively determined. However, the Competent Person has deep knowledge of SGS laboratories and considers the risk associated with the P2 fifth split low. The data resulting from the P2 fifth splits are considered fit for the purpose of estimation and high-confidence resource classification.

*RSC Wellington*

The data quality of the P2 fifth splitting was assessed following the determination that the process provided consistent data (7.3.4.6.2).

Scatter and QQ plots of the P2 fifth split repeat data (n=95) from pXRF Fe and Ti data are presented in Figure 80. The scatterplots show very low scatter. This is also reflected in the precisions ($CV^5$) of ~0.9% and ~3% for Fe and Ti, respectively. These are in range with expectations for the mineralisation style and comminution stage. The QQ plots do not indicate significant relative bias and ranked Wilcoxon tests confirm no statistically significant bias at 95% confidence.

The data resulting from the fifth split are accurate and highly precise, and therefore fit for the purpose of resource estimation in high-confidence classification categories.

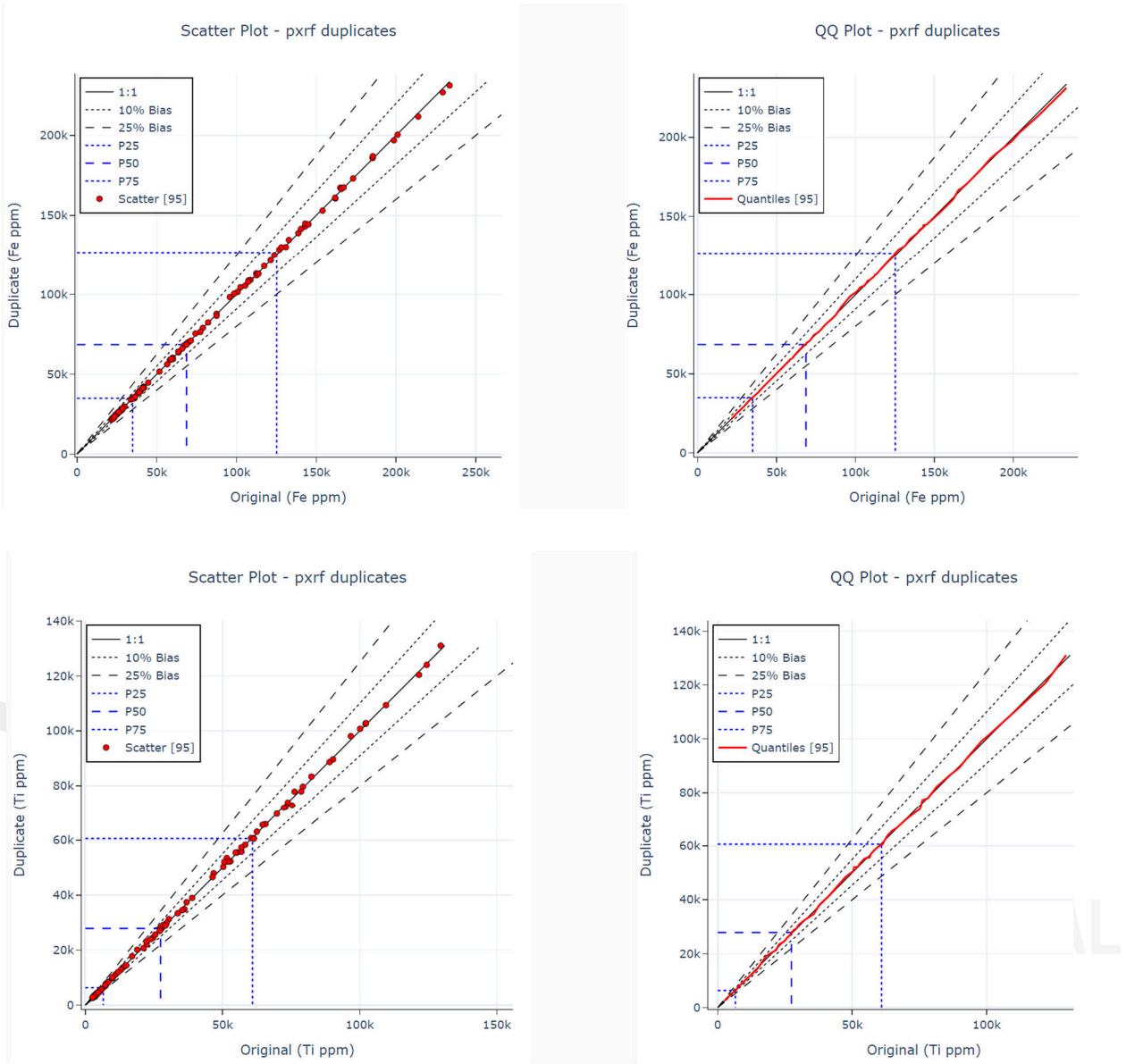


Figure 80: QQ plots for Fe (top) and Ti (bottom) pXRF P2 Split 5 repeats.

### *7.4.4.6.3 P2 Analytical (Fire Assay and pXRF) Process*

*Fire Assay (SGS Waihi)*

Since FA Au data were not used in the MRE, other than to identify the main gold-bearing domain, the quantitative accuracy and precision of the fire assay analytical process are not overly relevant. The data are suitable for the interpretation of estimation domains.

*pXRF*

Data from the pXRF were compared to laboratory XRF analysis from ALS Geochemistry, Brisbane. The samples are subsamples of those received for pXRF analysis and were selected to cover the variability of the geochemistry data in every element (section 6.3.2; Table 17). Scatter and QQ plots of the pXRF-XRF comparison are presented in Figure 81 and Figure 82, respectively. For most elements, the pXRF geochemical data slightly under-estimates the laboratory-derived geochemistry data (XRF; Figure 82); however, the precision is very good — appropriate sample preparation and calibration against standards have produced a high-quality pXRF dataset with a minor (~5%) low bias (Figure 82). Furthermore, the linear regression model to derive mineralogy from geochemistry is trained on the entire geochemical dataset and the absolute values do not impact the model performance. The Competent Person considers the calibrated pXRF geochemical data fit for purpose of resource estimation in high-confidence classification categories.

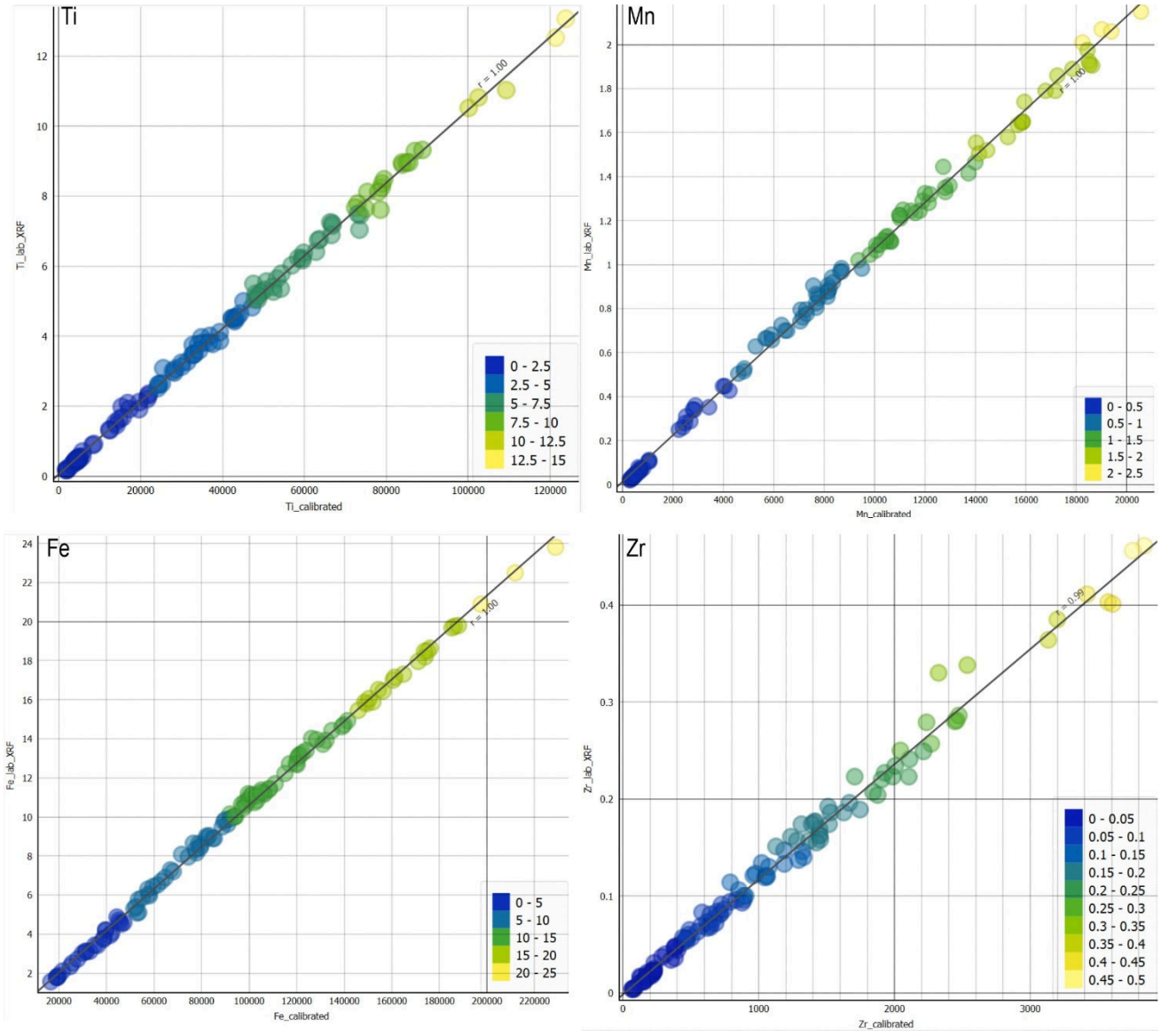


Figure 81: Validation of calibrated pXRF against laboratory XRF for the elements Ti, Fe, Mn and Zr.

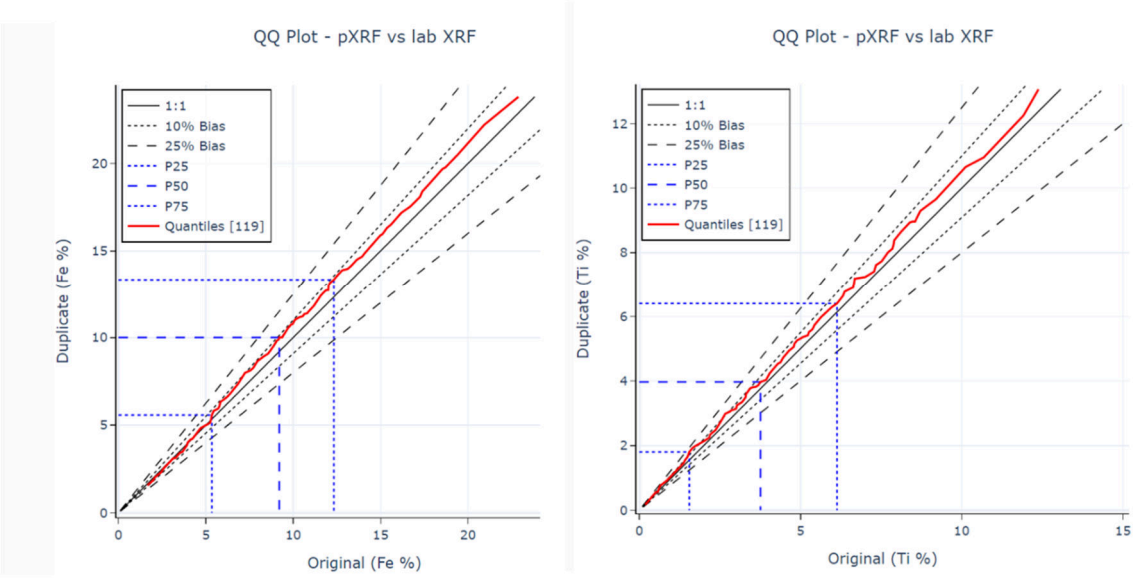


Figure 82: QQ plots for pXRF versus laboratory XRF for the elements Fe (left) and Ti (right).

#### *7.4.4.6.4 P2 Sixth Split*

No quality data are available for the P2 sixth split, hence the quality of the P2 sixth split cannot be quantitatively determined. Since the samples are finely pulverised, the Competent Person considers the risk associated with the P2 sixth split process to be low and the data fit for purpose.

#### *7.4.4.6.5 P2 Seventh Split*

The accuracy and precision of the scooping process at ALS Brisbane were not determined. Based on the accreditation of the laboratory, the use of industry-standard processes, systems and tools (section 7.2.4.6.5), including the laboratory's quality control processes to monitor inconsistencies in the splitting (section 7.3.4.6.5), the P2 seventh split data are considered fit for the purpose of estimation and high-confidence resource classification.

#### *7.4.4.6.6 P2 Analytical (XRF)*

The accuracy and precision of the XRF analytical process at ALS Brisbane were not determined. However, the laboratory's quality data suggest that the analytical process was fit for purpose and delivered accurate and precise data appropriate for estimation and high-confidence resource classification.

### *7.4.4.7 Priority 3 Subsample (P3)*

#### *7.4.4.7.1 P3 Fourth Split*

Insufficient quality data are available for the P3 fourth split. Based on the highly trained personnel and quality operating procedures (7.2.4.7.1), the Competent Person considers the P3 fourth split data fit for the purpose of estimation and high-confidence resource classification.

#### 7.4.4.7.2 P3 Analytical (SEM)

RSC analysed 70 samples for SEM-based automated mineralogy. The data collected via automated mineralogy with the SEM were used to guide mineral abundance modelling from the calibrated pXRF data.

The presence of fine particles (high slime content in 17 of the 70 samples; section 7.4.4.3) led to substantially longer scanning times and resulted in erroneous data. Data from samples with >10 wt% slime and organic material were excluded from training the heavy mineral abundance model; therefore, SEM data from 59 samples were accepted and used for the mineral abundance model.

Scatter and QQ plots of the paired pXRF and automated mineralogy data (n=59) are presented in Figure 40 and Figure 41. The scatterplots show very low scatter. The QQ plot suggests a bias (~10%) towards the automated mineralogy data; however, the pXRF data were found to have a minor bias (section 7.4.4.6.6) when compared with the XRF data. Based on the overall model performance results (sections 6.3.4.3 and 6.3.4.4), RSC considers the SEM-derived mineral abundances in the untrained data to be highly precise and sufficiently accurate for the purpose of estimation and high-confidence resource classification.

### 7.4.4.8 Priority 4 Subsample (P4)

No Priority 4 samples were submitted for analysis.

### 7.4.4.9 Cyanide Leach Samples

#### 7.4.4.9.1 Second Split

No quality data are available for the leach second split; hence, the quality of the split cannot be quantitatively determined. Based on the review of processes, systems and tools (section 7.2.4.9.1), the leach second split data are considered fit for the purpose of estimation and resource classification.

#### 7.4.4.9.2 Analytical (BLEG)

CRMs are not commonly inserted in BLEG analysis, and insufficient information was available to quantitatively assess any special-cause variation in the BLEG analytical process. Based on the review of processes, systems and tools (section 7.2.4.9.2), the leach analytical data are considered fit for the purpose of estimation and resource classification.

### 7.4.4.10 Legacy data

RSC also compared the distributions of ilmenite abundances between the 2022 and legacy data to establish whether the two datasets were comparable and suitable to be combined as an input for the MRE. The ilmenite distributions were compared within high- and low-abundance ilmenite domains that incorporate the legacy data, by visual assessment on cross-sections and comparison of geostatistical summaries including histograms, experimental variography, swath plots and nearest-neighbour analysis (specifically distance-buffered QQ plots).

When constrained to the high-abundance domain, the legacy ilmenite abundance data indicate a low bias (approximately -20%) compared to the 2022 results (Figure 83). Based on the apparent strong bias of the legacy data, and the fact that the legacy data do not provide strong additional spatial sampling coverage compared to the 2022 samples, these have been excluded from the final estimate. The legacy data, which preferentially sampled the high-abundance portion of the mineralisation were only used to help constrain the ilmenite high-abundance estimation domain boundary, as, in places, they improved the geometrical precision of the boundary.

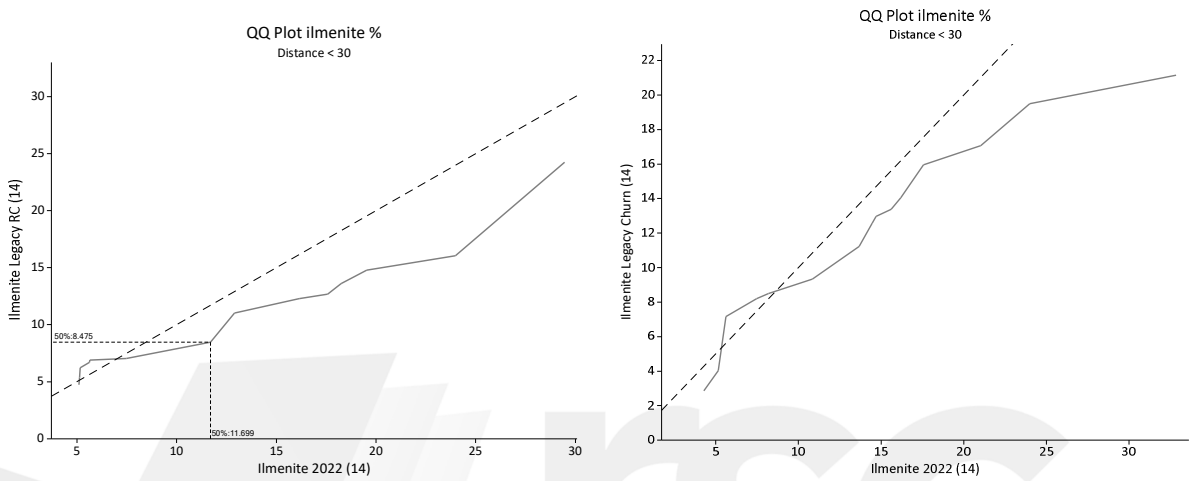


Figure 83: QQ plot of the 2022 and the legacy RC abundance data (left) and the 2022 and legacy churn abundance data (right), within the high-abundance ilmenite domain, using buffered pairs up to 30 m.

## 7.5 Data Verification

Data verification is the process of checking and verifying hard-copy logs and digital records for accuracy, ensuring the data on which Mineral Resource estimates are based can be linked from digital databases or records to log sheets and drilling or sampling intervals. It is an additional verification process to determine that QA and QC processes have been effectively applied, and that these were working to assure and control the quality of the data. Data verification is carried out after samples have been collected, assays have been returned, and data have been stored in the database. Where relevant, data verification may also include check sampling carried out by the Competent Person, especially if SOPs are not available or difficult to audit, and QC data are limited to demonstrate processes were in control.

### 7.5.1 Site Visit

Mr Sean Aldrich completed a site visit to the Barrytown Flats Project from 12–13 May 2022 and reviewed the project geology, drilling and sampling procedures, samples, drill sites and processing facilities. Mr Aldrich was granted full access to samples, certificates, and databases.

The objectives of the site visit included: auditing drilling, handling, and sampling procedures; examination of sampling and observation of mineralised intercepts; and a brief audit of the NZIMMR preparation laboratory in Greymouth (section 7.2).

However, the NZIMMR laboratory was not processing samples during the site visit. No verification samples were collected during the site visit. The locations of the points of interest visited during the site visit are presented in Table 19.

#### *7.5.1.1 Collar Locations*

During the site visit, the location data of a selection of collars were checked using a handheld GPS, all of which generally matched with what is recorded in the database (Table 19).

Table 19: Verification of collar locations.

| Drillhole ID | Database Easting | Database Northing | Check Easting | Check Northing | Difference Easting (m) | Difference Northing (m) |
|---|---|---|---|---|---|---|
| **TAC142** | 1461386.3 | 5326731.5 | 1461385 | 5326731 | 1.3 | 0.5 |
| **TAC143** | 1461401.0 | 5326724.1 | 1461401 | 5326719 | 0 | 5.1 |
| **TAC144** | 1461438.5 | 5326691.7 | 1461440 | 5326692 | -1.5 | -0.3 |
| **TAC145** | 1461467.0 | 5326681.3 | 1461465 | 5326685 | 2 | -3.7 |
| **TAC146** | 1461482.6 | 5326676.9 | 1461484 | 5326680 | -1.4 | -3.1 |
| **TAC147** | 1461504.5 | 5326679.0 | 1461506 | 5326680 | -1.5 | -1 |
| **TAC148** | 1461524.6 | 5326679.6 | 1461525 | 5326681 | -0.4 | -1.4 |
| **TAC149** | 1461541.0 | 5326680.3 | 1461545 | 5326681 | -4 | -0.7 |
| **TAC150** | 1461564.1 | 5326681.8 | 1461564 | 5326681 | 0.1 | 0.8 |

#### *7.5.1.2 Geological Logging*

During the site visit, several aircore drillholes were relogged by Mr Aldrich; the logs were found to be comparable with the logs recorded in the database. Mr Aldrich observed that the overburden is easily recognisable and separated from the mineralised domain by a distinct boundary. The mineralised domain consists of grey to dark-grey fine sand. The HM assemblage of the mineralised domain is difficult to assess with accuracy. The base of the mineralised domain is also distinct and marked by a decrease in HM and an increase in particle size. The overburden, the mineralised domain and their boundaries can easily be interpreted from photographs taken of the sample board.

## 7.6 Security & Chain of Custody

### 7.6.1 Sample Storage, Security & Chain of Custody

Following logging, samples were batched into polyweave bulka bags in groups of 40–60 samples. For the 2022 drilling, aircore samples were briefly stored on site before transportation to the sample preparation lab at NZIMMR. A locked gate restricts access to the site. Alton Drilling staff transferred samples from the rig to the storage area multiple times a day.

In the sample storage area, samples were unloaded and laid out for logging. Following logging, samples were recorded and then closed with a zip tie with a metal tag labelled with the sample number. An additional metal tag was placed inside the sample bag. The polyweave sample bags were placed in batches into large polyweave bulka bags which were then closed, ready for transportation. The site was securely locked overnight to prevent third party access.

NZIMMR laboratory staff picked the samples up from site and transported them directly to their facility. Samples were stored according to batch at the facility, both indoors and outdoors, awaiting sample preparation. Samples stored outdoors were covered in tarpaulins for protection from rainfall. Digital sample submission forms, including sample processing instructions, were sent directly to NZIMMR. NZIMMR used a spreadsheet to record sample processing data, and processed samples in batch order. The spreadsheet was maintained by the lead process engineer and periodically emailed to RSC.

### 7.6.2 Priority Sub-Split Samples

P1 sub-split samples were sent to IHC Robbins directly from NZIMMR in large batches. RSC was not provided with a sample list. IHC tracked sample data using spreadsheets.

P2 sub-split samples were sent in groups of batches to SGS Westport, where they were logged into SGS's sample tracking system throughout the subsequent processing. RSC received notification when samples were sent to SGS Waihi for fire assay analysis, and again following analysis. Samples were sent from SGS, Westport to SGS, Waihi facility by registered courier and remnant pulps were retained in Waihi. SGS Westport prepared P2 pulps for analysis by pXRF. Samples were sent by registered courier to RSC Wellington and sample submission lists accompanied these samples in hard copy format.

P3 sub-split samples were stored securely at NZIMMR, and then transported by NZIMMR staff to TiGa's secure storage facility in Greymouth awaiting selection for analysis. NZIMMR staff selected samples to send by registered courier to a preparation facility in Christchurch. Prior to analysis, RSC staff hand-couriered the prepared SEM samples.

Both the coarse reject, and the P4 samples were stored securely at NZIMMR, and at TiGa's Greymouth facility prior to selection. Selected samples were hand couriered to NZIMMR for preparation and dispatch to ALS Perth for analysis in several batches using two different registered couriers.

P2 pulp samples were retained in RSC Wellington in a secure locked office following pXRF analysis. Samples selected for XRF analysis were sent by registered courier, with accompanying sample submission forms, to ALS, Brisbane for analysis.

## 7.7 Summary Data Quality

A summary of the QA, QC and overall quality of the data informing the MRE is presented in Table 20.

Table 20: Summary of informing data quality for the purpose of resource estimation and classification.

| Data Type | Technique | QA | QC | Accuracy | Precision | Accepted/Fit for Purpose | Comment |
|---|---|---|---|---|---|---|---|
| **Location Data** | Collar | Pass | Pass | Not available | Not available | Yes | Quality data not recorded but collar location data fit for purpose based on process review. |
| | Downhole | Not available | Not available | Not available | Not available | Yes | No downhole surveys. Low risk as short vertical holes. |
| **Density** | Weight (Core tray) | Pass with minor issues | Pass with minor issues | Pass with minor issues | Pass with minor issues | Yes | Fit for purpose based on QC processes. |
| **Grade** | Primary sample | Pass with minor issues | Pass with minor issues | Pass with minor issues | Pass with minor issues | Yes | Possible minor low bias in aircore data |
| | First split | Pass | Pass | Pass | Pass | Yes | |
| | Second Split | Pass with minor issues | Pass with minor issues | Pass | Pass | Yes | Wet-screening issues |
| | Third Spilt | Pass | Pass | Pass | Pass | Yes | |
| | P1 Fourth Split | Not available | Pass with minor issues | Pass with minor issues | Pass with minor issues | Yes | Fit for purpose based on laboratory accreditation and QC processes. |
| | P1 Fifth Split | Not available | Pass with minor issues | Not available | Not available | Yes | Fit for purpose based on laboratory accreditation and QC processes. |
| | P1 Sixth Split | Not available | Pass with minor issues | Not available | Not available | Yes | Fit for purpose based on laboratory accreditation and QC processes. |
| | P1 Analytical | Not available | Not available | Not available | Not available | Yes | Fit for purpose based on laboratory accreditation and industry-standard processes. |
| | P2 Fourth Split | Not available | Not available | Not available | Not available | Yes | Fit for purpose based on laboratory accreditation and industry-standard processes. |
| | P2 Fifth Split (FA; SGS Waihi) | Not available | Not available | Not available | Not available | Yes | Fit for purpose based on laboratory accreditation and industry-standard processes. |
| | P2 Fifth Split (pXRF; RSC Wellington) | Pass | Pass | Pass | Pass | Yes | |
| | P2 Analytical (FA) | Not available | Pass | Not available | Not available | Yes | Gold FA data were only used for interpreting estimation domains. |

| Data Type | Technique | QA | QC | Accuracy | Precision | Accepted/Fit for Purpose | Comment |
|---|---|---|---|---|---|---|---|
| | P2 Analytical (pXRF) | Pass | Pass | Pass with minor issues | Pass | Yes | Minor low bias in pXRF data. |
| | P2 Sixth Splt | Pass | Not available | Not available | Not available | Yes | Fit for purpose based on process review. |
| | P2 Seventh Split | Not available | Pass | Not available | Not available | Yes | Fit for purpose based on laboratory accreditation and industry-standard processes. |
| | P2 Analytical (XRF) | Not available | Pass | Not available | Not available | Yes | Fit for purpose based on laboratory accreditation and industry-standard processes. |
| | P3 Fourth Split | Pass | Not available | Not available | Not available | Yes | Fit for purpose based on highly-trained personnel and process review. |
| | P3 Analytical (SEM) | Not available | Not available | Not available | Not available | Yes | Fit for purpose based on highly-trained personnel, process review and model performance. |
| | P4 Subsample | Not available | Not available | Not available | Not available | Not applicable | Samples not analysed or used in MRE |
| | Cyanide Leach Second Split | Pass | Not available | Not available | Not available | Yes | Fit for purpose based on laboratory accreditation and industry-standard processes. |
| | Cyanide Leach Analytical (BLEG) | Not available | Not available | Not available | Not available | Yes | Fit for purpose based on laboratory accreditation and industry-standard processes. |
| **Legacy** | Legacy data | Not available | Not available | Fail | Fail | Yes | Fit for the purpose of domaining only. |

# 8 Mineral Resources Coates South Block

## 8.1 Informing Data

### 8.1.1 Gold

The Au resource estimate is based on FA and BLEG data generated during the 2022 drill programme, which was supervised by RSC. These data include Au results from 261 drillholes, totalling 3,118 m. The 50-g fire assay data (selected from the 45-µm to 2-mm screened fraction) were only used to determine the domain from which to select more representative Au samples. Within this mineralised domain, all samples (n=281) were submitted for BLEG analysis, on which the estimate is based (see section 6.2 for sample preparation and section 6.3.3 for sample analysis details). The locations of the BLEG samples informing the Au estimate are plotted in Figure 84. Both fire assay and BLEG data were used to establish estimation domains (Figure 85).

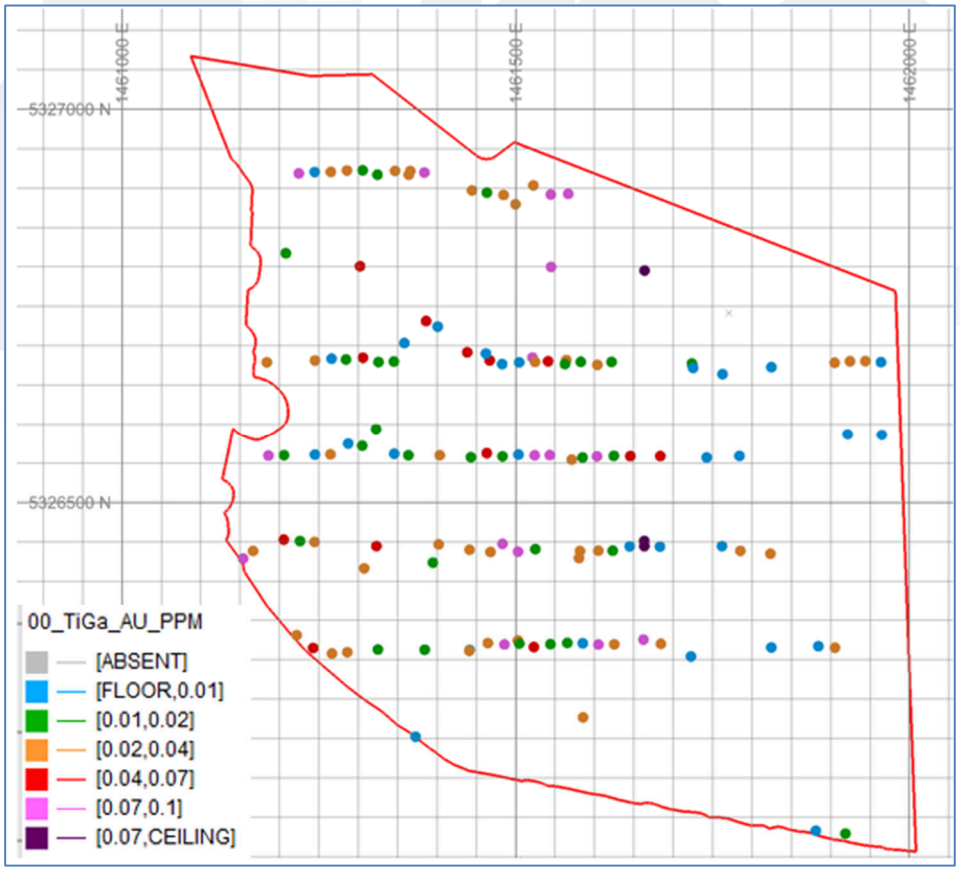


Figure 84: Location of the BLEG samples.

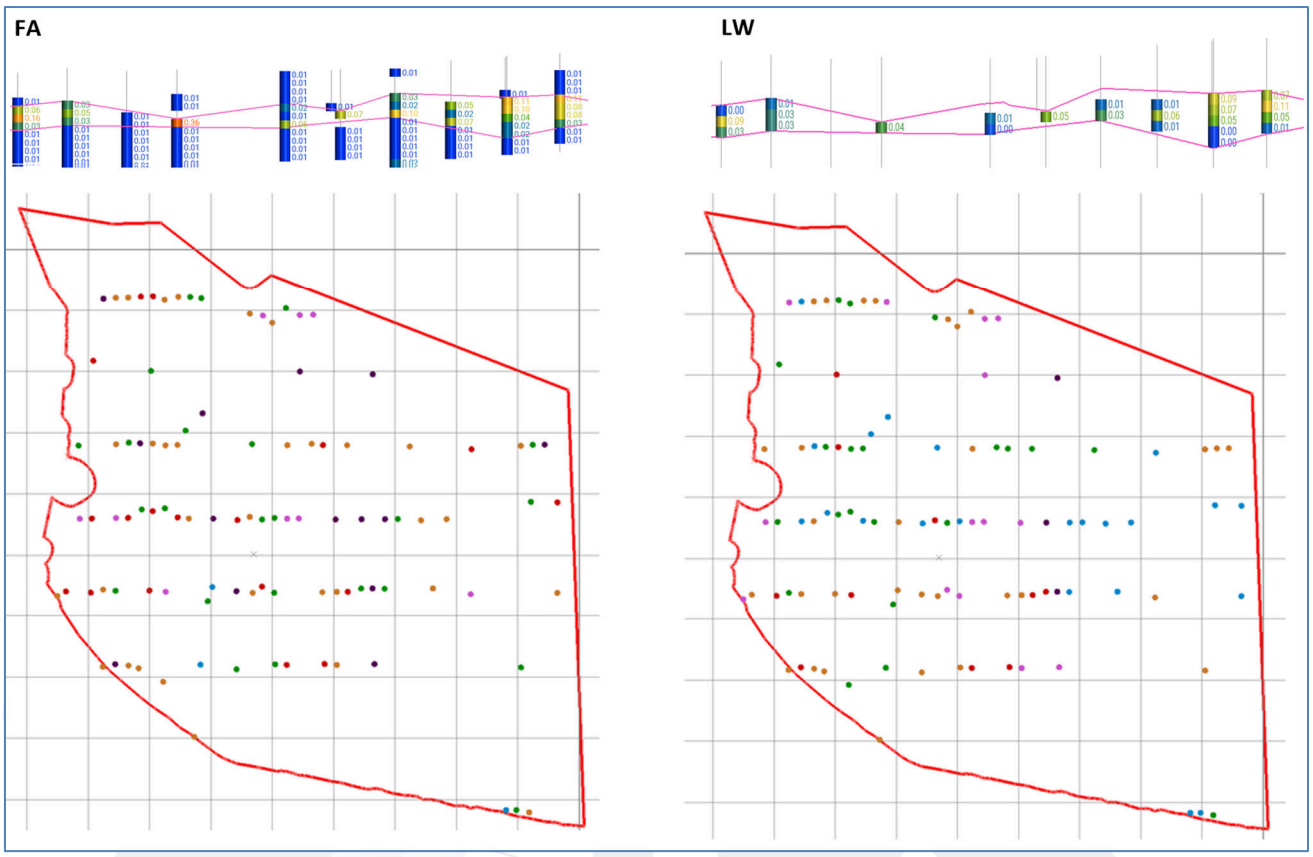


Figure 85: Visual comparison between fire assay (left) and BLEG (right). The top image is a selected cross-section, and the lower image is the plan view.

### 8.1.2 Heavy Minerals

Abundance data for the heavy minerals ilmenite, garnet, and zircon are used in the mineral resource estimate. These data were derived from 45-µm to 2-mm screened fraction of 1-m intervals from 3,118 m of aircore and sonic drilling, completed by TiGa during 2022. The process of determining heavy mineral abundances is described in section 6.3.4.

Data from legacy drilling completed within the project area (122 holes for 1,103 m, Table 6) were also used for the definition of the ilmenite high-abundance estimation domain boundary.

## 8.2 Interpretation & Model Definition

### 8.2.1 Geological Domains

The interpretation of geological domains is important for providing a first-pass constraint on grade populations, and ensuring the geological controls on mineralisation guide the modelling of estimation domains.

Nine geological domains were interpreted, based on downhole, lithological logging data from the 2022 drilling campaign.

The following geological domains were modelled using implicit techniques (Figure 86):

- Soil
- Gravel Base
- Top Clay-Silt
- Sands
- Sands, Minor Silt
- Sands, Minor Gravels
- Barren Gravel Strands
- Barren Silt Strands, and
- Eastern Gravel Unit.

The basal contact of the Soil unit (top) and the contact between the Sands and Gravel Base unit (bottom) provide a first-order constraint on mineralisation. Between these boundaries, mineralisation occurs predominantly within the Sands; Sands, Minor Silt; and Sands, Minor gravel geological domains.

In the Competent Person's opinion, given the strong geological continuity, high data density and relatively simple geology, alternative interpretations of the geology are not likely to deviate much from the current model and are unlikely to significantly impact the Mineral Resource.

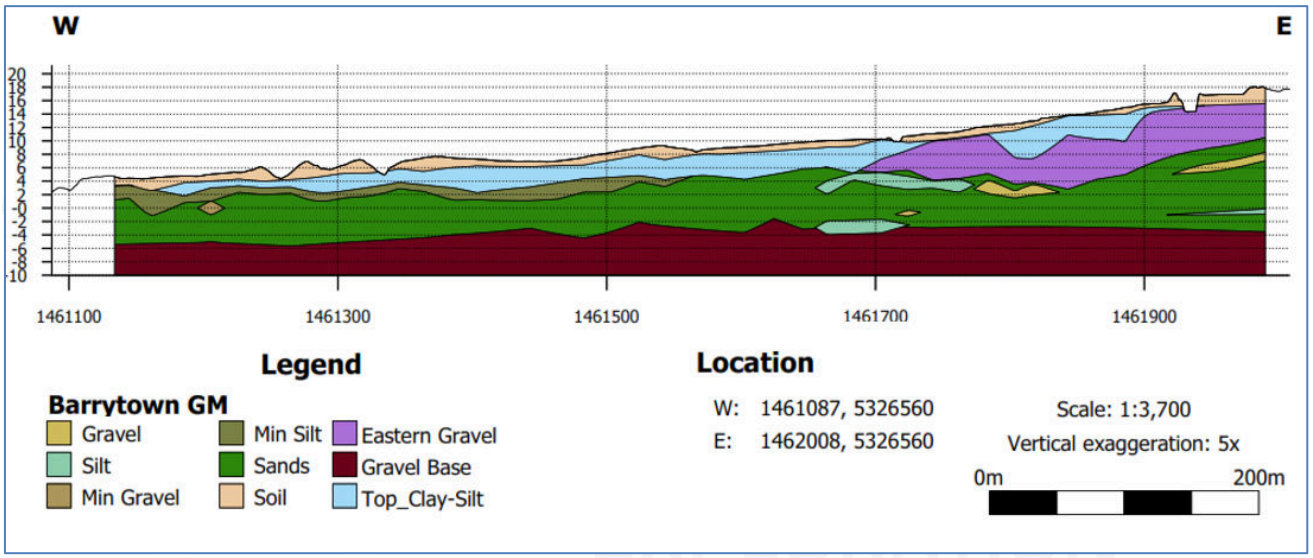


Figure 86: East–West cross-section (5,326,560N), looking to the north of the modelled and logged geological domains.

## 8.2.2 Estimation Domains

### *8.2.2.1 Gold*

The Au mineralisation is mostly constrained within the Sands geological domain (Figure 87). Within this domain, RSC assessed the continuity of the Au grades returned from both the fire assay and BLEG data. A 0.02 g/t Au numerical indicator offers a consistent representation of Au mineralisation within the Sands geological domain (Figure 88), and a grade shell based on that indicator was interpolated to model the Au estimation domain.

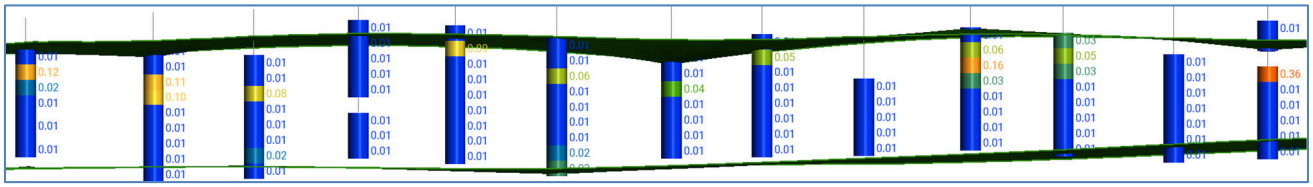

Figure 87: East–West cross-section (N 5,326,444), displaying drillholes coloured by Au mineralisation. The interpreted Sands unit is captured by the green triangles.

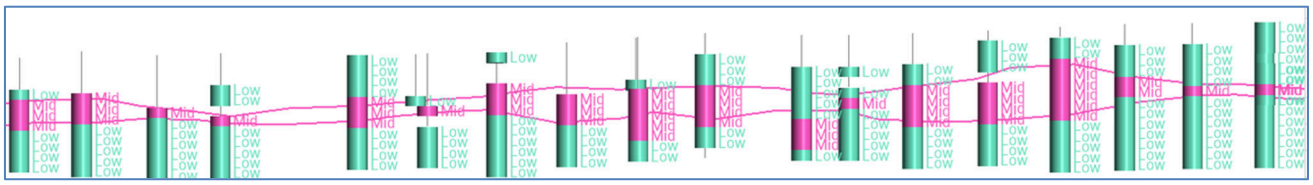

Figure 88: East–West cross-section (N 5,326,570), indicting the estimation domain based on a 0.02 pm Au indicator interpolant grade shell.

### *8.2.2.2 Heavy Minerals*

RSC assessed the continuity of the ilmenite, garnet, and zircon abundance, within the modelled geological domains, to ascertain whether populations could be combined or further subdivided for estimation.

Four estimation domains were created, based on the modelled geological domains (section 8.2.1). The geological domains representing the Minor Silts, and Sands with Minor Gravel, were combined with the main Sands domain to form a 'Sands' estimation domain. The Barren Gravel and Barren Silt Strands geological domains were combined into a 'Gravel and Silt' estimation domain. The Top Clay-Silt and the Eastern Gravels geological domains form the other two estimation domains.

A review of ilmenite, garnet, and zircon abundance, within the Sands estimation domain, revealed the presence of high-abundance sub-populations. High-abundance continuity trends, within the Sands unit, were assessed visually using numeric interpolant models. After determining the direction of maximum continuity to be approximately north–south in a sub-horizontal plane, numerical indicator models were further refined within the plane of maximum continuity. The indicator models represent heavy-mineral strandlines within the Sand unit and are characterised by high-abundance ilmenite (>4%, Figure 89), garnet (>10%), and zircon (>0.1%) domains, respectively.

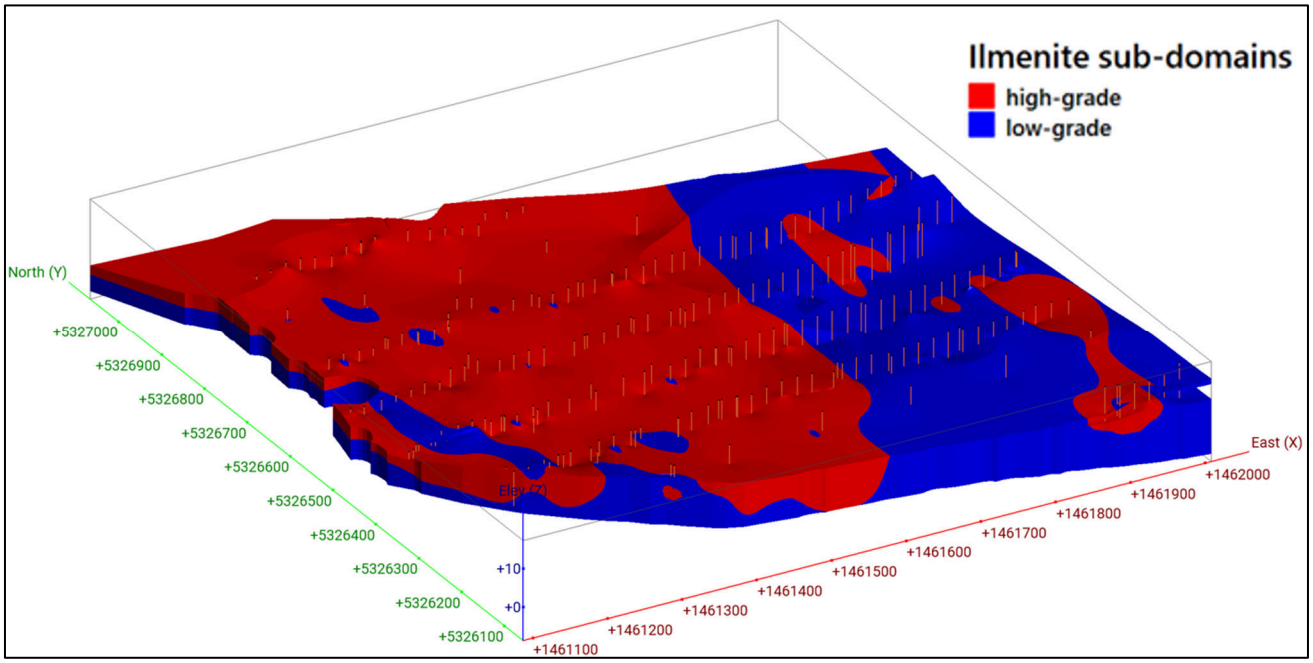


Figure 89: Perspective view to the northeast displaying the continuity of the High- and Low-Abundance Sands estimation domain for ilmenite.

### 8.2.3 Extrapolation

Mineralisation remains open in all lateral directions, and estimation domains do not extend beyond 50% of the drillhole spacing. The Competent Person considers the risk of uncertainty due to excessive extrapolation to be low.

## 8.3 Summary Statistics & Data Preparation

### 8.3.1 Gold

The BLEG data in the Au estimation domain was sampled at 1-m intervals and did not necessitate further compositing. The data distribution is monomodal with a low coefficient of variation (1.2). No top-cutting was applied. The distribution and summary statistics are plotted in Figure 90.

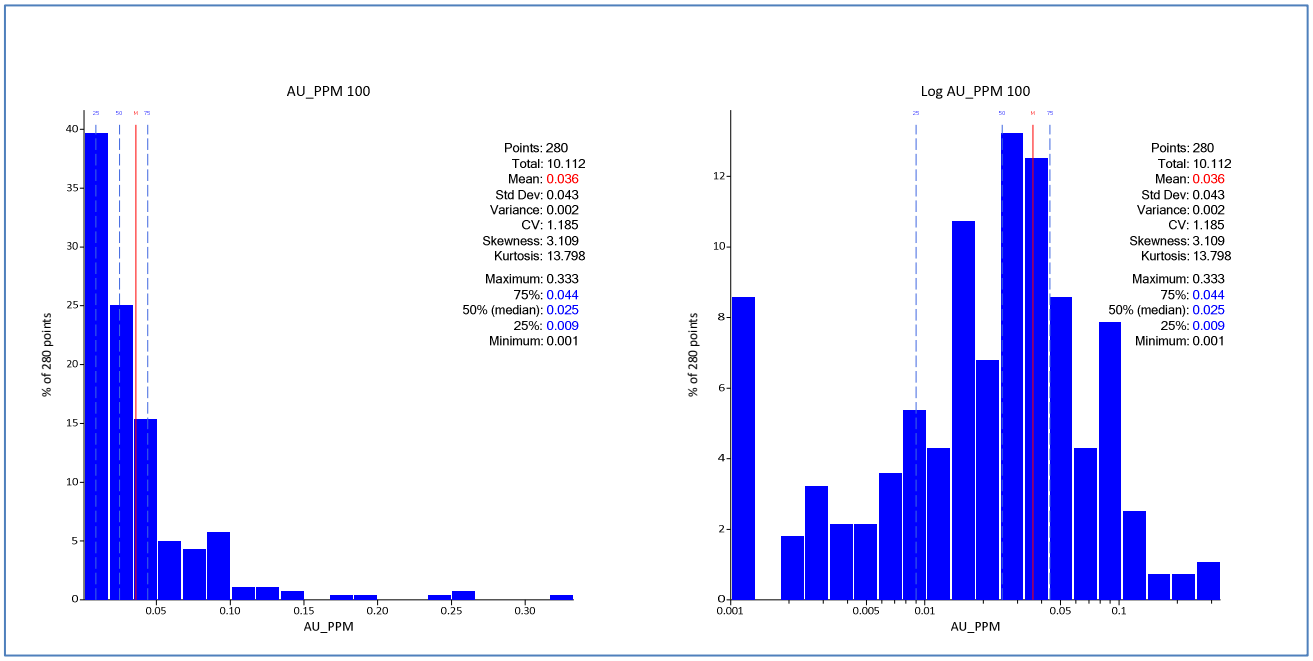


Figure 90: Histogram (left) and log-histogram for the Au data for Au estimation domain.

### 8.3.2 Heavy Minerals

All analyses and calculated abundances represent the 45-µm to 2-mm screened fraction of 1-m intervals. The estimation domains mainly indicate monomodal mineral abundance distributions (Figure 91). RSC notes that within the High-Abundance domain, the ilmenite abundance population suggests the existence of secondary modes around the first and third quartiles. RSC notes that despite this, the distribution has a low coefficient of variation (0.5), a mean value very close to the median value, and a relatively narrow interquartile range. These conditions present a low risk to the local estimation and therefore no additional sub-domaining to the ilmenite distribution was considered. All estimation domains exhibit low-to-moderate coefficient of variations (0.4–1.3; Table 21). The data have not been composited or top cut.

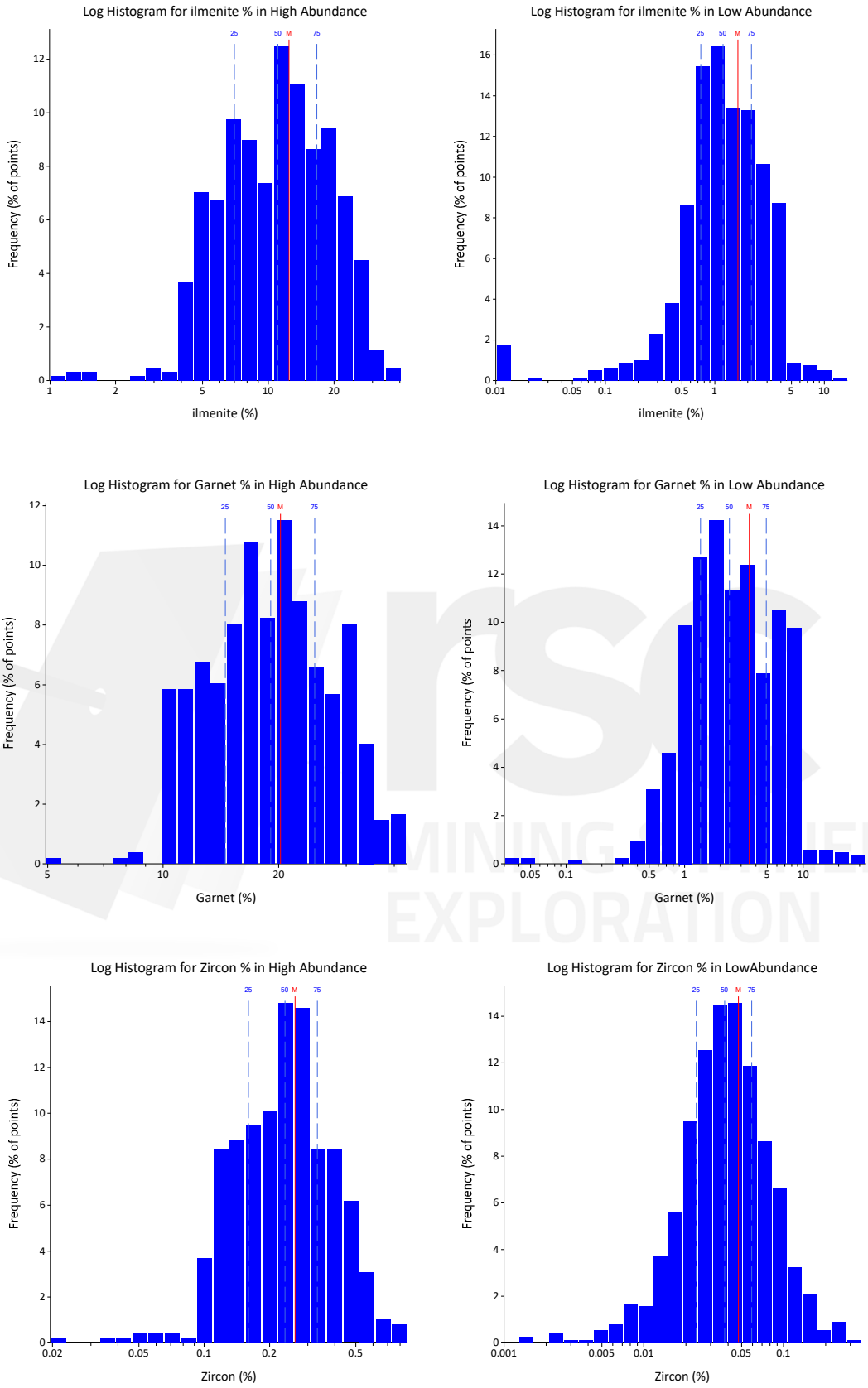


Figure 91: Log histograms of ilmenite, garnet and zircon (top to bottom) abundance, within the High-Abundance (left) and Low-Abundance (right) estimation domains.

Table 21: Summary statistics of mineral abundances within estimation domains.

| Mineral | Estimation Domain | Count | Mean (%) | Standard Deviation | CV | Variance | Minimum (%) | Median (%) | Maximum (%) |
|---|---|---|---|---|---|---|---|---|---|
| **Garnet** | Sands High-Abundance | 547 | 20.2 | 7.3 | 0.4 | 53.3 | 4.9 | 19.1 | 43.1 |
| **Garnet** | Sands Low-Abundance | 850 | 3.5 | 3.4 | 1.0 | 11.3 | 0.03 | 19.1 | 33.3 |
| **Garnet** | Gravel and Silt Strands | 171 | 5.5 | 6.4 | 1.2 | 40.6 | 0.6 | 3.0 | 50.0 |
| **Garnet** | Eastern Gravels | 123 | 3.6 | 3.4 | 0.9 | 11.3 | 0.3 | 2.7 | 22.8 |
| **Garnet** | Top Clay-Silt | 265 | 5.8 | 5.2 | 0.9 | 26.6 | 0.1 | 4.0 | 25.7 |
| **Ilmenite** | Sands High-Abundance | 624 | 12.4 | 6.7 | 0.5 | 44.4 | 1.0 | 11.1 | 40.5 |
| **Ilmenite** | Sands Low-Abundance | 775 | 1.62 | 1.3 | 0.8 | 1.8.0 | 0.01 | 1.2 | 11.5 |
| **Ilmenite** | Gravel and Silt Strands | 171 | 2.5 | 2.8 | 1.1 | 7.7 | 0.0 | 1.4 | 16.2 |
| **Ilmenite** | Eastern Gravel | 123 | 1.8 | 1.8 | 1.0 | 3.2 | 0.1 | 1.3 | 13.5 |
| **Ilmenite** | Top Clay-Silt | 265 | 2.9 | 4.1 | 1.4 | 16.7 | 0.0 | 1.2 | 21.0 |
| **Zircon** | Sands High-Abundance | 486 | 0.27 | 0.1 | 0.5 | 0.0 | 0.11 | 0.25 | 0.66 |
| **Zircon** | Sands Low-Abundance | 912 | 0.05 | 0.0 | 0.8 | 0.0 | 0.01 | 0.04 | 0.17 |
| **Zircon** | Gravel and Silt Strands | 171 | 0.05 | 0.1 | 0.9 | 0.0 | 0.01 | 0.05 | 0.28 |
| **Zircon** | Eastern Gravels | 123 | 0.05 | 0.0 | 0.8 | 0.0 | 0.02 | 0.05 | 0.17 |
| **Zircon** | Top Clay-Silt | 265 | 0.07 | 0.1 | 1.3 | 0.0 | 0.0 | 0.05 | 0.27 |

### 8.3.3 Total Heavy Minerals

The abundance of VHM has been calculated as the sum of the ilmenite, garnet, and zircon abundance, determined from pXRF data (section 6.3.4.4) from the 45-µm to 2-mm screened fraction of the 1-m sample intervals. The THM abundance, which includes all VHM and gangue minerals (e.g. epidote, magnetite), has been determined through the regression formula ($THM\ \% = \frac{\text{VHM}\ \%}{0.66}$) derived from the analysis of sink-float heavy fraction data (section 5.3.1). Summary statistics for THM abundance within each estimation domain are presented in Table 22.

Table 22: Summary statistics of THM and VHM abundance within estimation domains.

| Estimation Domain | Variable | Count | Mean (%) | Standard Deviation | CV | Variance | Minimum (%) | Median (%) | Maximum (%) |
|---|---|---|---|---|---|---|---|---|---|
| Sands Low-Abundance | THM | 827 | 7.4 | 7.4 | 1 | 55 | 0.1 | 5.2 | 100 |
| | VHM | 827 | 4.9 | 4.9 | 1.0 | 24.0 | 0.1 | 3.4 | 66.4 |
| Sands High-Abundance | THM | 639 | 47.4 | 21.9 | 0.5 | 524 | 4.7 | 44.3 | 100 |
| | VHM | 639 | 31.3 | 14.4 | 0.5 | 209 | 3.1 | 29.2 | 82.6 |
| Gravel and Silt Strands | THM | 171 | 12.2 | 13.5 | 1.1 | 183 | 1.3 | 6.7 | 100 |
| | VHM | 171 | 8.1 | 8.9 | 1.1 | 79.8 | 0.9 | 4.4 | 66.4 |
| Eastern Gravels | THM | 123 | 8.2 | 7.6 | 0.9 | 57 | 0.8 | 6.1 | 0.2 |
| | VHM | 123 | 5.4 | 5.0 | 0.9 | 24.9 | 0.6 | 4.0 | 32.5 |
| Top Clay-Silt | THM | 265 | 13.3 | 15.3 | 1 | 194 | 0.7 | 7.7 | 70.3 |
| | VHM | 265 | 8.8 | 9.2 | 1.0 | 84.7 | 0.5 | 5.1 | 46.4 |

### 8.3.4 Density

Dry bulk density data were collected from the sonic drillholes (section 6.4). Density values within estimation domains have very low CVs (Table 23).

Table 23: Summary statistics of density values within estimation domains.

| Estimation Domain | Count | Length of Sample (m) | Mean ($g/cm^3$) | Standard Deviation | CV | Variance | Minimum ($g/cm^3$) | Median ($g/cm^3$) | Maximum ($g/cm^3$) |
|---|---|---|---|---|---|---|---|---|---|
| Sands | 34 | 25.2 | 2.0 | 0.2 | 0.1 | 0.1 | 1.8 | 2.1 | 2.5 |
| Gravel and Silt Strands | 1 | 1.0 | 2.4 | - | - | - | 2.4 | 2.4 | 2.4 |
| Eastern Gravels | 16 | 13.3 | 1.9 | 0.3 | 0.2 | 0.1 | 1.7 | 1.9 | 2.6 |
| Top Clay-Silt | 11 | 7.45 | 1.4 | 0.6 | 0.4 | 0.3 | 1.0 | 1.3 | 2.3 |

### 8.3.5 Size Fraction Proportions

The three size fraction proportions (0–45 µm, 45 µm–2 mm, and >2 mm) of each sample were evaluated within each estimation domain. The distributions of size fraction proportions in all estimation domains are monomodal and characterised by low to moderate variance as expressed by their coefficient of variation (0.3–1.1, Table 24).

Table 24: Summary statistics of size fraction proportions within estimation domains.

| Estimation Domain | Size Fraction | Count | Mean % | Standard Deviation | CV | Variance | Minimum % | Median % | Maximum % |
|---|---|---|---|---|---|---|---|---|---|
| **Sands** | 0–45 µm | 1,267 | 20 | 0.2 | 1.1 | 0.0 | 0 | 10 | 100 |
| **Sands** | 45 –2 mm | 1,267 | 70 | 0.2 | 0.3 | 0.0 | 0 | 80 | 100 |
| **Sands** | >2 mm | 1,267 | 10 | 0.2 | 1.1 | 0.0 | 0 | 10 | 90 |
| **Gravel and Silt Strands** | 0–45 µm | 201 | 20 | 0.2 | 1.1 | 0.1 | 0 | 20 | 100 |
| **Gravel and Silt Strands** | 45 µm –2 mm | 201 | 50 | 0.2 | 0.5 | 0.0 | 0 | 50 | 80 |
| **Gravel and Silt Strands** | >2 mm | 201 | 30 | 0.2 | 0.7 | 0.0 | 0 | 30 | 90 |
| **Eastern Gravels** | 0–45 | 126 | 30 | 0.3 | 1.1 | 0.1 | 0 | 20 | 100 |
| **Eastern Gravels** | 45–2 | 126 | 40 | 0.2 | 0.5 | 0.0 | 0 | 40 | 80 |
| **Eastern Gravels** | >2 mm | 126 | 40 | 0.2 | 0.7 | 0.1 | 0 | 40 | 90 |
| **Top Clay-Silt** | 0–45 µm | 411 | 40 | 0.3 | 0.7 | 0.1 | 0 | 30 | 100 |
| **Top Clay-Silt** | 45 µm –2 mm | 411 | 40 | 0.2 | 0.7 | 0.1 | 0 | 40 | 90 |
| **Top Clay-Silt** | >2 mm | 411 | 20 | 0.2 | 1.0 | 0.0 | 0 | 10 | 80 |

## 8.4 Spatial Analysis & Variography

### 8.4.1 Gold

The spatial analysis was completed using Snowden Supervisor v8.14 and shows a north–northeast direction of major continuity. The experimental semi-variograms were modelled with a $\gamma_0$ value of 0.40 and two spherical structures. Following the analysis of the experimental variogram across a range of lags, two spherical structures were selected to better honour the short range in the principal direction. The orientation, modelled $\gamma_0$, structure and ranges represent the expected nature of Au mineralisation within a placer-style depositional setting, with the direction of maximum continuity in the general orientation of the observed strandlines. The modelled variogram parameters and plots are presented in Figure 92 and Table 25.

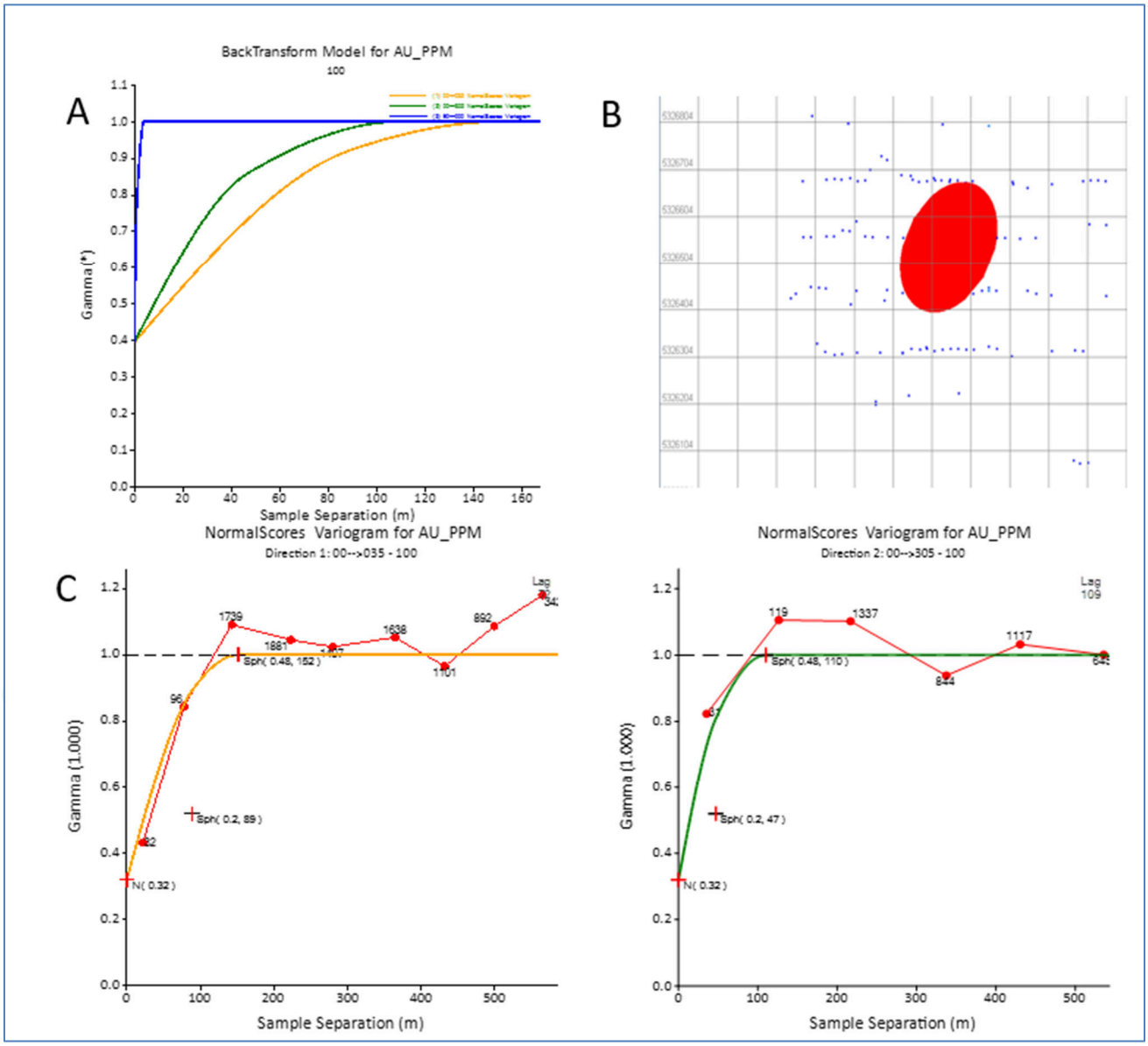


Figure 92: A. Back-transformed modelled variogram (Au), B. Plan view of anisotropy ellipse, C. Major and semi-major experimental and modelled normal-score variograms.

Table 25: Modelled Au variogram parameters (normalised sill).

| Variable | Estimation Domain | Structure | Model Type | Sill | Range Major (m) | Range Semi Major (m) | Range Minor (m) |
|---|---|---|---|---|---|---|---|
| **Au** | 100 | | Nugget | 0.40 | | | |
| | | 1 | Spherical | 0.25 | 90 | 50 | 5 |
| | | 2 | Spherical | 0.35 | 150 | 110 | 10 |

### 8.4.2 Heavy Minerals

The spatial continuity of heavy mineral abundance and THM abundance was independently modelled within the plane of mineralisation for each estimation domain.

For each estimation domain, experimental semi-variograms were modelled with a relatively low $\gamma_0$ value (0.1–0.2, estimated from downhole variograms) and two spherical structures (Table 26, Figure 92, Figure 93, and APPENDIX A:).

Table 26: Modelled Ilmenite variogram parameters.

| Variable | Estimation Domain | Structure | Model Type | Sill | Range Major (m) | Range Semi Major (m) | Range Minor (m) |
|---|---|---|---|---|---|---|---|
| **Ilmenite** | Sands High-Abundance | | Nugget | 0.15 | | | |
| | | 1 | Spherical | 0.70 | 180 | 25 | 2.5 |
| | | 2 | Spherical | 0.15 | 230 | 200 | 3.5 |
| **Ilmenite** | Sands Low-Abundance | | Nugget | 0.15 | | | |
| | | 1 | Spherical | 0.70 | 200 | 43 | 3 |
| | | 2 | Spherical | 0.15 | 250 | 75 | 4 |
| **Ilmenite** | Gravel and Silt Strands | | Nugget | 0.10 | | | |
| | | 1 | Spherical | 0.36 | 20 | 15 | 4 |
| | | 2 | Spherical | 0.54 | 350 | 175 | 8 |
| **Ilmenite** | Eastern Gravels | | Nugget | 0.10 | | | |
| | | 1 | Spherical | 0.34 | 150 | 45 | 2 |
| | | 2 | Spherical | 0.55 | 250 | 250 | 4 |
| **Ilmenite** | Top Clay-Silt | | Nugget | 0.15 | | | |
| | | 1 | Spherical | 0.37 | 200 | 30 | 4 |
| | | 2 | Spherical | 0.48 | 400 | 400 | 6 |

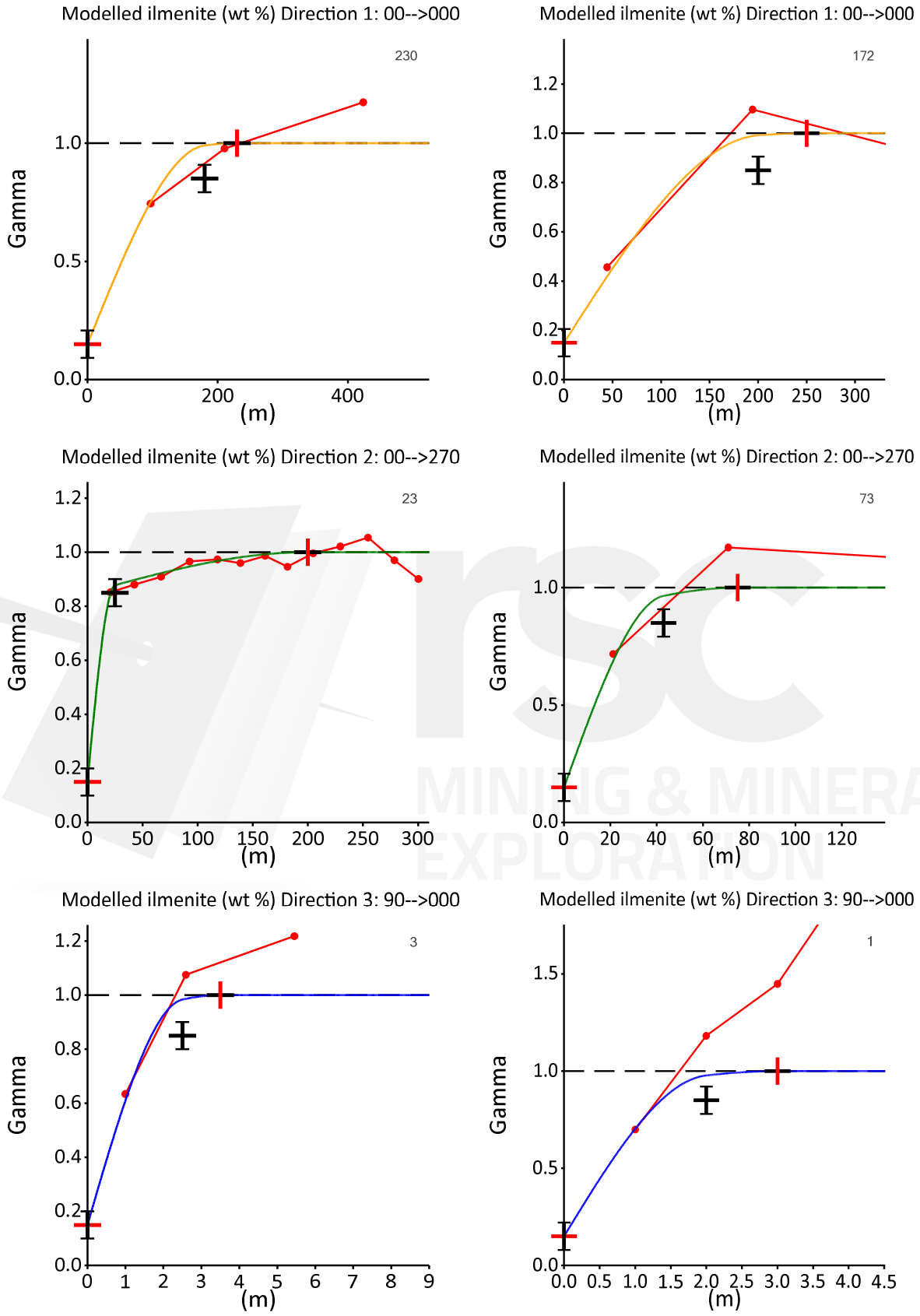


Figure 93: Experimental semi-variogram models for the Ilmenite High-Abundance Sands (left) and Low-Abundance Sands (right) estimation domains.

### 8.4.3 Size Fraction Proportions

The spatial continuity of the three size fraction proportions (0–45 µm, 45 µm to 2 mm, and >2 mm) were modelled using a single variogram model for each domain (Table 27), because the experimental variograms for each size fractions are similar in structure. By applying the single variogram, the conditions of a full co-kriging of the proportions are reproduced, ensuring that the consistency of the individual estimates is preserved with all proportions summing to 100%.

For each estimation domain, experimental semi-variograms were modelled with a relatively low $\gamma_0$ value (0.2, estimated from downhole variograms) and two spherical structures (Table 27 and APPENDIX B:).

Table 27: Modelled variogram parameters for the 45-µm to 2-mm size fraction.

| Variable | Estimation Domain | Structure | Model Type | Sill | Range Major (m) | Range Semi Major (m) | Range Minor (m) |
|---|---|---|---|---|---|---|---|
| **Proportion 0–45 µm** | Sands | | Nugget | 0.20 | | | |
| **45–2 mm** | | 1 | Spherical | 0.68 | 200 | 40 | 2 |
| **>2 mm** | | 2 | Spherical | 0.12 | 500 | 100 | 10 |

## 8.5 Block Model

### 8.5.1 Gold

Datamine Studio RM Pro version 1.11.300.0 was used to set up the block model and interpolate Au grades into the blocks. A parent block size of 10 m x 50 m x 3 m (x-y-z), sub-blocked to 1 m x 1 m x 0.5 m was selected. The parent blocks were discretised to 5 m x 5 m x 3 m. The parameters and dimensions are based on drill spacing and supported by kriging neighbourhood analysis (KNA). The block model parameters are described in Table 28.

Table 28: Au block model definition.

| Axis | Origin | Parent Block Size | Smallest Sub Block Size | Number of Blocks | Length (m) |
|---|---|---|---|---|---|
| **x** | 1,461,040 | 10 | 1 | 100 | 1,000 |
| **y** | 5,326,000 | 50 | 1 | 22 | 1,160 |
| **z** | -10 | 3 | 0.5 | 10 | 30 |

### 8.5.2 Heavy Minerals

A parent block size of 20 m x 20 m x 1 m (x-y-z), sub-blocked to 1 m x 1 m x 1 m, was selected for estimation, based on drill spacing and supported by KNA. Block model prototype definitions are outlined in Table 29. A discretisation of 5 m x 5 m x 1 m (x-y-z) was applied.

Separate block models were produced for the Au and heavy mineral estimates because each has a different parent cell architecture, based on the available data and modelled spatial continuity. Incidentally, the Au estimate does not account for size-fraction proportion as is the case with the HM model. The BLEG data informing the Au estimate is sourced from the

crush reject of the first split and does not represent any particular size fraction, whereas the HM data is informed by the 45-µm to 2-mm portion. As a consequence, size fraction proportions were only estimated for the heavy mineral block model.

Table 29: Block model definitions.

| Axis | Origin | Parent Block Size | Smallest Sub Block Size | Number of Blocks | Length (m) |
|---|---|---|---|---|---|
| **x** | 1,460,850 | 20 | 1 | 75 | 1,500 |
| **y** | 5,325,866 | 20 | 1 | 63 | 1,260 |
| **z** | -12 | 1 | 1 | 40 | 40 |

## 8.6 Search Neighbourhood Parameters

### 8.6.1 Gold

Given the very consistently flat geometry of the mineralisation, the Au estimate search neighbourhood applied a static ellipse of 150 m x 100 m x 10 m with the long axis orientated north–northeast. A minimum of eight and maximum of 40 samples were used per parent estimate. The blocks not informed by this search pass were estimated in a second pass, which increases the neighbourhood 3-fold and reduces the minimum and maximum samples to five and 40, respectively. Most (70%) of the estimate is informed by the first search. The search neighbourhood selected parameters are considered appropriate to support a robust estimate.

### 8.6.2 Heavy Minerals

The interpolation of heavy mineral abundance into blocks was completed using a single-pass search neighbourhood of 400 m x 300 m x 20 m (x-y-z) and applying a minimum of eight and a maximum of 30 samples to each estimated block. The regular spatial coverage from HM samples allows the use of a single-pass search to estimate the area of interest. The variogram models for ilmenite, zircon and garnet abundances provide good conditions for precise local estimation (modelled $\gamma_0$ of 10–20 %; ranges much longer than the sample spacing), and the maximum number of samples at 30 ensures conditional unbiasedness, while limiting the occurrence of negative weights in the kriging scheme.

## 8.7 Estimation

### 8.7.1 Gold

The Au grades were estimated into blocks in a single estimation domain using ordinary kriging (OK). OK is a suitable estimation technique at this stage of the Project; it honours the spatial continuity of the estimated variable, it provides the best unbiased estimate, and minimises the predicted error variance. The summary statistics for the block model estimate are provided in Table 30 and a plan view of the block model shown in Figure 94.

Table 30: Summary statistics for the Au-estimated block model (Domain 100).

| Estimation Domain | Variable | Parent Block Count | Mean (g/t) | Standard Deviation | CV | Variance | Minimum | Median | Maximum |
|---|---|---|---|---|---|---|---|---|---|
| **100** | Au | 5,788 | 0.034 | 0.017 | 0.498 | 0.000 | 0.005 | 0.031 | 0.139 |

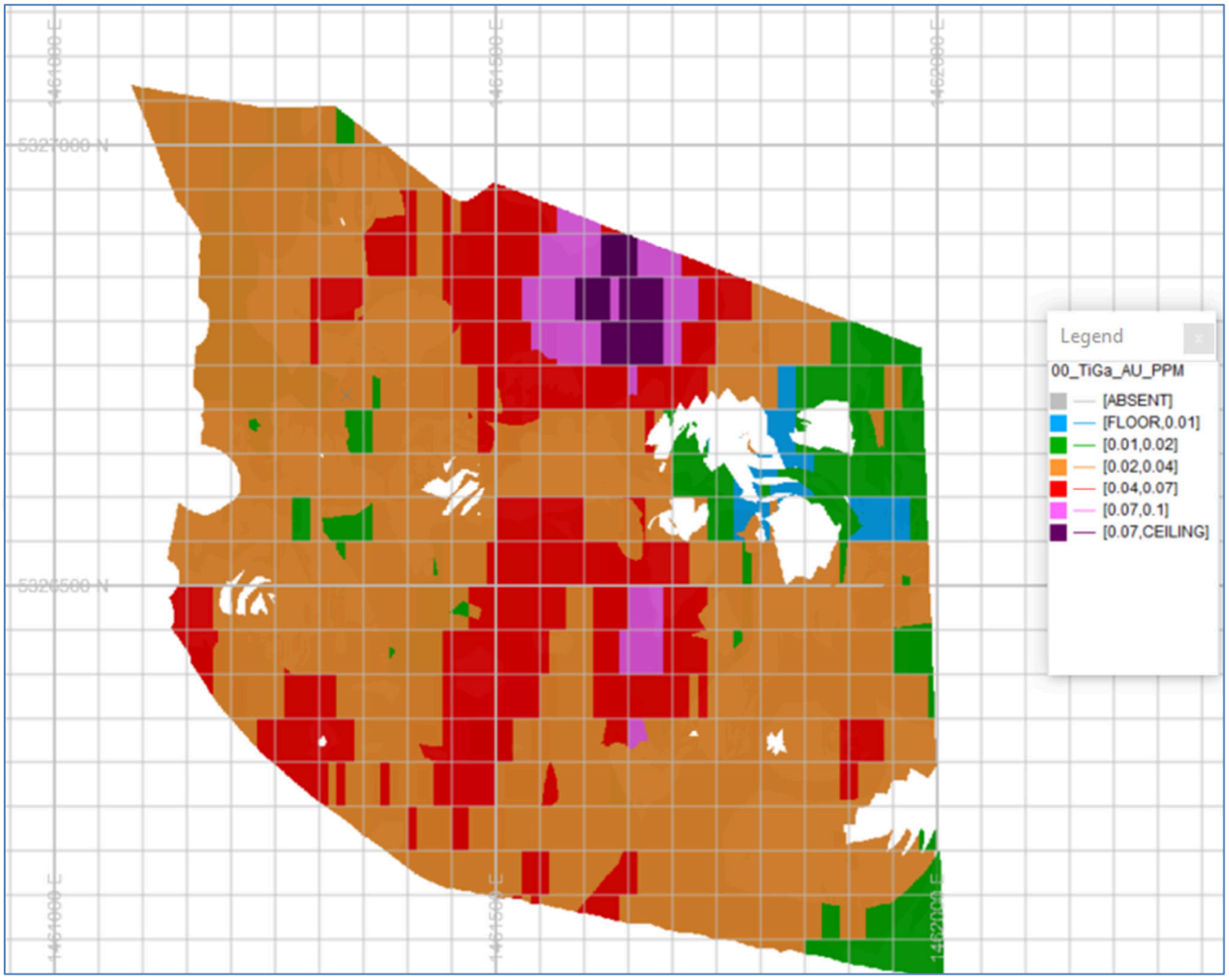


Figure 94: Plan view of the Coates South Block Au estimated model.

### 8.7.2 Heavy Minerals

The resource estimate was completed using OK. Hard domain boundaries were set for estimation, supported by domain contact analysis (Figure 95). The abundance of VHM has been calculated for each block as the sum of the estimated ilmenite, garnet, and zircon abundance. Summary statistics for the block model estimates are provided in Table 31. Plan and perspective views of the block model abundances are presented in Figure 96 and Figure 97.

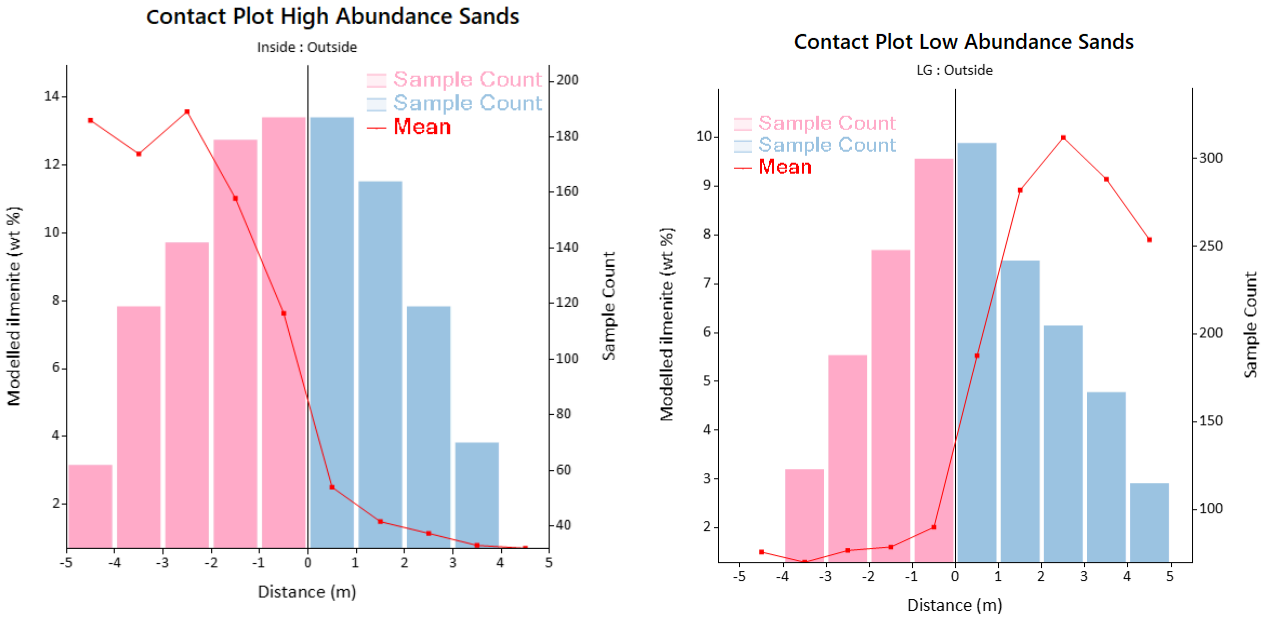


Figure 95: Contact analysis plots for the ilmenite within the High-Abundance (left) and Low-Abundance (right) estimation domains.

### 8.7.3 Density

The dry bulk density data obtained during the 2022 drilling campaign were used to assign (dry) bulk density values to parent estimation domains. For the Sands, Eastern Gravels, and the Top Clay-Silt unit, the median of the density values (section 6.4) was applied to determine tonnages. Due to the low sample support within the Gravel and Silt Strands estimation domains, a nominal value equal to that of the enclosing sand unit has been applied.

The following in-situ dry bulk densities were used:

- 2.08 g/cm$^3$ for the Sands and enclosed Gravel and Silt Strands;
- 1.93 g/cm$^3$ for the Eastern Gravels; and
- 1.34 g/cm$^3$ for the Top Clay-Silt unit.

Table 31: Summary statistics of estimated variables within estimation domains.

| Estimation Domain | Variable | Block Count | Mean % | Standard Deviation | CV | Variance | Minimum % | Median % | Maximum % |
|---|---|---|---|---|---|---|---|---|---|
| **Sands High-Abundance** | Ilmenite | 4,725 | 12.7 | 4.2 | 0.3 | 17.4 | 3.9 | 12.0 | 32.1 |
| | Garnet | 3,652 | 20.6 | 4.2 | 0.2 | 17.4 | 10.7 | 20.1 | 39.8 |
| | Zircon | 3,574 | 0.3 | 0.1 | 0.3 | 0.0 | 0.1 | 0.3 | 0.7 |
| | THM | 4,725 | 48.2 | 12.9 | 0.3 | 166.9 | 14.7 | 45.7 | 100.0 |
| | VHM | 4,725 | 29.2 | 11.3 | 0.4 | 128.4 | 8.6 | 29.4 | 69.0 |
| **Sands Low-Abundance** | Ilmenite | 9,443 | 1.6 | 0.8 | 0.5 | 0.6 | 0.1 | 1.4 | 7.0 |
| | Garnet | 10,513 | 3.5 | 1.7 | 0.5 | 2.9 | 0.6 | 3.2 | 18.9 |
| | Zircon | 10,591 | 0.0 | 0.0 | 0.4 | 0.0 | 0.0 | 0.0 | 0.2 |
| | THM | 9,443 | 7.1 | 4.0 | 0.6 | 16.2 | 0.9 | 6.2 | 39.5 |
| | VHM | 9,443 | 5.3 | 3.5 | 0.7 | 12.1 | 1.0 | 4.5 | 35.8 |
| **Sands** | Proportion 0–45 µm | 14,165 | 16.9% | 0.1 | 0.4 | 0.0 | 2.6% | 15.0% | 70.8% |
| | Proportion 45 µm–2 mm | 14,165 | 68.6% | 0.1 | 0.2 | 0.0 | 20.9% | 68.8% | 91.6% |
| | Proportion >2 mm | 14,165 | 14.6% | 0.1 | 0.7 | 0.0 | -0.3% | 12.8% | 70.6% |
| **Gravel and Silt Strands** | Ilmenite | 962 | 2.1 | 1.2 | 0.6 | 1.5 | 0.4 | 1.9 | 9.4 |
| | Garnet | 962 | 5.2 | 2.8 | 0.5 | 8.0 | 1.0 | 5.1 | 29.6 |
| | Zircon | 962 | 0.0 | 0.0 | 0.5 | 0.0 | 0.0 | 0.0 | 0.3 |
| | THM | 962 | 11.0 | 6.0 | 0.5 | 35.8 | 2.4 | 10.4 | 56.6 |
| | VHM | 962 | 7.3 | 3.8 | 0.5 | 14.6 | 1.4 | 7.0 | 39.0 |
| | Proportion 0–45 µm | 962 | 21.1% | 0.1 | 0.5 | 0.0 | 4.3% | 18.5% | 70.1% |
| | Proportion 45 µm –2 mm | 962 | 46.4% | 0.1 | 0.3 | 0.0 | 15.6% | 49.9% | 72.9% |
| | Proportion >2 mm | 962 | 32.5% | 0.2 | 0.5 | 0.0 | 7.6% | 28.5% | 77.1% |
| **Eastern Gravels** | Ilmenite | 1,087 | 1.7 | 0.6 | 0.4 | 0.4 | 0.4 | 1.6 | 6.9 |
| | Garnet | 1,087 | 3.5 | 1.4 | 0.4 | 1.8 | 0.8 | 3.3 | 10.4 |
| | Zircon | 1,087 | 0.0 | 0.0 | 0.3 | 0.0 | 0.0 | 0.0 | 0.2 |
| | THM | 1,087 | 7.8 | 3.0 | 0.4 | 9.1 | 1.9 | 7.3 | 25.3 |
| | VHM | 1,087 | 5.3 | 1.8 | 0.3 | 3.4 | 1.6 | 4.9 | 14.2 |
| | Proportion 0–45 µm | 1,087 | 27.7% | 0.2 | 0.5 | 0.0 | 5.7% | 22.8% | 91.7% |
| | Proportion 45 µm –2 mm | 1,087 | 36.6% | 0.1 | 0.3 | 0.0 | 3.7% | 38.1% | 59.8% |
| | Proportion >2 mm | 1,087 | 35.7% | 0.1 | 0.3 | 0.0 | 4.5% | 35.4% | 66.1% |
| **Top Clay-Silt** | Ilmenite | 3,316 | 3.2 | 3.1 | 1.0 | 9.4 | 0.1 | 1.7 | 16.6 |
| | Garnet | 3,316 | 6.0 | 3.2 | 0.5 | 10.1 | 1.6 | 5.1 | 20.1 |
| | Zircon | 3,316 | 0.1 | 0.0 | 0.7 | 0.0 | 0.0 | 0.0 | 0.3 |
| | THM | 3,316 | 13.9 | 9.9 | 0.7 | 97.8 | 3.4 | 9.8 | 54.2 |
| | VHM | 3,316 | 9.2 | 6.2 | 0.7 | 38.1 | 2.4 | 6.8 | 35.1 |
| | Proportion 0–45 µm | 3,316 | 42.2% | 0.2 | 0.4 | 0.0 | 11.8% | 39.5% | 100.0% |
| | Proportion 45 µm –2 mm | 3,316 | 37.3% | 0.1 | 0.3 | 0.0 | -2.5% | 38.6% | 65.6% |
| | Proportion >2 mm | 3,316 | 20.5% | 0.1 | 0.6 | 0.0 | -1.0% | 19.4% | 63.7% |

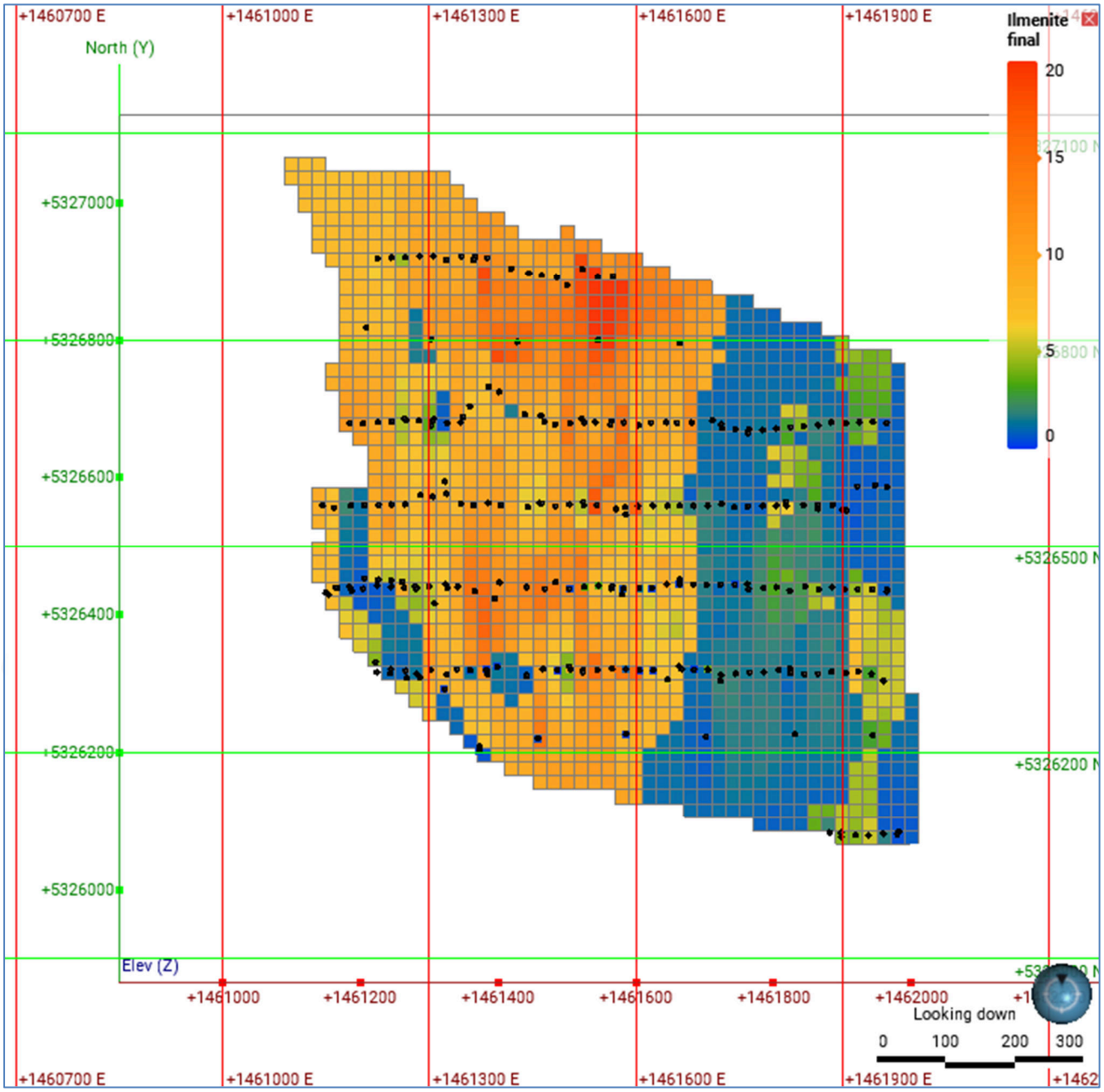


Figure 96: Plan view of estimated ilmenite abundance within the Sands estimation domains.

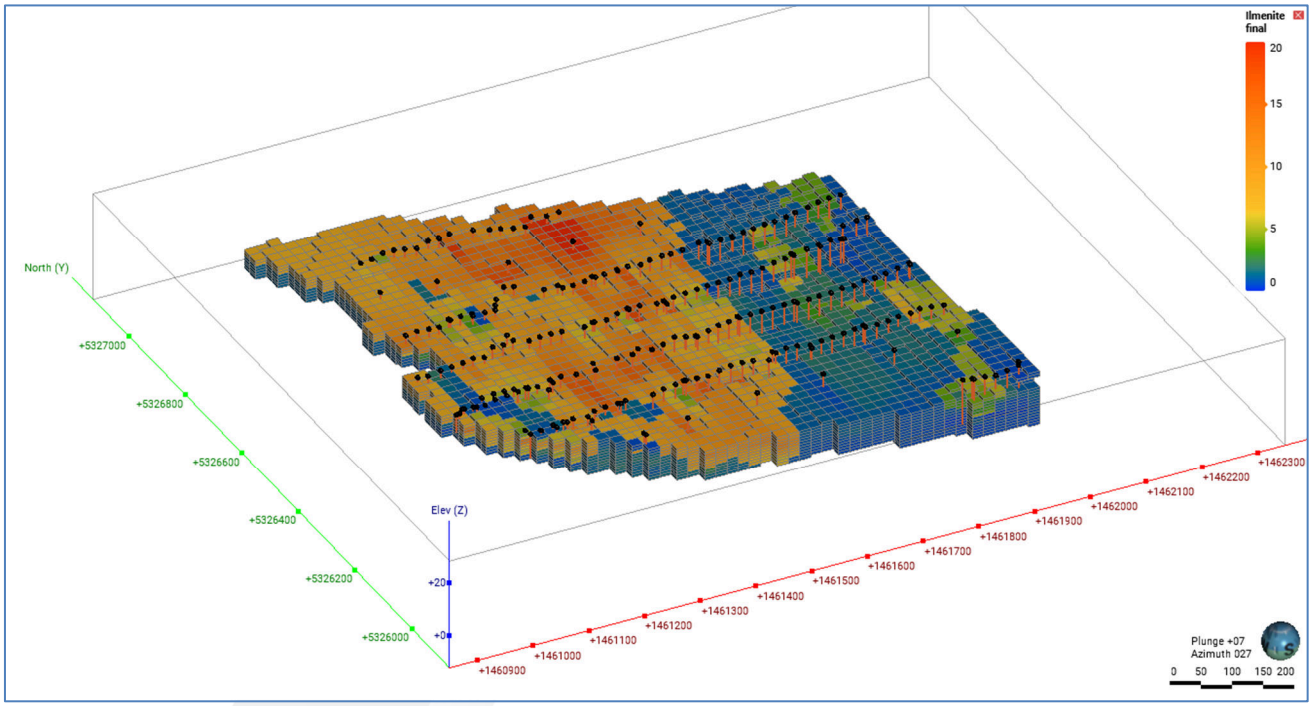


Figure 97: Perspective view towards the northeast of estimated ilmenite abundance within the Sands estimation domains.

## 8.8 Validation

### 8.8.1 Gold Estimation

The Au estimate has been validated through visual inspection of the input composite grades and the output estimate (Figure 98 and Figure 99), global statistical comparisons between composite data and model grades (Table 32), and swath plots analysis orientated in northing and easting slices (Figure 100). At the resolution of the parent cell estimate, the validations support acceptable representation of the model against the input grades.

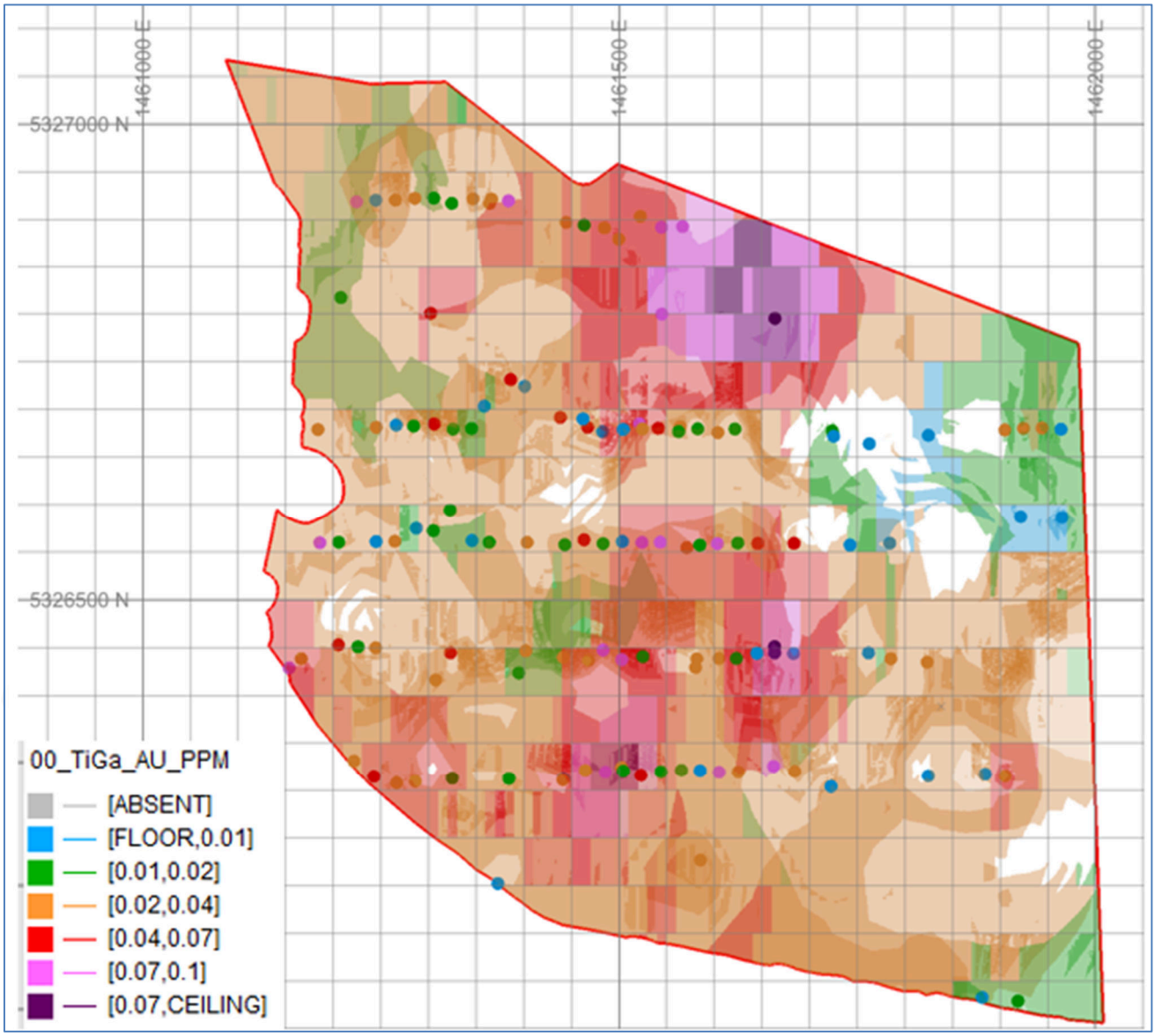


Figure 98: Plan view of the model and the composite data.

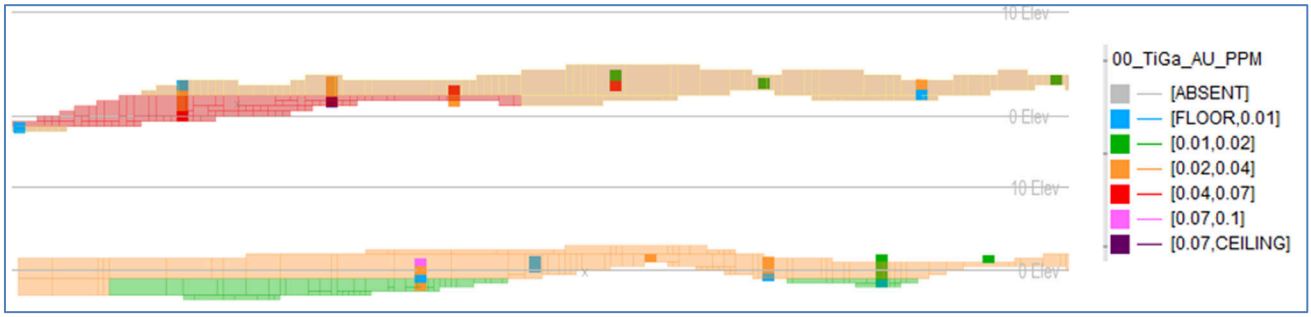


Figure 99: Two east–west cross-sections of the model and the composite data.

Table 32: Global grade comparison Domain 100 (composite vs model estimate).

| Estimation Domain | Variable | Model Grade (g/t) | Composite Grade (g/t) | % Difference |
|---|---|---|---|---|
| **100** | Au | 0.035 | 0.036 | -2% |

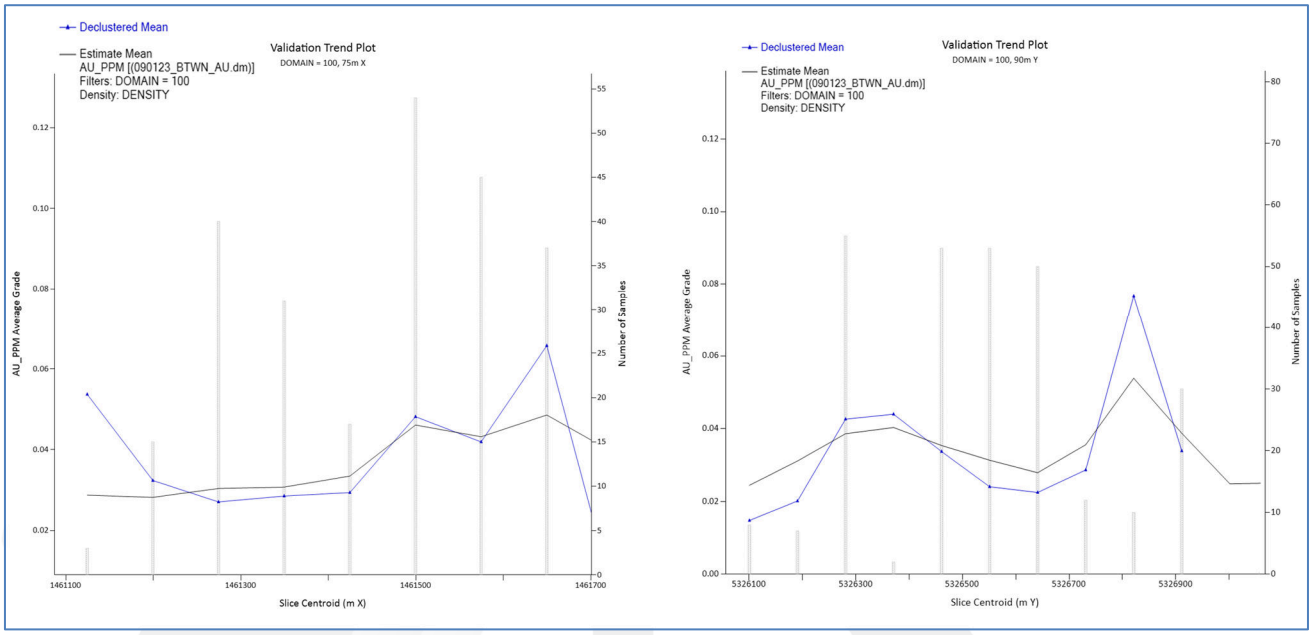


Figure 100: Easting (left) and Northing (right) Swath plots for Au domain 100. The de-clustered uncut data are in blue and the model estimate is in black. The bars represent the number of samples per slice.

### 8.8.2 Heavy Minerals

Block model abundances were validated by comparing the input mean abundances with the block model mean abundance, using swath plots, and visually, on cross-section including:

- the comparison of input mean abundance and estimated block means by estimation domain demonstrates good correlation (Table 33);
- visual validation along cross-section, comparing input and estimated block abundance, indicates that the estimates reasonably reflect the abundances of the input data (Figure 101); and
- swath plots (x-y-z) display good correlation between input and estimated abundance and proportions, and appropriate levels of smoothing within estimation domains (Figure 102, Figure 103 and APPENDIX C:).

Table 33: Mean comparison of input and estimated abundance and proportions.

| Estimation Domain | Variable | Mean % | Block Mean % | Relative Difference % |
|---|---|---|---|---|
| **Sands High Abundance** | Ilmenite | 12.4 | 12.7 | 2.8 |
| | Garnet | 20.2 | 20.6 | 2.1 |
| | Zircon | 0.26 | 0.26 | 0.0 |
| | THM | 47.4 | 48.2 | 1.7 |
| **Sands Low Abundance** | Ilmenite | 1.6 | 1.6 | -4.1 |
| | Garnet | 3.5 | 3.7 | 6.1 |
| | Zircon | 0.05 | 0.05 | 5.0 |
| | THM | 7.4 | 7.1 | -3.9 |
| **Sands** | Proportion 0–45 µm | 17.1 | 16.7 | -2.1 |
| | Proportion 45 µm–2 mm | 68.9 | 68.5 | -0.6 |
| | Proportion >2 mm | 14.0 | 14.8 | 5.7 |
| **Gravel and Silt Strands** | Ilmenite | 2.5 | 2.1 | -15.7 |
| | Garnet | 5.5 | 5.2 | -5.7 |
| | Zircon | 0.06 | 0.05 | -15.2 |
| | THM | 12.2 | 11.0 | -10.0 |
| | Proportion 0–45 µm | 22.4 | 21.0 | -6.3 |
| | Proportion 45 µm–2 µm | 48.1 | 47.0 | -2.4 |
| | Proportion >2 mm | 29.5 | 32.0 | 8.7 |
| **Eastern Gravels** | Ilmenite | 1.8 | 1.7 | -6.2 |
| | Garnet | 3.6 | 3.5 | -2.3 |
| | Zircon | 0.0 | 0.0 | -0.8 |
| | THM | 8.2 | 7.8 | -4.6 |
| | Proportion 0–45 µm | 26.6 | 27.5 | 3.4 |
| | Proportion 45 µm–2 mm | 37.7 | 37.1 | -1.6 |
| | Proportion >2 mm | 35.7 | 35.4 | -0.9 |
| **Top Clay-Silt** | Ilmenite | 2.9 | 3.2 | 10.6 |
| | Garnet | 5.8 | 6.0 | 2.6 |
| | Zircon | 0.1 | 0.1 | 13.0 |
| | THM | 13.3 | 13.9 | 4.6 |
| | Proportion 0–45 µm | 43.8 | 42.1 | -3.9 |
| | Proportion 45 µm –2 mm | 35.3 | 37.4 | 6.0 |
| | Proportion >2 mm | 20.9 | 20.5 | -2.0 |

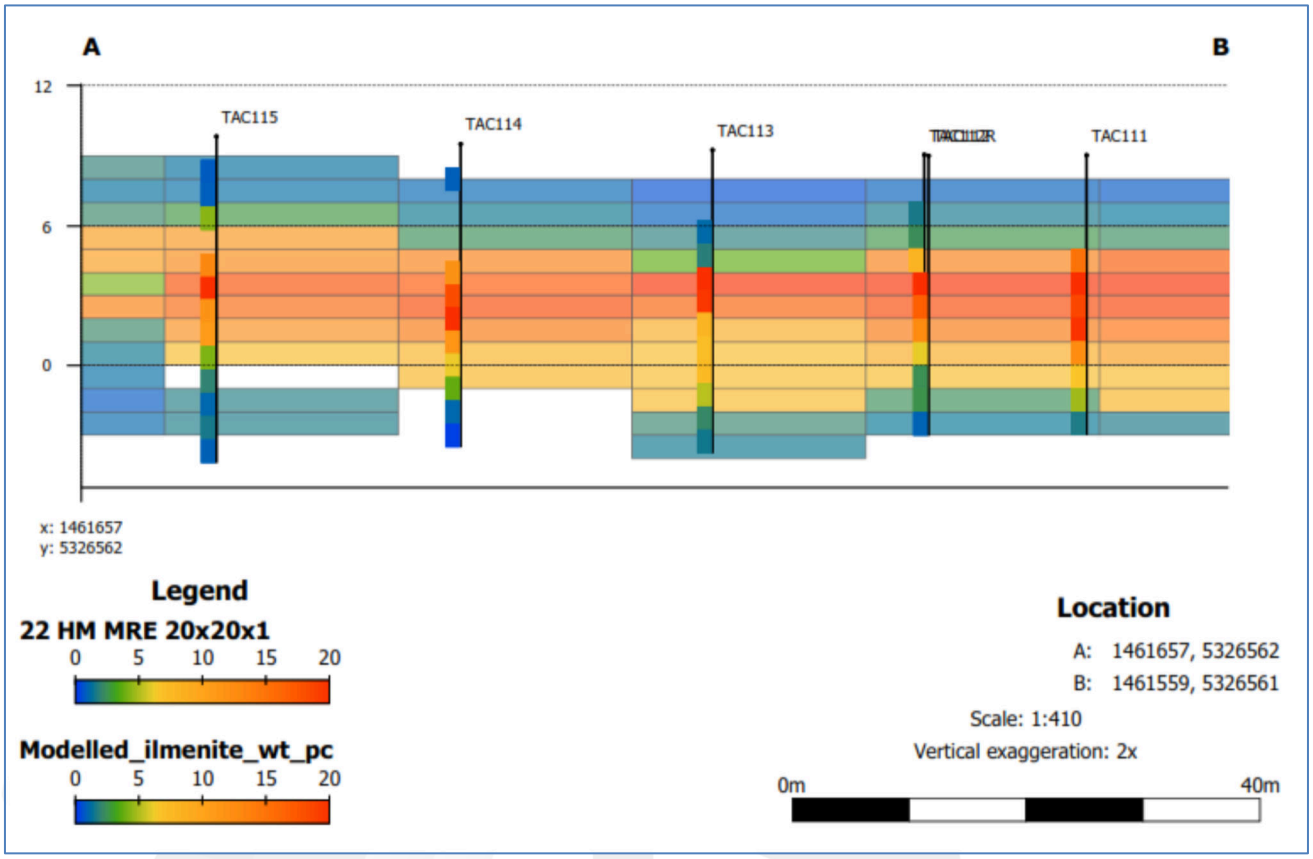


Figure 101: Visual comparison of a section of estimated ilmenite abundance and drillhole data.

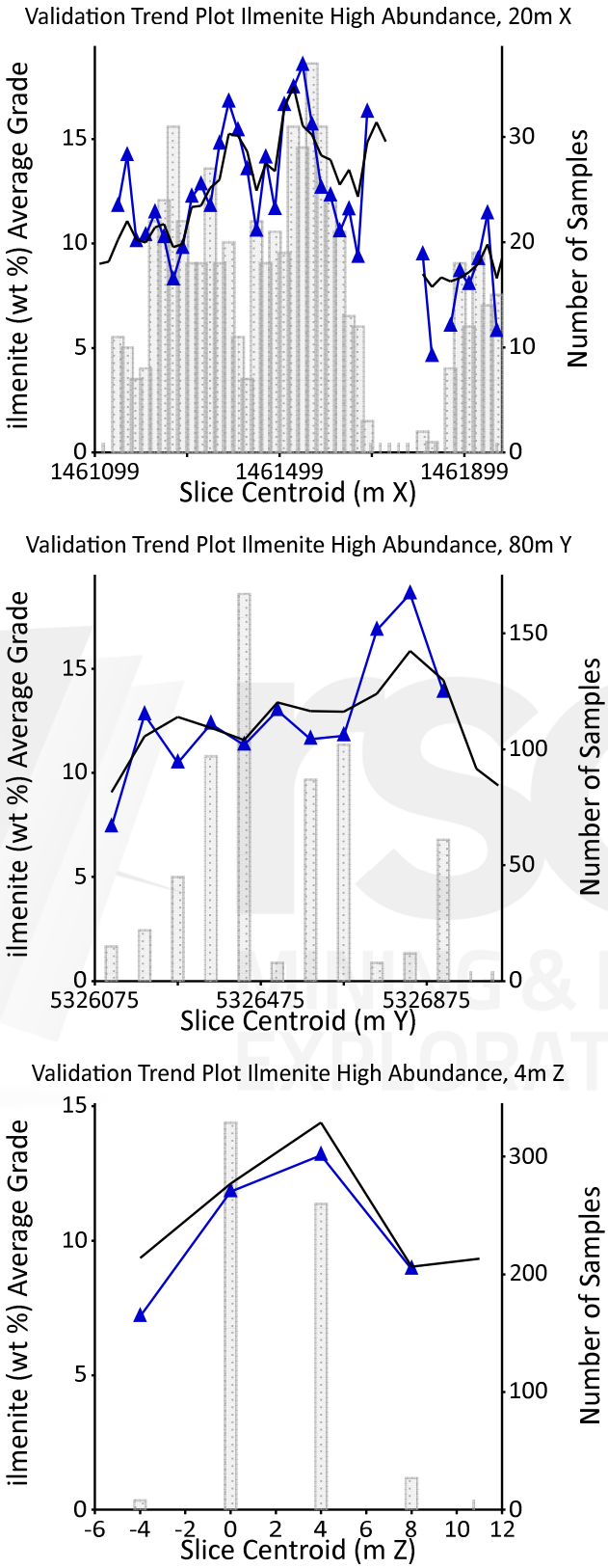


Figure 102: Swath plots displaying the average declustered sample (blue) and estimated (black) ilmenite abundance for the High-Abundance Sands domain along easting (20 m), northing (80 m), and elevation (4 m, top to bottom) slices.

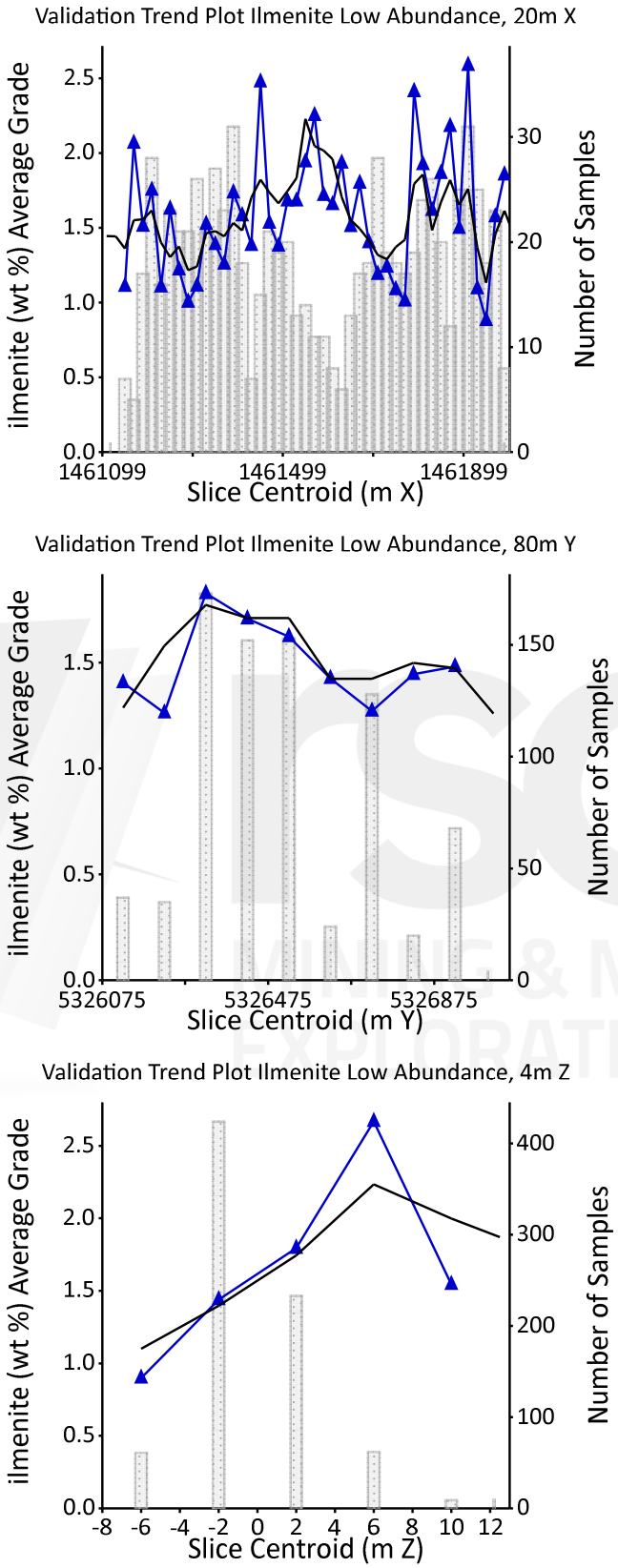


Figure 103: Swath plots displaying the declustered sample (blue) and estimated (black) ilmenite abundance for the Low-Abundance Sands domain along easting (20 m), northing (100 m), and elevation (4 m, top to bottom) slices.

## 8.9 Sensitivity Testing

Sensitivity testing was performed by comparing ilmenite block model estimates of the High- and Low-Abundance Sands domains:

- using an alternative block size conducive to the drill spacing (20 m x 60 m x 3 m, x-y-z);
- estimating with twice the number of maximum samples (60);
- estimating with half the number of maximum samples (15); and
- doubling the ranges of the variograms (see Table 26).

The comparison of ilmenite abundance for each sensitivity test demonstrates that the estimation settings testing (Table 34) had a minimal impact on estimated ilmenite abundance (≤2.6 % relative difference).

A test to compare mineral abundances within the Measured portion of the Resource estimated using only those samples with a recorded recovery of ≥50 % was carried out. This comparison (Table 35) shows that the relatively poor sample recoveries observed had no material impact on the estimated mineral abundances (≤5% relative difference for ilmenite, ≤4% for garnet and ≤3% for zircon).

The Competent Person considers the block model to be robustly estimated.

Table 34: Global comparison of ilmenite estimates using alternative estimation parameters.

| Estimation Domain | Parameter Tested | Sensitivity Test Ilmenite Mean (%) | Original Model Ilmenite Mean (%) | Relative Difference % |
|---|---|---|---|---|
| **High-Abundance Sands** | Block Size | 12.6 | 12.9 | -2.4% |
| | Reduced Max Samples | 13.0 | 12.9 | 0.2% |
| | Increased Max Samples | 12.9 | 12.9 | -0.2% |
| | Variogram Range | 12.9 | 12.9 | -0.5% |
| **Low-Abundance** | Block Size | 1.6 | 1.5 | 2.6% |
| | Reduced Max Samples | 1.5 | 1.5 | -1.9% |
| | Increased Max Samples | 1.6 | 1.5 | 1.3% |
| | Variogram Range | 1.5 | 1.5 | -0.6% |

Table 35: Global comparison of mineral concentration estimates within the Measured portion of the Resource using only those samples with ≥50 % recovery.

| Mineral | Original Model Mean (%) | Sensitivity Test Mean (%) | Relative Difference % |
|---|---|---|---|
| **Ilmenite** | 5.1 | 5.4 | 4.9% |
| **Garnet** | 8.2 | 8.5 | 3.8% |
| **Zircon** | 0.1 | 0.1 | 2.9% |

## 8.10 Depletion

Some minor historical mining for Au, ilmenite and other minerals has occurred within the Barrytown Project as discussed in sections 3.3 and 3.4; however, this has had no relevant impact on the volume of the Coates South Block resource estimate.

## 8.11 Classification

### 8.11.1 Gold

#### *8.11.1.1 Classification Statement*

The Competent Person has classified an Inferred Mineral Resource for Au of 3 Mt at 400 mg/t for 3.6 koz of Au (Table 36). The Mineral Resource has been classified in accordance with the JORC Code (2012) and is based on exploration, sampling and assaying information gathered through appropriate techniques from drillholes. Geological evidence is sufficient to imply, but not verify geological and grade continuity. Estimation quality measures (kriging efficiency and slope of regression), grade and geological continuity were considered in support of the classification.

#### *8.11.1.2 Cut-off Grade*

No cut-off has been applied in the classification of the Au Mineral Resource, as the Au represents a by-product of the heavy minerals, and the selectivity of mining is dependent on the cut-off grade applied to the resource estimate of the heavy minerals.

Table 36: Coates South Block Au estimate.

| Classification | Tonnes (Mt) | Grade (mg/t) | Ounces (koz) |
|---|---|---|---|
| **Inferred** | 3 | 400 | 3.6 |
| **Total** | 3 | 400 | 3.6 |

Notes:

1. The estimate is contained within the proposed mining disturbance area.
2. Estimate is rounded to reflect the level of confidence at the time of reporting.
3. No cut-off is applied to the reporting.

#### *8.11.1.3 Reasonable Prospects*

The recoverability of Au is mostly governed by heavy minerals economics. Gold is a by-product of the extraction of the heavy minerals, and the reasonable prospects of economic extraction depend on the reasonable assumption that the Au can be recovered through a relatively simple, conventional, and cost-efficient gravity process. The Competent Person considers the Au Mineral Resource reported as a realistic inventory of Au mineralisation which, under assumed and justifiable technical, economic, and developmental conditions, might, in whole or in part, become economically extractable.

## 8.11.2 Heavy Minerals

### *8.11.2.1 Classification Statement*

In accordance with Clause 49 of the JORC Code (2012), the likely product and its specifications have been considered by the Competent Person. The product is a 45-µm to 2-mm magnetic concentrate rich in ilmenite, garnet, and a non-magnetic concentrate rich in zircon. The MRE is reported in terms of the minerals on which the project is based and includes the specification of these minerals.

The Competent Person has classified a Measured Mineral Resource of 3.15 Mt at 7.69% ilmenite, 11.49% garnet and 0.14% zircon, and an Indicated Mineral Resource of 2.5 Mt at 7.5% ilmenite, 9.7% garnet and 0.14% zircon, reported at a cut-off abundance of 1% ilmenite and within a particle size range of 45 µm to 2 mm (Table 37 and Table 38). The Mineral Resource has been classified in accordance with the JORC Code (2012).

The Measured portion of the MRE (Figure 104) has been determined from an assessment of kriging statistics (kriging efficiency and slope of regression), drill spacing and assessment of geological and grade continuity. Geological evidence is derived from adequately detailed and reliable exploration, sampling and testing gathered through appropriate techniques from drillholes including SEM-based automated mineralogy, and is sufficient to confirm geological and grade continuity between points of observation where data and samples are gathered. The remainder of the Resource has been classified as Indicated as evidence is sufficient to assume but not confirm geological and grade continuity.

Table 37: Coates South Block Heavy Mineral Resource

| Classification | Mass (kt) | Ilmenite (%) | Garnet (%) | Zircon (%) | VHM (%) | Ilmenite (kt) | Garnet (kt) | Zircon (kt) |
|---|---|---|---|---|---|---|---|---|
| **Measured** | 3,150 | 7.69 | 11.49 | 0.14 | 19.32 | 240 | 360 | 4 |
| **Indicated** | 2,500 | 7.5 | 9.7 | 0.14 | 17.3 | 190 | 245 | 4 |
| **Total** | 5,650 | 7.6 | 10.7 | 0.14 | 18.4 | 430 | 610 | 8.0 |

Notes:

1. The Mineral Resource is classified in accordance with the JORC Code (2012).
2. The Mineral Resource is reported at a 1% ilmenite abundance cut-off.
3. Zircon is the tonnes of zircon within particle size range 45 µm to 2 mm.
4. Garnet is the tonnes of garnet within particle size range 45 µm to 2 mm.
5. Ilmenite is the tonnes of ilmenite within particle size range 45 µm to 2 mm.
6. VHM % is the abundance of ilmenite, garnet and zircon within a particle size range 45 µm to 2 mm.
7. The effective date of the MRE is 10 February 2023.
8. The Mineral Resources are contained within the proposed mining disturbance area.
9. Estimates are rounded to reflect the level of confidence at the time of reporting.

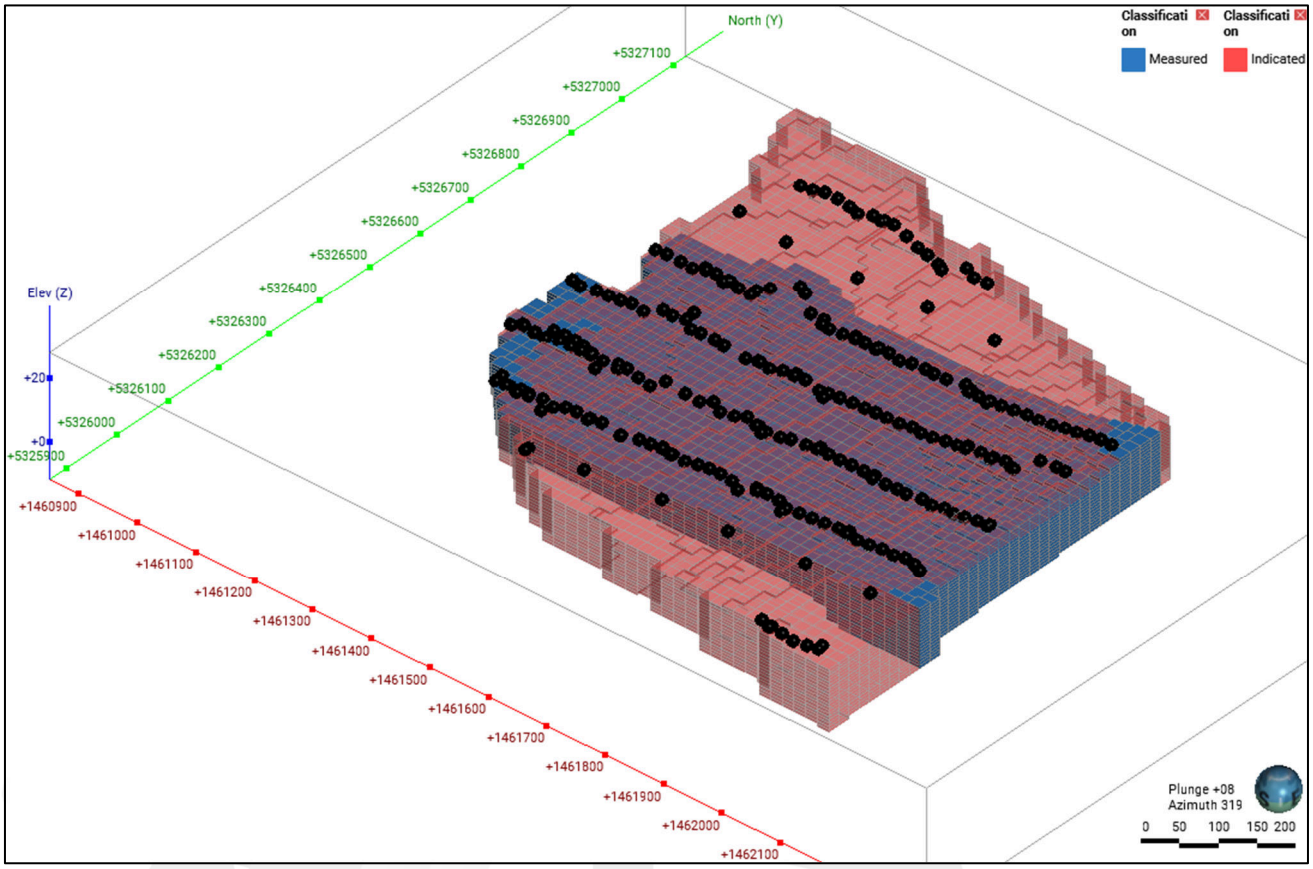


Figure 104: Oblique view to the northwest coloured by the classification of the heavy mineral Resource.

### 8.11.2.2 *Cut-Off Grade*

The abundance cut-off of 1% ilmenite was determined through an interim feasibility study (London, 2022) and is based on assumed operating costs of a conventional open pit mining operation and HM recoveries.

The ilmenite abundance–tonnage relationship for the estimate is demonstrated in Figure 105 and Table 38.

Table 38: Total Mineral Resource at various ilmenite cut-off abundances.

| Cut-Off | Mass (kt) | Average Ilmenite Abundance (%) |
|---|---|---|
| **0** | 9,400 | 5.0 |
| **1** | 5,670 | 7.6 |
| **2** | 3,250 | 11.7 |
| **4** | 2,725 | 13.1 |
| **6** | 2,290 | 13.9 |
| **8** | 1,640 | 15.3 |
| **10** | 1,050 | 17.1 |

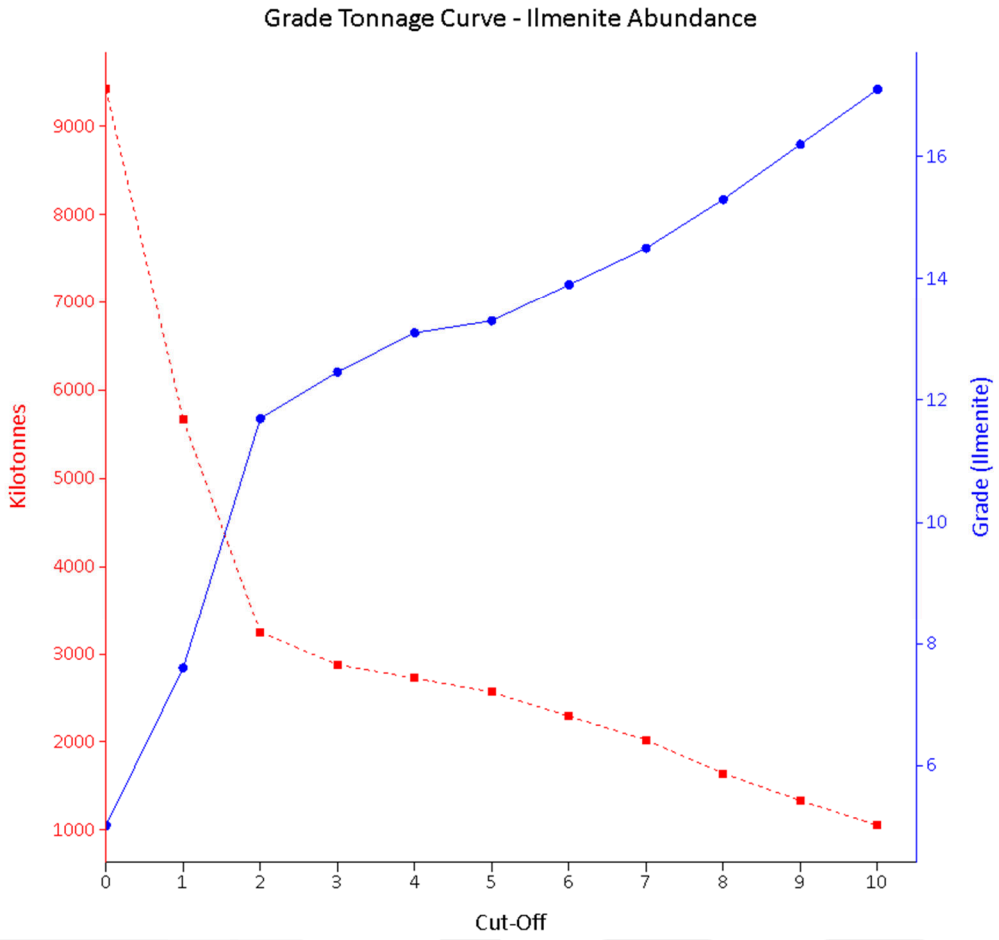


Figure 105: Ilmenite resource abundance-tonnage curve.

### *8.11.2.3 Reasonable Prospects*

In assessing the reasonable prospects, the Competent Person has evaluated preliminary mining, metallurgical, economic, environmental, social (section 9) and geotechnical parameters established in preliminary or internal pre-feasibility and feasibility studies (Banaszak et al., 2018; London, 2022), that have investigated various mining and processing methods for extracting and concentrating the ilmenite, garnet and zircon. The interim feasibility study (London, 2022), with engineering and design completed to a 20–30% level of precision, assumes a high level of mining recovery of the Sand unit (>95%) within the deposit.

London (2022) includes the outcomes of metallurgical testing of a bulk sample. The 2022 and previous metallurgical testing (section 5.3.2) results demonstrate reasonable pathways to produce marketable concentrates that contain ilmenite, garnet and zircon.

RSC considers that the Mineral Resource reported here is a realistic inventory of mineralisation which, under assumed and justifiable technical, economic and developmental conditions, might, in whole or in part, become economically extractable. Portions of the deposit that do not have reasonable prospects for economic extraction are not included in the Mineral Resource.

#### *8.11.2.4 Product Specification, Deleterious Elements and Marketability*

The heavy minerals product is a magnetic concentrate rich in ilmenite and garnet, and a non-magnetic concentrate rich in zircon with grains that range from 45 µm to 2 mm.

In the Competent Person's experience with similar projects and product types, from nearby locations in New Zealand and elsewhere, there are reasonable markets for these concentrate products. These will most likely be China, North America and/or Europe. Purchasers would separate the ilmenite, garnet and zircon from the concentrates for further processing and/or marketing.

Globally, the primary market for ilmenite is the supply of titanium raw materials for the manufacture of $TiO_2$ pigments and titanium metal. The Barrytown ilmenite product, recovered from the concentrate by downstream customers, would likely be used either for direct use in anatase production or as a blend feedstock for wider use in $TiO_2$ pigment production. The garnet product would likely be used for abrasive blasting and waterjet cutting. The zircon product may be suitable as an opacifier, whitening agent, or pigment for ceramic applications. Other zircon product markets include abrasives and machinery due to its hardness and resistance to corrosion and heat, respectively.

Key quality characteristics of the product containing ilmenite and garnet are the garnet composition and the proportion of impurities within the ilmenite and garnet grains (section 5.4). RSC notes that Barrytown ilmenite grains typically contain large inclusions of other deleterious minerals; however, using conventional processing techniques, the presence of other mineral inclusions in ilmenite is unlikely to be deleterious to the production of $TiO_2$ (pers. comm. Chris Bumby, Chief Scientist / Engineer – Materials, Robinson Institute). The Barrytown garnet grains are relatively fine (~100 µm; Figure 29), dominated by almandine and are typically free of inclusions (section 5.4); hence, the Barrytown garnets are suitable for the water-jet cutting market.

## 8.12 Reconciliation

Minor historical production was reported from the licence; however, no production data were available to reconcile the heavy mineral abundances of the Mineral Resource reported here. The head-grade of the bulk sample collected for metallurgical studies is 14% Ilmenite, compared with the block abundance of 10% for that location. The bulk sample only represents a small proportion of the total block volume (Indicated classification) at this location and was taken selectively from visible mineralisation; however, it provides a broad affirmation of the high-grade tenor at this location.

At a cut-off abundance of 4% ilmenite, the ilmenite resource abundance (13.1% ilmenite, Table 38) compares well with the previous estimates completed by Robbins (1989), Lee (1990 b, a) and Lee & Burlet (2018a) who reported average abundances of 11.6–14.3% ilmenite at a cut-off of 4% ilmenite (Table 7). At a cut-off abundance of 2.5% ilmenite, the ilmenite resource abundance (12.5% ilmenite) is around 25% higher than the estimate carried out by Maynard and Jones (2014, Table 7), who reported an average abundance of 6.5–-10% ilmenite at a cut-off of 2.5% Ilmenite. The difference is likely due to the Maynard and Jones (2014) resource relating to the Barrytown heavy mineral deposit in its entirety, including areas of lower abundance. RSC considers the abundances reported here to be broadly in line with previous mineral resource studies of the deposits.

# 9 Environmental & Social Factors

The drilling on the Coates South Block was undertaken within a planned mining disturbance area. This area was defined using boundaries and exclusion zones of the surrounding environmentally sensitive areas as discussed in section 2.4 and shown in Figure 3.

The Barrytown Flats and Coates South Block lie within an area of high average annual rainfall. Groundwater levels are high and landowners describe the area as very wet for large parts of the year. As such, effective groundwater management will be key to successful mining of HM deposits in this area, and in particular, the management of run-off with relation to the surrounding areas of environmental sensitivity. One of the conditions requested by the West Coast Regional Council for gaining resource consent to mine at Coates South concerns obtaining a detailed understanding of the hydrological conditions and groundwater for effective water management. As a result, in 2022, TiGa commissioned Komanawa Solutions Ltd to undertake a detailed hydrogeological study across the Project area. As part of this study, RSC supervised the drilling of water monitoring holes during the 2022 drilling campaign. A total of twenty holes were drilled with the aircore rig and fitted with standpipes and piezometers to act as dedicated water monitoring holes. In addition to these holes, four resource holes were retrofitted with mini piezometers to increase the density of data collection.

At the time of reporting, updated environmental technical studies have not been finalised. TiGa expects the new resource consent applications to be submitted in February 2023 and the company expects they will be approved by June 2023, allowing mining to start in early 2024[6]. While the outcomes of the environmental studies are not available, the Competent Person considers that the company is working towards an outcome where it is likely that resource consents will be granted. The Competent Person notes that if resource consents are not granted, it could affect the MRE's prospects of eventual economic extraction negatively.

Mining in New Zealand is a sensitive subject and like many other Western Countries, there are active anti-mining groups. Currently, there is a pending debate in the Central Government to consider the banning of mining on Department of Conservation land. While the outcome of this bill will not affect the Barrytown Project, as it is on private land, it could embolden local and online anti-mining groups. In 2019, Plaman Resources lost its social licence to operate at Foulden Hills, Diatomite Mine, Otago[7]. A negative Facebook social media campaign resulted in the project losing funding and therefore being unable to proceed. If TiGa was to lose its social licence to operate, it could affect the MRE's prospects of economic extraction negatively. The Competent Person notes that while there is some risk of social licence issues, the West Coast region has stronger support for mining than the rest of New Zealand. A similar heavy mineral sand project is consented and operating on private land ~50 km north of Barrytown at Nine Mile Beach with support from West Coast locals (section 4.5).

On balance, the Competent Person considers that the environmental, social and governance factors are sufficiently well-understood and proactively managed to support the MRE's reasonable prospects of economic extraction at the effective date of this Report.

[6] https://www.stuff.co.nz/environment/131052787/company-behind-barrytown-mine-proposal-100-confident-of-go-ahead
[7] https://www.newsroom.co.nz/southern-discomfort-at-fossil-mining-plans

# 10 Risks

The risks involved in the modelling and estimation for the Project are summarised in Table 39. The most pertinent risks have also been noted throughout this report.

rsc MINING & MINERAL EXPLORATION

Table 39: Overview of risk factors impacting the MRE.

| Category | Availability Data/Info | Score (1–10) | Impact Factor (1–5) | Risk Factor | Comment |
|---|---|---|---|---|---|
| **Database format** | Good | 9 | 3 | Low | Data are stored in a Microsoft Access database maintained by RSC. |
| **Drilling & primary sampling techniques** | Good | 8 (HM)<br>6 (Au) | 4 (HM)<br>4 (Au) | Low (HM)<br>Moderate (Au) | Sonic is considered the superior drilling method for this type of deposit. Aircore is suitable for drilling HM sand deposits but is generally not the recommended drilling technique for Au deposits. However given that the mineralised horizon is unconsolidated, there is support for applying aircore to sampling for Au sampling. There remains some risk associated with the quality of the aircore sampling and this is considered to have a moderate impact on the Au resource classification. |
| **Drilling & primary sampling recovery** | Good | 7 (HM)<br>7 (Au) | 3 (HM)<br>4 (Au) | Low (HM)<br>Moderate (Au) | Sample recoveries from the aircore drilling were variable. There is some risk of Au grade bias in samples with low recovery samples. This has been mitigated to an extent by selecting samples with higher recovery for the Au LeachWELLTM analyses, and taken into account in the Au classification. |
| **Logging** | Good | 4 | 9 | Low | Logging was completed to a high standard. It is consistent and provided a solid foundation for robust geological interpretations |
| **Sub-sampling techniques & sample preparation** | Good | 4 | 8 | Low | Subsampling procedures and quality control checks were acceptable. In general, Ti, Fe and Zr show low variation at all splitting stages. |
| **Quality of assay data & analytical techniques** | Good | 6 | 4 | Low (Au)<br>Moderate (pXRF)<br>Low (XRF, SEM) | There is a moderate risk that the pXRF data could be biased, due to errors in the sample preparation process, which would impact the quality of the mineral modelling. |
| **Verification of sampling and assaying** | Good | 4 | 8 | Low | Twin sampling results returned good results supporting low risk and positive verification of the sampling and assaying |
| **Location of data points** | Good | 4 | 9 | Low | Drill collar elevations were draped to the DTM with accuracy specifications of ± 0.2 m (95%) vertical. Considering the horizontal nature of the deposit, lack of cover, combined with the strong grade and geological continuity, the Competent Person considers the accuracy of the collar locations acceptable and the potential error present will not materially impact the Mineral Resource. |
| **Data spacing and distribution** | Good | 8 | 3 | Low | With drill fences 120 m apart and hole spacing of ~20 m, the Competent Person considers the data spacing sufficient to confirm geological and grade continuity for the HM and Au estimation. |
| **Bulk density** | Acceptable | 6 | 5 | Moderate | Core tray method applied to the collected sonic samples is not considered best practice. It does not yield accurate results however the more granular measurements taken per sample are the data that were used in the MRE and this is considered fit for purpose. This is considered a moderate risk. |

| Category | Availability Data/Info | Score (1–10) | Impact Factor (1–5) | Risk Factor | Comment |
|---|---|---|---|---|---|
| **Orientation of data/drilling** | Good | 8 | 2 | Low | All drilling used in the estimate was appropriately oriented, and perpendicular to the flat-lying deposit. |
| **Database integrity** | Good | 9 | 3 | Low | All data are maintained in a database and checked by RSC. |
| **Geological interpretation** | Good | 8 | 4 | Low | The geological interpretation is based on downhole lithological logging, which provides good correlation between drillholes. |
| **Estimation and modelling: Domaining** | Good | 8 | 4 | Low | Estimation domains are constrained by the geological interpretation and produced populations with low to moderate internal grade variation, as expressed by the CV. |
| **Estimation and modelling: compositing** | Good | 9 | 2 | Low | Samples were collected in 1 m intervals. There was no requirement to composite. Low risk |
| **Estimation and modelling: grade capping** | Good | 8 | 3 | Low | Estimation domains exhibit low to moderate CVs; top cutting was not applied. |
| **Estimation and modelling: variography** | Good | 7 | 3 | Low | Variogram structures are typically well defined and extend beyond drill spacing. Nugget values inferred from the downhole variograms are relatively low (0.1–0.2). For Au mineralisation, the nugget is appropriately higher at 0.4. |
| **Estimation and modelling: interpolation and extrapolation** | Good | 8 | 3 | Low | Interpolation is controlled by kriging weights within each domain.<br>Extrapolation typically does not exceed 50% of the drillhole spacing, and the extrapolation distance is considered reasonable by the Competent Person. |
| **Estimation and modelling: checks and validation** | Good | 8 | 3 | Low | The model was validated through visual validation, mean comparison checks, and review of swath plots. RSC considers the block model to be robustly estimated, with block grades representative of the input data. |
| **Estimation and modelling: cut-off** | Good | 8 | 3 | Low | The abundance cut-off of 1% ilmenite was determined through a pre-feasibility study (London, 2022) and is based on assumed operating costs and heavy mineral recoveries. No cut-off criteria were applied to the reported Au estimation. |
| **Estimation and modelling: density** | Acceptable | 6 | 5 | Moderate | Dry bulk density data were collected from sonic drillholes following the core tray method. Density values within estimation domains display very low CVs and variability. RSC considers the density assignment sufficient due to the low variability of the density values within domains. |
| **Estimation and modelling: Classification** | Good | 7 | 4 | Moderate | The HM model is classified as Measured and Indicated based on sample spacing, sample quality, geological understanding, and kriging statistics.<br>The HM Measured portion of the MRE has been confined to the Sands domain of the Resource.<br>The Au MRE is classified as Inferred, reflective of the data spacing, geological and grade continuity. |

# 11 Exploration Potential

The MRE presented in this Report relates to exploration undertaken within a planned mining area on the Coates South property. The area is sited within a buffer zone to environmentally sensitive areas which require special consent to explore or mine. The exploration area is thus bound to the north, south, and west largely by environmentally protected margins that limit exploration and mining in those directions. To the east of the area of the MRE, is a strip of land approximately 200–300-m wide which is bound by both the State Highway and private property. Previous work indicates that there are buried marine strandlines running through this area; however, RSC has not undertaken an evaluation of this area, and cannot comment on the potential of any resources, or mine potential under this area.

TiGa is in the process of undertaking further exploration activities on the wider Barrytown Flats under the existing mining licence. During 2022, RSC supervised exploration drilling at Barrytown Farms which intercepted similar deposits of HMS. RSC understands that TiGa initiated the processing of these samples, and RSC has not undertaken any further work to date. RSC cannot comment on the potential size or nature of any Exploration Targets on Barrytown Flats. Previous MREs have attempted to estimate the global resources across the flats; however, they have not led to further and more advanced technical evaluations, considering the varied land use and ownership across the area.

# 12 Conclusions

The Au, ilmenite, garnet, and zircon MRE presented in this Report is a realistic inventory of mineralisation which, under assumed and justifiable technical, economic and developmental conditions, might, in whole or in part, become economically extractable. The heavy-mineral product is a 45-µm to 2-mm magnetic concentrate rich in ilmenite, garnet, and a non-magnetic concentrate rich in zircon. Geological evidence is derived from adequately detailed and reliable exploration, sampling and testing, gathered through appropriate techniques from drillholes including SEM-based automated mineralogy, and is sufficient to confirm geological and grade continuity between drill holes for a significant part of the deposit.

The machine learning approach to quantify the ilmenite, garnet and zircon abundance from XRF-derived elemental concentrations in drill samples has performed well, and is supported through robust, repeatable and demonstrable quality control processes.

# 13 Recommendations

The method of using aircore drilling is suitable to sampling soft sediments, but struggles to obtain high-quality samples where large-diameter gravel, beach pebbles, or other clasts are present; whereby the material is either rejected by the bit, or causes a blockage to either the bit, casing, or sample hose. As a result of this, and/or efforts to clear this material, the resulting samples can be unrepresentative of the mineralisation domain. There is a potential for the under-estimation of coarse/over-size material, or the over-estimation of finer material, which would introduce bias towards subsequent estimation of HM and Au within size fractions. RSC recommends a series of test pits are excavated to further evaluate the true size fraction proportions and abundances across key areas. It is also recommended to drill a close-spaced (say ~5 m spaced) sonic drill programme to further resolve any abundance bias and better understand short-range variability in the deposit.

Water saturation was high owing to high groundwater levels and run-off from heavy rainfall during the autumn–winter period. Sample quality in future drilling programmes could be improved by drilling during the drier summer months.

RSC understands that geotechnical studies have been carried out at Coates South Block and recommends that more density data are collected across the ore body to get more confidence in tonnages and variation in densities across the project area.

Amendments and adjustments were made to sample processing during the programme as a result of budget constraints, and tight timelines. This created complicated sampling protocols, which in itself is a common source of errors in data. Limitations with equipment, experience, personnel, size and capacity at NZIMMR all contributed to small but cumulative errors in handling of samples, or errors in digital data reporting. RSC recommends that future samples are processed at a single accredited facility, and that all sample processing is defined before the programme starts.

All future Au estimates should be based on large-volume samples and ideally not on only a part of the size fraction. It is recommended that to obtain further confidence in the Au estimate, single, sonic-derived, whole-core samples should be processed on site through a small concentrator (i.e. 7-inch Knelson, or similar), with the concentrate sent for total leaching, and the undersize and oversize sub-sampled for standard fire assaying.

There is a robust relationship between the mineralogy abundance data (derived from pXRF) and automated mineralogy data with the sink-float data. This suggests that TiGa can reduce the quantity of sink float analyses in future studies on the Barrytown project

# 14 References

Abzalov, M., 2008, Quality control of assay data: a review of procedures for measuring and monitoring precision and accuracy. *Exploration and Mining Geology*, **17**, 131-144.

Banaszak, P., Mann, S., Pearce, R., and Straface, D., 2018, Prefeasibility Study, Barrytown Mineral Sands Project, New Zealand. Prefeasibility Study prepared by Barrytown JV Limited for Exploration Permit EP51803.

Barrows, T. T., Almond, P., Rose, R., Fifield, L. K., Mills, S. C., and Tims, S. G., 2013, Late Pleistocene glacial stratigraphy of the Kumara-Moana region, west coast of South Island, New Zealand. *Quaternary Science Reviews*, **74**, 139-159.

Best, R., 1972, Review of operations to January 1972 - Barrytown, New Zealand. Phase 2: Review of field work, laboratory work, ore reserves, Barrytown Mineral Sands, MR3018. Carpentaria Exploration Co Pty Ltd.

Bradley, J., Chew, P., and Wilkins, C., 2002, Transport and distribution of magnetite and ilmenite on Westland beaches of New Zealand; with comment on the accumulation of other high-density minerals. *Journal of the Royal Society of New Zealand*, **32**, 169-181.

Bruker, 2020, SEM AMICS.

Burlet, L., and Lee, G., 2019, Old Data, Changed Times, New Resource? A Case Study, Barrytown, New Zealand, Ilmenite Garnet Gold Zircon. *ASEG Extended Abstracts*, **2019**, 1-5.

Caffyn, P. H., 1976, Ilmenite reserves at Barrytown, New Zealand, MR1327. Carpentaria Exploration Co Pty Ltd.

Christie, A. B., and Brathwaite, R. L., Geology and exploration of New Zealand mineral deposits2006, Australasian Institute of Mining and Metallurgy.

Clifton, H. E., 1969, Beach lamination: nature and origin. *Marine Geology*, **7**, 553-559.

Fisher, L., Gazley, M. F., Baensch, A., Barnes, S. J., Cleverley, J., and Duclaux, G., 2014, Resolution of geochemical and lithostratigraphic complexity: a workflow for application of portable X-ray fluorescence to mineral exploration.

Force, E. R., 1991, Geology of titanium-mineral deposits, Geological Society of America.

Furkert, F., Westport harbour, *in* Proceedings *Transactions of the Royal Society of New Zealand*1947, Volume **76**, p. 373-402.

Furlong, K. P., and Kamp, P. J., 2013, Changes in plate boundary kinematics: Punctuated or smoothly varying—Evidence from the Mid-Cenozoic transition from lithospheric extension to shortening in New Zealand. *Tectonophysics*, **608**, 1328-1342.

Gallagher, E., Wadman, H., McNinch, J., Reniers, A., and Koktas, M., 2016, A conceptual model for spatial grain size variability on the surface of and within beaches. *Journal of Marine Science and Engineering*, **4**, 38.

Gazley, M., and Fisher, L., 2014, A review of the reliability and validity of portable X-ray fluorescence spectrometry (pXRF) data. *Mineral resource and ore reserve estimation–The AusIMM guide to good practice*, **69**, 82.

Hancock, and Associates, 1980, Report on potential of EL 33086, Barrytown, MR1349. Mineral Resources NZ Ltd.

Haverkamp, R. G., Kruger, D., and Rajashekar, R., 2016, The digestion of New Zealand ilmenite by hydrochloric acid. *Hydrometallurgy*, **163**, 198-203.

Hutton, C. O., 1950, Studies of heavy detrital minerals. *Geological Society of America Bulletin*, **61**, 635-710.

IHC, 2022, 2263 Characterisation Data, *in* Love, J., ed.

James, J. G., 2001, Evaluation of the Gold Potential of the Barrytown Beach Placer Project, Report No PCRE 01:10.

Kenex, 2013a, Barrytown Project - Historical data compilation and QC of current database progress report, EP 51803, MR4934.

-, 2013b, EP 51803 Barrytown Flats annual technical report – 2013, MR5069.

-, 2016, MEP 51803 Annual Technical Report 2015, MR5266.

-, 2017, Annual Technical Report 2016 – EP 51803 – Barrytown, MR5406.

Kimbrough, D. L., and Tulloch, A. J., 1989, Early Cretaceous age of orthogneiss from the Charleston Metamorphic Group, New Zealand. *Earth and planetary science letters*, **95**, 130-140.

Laird, M., 1988, Sheet S37-Punakaiki. Geological map of New Zealand 1: 63,360. *New Zealand Geological Survey. Wellington, Department of Scientific and Industrial Research*.

Laird, M., and Bradshaw, J., 2004, The break-up of a long-term relationship: the Cretaceous separation of New Zealand from Gondwana. *Gondwana Research*, **7**, 273-286.

Laird, M., and Shelley, D., 1974, Sedimentation and early tectonic history of the Greenland Group, Reefton, New Zealand. *New Zealand journal of geology and geophysics*, **17**, 839-854.

Lee, G., 1990a, Bulk Density Sampling. Barrytown Ilmenite Deposit, South Island, New Zealand, Technical Note 4/90.

-, 1990b, Statement of Ilmenite Sand Resources at Barrytown, Report No. 9/90.

-, 1991, Statement of Ilmenite Sand Resources at Barrytown, MR4287. Westland Ilmenite Ltd.

Lee, G., and Burlet, L. A., 2018a, Barrytown Ilmenite Mineral Resource Estimate. Prepared by G Lee & Associates and H&S Consultants.

-, 2018b, Supplementary Report Barrytown Gold Exploration Target. Prepared by G Lee & Associates and H&S Consultants.

Lipton, I., and Horton, J., 2014, Measurement of bulk density for resource estimation–methods, guidelines and quality control: Mineral Resource and Ore Reserve Estimation–The AusIMM Guide to Good Practice. *Monograph*, **30**, 97-108.

London, J., 2022, Draft Barrytown Sands Feasibility Study. Prepared by Palaris for TiGa Minerals and Metals Ltd. Document No. BJL5790-001.

Maynard, A. J., and Jones, P. A., 2014, Geological and resource report: Barrytown resource estimates. Al Maynard & Associates Pty Ltd.

McOnie, A., and Bull, V., 2007, Work on EP40760 Barrytown to 30 September 2007, MR4265. NZ Gold Ltd.

McPherson, R., 1978, Geology of Quaternary ilmenite-bearing coastal deposits at Westport.

Minehan, P. J., 1989, The occurrence and identification of economic detrital minerals associated with alluvial gold mining in New Zealand. *Mineral Deposits of New Zealand. Australasian Institute of Mining and Metallurgy monograph*, **13**, 159-167.

Nathan, S., 1974, Stratigraphic nomenclature for the cretaceous-lower quaternary rocks of Buller and North Westland, west coast, South Island, New Zealand. *New Zealand journal of geology and geophysics*, **17**, 423-445.

Nathan, S., Anderson, H. J., Cook, R. A., Herzer, R., Hoskins, R., Raine, J., and Smale, D., 1986, Cretaceous and Cenozoic sedimentary basins of the West Coast region, South Island, New Zealand, Science Information Publishing Centre, DSIR, for the New Zealand Geological Survey.

Nathan, S., Rattenbury, M., and Suggate, R., 2002, Geology of the Greymouth area (compilers). *Institute of Geological and Nuclear Sciences. Geological Map*, **12**.

Newman, N. A., 1989, Barrytown ilmenite evaluation—Borehole reports, MR1434. Ministry of Economic Development: Wellington, New Zealand.

Nicol, A., Seebeck, H., and Wallace, L., 2017, Quaternary tectonics of New Zealand, Landscape and Quaternary environmental change in New Zealand, Springer, p. 1-34.

Pillans, B., 1990, Pleistocene marine terraces in New Zealand: a review. *New Zealand journal of geology and geophysics*, **33**, 219–231.

Riordan, N., Reid, C., Bassett, K., and Bradshaw, J., 2014, Reconsidering basin geometries of the West Coast: the influence of the Paparoa Core Complex on Oligocene Rift Systems. *New Zealand Journal of Geology and Geophysics*, **57**, 170-184.

Ritchie, T. W., Scott, J. M., and Craw, D., 2019, Garnet compositions track longshore migration of beach placers in western New Zealand. *Economic Geology*, **114**, 513-540.

Robbins, C. M., 1989, Barrytown Ilmenite Project Prefeasibility Study. Prepared for Fletcher Titanium.

RSC, 2017, ANNUAL TECHNICAL REPORT: EP 51803 – Barrytown, MR5499. Barrytown JV Ltd. (Alloy Resources Ltd.).

Schulte, D. O., Ring, U., Thomson, S. N., Glodny, J., and Carrad, H., 2014, Two-stage development of the Paparoa metamorphic core complex, West Coast, South Island, New Zealand: Hot continental extension precedes sea-floor spreading by∼ 25 my. *Lithosphere*, **6**, 177-194.

Stanley, C. R., and Lawie, D., 2007, Average relative error in geochemical determinations: Clarification, calculation, and a plea for consistency. *Exploration and Mining Geology*, **16**, 267-275.

Suggate, R., 1968, The thirty-foot raised beach at Rapahoe, North Westland. *New Zealand journal of geology and geophysics*, **11**, 648-650.

-, 1989, The postglacial shorelines and tectonic development of the Barrytown coastal lowland, North Westland, New Zealand. *New Zealand Journal of Geology and Geophysics*, **32**, 443-450.

Tay, S. L., Scott, J. M., Palmer, M. C., Reid, M. R., and Stirling, C. H., 2021, Occurrence, geochemistry and provenance of REE-bearing minerals in marine placers on the West Coast of the South Island, New Zealand. *New Zealand Journal of Geology and Geophysics*, **64**, 89–106.

Tulloch, A., and Kimbrough, D., 1989, The Paparoa metamorphic core complex, New Zealand: cretaceous extension associated with fragmeotation of the pacific margin of Gondwana. *Tectonics*, **8**, 1217-1234.

Van Gosen, B. S., Fey, D. L., Shah, A. K., Verplanck, P. L., and Hoefen, T. M., 2014, Deposit model for heavy-mineral sands in coastal environments. US Geological Survey, 2328-0328.

Vidanovich, P., 2008, Barrytown Airborne Geophysics Survey, MR4438. NZ Gold Ltd.

Wallace, Y., and Peters, B., 2016, Identification of heavy mineral sands strandlines from airborne magnetic and radiometric data, SGC3131.

Wells, H. C., and Haverkamp, R. G., 2020, Characterization of the heavy mineral suite in a holocene beach placer, Barrytown, New Zealand. *Minerals*, **10**, 86.

rsc
MINING & MINERAL EXPLORATION

# APPENDIX A: Summary Statistics

## A.1 Estimation Domain Summary Statistics

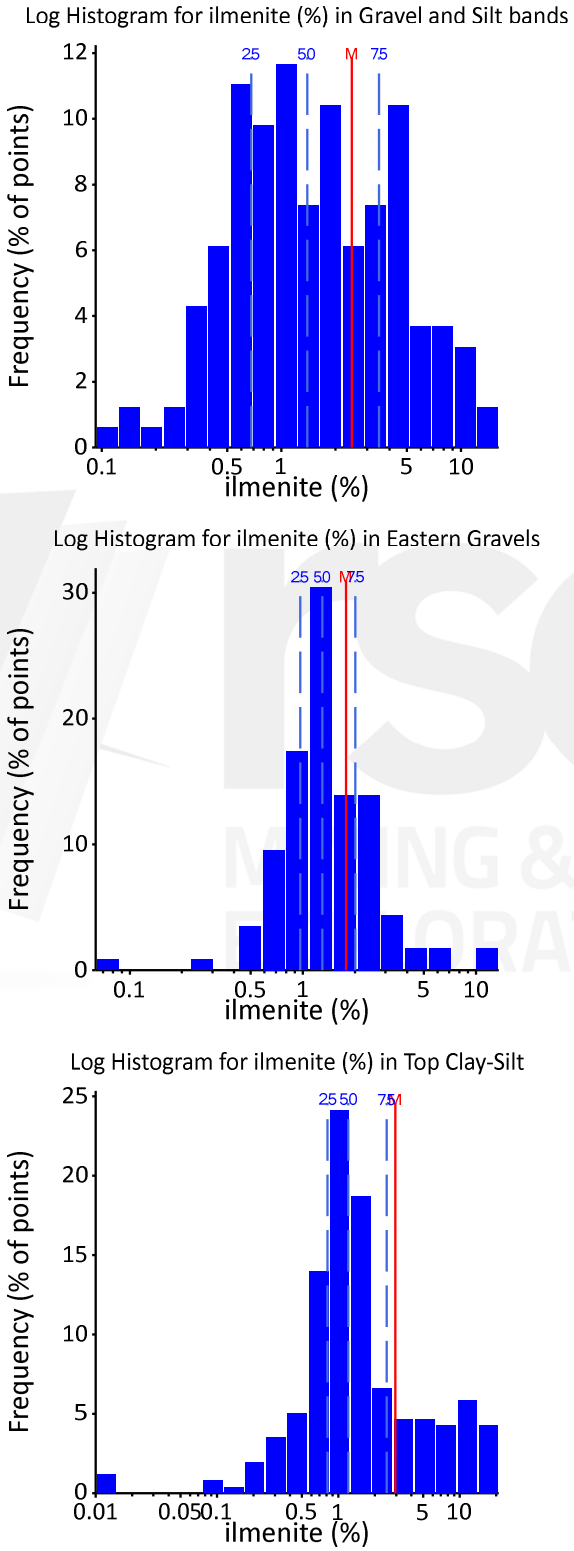


Figure 106: Log histograms of ilmenite abundance within estimation domains.

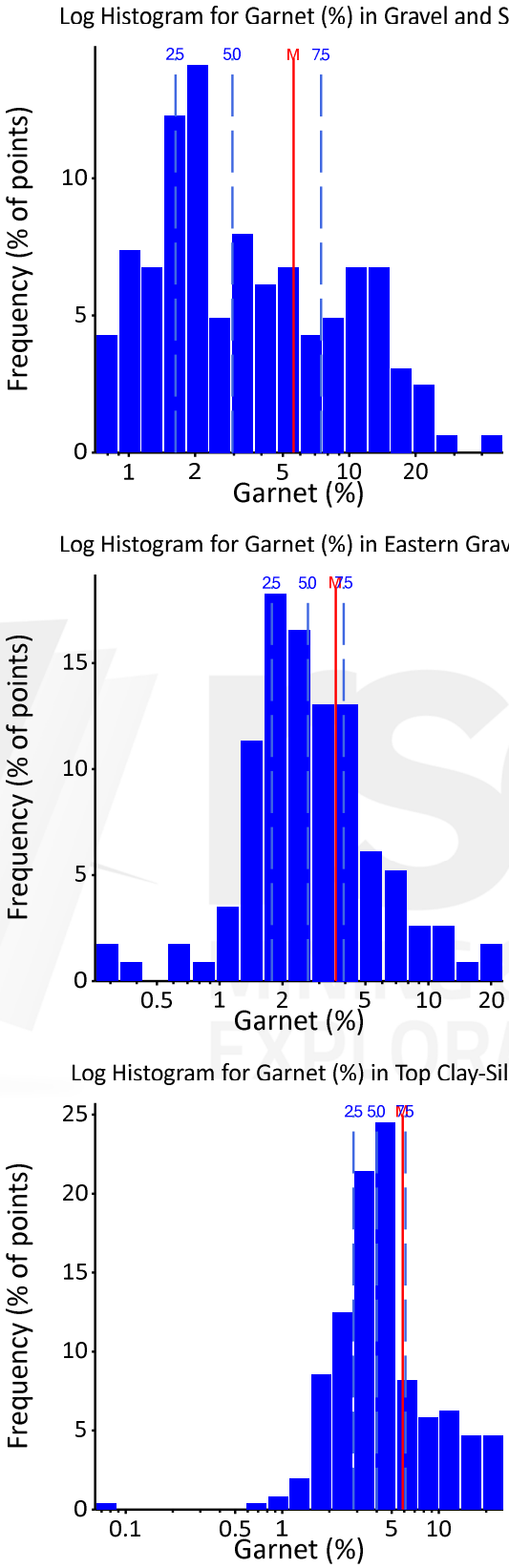


Figure 107: Log histograms of garnet abundance within estimation domains.

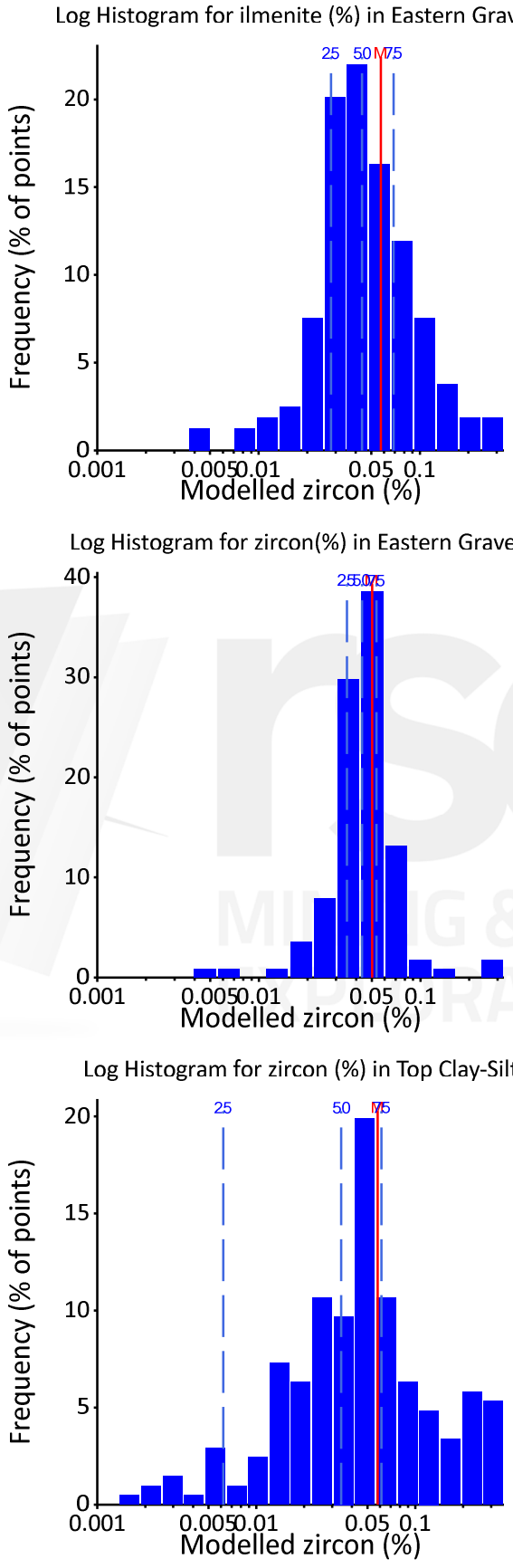


Figure 108: Log histograms of zircon abundance within estimation domains.

# APPENDIX B: Variogram Parameters and Models

## B.1 Heavy Minerals Variogram Parameters

| Variable | Estimation Domain | Structure | Model Type | Sill | Range Major (m) | Range Semi Major (m) | Range Minor (m) |
|---|---|---|---|---|---|---|---|
| **Garnet** | Sands High-Abundance | | Nugget | 0.15 | | | |
| | | 1 | Spherical | 0.72 | 155 | 28 | 2 |
| | | 2 | Spherical | 0.13 | 500 | 50 | 4 |
| **Garnet** | Sands Low-Abundance | | Nugget | 0.15 | | | |
| | | 1 | Spherical | 0.66 | 130 | 20 | 2 |
| | | 2 | Spherical | 0.19 | 250 | 150 | 3 |
| **Garnet** | Gravel and Silt Strands | | Nugget | 0.20 | | | |
| | | 1 | Spherical | 0.40 | 70 | 70 | 8 |
| | | 2 | Spherical | 0.40 | 250 | 250 | 10 |
| **Garnet** | Eastern Gravels | | Nugget | 0.20 | | | |
| | | 1 | Spherical | 0.10 | 200 | 200 | 2 |
| | | 2 | Spherical | 0.70 | 300 | 300 | 5 |
| **Garnet** | Top Clay-Silt | | Nugget | 0.20 | | | |
| | | 1 | Spherical | 0.40 | 70 | 70 | 4 |
| | | 2 | Spherical | 0.40 | 450 | 450 | 10 |
| **Zircon** | Sands High-Abundance | | Nugget | 0.20 | | | |
| | | 1 | Spherical | 0.7 | 160 | 30 | 2 |
| | | 2 | Spherical | 0.10 | 300 | 300 | 3 |
| **Zircon** | Sands Low-Abundance | | Nugget | 0.20 | | | |
| | | 1 | Spherical | 0.53 | 15 | 30 | 3 |
| | | 2 | Spherical | 0.27 | 100 | 60 | 4 |
| **Zircon** | Gravel and Silt Strands | | Nugget | 0.10 | | | |
| | | 1 | Spherical | 0.25 | 90 | 60 | 4 |
| | | 2 | Spherical | 0.65 | 425 | 80 | 6 |
| **Zircon** | Eastern Gravels | | Nugget | 0.10 | | | |
| | | 1 | Spherical | 0.32 | 150 | 20 | 1 |
| | | 2 | Spherical | 0.58 | 400 | 200 | 3 |
| **Zircon** | Top Clay-Silt | | Nugget | 0.25 | | | |
| | | 1 | Spherical | 0.35 | 100 | 30 | 4 |
| | | 2 | Spherical | 0.40 | 425 | 425 | 5 |
| **THM** | Sands High-Abundance | | Nugget | 0.15 | | | |
| | | 1 | Spherical | 0.70 | 180 | 25 | 2.5 |
| | | 2 | Spherical | 0.15 | 230 | 200 | 3.5 |

| | | | | | | | |
|---|---|---|---|---|---|---|---|
| **THM** | Sands Low-Abundance | | Nugget | 0.15 | | | |
| | | 1 | Spherical | 0.7 | 200 | 43 | 3 |
| | | 2 | Spherical | 0.15 | 250 | 75 | 4 |
| **THM** | Gravel and Silt Strands | | Nugget | 0.1 | | | |
| | | 1 | Spherical | 0.36 | 20 | 15 | 4 |
| | | 2 | Spherical | 0.54 | 350 | 175 | 8 |
| **THM** | Eastern Gravels | | Nugget | 0.1 | | | |
| | | 1 | Spherical | 0.34 | 150 | 45 | 2 |
| | | 2 | Spherical | 0.56 | 250 | 250 | 4 |
| **THM** | Top Clay-Silt | | Nugget | 0.15 | | | |
| | | 1 | Spherical | 0.37 | 200 | 30 | 4 |
| | | 2 | Spherical | 0.48 | 400 | 400 | 6 |

## B.2 Size Fraction Proportion Variogram Parameters

| Variable | Estimation Domain | Structure | Model Type | Sill | Range Major (m) | Range Semi Major (m) | Range Minor (m) |
|---|---|---|---|---|---|---|---|
| **All proportions** | Sands | | Nugget | 0.20 | | | |
| | | 1 | Spherical | 0.68 | 200 | 40 | 2 |
| | | 2 | Spherical | 0.12 | 500 | 100 | 10 |
| **All proportions** | Gravel and Silt Strands | | Nugget | 0.20 | | | |
| | | 1 | Spherical | 0.68 | 200 | 30 | 2 |
| | | 2 | Spherical | 0.12 | 500 | 100 | 10 |
| **All proportions** | Eastern Gravels | | Nugget | 0.20 | | | |
| | | 1 | Spherical | 0.58 | 150 | 40 | 2 |
| | | 2 | Spherical | 0.12 | 500 | 100 | 10 |
| **All proportions** | Top Clay-Silt | | Nugget | 0.20 | | | |
| | | 1 | Spherical | 0.68 | 200 | 40 | 2 |
| | | 2 | Spherical | 0.12 | 500 | 100 | 10 |

## B.3 Variogram Models

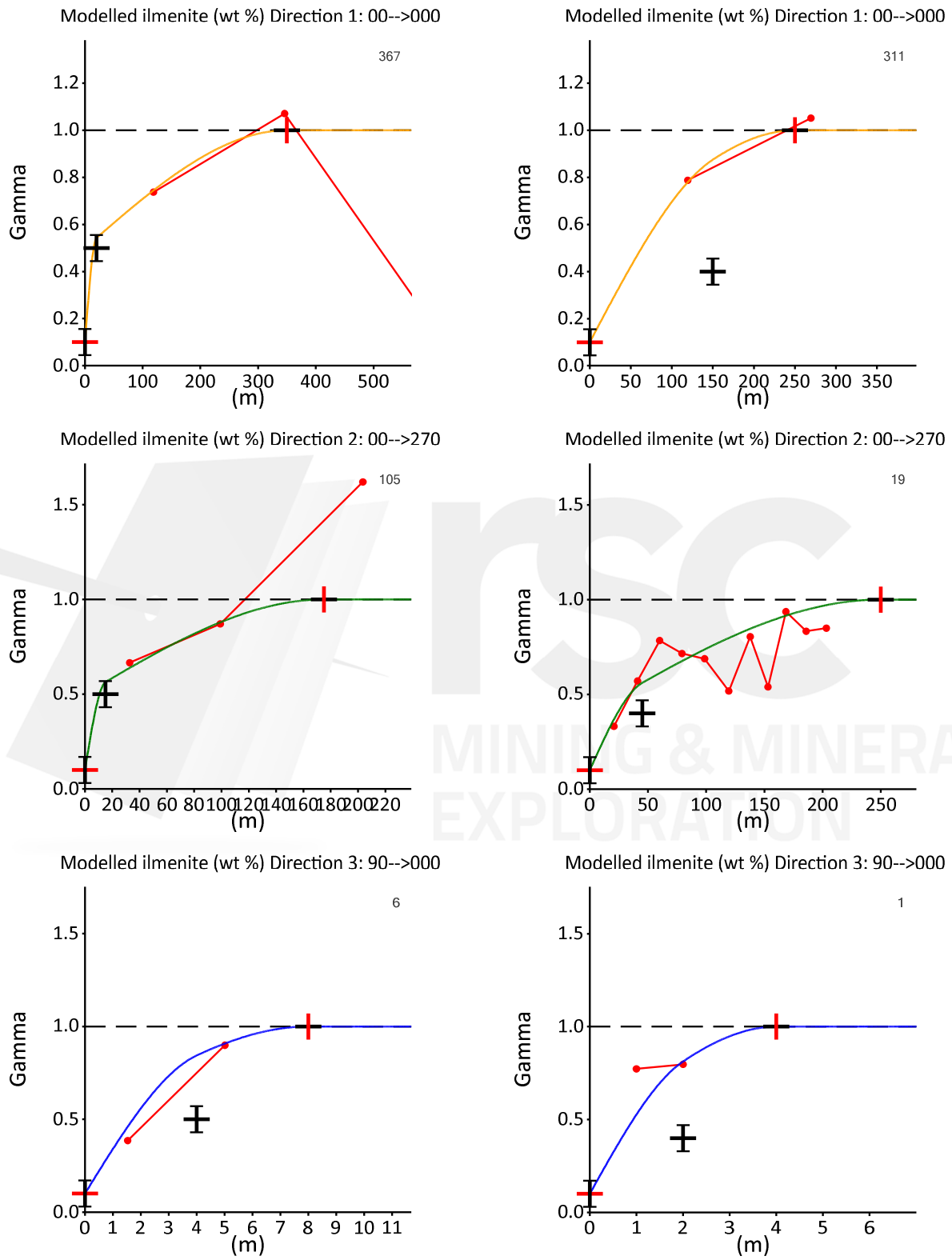


Figure 109: Experimental semi-variogram models for ilmenite within the Gravel and Silt Strands (left) and Eastern Gravels (right).

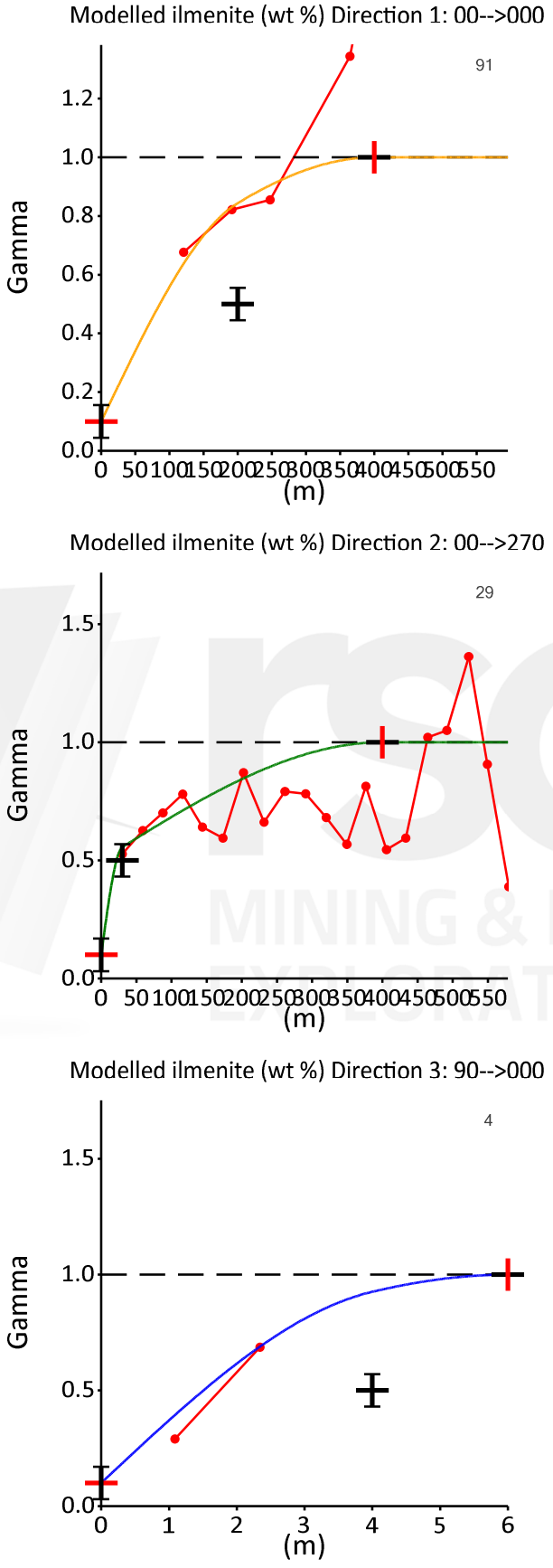


Figure 110: Experimental semi-variogram models for Ilmenite within the Top Clay-Silt estimation domain.

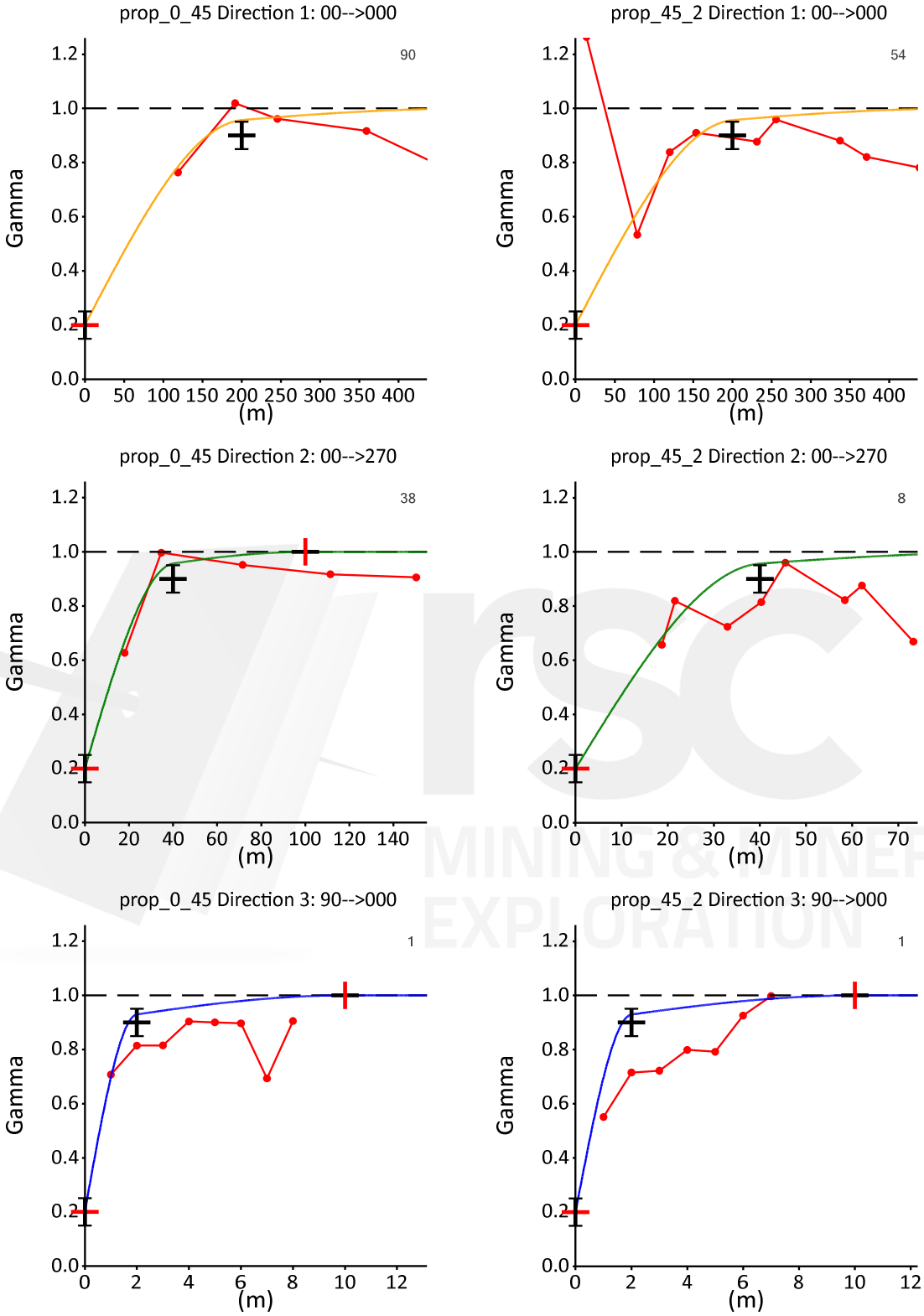


Figure 111: Experimental semi-variogram models for the 0–45 µm (left) and 45 µm to 2 mm (right) portion within the Sands estimation domain.

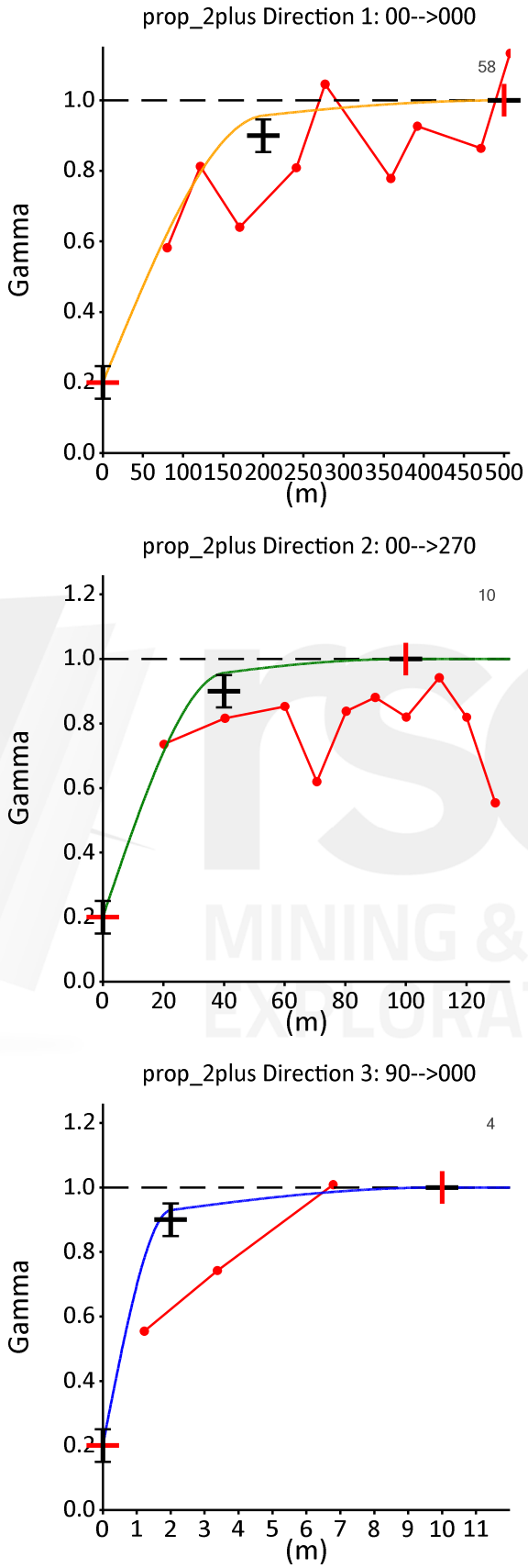


Figure 112: Experimental semi-variogram models for the >2 mm portion within the Sands estimation domain.

# APPENDIX C: Swath Plots

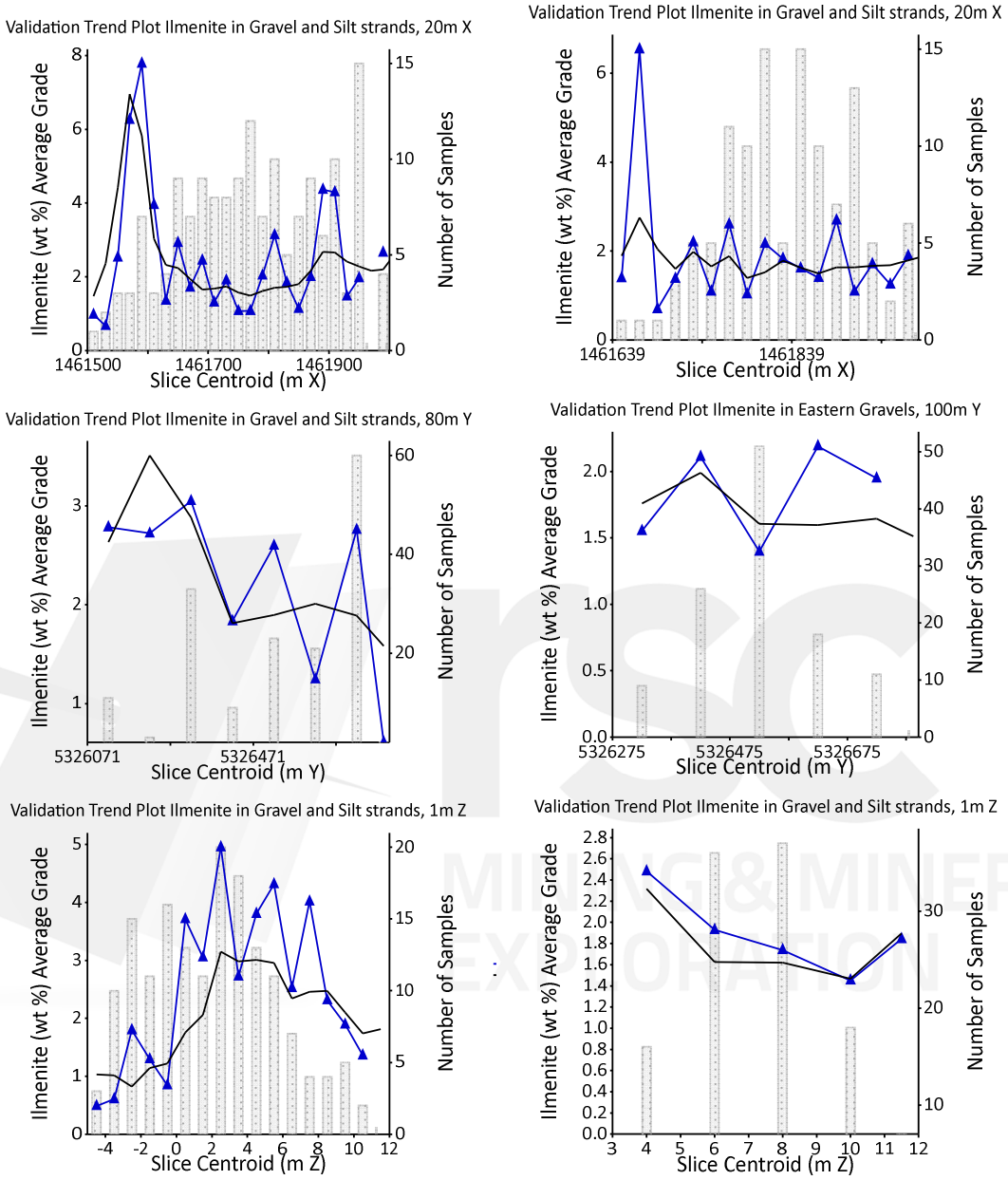


Figure 113: Swath plots displaying the average declustered sample (blue) and estimated (black) ilmenite abundance for the Gravel and Silt strands domain (left) and Eastern Gravels domain (right) along easting (20 m), northing (100 m), and elevation (2 m, top to bottom) slices.

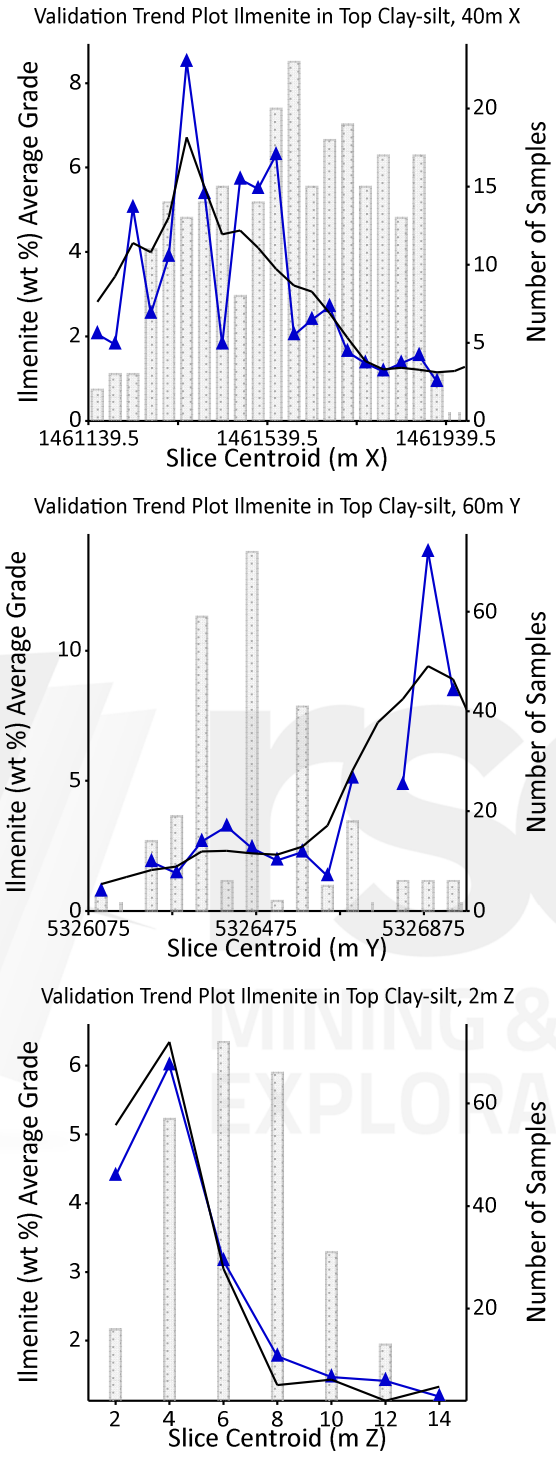


Figure 114: Swath plots displaying the average declustered sample (blue) and estimated (black) ilmenite abundance for the Top Clay-Silt domain along easting (40 m), northing (60 m), and elevation (2 m, top to bottom) slices.